

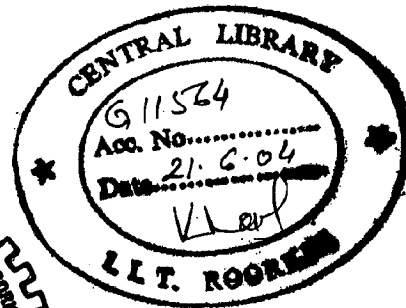
MATHEMATICAL MODELING OF PULP WASHING SYSTEMS AND SOLUTIONS

A THESIS

*Submitted in fulfillment of the
requirements for the award of the degree
of*
DOCTOR OF PHILOSOPHY

By

MUKESH KUMAR



DEPARTMENT OF PAPER TECHNOLOGY
INDIAN INSTITUTE OF TECHNOLOGY ROORKEE
SAHARANPUR CAMPUS
SAHARANPUR-247 001 (INDIA)

JULY, 2002

INDIAN INSTITUTE OF TECHNOLOGY ROORKEE

(Formerly University of Roorkee)

CANDIDATE'S DECLARATION

I hereby certify that the work which is being presented in the thesis entitled, "**Mathematical Modeling of Pulp Washing Systems and Solutions**", in fulfilment of the requirement for the award of the Degree of **Doctor of Philosophy** submitted in the "**Indian Institute of Technology Roorkee**" is an authentic record of my own work carried out during the period from Aug. 1998 to May, 2002, under the supervision of Dr. A.K. Ray and Dr. V.P. Singh. The matter presented in this thesis has not been submitted by me for the award of any other degree of this or any other institute/university.

Dated: 22.07.2002

Mukesh Kumar

Place: Saharanpur, U.P. (INDIA)

(Mukesh Kumar)

This is to certify that the above statement made by the candidate is correct to the best of our knowledge.

A.K. Ray

(A.K. Ray)

Professor
Department of Paper Technology
Indian Institute of Technology, Roorkee
Saharanpur Campus
Saharanpur (U.P.) 247001, INDIA

V.P. Singh

(V.P. Singh)

Associate Professor
Department of Paper Technology
Indian Institute of Technology, Roorkee
Saharanpur Campus
Saharanpur (U.P.) 247001, INDIA

The viva – voce examination of Mr. Mukesh Kumar, Research Scholar, has been held on

25/10-2002
A.K. Ray 25/10/02

V.P. Singh
25/10/02

Signature of Supervisors

J.S. Dhyaya
Signature of H.O.D.
(J.S. DHYAYA)
Professor & Head

Signature of External Examiner

Department of Paper Technology
(I.I.T. Roorkee) Saharanpur Campus
SAHARANPUR-247001

25/10/2002

ACKNOWLEDGEMENT

I would like to express my humble gratitude and deep sense of indebtedness to my learned supervisors Dr. A.K.Ray, Professor and Dr. V.P.Singh, Associate Professor, both from Department of Paper Technology, Indian Institute of Technology, Roorkee for their erudite guidance, co-operation and encouragement throughout the duration of research work.

I am thankful to Dr. J.S.Upadhyaya, Head, Department of Paper Technology upto the utmost possible extend for ultimate encouragement, co-operation and providing all kinds of help, academic and administrative during the research work. If he had not provided the computer facility from his own, this work could not be completed in time.

I am thankful to Dr.A.K.Ray, Professor and Dr. Satish Kumar, Professor, both from Department of Paper Technology and Dr. R.K.Gupta, Professor from Department of Mathematics who taught me the courses Heat and Mass Transfer, Washing and Bleaching and C++ Object Oriented Programming respectively to clear the courses on these topics during my research work.

My regards are due to Dr. Bani Singh, Professor, Department of Mathematics who encouraged and helped me a lot constantly during my research work.

I respect Dr. H.S.Kasana, Professor, Thapar Institute of Engineering and Technology, Patiala, India, Dr. M.P.Singh, Assistant Professor, Govt, College, Gwalior, India and Dr. Peeyush Tewari, Lecturer, Birla Institute of Technology, Ranchi, India, who motivated me to do research work and encouraged me during the whole period.

Co-operation of Mrs. Anjali Ray and Mrs. Vimlesh Singh is unlimited who supported a lot directly and indirectly during the preparation of this thesis.

It don't find words to express my regards towards Mrs. Santosh Upadhyaya and love to Mr. Siddhartha Upadhyaya who supported me like anything during the whole period.

I feel privileged to express my endless thanks to Mr. Sanjay Kumar, Mr. Joy Biswas and Mr. Reddy, students of M.E. (Communication Engineering), Department of Electronics and Computers, IITR, Roorkee, who helped me constantly sparing hours to make me acquainted with the software MATLAB.

I acknowledge the support rendered by Miss Anjana Rani Gupta and Mrs. Seema Saini, research scholars of this institute during the whole period of the work.

With gratitude, I acknowledge the co-operation rendered by the staff members of various offices of this Department of Paper Technology.

My heartiest regards are due to my respected parents who are blessing me from heaven each and every moment.

Motivation, inspiration, patience and constant support of my respected brother Shri Pawan Kumar, my beloved wife Mrs. Archana Singhal and my pretty daughters Smriti and Mansi were unlimited.

This work could not be possible without their support.

ABSTRACT

Pulp and paper industry is highly capital intensive industry. It is intensive in terms of raw materials, water, chemicals, thermal and electrical energy, labour and pollution loads. Approximately 2.5-3.0 t of raw materials, 200-350m³ of water, 9 -20 t of steam, 1000-1700 kWh of electric energy are required for one tonne of pulp. This leads to generation of pollution loads to the extent of 24-45 kg of BOD₅, 80-150 kg of COD, 2.5-8 kg of AOX in the effluents. There are all round efforts globally to reduce the above intakes and outflows from a paper mill keeping the quality for its acceptance in the international market. Concerted efforts are also being made in Indian paper mills to address these issues for mere survival point of view and also to keep pace with sustainable production to meet the demands of paper. Some of the measures taken into consideration by mills are: seeking of optimum design and operational parameters, adaptation of modern control measures and use of new equipment and process technology.

Mathematical model can help significantly to fulfill the above objective. For research work a model can be highly complicated to obtain higher accuracy but in actual practice there is a compromise between the accuracy and the complexity of the model. A mathematical model can be macroscopic, microscopic or semi quantitative in nature. Macroscopic / empirical / black box / white box models give a general outside description (in terms of material balance) of a brown stock washer. As a whole microscopic / physical / gray box models gives a deep inside description (in terms of fundamental parameters) of a brown stock washer. Semi quantitative models are intermediate between macroscopic and microscopic models. Higher is the order of the model, higher is the degree of difficulty expected to solve the problem.

In this present study up-to date review of mathematical models relating to displacement washing or similar systems with or without adsorption or dispersion is made. The models developed very recently for some other systems (quite similar to pulp fibers) are also presented.

It is found from the literature that there is abundant of information regarding steady state models mainly required for the material balances for the macroscopic evaluation of the design estimates. However, there is little information about the interaction of various time dependent operational parameters for control purposes. Very few investigators have attempted to throw light on these aspects. Majority of the investigators have concentrated on displacement washing studies though in normal practice the process is related to dilution and extraction and also with displacement. Many investigators did not take into account the parameters related to diffusion, dispersion, adsorption, desorption, multiporosity values for inter particle and intra particle voids. Although some mathematical models are available in literature limited studies are carried out for pulp washing under the influence of longitudinal dispersion coefficient, mass transfer coefficients and solute accumulation capacity of pulp fibers. Many works are also applicable to only nonporous solids. Though these are fantastic in their approach and the corresponding solution techniques, these are not truly applicable to porous adsorptive beds like pulp mat. Besides, there are significant variations noted among the models of many investigators in their adsorption-desorption isotherm equations. The solution techniques (either analytical or numerical or quasi- analytical or statistical) are also remarkably different. No investigator has ever compared the results evolved out by assuming different adsorption isotherms that too for different boundary conditions with mill practice values. Very few workers applied the results of simulation with displacement washing data to brown stock washer operation in rotary vacuum filter equipment in a very concise form but it lacks clarity. From design point of view these are of little relevance.

The solution of partial differential equation can also be possible with numerical techniques which is not very complex yet preserving the required accuracy for evaluating an industrial system. The system equation must address the issues of practical significance. It therefore demands a rational approach for interlinking the output data from a mathematical problem and the parameters normally known to the practicing engineers of a pulp and paper industry.

In this investigation mathematical models are derived for displacement washing in the washing zone of a rotary vacuum washer from basic equation of continuity in one dimensional form for flow through porous media, Fick's law of diffusion and dispersion with adsorption and desorption isotherm equations for two species namely Na^+ and lignin. The equations are coupled with many other fluid mechanical parameters and thus general in nature. The models resulted in the form of a linear parabolic partial differential equation.

For solving the models varying initial and boundary conditions applicable to rotary vacuum brown stock washer are proposed. The developed models have been reduced to various earlier proposed models using simplifying assumptions and neglecting certain terms. .

As the developed models are mathematically complex to solve, these are simplified for further investigation in order to compare with some of the models proposed by Grah [24], Brenner [6], Sherman [88], and Pellett [71] but with different numerical techniques. Four set of models differing in adsorption isotherm with same boundary conditions are proposed to solve through finite difference method. In fact earlier investigators did not attempt to use this simple technique. In order to solve the proposed models, various equations for parameters like porosity, permeability, specific cake resistance, filter medium resistance, compressibility constants, design equations for filtration are reviewed in detail and selected for our investigation.

For the solution of the models developed above, MATLAB software is employed after developing some specially designed C++ programmes.

The present models (four models) are validated with those of Grah [24] based on numerical technique (Orthogonal Collocation) and Brenner [6] with analytical methods with same species and Pe numbers estimated by Grah [23].

In the present investigation the sorption values are also calculated using non-linear adsorption isotherm which is of Langmuir type for estimation of Na^+ / soda loss and lignin. At practical values of kappa number for bleachable grade kraft pulp, the adsorption of Na^+ and soda loss will be on the order of 1.5-1.75 kg / t and 4.8-5.5 kg / t respectively. At kappa number admissible for bleachable grade pulp the amount of lignin sorption will be on the order of 3 kg / t to 5.5 kg / t.

Expressions are given for dimensionless concentration of solute in liquid phase C at any dimensionless pseudo time T , and dimensionless concentration of solute in solid phase, N as a function of T and also as a function of dimensionless distance (bed depth). The C - T profiles are in excellent agreement with those of Grah [24], Poirier et. al.[79] as well as Sherman [88], and Brenner [6]. The C - T profile closely agrees also with Kuo and Barrett [43] and Kukreja [40]. However, there is no work available for pulp washing system with N - T profiles though Kuo [42], Kuo and Barrette [43] and later Kukreja [40] have attempted to show the profile for stagnant liquor. The N - T profile for the present investigation has been in close agreement with many other investigators [17,45,51,92] working with adsorption in solid phase for allied type of systems. Therefore this investigation with N - T profile can claim for the first time a new dimension for solving adsorption related issues in pulp washing situation using the concentration terms in solid phase. The N - T profile in this present study gives an opposite trend with C - T profile of solute in liquor phase or solute in stagnant liquor phase as advocated by Kuo [42] and Kukreja [40]. The four different models are used to predict for two species, namely Na^+ and lignin to examine their washing behavior. Parameters like bed thickness, Peclet number, liquor velocity through cake

pores, dispersion coefficient, porosity and mass transfer coefficients are varied in the C-T and N-T profiles of both Na^+ and Lignin species to examine their influences.

From the displacement washing study for which our models are based the following important conclusions can be drawn.

Investigations of the simultaneous displacement washing of Na^+ and Lignin in sulphate pulp have shown great difference between the two substances in their behavior during washing.

At the same time interval the A_T values (proportional to solute removal) of lignin are equal to or higher than those of Na^+ for the models 1 and 2 but it is reversed in case models 3 and 4 (i.e. Na^+ is higher than lignin) though the differences are very marginal. Poirier et. al.[77] however found the similar or slightly higher values in case of Na^+ . It is probable that Poirier et. al.[77] did not consider the dispersion effects.

The model predicted data can be used reliably for brown stock washer simulation.

The simulated data on DR from displacement washing are in close agreement with mill data.

The washing efficiency WE based on total solute removal in a brown stock washer closely tally with data calculated from the breakthrough curve obtained from the model. The difference arises due to different conditions employed by different investigators for brown stock washer. It however does not consider the removal efficiency of nature of solutes namely, Na^+ and lignin species.

The DR and WE values increases with time, valid for both Na^+ and lignin. This is in excellent agreement with those of Grah [25].

The DR and WE data for sodium are slightly higher than those for lignin for model 1 and model 2. However, for the case of model 3 and model 4 they yield identical values. The model 1 and model 2 give the same value whereas model 3 and model 4 yield identical value for both Na and lignin species. The latter models (models 3 and 4) however provide higher values of C than those from

the former (models 1 and 2). This is caused as earlier indicated by the dispersion which hampers adsorption.

All the above experimental and theoretical findings suggest that the present model agrees quite well with the experimental data and takes care of many of the important aspects of diffusion, dispersion, adsorption-desorption and different porosity values in the system. This verifies that numerical solution of resultant non-linear parabolic partial differential equation with finite difference method can be used though it is simpler and approximate compared to Orthogonal Collocation method employed by many authors.

Present investigation also attempted to correlate the DR and WE obtained from microscopic models (mathematically complex) with those from industrial system of brown stock washer after modifying certain parameter as suggested by Grah [24] using one or two parameter models.

The present study also designed a systematic procedure to examine whether a displacement washing data can be used as a guideline to simulate a BSW or not. It is found that the present computer simulation can be employed to find optimum operating conditions for practical washers, however, it is limited to only washing zone of BSW and also for a single stage equipment.

The present mathematical model is suitable for the simulation of displacement washing in other existing equipment and in equipment under design.

This present analysis can also be extended for the simulation of the washing operation on a multistage rotary washing filter for pulp mill.

LIST OF CONTENTS

| Subject | Page Number |
|---|--------------------|
| Candidate's declaration | i |
| Acknowledgement | ii |
| Abstract | iv |
| List of contents | x |
| Chapter 1. Introduction | 1 |
| 1.1 Status of Indian pulp and paper mill | 1 |
| 1.2 Mathematical models and its relevance with regard to mechanism and operation of BSW | 3 |
| 1.3 Present objectives | 15 |
| Chapter 2. Literature Review | 16 |
| 2.1 Mathematical models for displacement washing and their analytical description | 16 |
| 2.2 Conclusions | 49 |
| Chapter 3. Development of Mathematical models | 51 |
| 3.1 Principles | 51 |
| 3.2 Role of dispersion-diffusion | 51 |
| 3.3 Mathematical modelling of the physical problem | 53 |
| 3.4 Equation of continuity | 54 |
| 3.5 Equation for stagnant layer | 57 |
| 3.6 Equation for fibers | 58 |
| 3.7 Adsorption-desorption isotherm for various species of black liquor | 58 |
| 3.8 Boundary condition for Langmuir type | 58 |
| 3.9 Equation in terms of Na^+ and lignin | 59 |
| 3.10 Corollaries from the developed model | 59 |
| 3.11 Simplification of the present model | 62 |
| 3.12 Simplification of the transport model derived in equ.(4.14) | 62 |

| | |
|--|------------|
| 3.13 Conclusions | 65 |
| Chapter 4. Solution Technique | 66 |
| 4.1 Solution of the problem through MATLAB | 72 |
| Chapter 5. Parameter estimation, data analysis and validity of models | 74 |
| 5.1 Review of modeling of fluid-mechanical parameters | 74 |
| 5.2 Displacement washing data | 87 |
| 5.3 Estimation of data for viscous fiber and bed parameters used for simulation | 88 |
| 5.4 Model validation and simulation | 100 |
| 5.5 conclusions | 104 |
| Chapter 6. Results and discussions of the models | 107 |
| 6.1 Effect of various input parameters on concentration | 108 |
| 6.2 Conclusions | 211 |
| Chapter 7. Simulation of models for efficiencies for single and multistage washer | |
| 7.0 Models to predict washing efficiency in mill equipment | 216 |
| 7.1 Steady state material balance around single stage BSW | 219 |
| 7.2 Selected process and design parameters from the respective models | 219 |
| 7.3 Parameters required for evaluating washer performance | 221 |
| 7.4 Interrelationship among different parameters | 223 |
| 7.5 Comparison of data among various investigators | 224 |
| 7.6 Data obtained from Potucek model | 225 |
| 7.7 Data for multistage BSW | 226 |
| 7.8 Simulation of BSW with the Present investigation | 227 |
| 7.9 Conclusions | 229 |
| Chapter 8. Conclusions and recommendations | 231 |
| 8.1 Main conclusions from the present study | 231 |
| 8.2 Recommendations based on present study | 236 |
| Nomenclature | 238 |
| References | 243 |

Appendices

| | |
|---|-----|
| Appendix I: Base data for the present work for chapter 5 | 252 |
| Appendix II: Base data for chapters 5 and 6 | 258 |
| Appendix III: Algorithm for calculating approximate peclet number | 263 |
| Appendix IV: Base data for comparison between displacement washing and brown stock washing in rotary vacuum filter of a mill | 265 |
| Appendix V: Algorithm for calculation of relevant washing performance parameters in brown stock washing operation | 267 |
| Appendix VI: A set of data obtained from model solution | 268 |

CHAPTER-1

INTRODUCTION

1.1 Status of Indian pulp and paper mill

Pulp and paper industry is highly capital intensive industry. It is intensive in terms of raw materials, water, chemicals, thermal and electrical energy, labour and pollution loads. Approximately 2.5-3.0 t of raw materials, 200-350m³ of water, 9 -20 t of steam, 1000-1700 kWh of electric energy are required for one tonne of pulp. This leads to generation of pollution loads to the extent of 24-45 kg of BOD₅, 80-150 kg of COD, 2.5-8 kg of AOX in the effluents. There are all round efforts globally to reduce the above intakes and outflows from a paper mill keeping the quality for its acceptance in the international market. Concerted efforts are also being made in Indian paper mills to address these issues for mere survival point of view and also to keep pace with sustainable production to meet the demands of paper. Some of the measures taken into consideration by mills are: seeking of optimum design and operational parameters, adaptation of modern control measures and use of new equipment and process technology. Paper plant is composed of many subsystems such as size reduction, size separation, cooking, washing of brown stock, bleaching, stock preparation, approach flow system, wet end operation, drying, calendering and chemical recovery operation. Surface sizing, filling and coating are rather additional operations. Chemical recovery operation in turn consists of concentration of waste liquor, combustion, causticization and calcination of lime sludge. Fig. 1.1 shows the block diagram of a typical pulp mill. It is evident that the process necessitates washing of pulp obtained from digester blow operation to remove organic and inorganic solutes present in water medium (called black liquor). It is evident that Brown stock washing is one of the key steps for pulp mill which interlinks among various operations such as

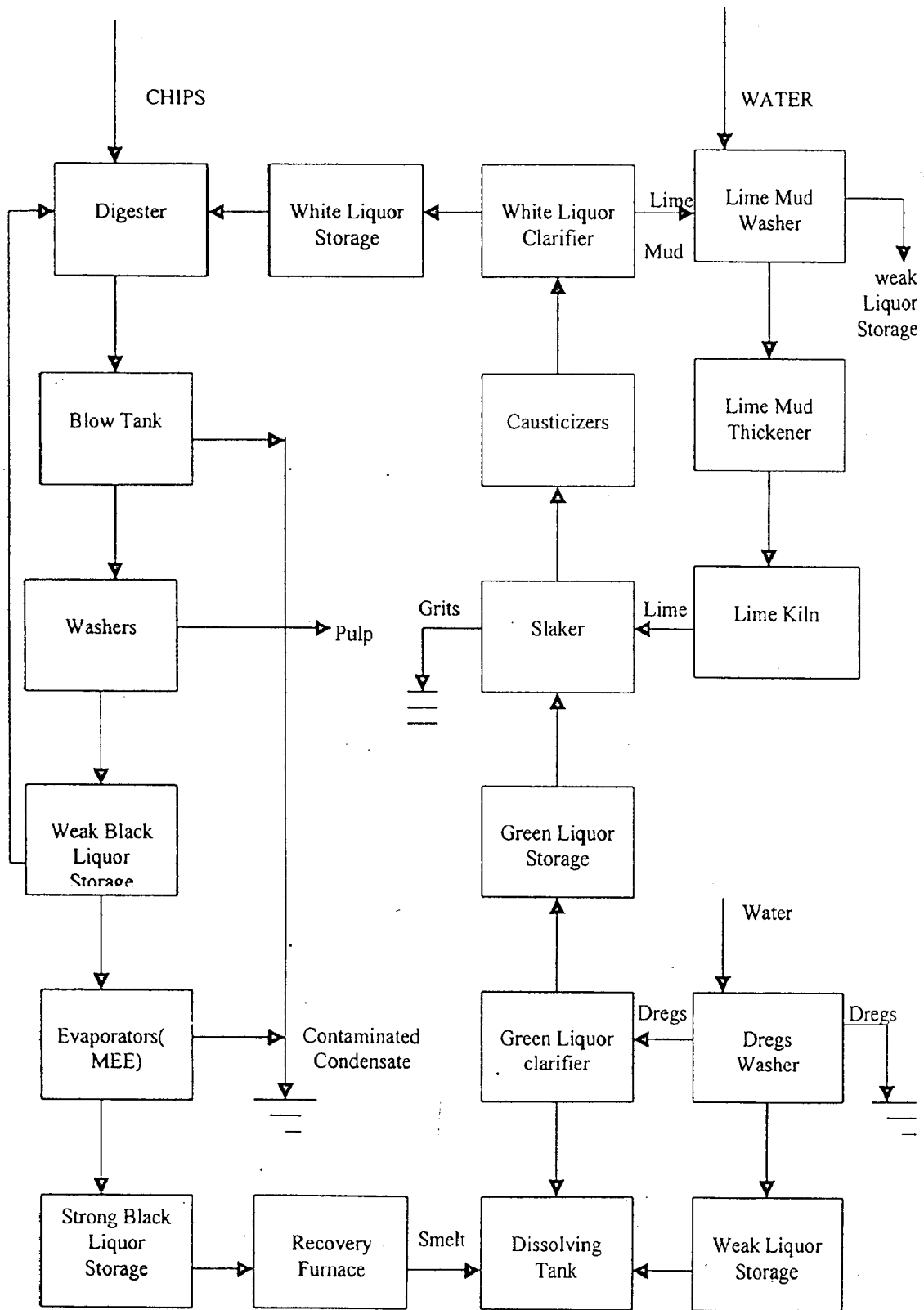


Fig. 1.1 Block Diagram of a Typical Pulp Mill.

pulping, bleaching of pulp, bleach plant and evaporation of black liquor. It has also direct impact on the economy and the environment. The energy, water and chemical consumptions and the resultant pollution loads are cumulative of the contributions of each subsystem. Optimum parameters and controlling the plant can only be ascertained through development of mathematical models and optimization for the right process parameters required for better quality products in all subsystems of a paper mill.

Rising chemical cost and stringent pollution regulations have forced the paper industry to increase the recovery of chemicals by utilizing dissolved organic constituents for steam and power generation. This is achieved via efficient washing of pulp in multistage brown stock washer with close control of various parameters. The parameters are interactive in nature. Therefore to examine the parametric effect on washing effectiveness or washing efficiency, detailed analysis of washing system is essential.

1.2 Mathematical models and its relevance with regard to mechanism and operation of BSW

Mathematical model can help significantly to fulfil the above objective. For research work a model can be highly complicated to obtain higher accuracy but in actual practice there is a compromise between the accuracy and the complexity of the model. A mathematical model can be macroscopic, microscopic or semi quantitative in nature. Macroscopic / empirical / black box models give a general outside description (in terms of material balance) of a brown stock washer. As a whole microscopic / physical / gray box models gives a deep inside description (in terms of fundamental parameters) of a brown stock washer. Semi quantitative models are intermediate between macroscopic and microscopic models. Higher is the order of the model, higher is the degree of difficulty expected to solve the problem.

Grah [23] has presented a simple model of a packed bed, which is given in Fig. 1.2. In this diagram the packed bed of cellulose fibers is divided into three different zones namely, flowing

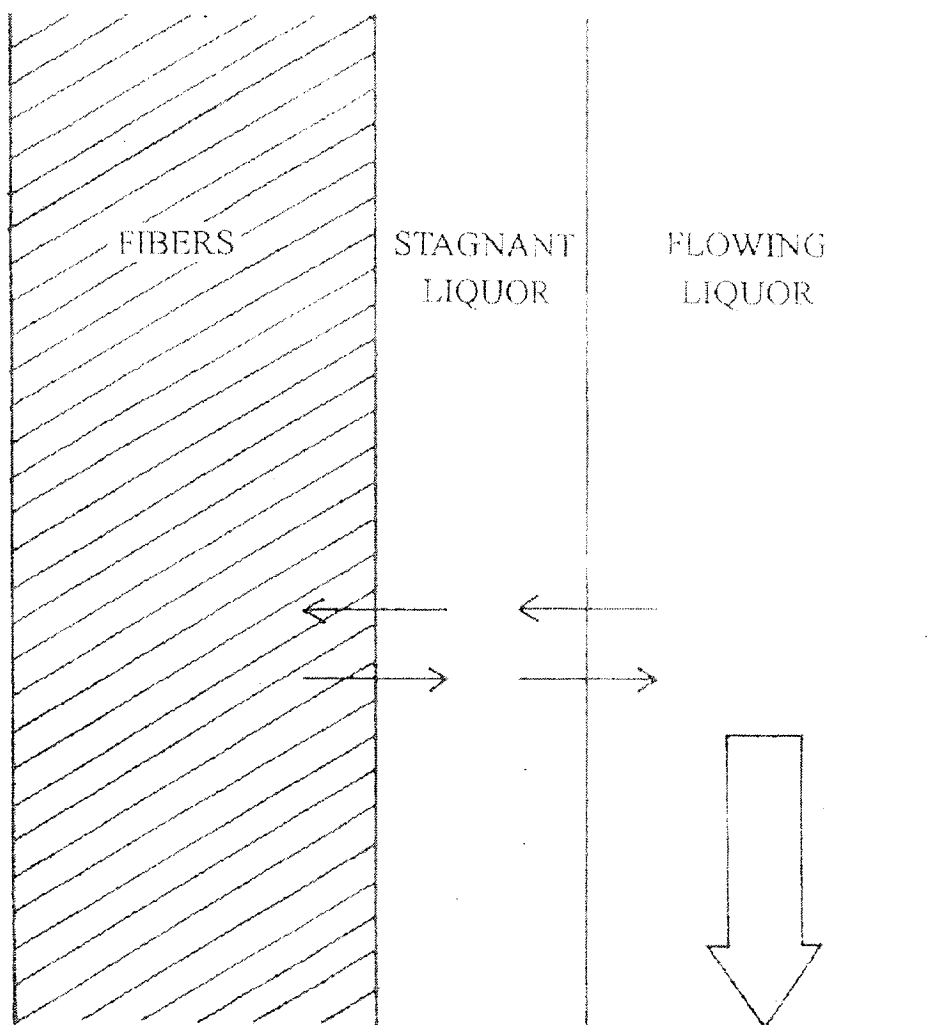


Fig. 1.2 A Packed Bed of Cellulose Fibers.

liquor, stagnant liquor and fibers. Mass transfer is assumed to take place from fibers to stagnant liquor and then back from stagnant liquor to flowing liquor. This clearly indicates that the porosity value varies significantly from zone to zone. Therefore multiporosity values must be considered in the mathematical analysis of pulp washers. Majority of investigators, however, neglected the above aspects.

A variety of equipments are available in the market for brown stock washing. Notable equipments among them are rotary vacuum washer, pressure washer, belt washer, wash press, screw press, diffusion washer, pressure diffusion washer, fiberfuge, continuous centrifuge washer and High heat washer. Among all these equipments rotary vacuum washer is the oldest one and is very commonly used in the industry globally. It has undergone continuous modification and development in its seven decades of applications. At present, in industry a battery of 3 to 5 rotary vacuum washers connected in a counter current manner is used to wash the pulp discharged from the digester.

A rotary vacuum washer consists of a wire mesh screen or cloth covered cylinder which rotates in a vat containing slurry of pulp (brown stock). As the drum rotates inside the vat various zones are formed. These are: cake formation, first stage cake dewatering, cake washing, second stage cake dewatering, blow/discharge and dead zones. Cross sectional view of a rotary vacuum washer is given in Fig. 1.3. The mechanism of each zone is explained therein. A battery of 3 to 5 rotary vacuum washers connected in a counter current manner is shown in Fig. 1.4.

The formation of cake during cake formation zone is highly dependent upon the inlet vat consistency, fractional submergence of drum, speed of drum, pressure drop across the cake and specific resistance of the cake. During cake washing porosity, cake thickness, time of washing, liquor speed inside the cake pores, amount of wash water applied and mass transfer rate are major variables. Whereas in cake dewatering or drying zones cake saturation is a key variable

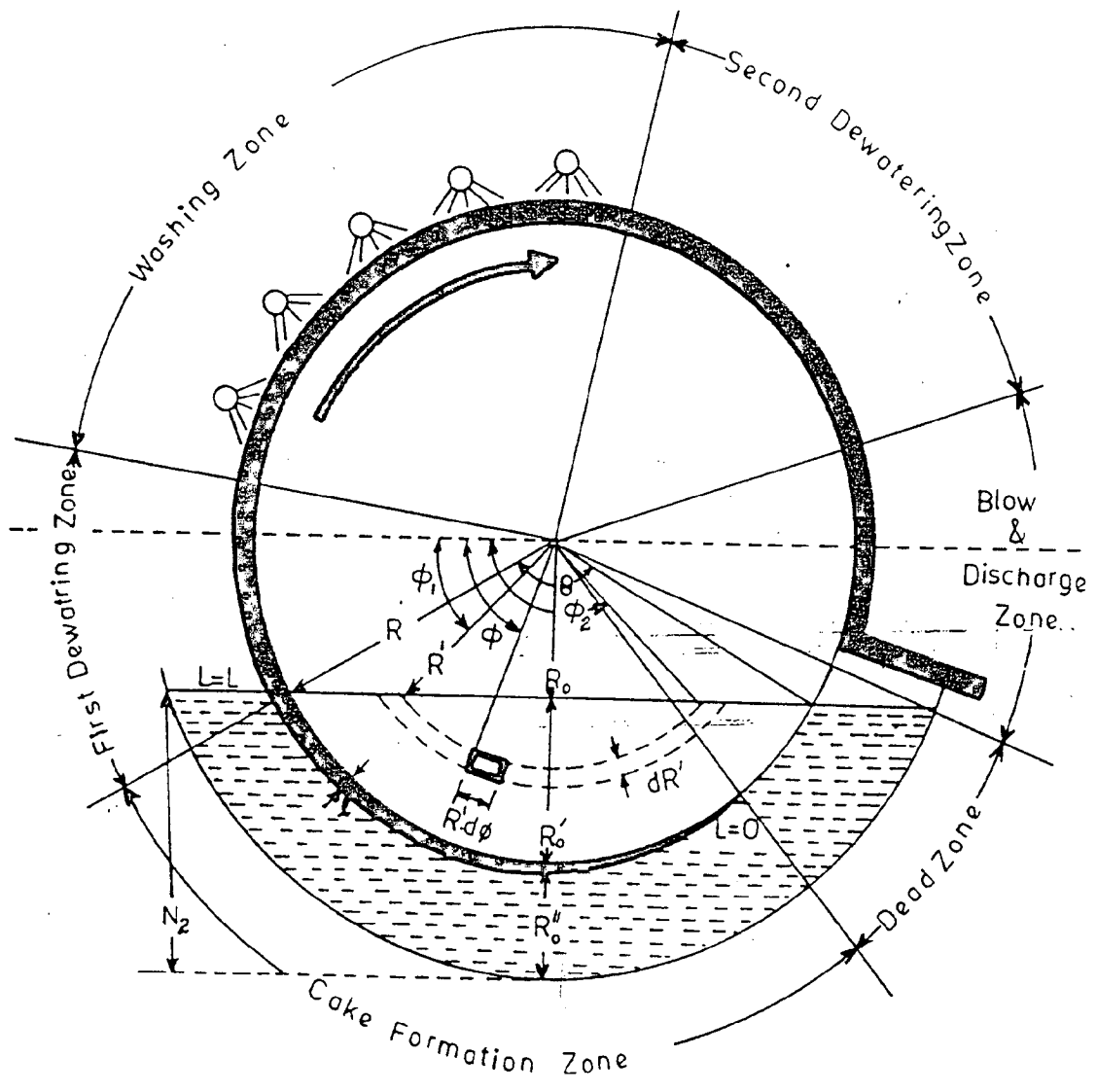


Fig. 1.3 Cross-Sectional View of a Rotary Vacuum Washer.

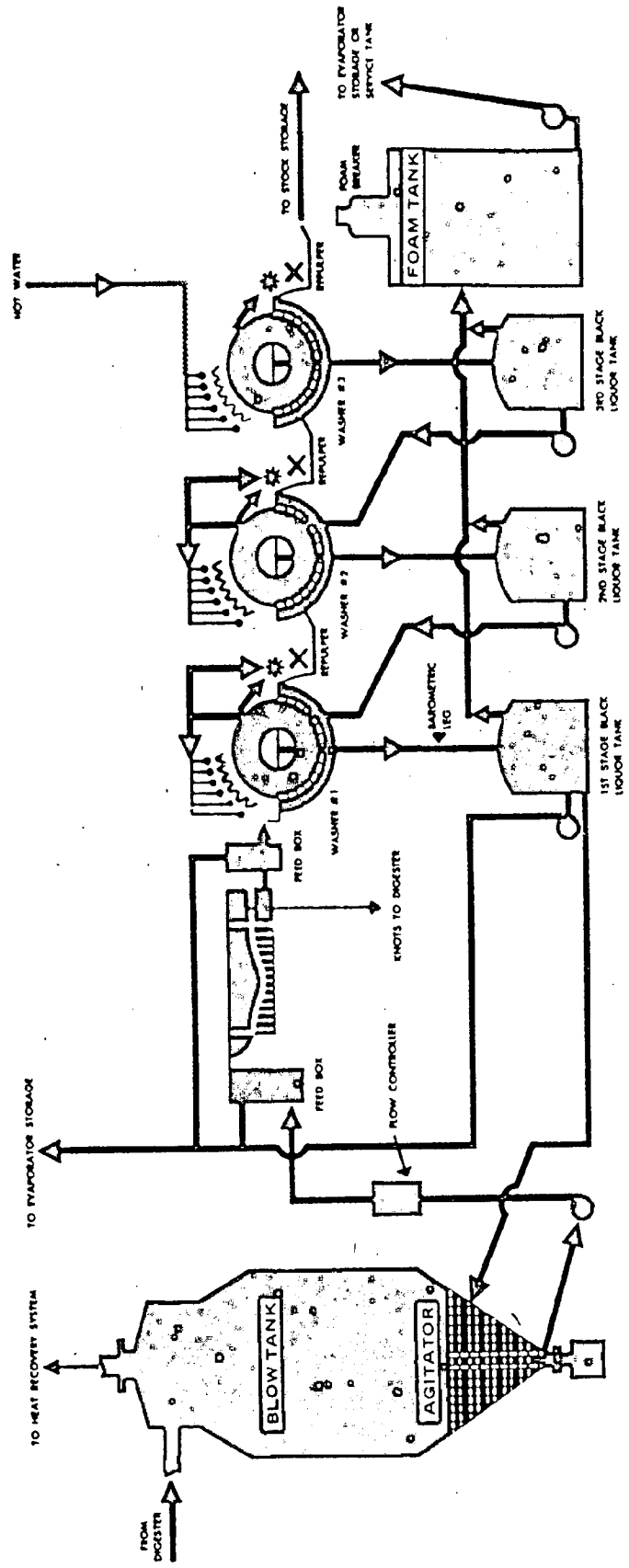


Fig. 1.4 A Battery of Three Rotary Vacuum Washers Connected in Counter Current Manner.

because of simultaneous flow of liquor and air. Hence it can be concluded that the conditions and mechanism involved in each zone varies significantly and a single model can't describe the entire system. Therefore individual models are required for each zone to assess the pulp washing behavior on a rotary vacuum washer.

The method of cake removal is however not a critical factor in the operation of each filter but the rate at which one or more of the first four operations can be carried out will critically affect the size of the filters. The above control can be achieved by suitably designing a realistic model of each operation. Pulp of approximately 1-2 % consistency is fed inside the vat. A layer of fibers is deposited on the outer surface of the filter (washer) due to vacuum inside the drum. This layer of fibers becomes progressively thicker and thicker till the end of cake formation zone. At the outlet of the cake formation zone the mat consistency is usually 10-16 %. On the upper part of the drum, a definite quantity of water/weak wash liquor is applied with the help of nozzles at a predetermined temperature (60-70 °C). Certain portion of the drum before and after the washing zone is left out under the influence of the driving force (vacuum) to assist in the removal of some residual black liquor trapped inside the fibers. As the mat is porous, the applied vacuum sucks black liquor as well as air in the first dewatering zone. In the second dewatering zone, the black liquor will be much more diluted compared to the former. Black liquor solutes, water and air collected through different zones are withdrawn with the help of pipes connected with the respective zones. Pressure differential (vacuum) is not applied after the second stage cake dewatering zone which causes the cake to lift up from the wire mesh. The cake is removed with the help of a doctor blade. In a counter current washing system cleanest wash water is applied only at the showers of the final washer for economic reasons. The black liquor from different zones is now accumulated in the seal tank of each filter stage. Effluent from any stage is used for two purposes: to dilute the pulp coming from the previous

and as shower liquor for previous washer. This effluent recycle is continued till the first stage of the washer train is reached in the direction opposite to the pulp flow in a similar manner.

Ideally, there should be no overflow of black liquor solutes with the washed pulp to the bleached plant and no overflow of fibers with the filtrate i.e. black liquor leaving from the washing plant for concentration in multiple effect evaporator. But these ideal stipulations can never be met in the industry.

Therefore the basic goal of brown stock washing is to remove maximum black liquor solids from the pulp by spraying of water or weak wash liquor as minimum as possible. More exclusively, the objective can be explained as follows:

- (a) To obtain clean pulp for further processing in bleaching, thereby to reduce the consumption of bleaching chemicals in bleach plant and to reduce the cost of effluent treatment.
- (b) To recover expensive inorganic Na-salts in recovery section.
- (c) To recover lignin based organic solutes for their heating values.
- (d) To forbid the sewerage of chemicals to maintain strict pollution regulations.

Black liquor consists of dissolved organic (lignin derivatives such as Thiolignin, Na-lignate etc.) and inorganic (Na, Mg, Ca and K ions) solids. As indicated, aqueous organic (primarily lignin), if not separated from the pulp stream before bleaching, consumes excess bleaching chemicals which generate more undesirable effluents such as AOX, colour, BOD, COD and other toxic and acute toxic compounds. Two of the acute pollutants are dioxins and chlorinated furans [36].

It may be pointed out that as a thumb rule 1 kg of COD consumes about 0.4 to 0.8 kg of active chlorine. The higher the Kappa number of the pulp entering in the bleach plant, more amount of COD is generated and as a result more chlorine per kg of COD has to be used to get more

of COD is generated and as a result more chlorine per kg of COD has to be used to get more bright pulp with less generation of pollutants. Accordingly less expenditure is to be incurred in effluent treatment plant. McCubbin [55] has estimated the cost of removing AOX of the order of \$ 84 / kg of AOX. [93,94].

For economic optimization soda loss vs. dilution water and the cost of various inputs are taken into consideration. The various parameters used for optimization are: excess water, dilution factor, displacement ratio, entrainment factor, Norden and modified Norden efficiency factor etc. In order to make the optimization feasible, it is necessary to describe the washing process by models in a realistic way and then carryout the simulation through the models.

Normal range of different parameters is given in Table (1.1).

Table (1.1): Normal range of different parameters

| Parameter | Unit | Value |
|--------------------------------|---------|-------------|
| Inlet vat consistency | % | 1 -2 |
| Outlet vat consistency | % | 10 -12 |
| Cake thickness | m | 0.015-0.040 |
| Dilution factor | kg / kg | 1-5 |
| Fractional submergence of drum | - | 0.25-0.45 |
| Liquor speed in cake pores | m / s | 0.003-0.026 |
| Pressure drop across the cake | Pascal | 20000-50000 |
| Pulp temperature | °C | 60-90 |
| rpm | - | 1-4 |

A variety of parameters is available to describe the performance of a rotary vacuum washer in steady state. These can be mainly divided into three categories namely, wash liquor usage (dilution factor, wash liquor ratio, weight liquor ratio), solute removal (wash yield, displacement ratio, solid reduction ratio) and efficiency parameters (soda loss, Norden's and modified Norden efficiency factor, % efficiency, equivalent displacement ratio). All these parameters are not used by all investigators and therefore equipment performance can not be compared in coherent manner from different investigations for steady state models.

In order to attempt a robust modeling, one has to quantitatively understand the mechanism of washing process / operation. This is discussed as under.

1.2.1 Mechanism of Washing

The washing methodology is based on the following operations,

- (a) displacement
- (b) dilution -agitation -extraction
- (c) dilution -displacement -extraction

The mechanism of pulp washing involves fluid mechanics superimposed by mass transport phenomena like diffusion. This is further complicated by dispersion, adsorption, desorption, foaming and channeling. Further, various studies [30,49,72,73] have shown that foam affects the brown stock performance to a significant extent. Out of the above the displacement washing is very important step which is accompanied by dilution and drainage. However displacement (extraction of liquor between the fibers by piston effect with another liquid) and diffusion (extraction of the liquor within the fibers by diffusion of the dissolved components towards an external liquid which is less concentrated) occur simultaneously. In actual situation these two operations overlap each other. In case of washing on rotary drums the major operation is the displacement and the entire process is affected by this step. Therefore, the

these two operations overlap each other. In case of washing on rotary drums the major operation is the displacement and the entire process is affected by this step. Therefore, the displacement of solute from the irregular channels of voids of the bed is associated with a diffusion like dispersion of the washing liquid in the direction of flow. If the fibers are porous, stagnant liquid that contains solute is present in the intra-fiber voids. Thus the solute must diffuse out of the porous fibers before it is dispersed by the flowing liquor. In case of an adsorbable solute, its adsorption and transfer from internal and external fiber surfaces to the liquid must be taken into account for model development.

In displacement washing of wood pulp, wash liquor is forced to flow through a pulp pad, displacing the liquor from it. Solute such as lignin or the inorganic chemicals used in pulping or bleaching, which are adsorbed and / or absorbed by the pulp fibers, are released into the wash water during this washing operation and are removed by displacement. The amount of solute that is thus leached from the fibers is negligible compared to the amount in the concentrated liquor being displaced during the initial stages of an industrial pulp washing operation. However, in the final stage of washing, where solute concentration in the liquor surrounding the pulp fibers have been reduced substantially, the contribution of the leached solute becomes very significant.

Lee [50], Hakamaki and Kosavin [30] and Poirier et. al.[77] have given contradictory conclusions about the effect of temperature on displacement washing. Lee [50] observed that displacement washing efficiency increased markedly when the temperature was in the 20-25 °C range and consistency was high enough. Hakamaki and Kosavin [30] found an increase in washer capacity with increasing temperature. Result in terms of washing efficiency is not found in their study. Poirier et.al.[77] observed that temperature has no significant effect on washing efficiency in the range 30-60 °C. Therefore it is to be studied whether there is any benefit of high temperature on displacement washing or not.

Poirier et. al.[79] in a later study observed that the effectiveness of displacement washing, either in the earlier or later stages, is not changed by variation of washing temperature over the range 60-90 °C.

Time allowed for diffusion of washable substance out of fibers is also an important factor.

During washing the speed at which the diffusion of black liquor solids inside the fiber voids and the surrounding liquor takes place is dependent on the concentration difference between black liquor solutes at the inside and at the outside of the fibers, temperature, turbulence around the fibers and coefficient of diffusion. The later in turn is dependent on molar volume or size, viscosity and molar mass. The larger the concentration difference, the higher the temperature and turbulence and the smaller the molecule size, the faster the diffusion will be and the quicker the equilibrium will be reached [91].

According to Lindsay [52] dispersion is a connective mixing process that arises because of velocity profiles in individual pores and because of the complex branching and intertwaving of flow paths in a porous medium.

To analyze the performance of washers in different plants or in a same plant using different pulping techniques, in a uniform and coherent manner, interrelations between various parameters are required. Some relations between various efficiency parameters are, however, already known. More broad base correlations are still essential to define the effect of one variable on the others.

In all commonly used industrial pulp washers, washing is achieved by dilution / extraction, by displacement or by a combination of these two principles. In dilution / extraction, the pulp slurry is diluted with weaker wash liquor and then thickened the slurry by filtering or pressing. This process is the oldest one and will not remove all solute even if it is repeated a very large

number of times or unless all the liquid is removed in the dewatering stage and adsorption is not there at all. These conditions can't be met in industry.

In displacement washing, ideally, the pulp is left clean if pure water is used but this is never achieved because of mixing of the wash water and liquor, slow diffusion of solutes from the fibers and sorption of solutes on the pulp fibers. Displacement washing can only be applied to pulps which are sufficiently permeable, such as most kraft pulps.

Displacement velocity, pulp pad thickness and consistency have been shown by various investigators to influence the displacement washing efficiency. Lee [50] found that increasing washing velocity has no effect on washing efficiency. Grahs [25] found that increasing washing velocity improves washing efficiency. Hakamaki & Kosavin [30] and Gren U.R. & Strom K.H.U.[28] found that increasing washing velocity lowers washing efficiency. Hakamaki & Kosavin [30] and Gren U.R. & Strom K.H.U.[28] observed higher consistency beneficial for displacement washing while Lee [50] observed it detrimental. Grahs [25] and Gren U.R. & Strom K.H.U.[28] observed that the increasing pad thickness is beneficial for displacement washing. This observation has not been contradicted by any investigator. Trinh et. al.[2nd paper] observed that the washing efficiencies are on average approximately 3 % higher for lignin than for sodium. The difference is due to the effect of desorbing sodium which increases the sodium breakthrough curve area relative to that of lignin (breakthrough curve area is proportional to the amount of solute removal).

On closer look of the expression, it is revealed that the amount of sodium removed before $W=1$ is slightly larger than that for lignin but the total area of the sodium breakthrough curve is much larger than that of lignin and $WE_{1,0}$ is thus lower for sodium than for lignin. The desorption of sodium from the pulp fibers is attributed to both decreasing pH and concentration of the surrounding fluid as the wash water passes through the pulp pad.

From the above it is evident that different investigators have put forward different views regarding parametric effects on washing equipment performance. To predict the washing efficiency of displacement washing as well as rotary vacuum brown stock washer there is enough room to further investigate these aspects in more comprehensive but coherent manner. In order to achieve the goal the following stepwise investigation are carried out.

1.3 Present Objectives

The present investigation deals with the following distinct stepwise investigations:

- (a) To develop mathematical models through equation of continuity for a single solute as well as multiple solutes present in black liquor like Na^+ based compounds and lignin based compounds, which are the usual diffusing components during brown stock washing operation in a pulp mill.
- (b) To include in the above models the relevant mathematical equations for adsorption-desorption isotherms, specially applicable for brown stock washing process.
- (c) To identify the expressions of parameters including overall porosity in the various phases of the system and to incorporate them in the models as developed in step-1.
- (d) To solve the system of simultaneous differential equations thus developed in step-1 by suitable Numerical Technique i.e. Finite Difference Method with various initial and boundary conditions pertinent to multi-stage Brown Stock Washers for the species as mentioned.
- (e) To validate the models through experimental data obtained from a similar system
- (f) To simulate the industrial system of BSW.

CHAPTER-2

LITERATURE REVIEW

2.1 Mathematical models for displacement washing and their analytical description

Modeling of pulp washing is done mainly using two approaches which are different in nature.

- (i) Process modeling.
- (ii) Physical modeling.

Most models adopted microscopic black box approach.

There are other approaches also. One of these is statistical modeling.

A complete review of the various models used to describe pulp washing has been presented by Pekkanen and Norden [70].

Process models are used by various investigators such as Perkins et.al.[74], Norden [], Baldus et.al.[4], Phillips et.al.[76], Luthi [53], Edward et.al.[15] and Tomiak [103] for design and optimization of pulp washers. Each stage in pulp washing is treated as black box. No attempt has been made to describe the processes occurring within them. Using material balances, process models express the efficiency of an individual washing stage in terms of some performance parameters such as Displacement Ratio [74], Norden Efficiency Factor [67], and Equivalent Displacement Ratio [53]. Although these models are useful for routine process design calculation, these provide little insight into how the design or operation of a washer might be altered to improve its efficiency.

Physical models are also used by various investigators such as Sherman [88], Pellett [71], Grahs[23], Kuo [42], Han [31], Perron and Lebeau [75] and Kukreja [40]. These models are used to describe the washing operation in terms of fundamental fluid flow and mass transfer principles occurring on microscopic level during displacement washing of a fibrous bed. These models involve parameters such as longitudinal dispersion coefficient and mass transfer coefficients. Physical models are used to know the factors which limit or control washing rate and efficiency and could thus provide the insight needed for the development of new and improved pulp washing systems.

Although physical models are used to provide a clear understanding of the physical phenomena, but the quantitative application is not adequate to analyze the real washing systems because the parameters, such as mass transfer coefficients, mass transfer area, dispersion coefficients and porosities, on which the models are based, have not been related properly to process variables such as pad thickness, consistency, superficial wash water velocity and temperature.

Of these few models, two given by Sherman [88] and Pellett [71] are based on packed beds of synthetic fibers and although they provide insight into the modeling of pulp washing, their results have no quantitative relevance to the washing of cellulose fibers. Another model, given by Grah [24], based on a packed bed of cellulose fibers, accounts for desorption as well as two mass transfer resistances in the fluid phase. However, the complexity of that model is inconsistent with the limited experimental data available for testing. Of the two mass transfer coefficients; one showed no trend with experimental conditions and the other was responsible to determine [24].

A simple model was recently developed by Poirier et. al.[79] to describe with a minimum number of parameters the information contained in experimental displacement washing breakthrough curves. The model does not account for the release of solutes from the pulp fibers

to the bulk fluid. This model could therefore be successfully applied to the experiments performed at high initial pad liquor concentration by Trinh et. al.[100] as the amount of solute released was insignificant compared to that in the concentrated (10,000 mg sodium / l; 25,000 mg lignin / l) initial pad liquor. However, model does not describe the breakthrough curves performed at low initial pad liquor concentration by Poirier et. al.[78], since the amount of solute released from the pulp fibers was large relative to the total amount initially in the pad. Therefore a model without a source term (concentration of solute in solid phase) is unable to describe the breakthrough curves for low initial pad liquor concentration experiments.

Among the various models proposed by various investigators [6,88,71,23,24,42,33,57,75,105,63,4,10,64,15] and also Fitch & Pitkin [c.f.75] and Fogelberg & Fugleberg [c.f.49] classification has also been made into two types based on mass transfer principles: Differential contact models (macroscopic) and the dispersion models (microscopic). These are solved either by numerical / analytical technique or by graphical methods. The dispersion models differ from investigators to investigators due to various assumptions chosen by them for model development. Adsorption of dissolved substance in the liquor on the fibers to a variable extent depending on the solute-fiber combination and the solute concentration effects are neglected in the model development by some investigators. Compressible nature of the fiber network also has distracted the building of a realistic model.

Brenner [6], Sherman [88], Pellett [71], Neretnieks [57], Grahs [24] and Rydin et al.[33] have considered the linear or non linear adsorption isotherm equation alongwith the dispersion-diffusion based models whereas Perron and Lebeau [75] developed without taking adsorption-desorption phenomena into consideration. Porosity values for displacable liquid (flowing liquid), non displacable liquor (stagnant layer) and pulp fibers are added complexities in the models of Grahs [24] and Perron et al [75]. Multistage washing system design through finite stage contact method for the estimation of number of stages and other operational parameters

solved by Norden et al.[64] by Matrix method is also available and is not discussed here. Baldus and Warnqvist [4] and Crotagino et al. [10] after discussing the various models indicated the suitability of the models from design point of view. However the role of displacement washing has not been elaborated. Fitch & Pitkin [c.f.75] correlated the mill data through material balance equations. Fogelberg and Fugleberg [c.f.49] have given emphasis on desorption equation. Statistical analysis of pulp washing on industrial rotary drum washers has been made by Norden, Pohjola and Sappanen [63]. Viljakainen [105] has considered models; one based on Kuo [42] and other on Lapidus and Amundson [48].

No due attention has been paid for the models on the displacement washing which is a coupling mechanism among dispersion, diffusion and adsorption.

A few mathematical models are cited below alongwith their development methods for only displacement washing.

(1) Model due to Edeskurty and Amundson (1950):

Edeskurty and Amundson [14] studied the effect of intraparticle diffusion in agitated static system. They quoted in their work that there is evidence according to Amis [c.f.14] that adsorption equilibrium attains always in a finite time although a period of years may be required. The investigators considered a spherical shell of inside radius r and thickness Δr . They equated inflow minus outflow by diffusion to the rate of accumulation in the shell and obtained the following equation.

$$(4 \pi r^2 D_v \alpha \frac{\partial c}{\partial r})_{r+\Delta r} - (4 \pi r^2 D_v \alpha \frac{\partial c}{\partial r})_r = (4 \pi r^2 \alpha \frac{\partial c}{\partial t})_{\bar{r}} \cdot \Delta r + (4 \pi r^2 \frac{\partial n}{\partial t})_{\bar{r}} \cdot \Delta r$$

where $r < \bar{r} < r + \Delta r$.

On letting $\Delta r \rightarrow 0$, the equation reduces to

$$D_v (\frac{\partial^2 c}{\partial r^2} + 2 / r \frac{\partial c}{\partial r}) = \frac{\partial c}{\partial t} + 1 / \alpha \frac{\partial n}{\partial t}.$$

If one assumes pointwise equilibrium inside the particles then the equilibrium attained is that of an adsorption isotherm

$$n = f(c)$$

$$\text{or, } \partial n / \partial t = f'(c) \partial c / \partial t.$$

For non-equilibrium, the adsorption equation considered is

$$l / \alpha \partial n / \partial t = k_1 c - k_2 n, \alpha \text{ being treated for convenience only.}$$

$$c(r,0) = C_i, \forall r.$$

$$c(0,t) = C_s, \forall t.$$

$$n(r,0) = n_i, \forall r.$$

The solution is obtained analytically with the help of Laplace Transform technique. Laplace Transform technique is used for solving linear partial differential equations.

The investigators obtained a formula to predict the change in the concentration of solute in the solution with time. An equation is also considered to relate the change in concentration of the solute in the solution with the rate at which adsorbate enters the adsorbent. The equation is merely a material balance over the adsorber made on the adsorbate.

In the paper quoted here the investigator investigated the problem and didn't report.

(2) Model due to Lapidus and Amundson (1952):

Lapidus and Amundson [48] assumed that a column of unit cross sectional area is packed with a finely divided adsorbent such as the interparticle volume is filled with solvent or solution. The column may have an initial adsorbate content on the adsorbent as well as in the interparticle volume. At time zero, a solution, whose concentration may vary with the time, is

admitted to the column. It is desired to know the concentration of the interparticle solution and the adsorbate content of the adsorbent at any time and at any position in the bed.

The model considered is

$$D \frac{\partial^2 c}{\partial z^2} = u \frac{\partial c}{\partial z} + \frac{\partial c}{\partial t} + \frac{1}{\alpha} \frac{\partial n}{\partial t},$$

where D is diffusion coefficient of the adsorbate in the solution in the bed. α is fractional void volume in the bed.

Two adsorption-desorption equations are considered:

$$(i) \quad n = k_1 c + k_2$$

$$(i) \quad \frac{\partial n}{\partial t} = k_1 c + k_2 n$$

Equation (i) implies that equilibrium is established at each point in the bed while eqn. (ii) assumes that the rate of adsorption is finite.

The solution is obtained analytically with the help of Laplace Transform technique.

The investigators plotted the effect of longitudinal diffusion for an infinite column in which equilibrium is established locally. Initial adsorbate concentration was assumed to be zero.

(3) Model due to Kuo (1960):

Kuo [42] derived differential equations for a filter cake wash cycle. The derivation is based on the assumption that the wash liquor executes plug flow in the pores of the cake, with continuous mass transfer between the liquor and a boundary film of filtrate. The appropriate differential equation turns out to be a simple form of those studied by Goldstein [21].

Differential equations for the wash liquor due to Kuo is

$$\frac{\partial c}{\partial t} = k_1 (n - c) - u \frac{\partial c}{\partial z}, \quad 0 < z < L, \quad t > z / u$$

and for the stagnant layer is

$$\frac{\partial n}{\partial t} = k_2 (c - n), \quad 0 < z < L, \quad t > z / u.$$

Associated inlet condition on the solute concentration in the wash liquor is

$$c(0,t) = C_s, \quad t > 0.$$

Also an initial condition on the solute concentration in the stagnant layer is

$$n(z,t) = n_i, \quad 0 < z < L, \quad t > 0.$$

n_i is initial concentration of solute in stagnant film.

The estimates of the various parameters was done on analyzing the data from the experiments performed in a mill on a system of calcium carbonate cake containing an ammonium chloride solution and washed with water.

The investigators plotted the dimensionless concentration of solute in wash liquor and in filtrate film against dimensionless time at various bed depths. He also plotted the solute concentration in exit wash liquor against time.

(4) Model due to Brenner (1962):

Brenner [6] gave a diffusion model of longitudinal mixing in beds of finite length. He considered a reasonably well established fact that the extent of mixing between solvent and solute “phases” can be characterized by a diffusion type equation in which an axial dispersion coefficient appears in place of usual molecular / volumetric diffusivity. The equation considered is

$$\frac{\partial c}{\partial t} + u \frac{\partial c}{\partial z} = D_L \frac{\partial^2 c}{\partial z^2}.$$

The boundary conditions considered are:

At the inlet to the bed i.e. at $z = 0$,

$$u c - D_L \frac{\partial^2 c}{\partial z^2} = u C_s, \quad t > 0.$$

At bed exit,

$$\frac{\partial c}{\partial z} = 0, \quad \text{at } z = L, t > 0.$$

The initial concentration is

$$c(z,0) = C_i.$$

Results are given in dimensional form for (i) the instantaneous concentration of solute leaving the bed and (ii) the average solute concentration in the bed at any instant. Various limiting cases are discussed.

The model is solved analytically using Laplace Transform technique.

The investigators plotted semi-logarithmic plots of dimensionless exit solute concentration in wash liquor and dimensionless average solute concentration in bed vs. dimensionless time T and found that the graph asymptotically approach a straight line for sufficiently large T . The smaller the Peclet number, the more rapid is the asymptotic approach.

Numerical calculations of the Dimensionless exit and average solute concentrations were carried out for a large number of Peclet numbers and dimensionless time. The results are tabulated to a fixed number of significant figures rather than to a fixed number of decimal places. The entries in tables are correct to three significant figures and in most instances to four significant figures, as quoted by the investigator himself.

The investigator also quoted that wherever infinite summation was required, only twelve terms were used as per the availability. Values for the exponentials and complimentary error functions required in the modified asymptotic solution were done on a desk calculator.

(5) Model due to Sherman (1964):

Sherman [88] treated the problem of the washing of packed beds of porous viscose fibers saturated with diacetyl solution. He used an equation originally proposed by Lapidus and Amundson [48] which included parameters to account for longitudinal dispersion in the packed bed and the absorption of diacetyl solution by porous viscose fibers. He assumed the liquid solid concentration inside the fibers and surrounding the fibers to be identical at any time and at any position within the bed, implying that diffusion, both within the fiber and between the fiber and the surrounding fluid is sufficiently rapid which does not affect the rate of the overall transport process.

Sherman used a diffusion like differential equation

$$D_L \frac{\partial^2 c}{\partial z^2} - u \frac{\partial c}{\partial z} = \frac{\partial c}{\partial t} + (1-\epsilon) / \epsilon \frac{\partial n}{\partial t}.$$

The equation connecting n and c as $n = K c$ was used which gives $\frac{\partial n}{\partial t} = K \frac{\partial c}{\partial t}$.

Substituting this in transport equation, we get

$$D_L \frac{\partial^2 c}{\partial z^2} - u \frac{\partial c}{\partial z} = 1 / \lambda \frac{\partial c}{\partial t},$$

where $\lambda = 1 / (1 - K + K / \epsilon)$.

The initial condition used is

$$c(z,0) = C_i \quad z > 0$$

and the boundary condition used is

$$c(0,t) = f(t) = C_i (k_0 + k_1 t + k_2 t^2 + k_3 t^3 + k_4 t^4) \cdot \exp(-\gamma t), \quad t > 0.$$

This equation is an empirical representation of the concentration at $z = 0$, as a function of time, in which the constants k_0 , k_1 , k_2 , k_3 , and k_4 are adjusted so that the equation agrees with the experimentally determined curve of c vs. t .

In the case of the glass bead and the dacron fibers, no sorption of diacetyl occurred; thus n was zero and λ was 1. In the case of the viscose fibers, however, sorption of diacetyl did occur; thus n was not equal to zero. If equilibrium exists between the fiber and the surrounding solution (very rapid diffusion within the fiber) and the only solute in the fiber is contained in the solution absorbed by the swollen fiber, one may write

$$n = \varepsilon_f c.$$

Thus $\lambda = 1 / (1 - \varepsilon_f + \varepsilon_f / \varepsilon)$, ε_f being porosity of fiber while ε was bed porosity.

The purpose of this investigation was to study the movement of a solute in a bed of packed solids, during the washing process, with particular emphasis on fibrous systems. Since it was deemed impractical to form thick beds of fibrous media, this study was limited to thin beds of packed solids (glass beads, dacron fibers and viscose fibers). The glass bead system was primarily used to checkout the experimental system and verify the mathematical model. The dacron fiber system was investigated in order to indicate the important variables in a non-porous fiber system and to show the differences between a fiber system and a granular system. The viscose fiber system was investigated in order to indicate importance of the movement of solute within the fibers.

The mixing parameter D_L / u was found to be a constant for all runs on any single bed regardless of the particles used to pack the bed. The value of D_L / u (0.233 cm) for the 3 mm glass bead bed is in general agreement with that determined in other investigations.

The same basic mechanism of fluid particle dispersion applies to beds of fibrous media as that which applies to beds of granular media; however the physical differences in the two types of systems cause the mixing parameter D_L / u to behave differently in the two systems.

The differences in geometry, that is in average pore size and in pore size distribution, between a bed of fibrous media and a bed of granular media of the same particle diameter is believed to account for the fact that D_L / u for the Dacron fiber beds was about sixty times as great (ratio of 100, 60 and 30 were obtained for the three beds) as it would be for a bed of granular media of the same diameter.

In beds of granular media of uniform size particles, where geometrical similarity exists, the mixing parameter D_L / u is generally proportional to the particle diameter. In this study the fiber diameter was changed by a factor of 8 without a noticeable change in D_L / u . On the other hand, the three Dacron fiber beds, with a fixed particle diameter, had widely different values of D_L / u . Although the porosity was different for each of these beds, it is believed that the observed difference in D_L / u was probably due to a difference in packing or formation, of the beds rather than the difference in porosity. Thus, it appears that a single parameter, such as particle diameter, does not define a bed of fibrous media since geometric similarity is not necessarily maintained from bed to bed.

The theoretical equation for the washing of the viscose fiber beds was written with equilibrium assumed between the fibers and the surrounding solution. The assumption of equilibrium was found to be satisfactory over the range of flow rates investigated for the 1-denier fibers (16- μ diameter). For the 64-denier (120- μ) fibers, the assumption of equilibrium was satisfactory at low flow rates; however at higher flow rates this assumption was not satisfactory. In this case the experimental curve exhibited an appreciable tail due to the relatively slow intrafiber diffusion of the solute.

(6) Model due to Pellett (1966):

Pellett [71] extended Sherman's model by accounting for intra-fiber diffusion of a solute linearly adsorbed to the viscose fibers, as well as for fiber to liquid phase mass transfer resistance. Pellet proposed a mathematical model for breakthrough curves that incorporates longitudinal dispersion, intrafiber diffusion of a solute that is linearly adsorbed and a finite liquid phase mass transfer resistance. Caution is advised in applying the model to systems where particle geometry and solute-particle diffusion and adsorption are non-ideal or where ionic solutes are employed.

Pellett considered that if a porous medium of void fraction ϵ consists of solids that have a finite capacity Q for solute, the differential equation that describes the longitudinal dispersion of a fluid containing a dynamically neutral solute of concentration c is

$$D_L \frac{\partial^2 c}{\partial z^2} - u \frac{\partial c}{\partial z} = \frac{\partial c}{\partial t} + (1-\epsilon) / \epsilon \frac{\partial Q}{\partial t}.$$

Initial condition is

$$c(z,0) = C_i, \quad z \geq 0.$$

Boundary condition is at bed inlet is

$$c(0,t) = C_i (k_0 + k_1 t + k_2 t^2 + k_3 t^3 + \dots). \exp(-\gamma t).$$

This is the modified step-function input. The accumulation capacity of the particles is due to adsorption and hence this must be expressed in terms of adsorption isotherm equation.

Analytic solution of the no-sorption case, gives $\frac{\partial Q}{\partial t} = 0$ and with the equilibrium case $\frac{\partial Q}{\partial t} = K \frac{\partial c}{\partial t}$.

If the intraparticle diffusion is not described by the equilibrium case, $\partial Q/\partial t$ must be obtained from the appropriate diffusion equation (Fick's law) and boundary conditions. Using fiber as long circular cylinder system the radial movement of solute can be depicted as:

$$D_F [\partial^2 A/\partial r^2 + 1/r \partial A/\partial r] = \partial A/\partial t, \quad \dots(1)$$

where A, the local solute concentration includes the solute that is adsorbed on solid surface with the fiber and is contained by solution within intrafiber pores. D_F is interfiber diffusion coefficient (cm^2/sec). As the intraparticle pore network is a swollen solid (neglecting true surface and solid phase diffusion effects) the transport of solute within a fiber should be described by diffusion in solution phase only. If the driving force for diffusion is intraparticle concentration gradient $\partial P/\partial r$, P being local intrapore solution concentration (mg / ml) in a swollen fiber at r, the above equation can be written as:

$$D_F' [\partial^2 P/\partial r^2 + 1/r \partial P/\partial r] = \partial P/\partial t + 1/\epsilon' \partial S'/\partial t.$$

Where D_F' is the intrapore diffusion coefficient, $\partial S'/\partial t$ is the rate of exchange of solute between local adsorption sites and adjacent solution in the pores of the fiber and ϵ' is the internal porosity of the swollen fiber. Now the local solute concentration in a swollen fiber can be expressed as $A = \epsilon' P + S'$. Assuming the existence of local equilibrium in the intrafiber pores in the form of a linear adsorption equilibrium as $A = K P$ and $S' = (K - \epsilon') P$, differentiating it to obtain dS'/dt and substituting in the above equation, the following differential equation for intrafiber diffusion is obtained.

$$D_F' [\partial^2 P/\partial r^2 + 1/r \partial P/\partial r] = K/\epsilon' \partial P/\partial t, \quad \dots(2)$$

where $D_F = D_F' \epsilon'/K$

If A/K is substituted for P, equation (2) becomes identical with equation (1).

The differential equation for intraparticle diffusion may be rewritten as:

$$D_F [\partial^2 P / \partial r^2 + \alpha / r \partial P / \partial r] = \partial P / \partial t$$

where α , the shape factor is 1 for long circular cylindrical fibers and 2 for spherical fibers. The necessary initial and boundary conditions are as follows:

$$\text{I.C.: } P = C_i, \quad 0 \leq r \leq a, \quad t = 0.$$

$$\text{B.C.: } P = c(z, t), \quad t > 0.$$

The investigator calculated that the longitudinal dispersion had a highly significant effect in the smoothing or diffusion like destruction of concentration fronts during laminar flow through fiber beds. The extend of the longitudinal dispersion effect as measured by D_L / u was shown to be approximately proportional to fiber diameter and average bed porosity and a strongly increasing function of the fiber length-to-diameter ratio l / d . He also observed that it is likely that the observed liquid phase mass transfer resistances were due primarily to radial molecular diffusion in interfiber pores, rather than to axial molecular diffusion which would become important at somewhat lower fluid velocities.

The studies of Sherman [88] and Pellett [71] provide insight into the modeling of washing of pulp fiber beds. However, unlike pulp fibers, viscose fibers are uniform cylinders with simple, linearly adsorbed non-ionic solutes. The results of these two studies thus have no quantitative relevance to the washing of geometrically complex pulp fibers with non-linearly adsorbed ionic solutes.

(7) Model due to Grah (1975):

A more complex model of displacement washing of pulp fiber beds was developed by Grah [23]. He accounted for the mass transfer rates between three separate zones in the packed bed of cellulose fibers: a zone of flowing liquor, a zone of stagnant liquor and the fibers. The amount of adsorbed sodium on the pulp fibers was described by a non-linear Langmuir type

adsorption isotherm which was determined experimentally, as well as the total bed porosity and the fiber consistency profile throughout the bed.

The model considered by Graessle is

$$\varepsilon_d(z) \frac{\partial c}{\partial t} + \varepsilon_s(z) \frac{\partial c_{st}}{\partial t} + C_F(z) \frac{\partial n}{\partial t} = \varepsilon_d(z) D_L(z) \frac{\partial^2 c}{\partial z^2} - \varepsilon_d(z) u(z) \frac{\partial c}{\partial z}$$

It is assumed that D_L is directly proportional to the interstitial velocity u , which implies that

$$D_L \varepsilon_d = \text{constant.}$$

For the stagnant liquor the following equation applies:

$$\varepsilon_s(z) \frac{\partial c_{st}}{\partial t} = k_1 (c - c_{st}) - C_F(z) \frac{\partial n}{\partial t}$$

and for the fibers:

$$C_F(z) \frac{\partial n}{\partial t} = k_2 (c_{st} - c_{st}^*)$$

where $w = \text{func}(c_{st}^*)$

For instance, the non-linear Langmuir isotherm of the following type has been described:

$w = A c_{st}^* / (1 + B c_{st}^*)$, A and B being constants and c_{st}^* being concentration in zone of stagnant liquor at equilibrium.

The boundary conditions and initial conditions are

$$u C_m = u c - D_L \frac{\partial c}{\partial z}, \quad z = 0+, \quad \forall t;$$

$$\frac{\partial c}{\partial z} = 0, \quad z = L-, \quad \forall t;$$

$$c = c_{st} = c_{st}^* = C_i, \quad \forall z, \quad t = 0$$

$$\text{and } n = n_i, \quad \forall z, \quad t = 0.$$

The model was solved numerically using a double collocation method.

From model parameters, the fractional bed volume occupied by flowing liquor, the axial dispersion coefficient and two mass transfer coefficients were then adjusted until the calculated breakthrough curve for the bed exit concentration satisfactorily fitted the experimentally obtained breakthrough curve.

The investigator found that the dispersion coefficient D_L increased when the rate of flow of liquor through the bed was increased. The mean value of the porosity in the zone of flowing liquor, ε_{dm} was increasing too when the liquor flow rate was increased. That means that a larger part of the bed volume was used for liquor in motion when the flow rate was increased.

The experiments were performed at low solute concentration and carried out on packed beds at a temperature of 50°C using a laboratory displacement cell. The sodium and lignin contents in the outlet stream were determined. An isotherm for the adsorption of sodium ions on the pulp has been obtained. The adsorption of lignin on the pulp was considered negligible.

The results of Grah showed great differences between the washing of sodium and of lignin. The mass transport between flowing and stagnant liquors was found to be much larger for sodium than for lignin. Sodium was found to have a longer residence time in the bed than lignin, probably due to the larger size of the lignin molecules.

The dispersion was found to be almost equal for the two substances.

It was also observed by the investigator that lignin is the easiest to wash out. The difference between lignin and sodium in this respect is by the difference in their adsorption onto the pulp and their different mass transport times. Very little information with respect to the effect of the experimental conditions on the model parameters was obtained. No intrafiber diffusional resistance was included in the model, although the diffusivity is smaller within the fiber than in

the stagnant film. One of the two mass transfer coefficients showed no trends with the experimental conditions and the other could not be determined.

As the complexity of this model would have required a more extensive experimental program for an adequate experimental test, the results serve no practical purpose from a predictive standpoint.

(8) Model due to Perron and Lebeau (1977):

Perron and Lebeau [75] presented static models of washers after a theoretical analysis of the different phenomena taking place on a drum of a rotary drum washer, then dynamic models are reported. A mathematical expression has been formulated for cake length and filtrate flow rate through cake formation zone using Darcy's law by assuming constant pressure drop, negligible hydrostatic pressure and non compressibility of cake. Permeability is calculated using modified Kozeny model. The diffusion of the solute within the fibers towards the washing liquor is described by a differential equation which is solved assuming that the mass transfer rate through the stagnant film is finite.

The model is

$$u \epsilon_d \frac{\partial c}{\partial z} + \epsilon_d \frac{\partial c}{\partial t} + \epsilon_s \frac{\partial n}{\partial t} = 0.$$

For stagnant film

$$\frac{\partial n}{\partial t} = -k(n - c).$$

Initial and Boundary conditions are

$$c(0,t) = C_s, \quad t > 0$$

$$c(z,t) = C_i, \quad t < L/u$$

$$n(z,t) = C_i, \quad t < z/u \quad (t < z/u \text{ corresponds to the displacement phase}).$$

The model has been solved analytically using Laplace Transform technique.

The solution is in terms of zero order Bessel's function with imaginary arguments. Models are simulated by taking data from industry. Mathematical expressions for mean concentration of solute in filtrate, pulp level inside the vat, concentration of solute in cake pores after washing, filtrate flow rate through dewatering zone and fiber production rate are also given. Graphs depicting the effects of different variables are also drawn.

(9) Model due to Rasmuson and Neretnieks (1980):

Rasmuson and Neretnieks [82] considered the following model for exact solution for diffusion in particles and longitudinal dispersion in packed beds.

$$\partial c / \partial t + u \partial c / \partial z - D_L \partial^2 c / \partial z^2 = - (1 - \epsilon) / \epsilon \partial \bar{n} / \partial t;$$

$$\partial n_i / \partial t = D_v (\partial^2 n_i / \partial r^2 + 2 / r \partial n_i / \partial r).$$

\bar{n} is volume averaged concentration in particles. (mol / m³)

n_i is internal concentration in particles. (mol / m³)

r is radial distance from center of spherical particle. (m)

Boundary conditions considered are:

$$c(0,t) = C_s;$$

$$c(\infty,t) = 0;$$

$$c(z,t) = 0;$$

$$n_i(r,z,t) \neq \infty, \quad r = 0;$$

$$\partial \bar{n} / \partial t = 3 k / b (c - n_i(b,z,t) / K);$$

$n_i(r,z,0) = 0$.

k is the mass transfer coefficient. (m / s)

K is the volume equilibrium constant. (m^3 / m^3)

b is the particle radius. (m)

The above investigators solved the model analytically using Laplace Transform technique.

The investigators found the solution of Babcock et.al.[c.f.82] to be in error for $D_L > 0$. They showed that Babcock's solution is actually a limiting solution for low values of D_L . For $D_L = 0$, the solution is identical to that given by Rosen [84]. Rosen's solution for $D_L = 0$ is obtained by letting $Pe \rightarrow \infty$. In the solution procedure the investigators arrived at a stage where numerical integration had to be performed because of complicated nature of the integral expression for $u(z,t)$. The integrand is the product of an exponential decaying function and a periodic sine function. The total function is thus a decaying sine wave, in which both the period of oscillation and the degree of decay are functions of the system parameters. Due to the very rapid oscillation of the integrand for certain parameter values, a straightforward integration method may fail. In some instances, the magnitude of the integrand is not negligible, even after a thousand oscillations of the wave.

Furthermore, with ordinary integration methods, one must choose a step size which is small with respect to the wave length. A special integration method was therefore developed, where the oscillatory behavior of the integrand is utilized. The integration is performed over each half-period of the sine wave, respectively. The convergence of the alternating series obtained is then accelerated by repeated averaging of the partial sums. The solution was checked against the analytical solution of Lapidus and Amundson [48] for the case of negligible external and internal diffusion resistance. The agreement was excellent.

(10) Model due to Gren and Strom (1985, September):

Gren and Strom [28] performed experiments with packed beds of mixed pine / spruce sulphate pulps (Kappa number 32). The influence of some fundamental variables of the displacement washing operations on softwood kraft pulps has been studied. The effectiveness, expressed as the displacement or wash ratio was determined for varying conditions (e.g. varying bed length, bed porosity, flow rate) as a function of the relative wash liquor volume.

In this study the investigators made the concentration dimensionless by assuming

$$C = (c - C_s) / (c - C_i) \text{ and } T = t V^* / BV \varepsilon_t$$

V^* being the volume flow rate and BV , the volume of the bed.

The amount of the substance washed out of the bed at the time T is

$$WO(T) = (C_i - C_s) BV \varepsilon_t \int_0^T (C_u - C_{in}) dT;$$

$$C_u = C(L, T) \text{ and } C_{in} = C(0, T).$$

The investigators concluded from their experiments that the wash ratio

- increases with increasing bed length.
- is relatively independent of fluid velocity, decreasing slightly for higher flow rates.
- increases very slightly with porosity.

It was also found that pine sulphate pulp renders a slightly higher wash ratio than spruce sulphate pulp, if they have similar kappa number but with decreasing difference at lower flow rates and longer beds. The experimental data obtained in this method can be a basis for the design of efficient washing equipments and can be used in the study of the fundamental mechanism of displacement washing.

(11) Model due to Viljakainen (1985, October):

Viljakainen [105] used the following dispersion model for pulp washing.

$$D_L \frac{\partial^2 c}{\partial z^2} - u \frac{\partial c}{\partial z} = \frac{\partial c}{\partial t} + (1 - \epsilon_t) / \epsilon_t \frac{\partial n}{\partial t}.$$

He solved this equation for the equilibrium isotherm $n = c$.

The investigator showed how to carry out the mass balance calculations for different mass transfer models and washing system flowsheets. The calculation method is kept as simple as possible by the use of Norden's efficiency factor and dimensionless mass transfer parameters. The effect of choosing different mass transfer models and mass transfer parameters on the washer efficiency is shown. The investigator observed that there is only a slight difference in the washer efficiency obtained between the differential contact model and the dispersion model. In practice this means that the dimensionless concentration in the filter cake after washing is numerically a similar function of the wash liquor ratio in the two models.

The effect of the wash liquor ratio, the mass transfer model and mass transfer parameters on the washer efficiency is shown.

(12) Model due to Wong and Reeve (1990, February):

Wong and Reeve [107] carried out experiments on nylon and various modified pulp fibers using Potassium Chloride. They studied the unsteady state diffusion in fiber beds using following equation.

$$D_L \frac{\partial^2 c}{\partial z^2} = \frac{\partial c}{\partial t}.$$

The investigators observed that in fiber suspension, the effective diffusivity decreases linearly with increasing fiber volume fraction, where this fraction represents the total volume of fibers and encumbered water. They also observed that fiber volume fraction can be estimated by the

water retention value or hydrodynamic specific volume and hence the effective diffusivity of a solute in any bed of fibers can be calculated.

(13) Model due to Teruo Takahashi, Takashi Korenaga and Fenguha Sen (1990, April):

Fenguha Sen et.al.[18] studied fully developed steady laminar flow in a straight tube of circular cross section. They assumed that if molecular diffusion coefficient is assumed to be constant, the local concentration c of a solute as a function of axial distance z , radial distance r and time t is described by the convective diffusion equation

$$\frac{\partial c}{\partial t} = D_v \left(\frac{\partial^2 c}{\partial r^2} + \frac{1}{r} \frac{\partial c}{\partial r} + \frac{\partial^2 c}{\partial z^2} \right) - u_0 \left(1 - \frac{r^2}{R^2} \right) \frac{\partial c}{\partial z},$$

where u_0 is the velocity at the center of the tube, R is the radius of the tube and D_v is the molecular diffusion coefficient.

The boundary condition is

$$\frac{\partial c(z,0,t)}{\partial r} = \frac{\partial c(z,R,t)}{\partial r} = 0.$$

The initial condition is

$$c(z,r,0) = C_i, \text{ the initial concentration.}$$

In dimensionless form, the above equation can be written as

$$\frac{\partial C}{\partial T} = \frac{\partial^2 C}{\partial y^2} + \frac{1}{y} \frac{\partial C}{\partial y} + \frac{\partial^2 C}{\partial Z^2} - Pe \left(1 - y^2 \right) \frac{\partial C}{\partial Z}.$$

Boundary conditions are

$$\frac{\partial C(Z,0,T)}{\partial y} = \frac{\partial C(Z,1,T)}{\partial y} = 0.$$

Initial condition is

$$C(Z,y,0) = 1.$$

Here $C = c / C_i$, $Pe = R u_0 / D_v$, $Z = z / R$, $y = r / R$, $T = D_v t / R^2$.

First of all the investigators applied the analytical method of separation of variables to convert an equation into another equation and then applied finite difference method to solve this converted equation numerically.

The investigator developed an improved numerical method based on Bailey and Gogarty [c.f.18] work to solve the dispersion problem in laminar flow through a circular tube. The numerical solution can give very accurate results at least for $T < 0.7$ and arbitrary Peclet numbers. It can be used as a complementary solution to the Taylor-Aries and Gill solution. The numerical solution involves less computation compared with Yu's [c.f.18] solution and with other numerical methods. It also has a distinct physical significance and is easily understood.

(14) Model due to Farooq and Ruthven (1991, February):

Farooq and Ruthven [17] required a model for a three component system, in which two components are adsorbable and the third component (He) is inert. They considered an isothermal, dispersed plug flow system, in which frictional pressure drop in the bed is negligible. The equilibrium relationships are represented by the ternary Langmuir isotherm and the mass transfer rates are given by linear driving force (LDF) rate expressions. The model is as follows:

Mass balance:

$$D_L \partial^2 c_i / \partial z^2 + \partial(u c_i) / \partial z + \partial c_i / \partial t + (1-\varepsilon) / \varepsilon \partial n_i / \partial t = 0.$$

Continuity condition:

$$\sum C_i = C \text{ (constant), } i = 1, 2, 3 \text{ for three components.}$$

Overall balance:

$$C \frac{\partial u}{\partial z} + (1-\epsilon)/\epsilon \sum \frac{\partial n_i}{\partial t} = 0.$$

Mass transfer rates:

$$\frac{\partial n_i}{\partial t} = k_i (n_i^* - n_i). \text{ Here } * \text{ is used for equilibrium with } c.$$

Adsorption equilibrium:

$$n_i^* / n_{is} = b_i c_i / (1 + \sum b_i c_i).$$

Boundary condition:

$$D_L (\frac{\partial c_i}{\partial z})_{z=0} = -u_0 ((c_i)_{z=0-} - (c_i)_{z=0+}), u_0 \text{ is interstitial velocity at bed inlet.}$$

The model was solved numerically by the method of Orthogonal Collocation.

In an equilibrium-controlled system, the phenomenon of “roll-up” is commonly observed in the concentration profiles (or breakthrough curves) whenever the equilibrium relationship is of favorable form. Under these circumstances, the more strongly adsorbed (and therefore slower travelling) species, leading to a rise in the effluent concentration of the less strongly adsorbed species above the inlet value. Roll-up is not observed for the heaviest component, although, in a multicomponent system, it is commonly observed for all the lighter species in sequence.

The investigators observed that the roll-up of the faster component also originates from the difference in sorption kinetics, but for a given L / u ratio the extent of roll-up will depend on the equilibrium selectivity.

(15) Model due to Lai and Tan (1991, March):

Lai and Tan [45] developed approximate models for nonlinear adsorption in a packed bed adsorber. Model given by them is

$$\partial c_s / \partial T = 10 B_i (C_B - C_s) / (dQ/dc)_{C_s} - (35 (Q_s - \bar{Q}) + (d^2Q/dc^2)_{C_s} (B_i (C_B - C_s))^2) / ((dQ/dc)_{C_s})^2 \text{ and}$$

$$\partial \bar{Q} / \partial T = 3 B_i (C_B - C_s).$$

Here C_s is the dimensionless surface concentration, C_B is the concentration in the bulk phase, C is the dimensionless concentration in the void fraction of an adsorbent particle, B_i is the Boit number ($k_f R / De$), k_f is the interphase mass transfer coefficient (m / s), R is the radius of adsorbent particle (m), De is the effective diffusivity (m^2 / s), Q is the dimensionless sum of the adsorbates in void fraction and adsorbate phase, \bar{Q} is the dimensionless averaged sum of adsorbates, Q_s is the dimensionless sum of adsorbates on the surphase of an adsorbent particle, t is the time and T is the dimensionless time ($t De / R^2$).

The numerical solution of the model was obtained numerically by applying the Orthogonal Collocation method to the radial direction x and the cross integral scheme and the modified Adam predictor-corrector method to both the Z and θ directions.

The numerical solution to the pore-diffusion model and the proposed approximate models based on parabolic profile assumption and quartic profile assumption are shown in figures.

To quantitatively justify the validity of the approximate models, the relative error, E_R is defined and it was indicated that E_R increases with increase in the degree of non-linearity. It was noticed that for a linear isotherm, all the approximate models behave similarly to the pore-diffusion model. Further, it was also indicated that the quartic profile assumption provided more accurate prediction than did the parabolic profile assumption and the linear deriving force (LDF) model specially at beginning times.

(16) Model due to Sun and Levan (1994):

Sun and Levan [95] considered one dimensional unsteady diffusion in a spherical particle which is described by the following dimensionless equation:

$$\partial C/\partial T = 2 / Z \partial C/\partial Z + \partial^2 C/\partial Z^2.$$

Boundary conditions are

$$\partial C/\partial Z = 0, Z = 0, \forall T \text{ and } C(1, T) = C_{st}(T).$$

In this model Z is the normalized radial coordinate, C_{st} is the dimensionless surface concentration.

The problem has been solved numerically using finite difference technique.

The investigators further confirmed that the efficiency of the finite difference method can be improved if the grid density in the particle is better distributed. The iso-volumetric discretization, which gives a constant grid density per unit volume in the particle, has been found to be significantly more accurate than the usually used equal-spacing discretization.

The investigators considered the simple case of single component diffusion with a constant diffusion coefficient and found that the iso-volumetric discretization performs better than the equal-spacing discretization in more complicated problems as well.

(17) Model due to Westerterp, Dil'man and Kronberg (1995):

Westerterp et. al.[108] considered classic 1953 article of Taylor to derive a longitudinal dispersion model of dispersion of a solute in a laminar flow through a tube. They considered the following equation:

$$\partial c/\partial t + u \partial c/\partial z = D_L (\partial^2 c/\partial r^2 + 1/r \partial c/\partial r)$$

alongwith the boundary condition

$\partial c / \partial r = 0$ at $r = 0$ and a , where a is the tube radius, r being radial coordinate and the velocity u is given by $u = 2 \bar{u} (1 - r^2 / a^2)$, \bar{u} being the cross sectionally averaged value.

They neglected the molecular diffusion in axial direction as Taylor (1953) did, on the assumption that the longitudinal mixing is completely dominated by shear dispersion and developed a more realistic model.

A new 1-D model for longitudinal dispersion is proposed as an alternative to the Fickian-type dispersed plug-flow model. Accounting for significant features of longitudinal mixing gives rise to a quasilinear hyperbolic system of two first-order equations for the average concentration and the dispersion flux instead of one second-order parabolic equation for the average concentration. The model equations are obtained based on minor extensions of the heuristic equilibrium analysis of Taylor. A qualitative, more general derivation of the equations is given on the basis of a simple generalization of Fick's law, taking into account the finite velocity of fluid elements. For linear problems the mean concentration and the dispersion flux obey a hyperbolic equation of the second order. The proposed hyperbolic model contains three parameters that depend only on the flow conditions, the physical properties of the fluid and the geometry of the system. It effectively resolves the well-known problem of boundary conditions that, for unidirectional flow, are formulated now only at the reactor inlet. The new model eliminates the conceptual shortcomings inherent to the Fickian dispersed plug-flow model; it predicts a finite velocity of signal propagation and does not involve backmixing in the case of unidirectional flow.

(18) Model due to Potucek (1996):

Frantisek Potucek [81] investigated the mechanics of the displacement washing of unbleached kraft pulp. The flow of the wash liquid through a pulp pad was described by the dispersion model using one dimensional parameter known as the Peclet number.

The model considered is

$$\partial c / \partial t = D_L \partial^2 c / \partial z^2 - u \partial c / \partial z.$$

Boundary condition is

$$u c - D_L \partial c / \partial z = u C_s, \quad z = 0, \quad t > 0.$$

This condition is imposed by the requirement that there be no loss of solute from the bed through the plane at which the displacing liquid is introduced. In order to avoid the unacceptable conclusion that the solute concentration passes through a maximum or minimum in the interior of the bed, it is necessary to impose the second boundary condition

$$\partial c / \partial z = 0, \quad z = L, \quad t > 0.$$

$$\text{Also, } c(z, 0) = C_i, \quad \forall z.$$

To convert into dimensionless form, the following procedures are adopted:

$$C = (c - C_s) / (C_i - C_s), \quad Z = z / L \quad \text{and} \quad T = u t / L.$$

The transport equation in dimensionless form is

$$\partial C / \partial T = 1 / Pe \partial^2 C / \partial Z^2 - \partial C / \partial Z, \quad \text{where } Pe = u L / D_L.$$

T is equal to the ratio of total fluid volume introduced per unit time into the free volume of the bed.

To characterize the displacement washing, the wash yield, dispersion coefficient, the bed efficiency, as well as time parameters such as the mean residence time of lignin and space time were evaluated. Results obtained for kraft pulp were compared with those for static bed of glass spheres.

The investigator observed that the wash yield depends not only upon the hydrodynamics of washing but also on the initial bed lignin concentration in black liquor. The wash yield decreases with increasing initial bed lignin concentration.

The bed efficiency may be expressed as

$E = -\ln(1 - WY) / RW$, where WY is wash yield and RW is wash liquor ratio.

The investigator simulated the displacement washing of kraft pulp at the dimensionless length ratio $L / d = 0.82$, d being the inside diameter of washing cell. The result obtained showed several differences between a bed of non-porous, non-compressible glass spheres and a bed of the more complex fibrous system. Because of a much wider pore size distribution and fiber swelling, the wash yield as well as the bed efficiency are lower for pulp bed in comparison with bed of glass spheres.

The investigator noticed that the dependence of the dispersion coefficient on the superficial wash liquid velocity shows an increasing trend. The presence of undercooks in pulp used in the experiments led to an increase in the dispersion coefficient. He also noticed that the pulp type, i.e. fiber characteristics, was the main variable affecting the dispersion coefficient. Also, the difference in geometry, that is, in average pore size and in pore size distribution, occurring in fiber material influenced dispersion in the given pulp bed.

The mean residence time, t_m is given as

$t_m = \int_0^{\infty} C_e / C_i dt$, where C_i is the exit concentration of solute in the wash liquor.

The space time is defined as the void volume of the bed divided by the volumetric flow rate of wash liquid. The investigator obtained a relationship between the mean residence time and the space time for pulp bed. He noticed that this relationship confirmed that the displacement washing was not a purely mechanical process but diffusion must be taken into account in the case when the presence of mother liquor inside fibers can't be neglected.

Displacement of mother liquor from pulp bed was evidently accompanied by diffusion process. In spite of small diffusion rate, the contribution of diffusion to the washing effectiveness can be distinguished in cases of sufficiently long contact time between fibers and wash liquid.

(19) Model due to Kukreja (1997):

Kukreja [40] considered a model based on the work of Kuo [42], Kuo and Barrette [43] and also Perron and Lebeau [75] for effective washing in the different zones of a brown stock washer with particular emphasis on the washing zone. The investigator attempted to define possible applicable performance evaluation parameters used by various investigators and to compare each other. The model considered is

$$D_L \frac{\partial^2 c}{\partial z^2} = u \frac{\partial c}{\partial z} + \frac{\partial c}{\partial t} + \mu \frac{\partial n}{\partial t}.$$

The adsorption-desorption isotherm considered is

$$\frac{\partial n}{\partial t} = k_1 c + k_2 n.$$

The investigators converted this couple of equations in dimensionless form by using

$$C = (c - C_s) / (C_1 - C_s), N = (n - C_s) / (C_1 - C_s), Pe = u L / D_L, Z = z / L, T = u t / L, K' = k_1 / k_2,$$

$$G = k_2 L / u \text{ and } H = (K' - 1) C_s / (C_1 - C_s).$$

The equations in dimensionless form are

$$\frac{\partial^2 C}{\partial Z^2} = Pe \left(\frac{\partial C}{\partial Z} + \frac{\partial C}{\partial T} + \mu \frac{\partial N}{\partial T} \right)$$

$$\text{and } \frac{\partial N}{\partial T} = G (H + K' C - N).$$

The boundary conditions and initial condition used in dimensionless form are

$$C(Z,0) = N(Z,0) = 1.$$

$$C(0,T) = 0, \frac{\partial C}{\partial Z} = 0 \text{ at } Z = 1.$$

The investigators solved the model using Laplace Transform technique.

The investigators considered u , ε_i and D_L as function of z while c and n as function of z and t both. They claimed the equation in non-dimensionless form as non-linear.

Drawbacks:

The following observations are made in the work of Kukreja [40] by the present investigator.

The equation in non-dimensionless form is a linear one, not a non-linear one because no convective term is present in the equation.

The boundary conditions give contradictory information, viz.

$$N = 1 \Rightarrow n = C_i \text{ while } N = 0 \Rightarrow n = C_s.$$

In this way $C_i = C_s$ is concluded. With this condition washing is not possible.

Also $C(Z,0) = 1$ is given for all values of Z . Therefore $C(0,0) = 1$.

$C(0,T) = 0$ is given for all T . Therefore $C(0,0) = 0$.

It is a contradiction again.

In development of model an equation contains the term $\partial c/\partial t$, which must be $\partial u/\partial t$.

No description of Fick's law of diffusion is given.

In the work of Kukreja [40] a table depicting normal range of different parameters is given. In the table fractional submergence of drum is given to be of the order of 25 to 40 which is beyond the normal range.

The dewatering zone is named as drying zone while no heat is applied in this zone.

(20) Model due to Miroslaw K. Szukiewicz (2000, March):

Miroslaw K. Szukiewicz [96] developed an approximate model for diffusion and reaction in a porous catalyst. The method applied for the derivation of the approximate model can be useful not only for diffusion and reaction process in porous catalyst, but also for any process that takes into account the internal diffusion, adsorption and the like.

The model is

$$\partial c / \partial t = 1 / r^2 \partial / \partial r (D_v r^2 \partial c / \partial r) - k c, \quad k \text{ being reaction rate constant.}$$

Initial Condition is

$$c(r, 0) = C_i.$$

Boundary Conditions are

$$c(0, t) = \text{extremum} \quad \text{or,} \quad \partial c / \partial r = 0 \text{ at } r = 0.$$

$$c(R, t) = C_{st}.$$

R = radius of the catalyst pellet.

The model is solved analytically applying Laplace-Larson transform technique.

The linear driving-force formula, which approximates diffusion with the chemical reaction processes (such as heterogeneous catalysis), is distinguished by the high accuracy of its calculations and the simplicity of its form. The simplicity of the form is important because it makes it possible to extend the validity of the LDF formula, for example, to another type of kinetic equation, in a relatively easy way. The formula has been derived as a "long-time" approximation, and its accuracy rises for longer times. A simple relation that defines the validity range of the approximate model was presented. It was shown, that the higher the value of the Thiele modulus, the greater the accuracy of the calculations for shorter times. This

means that the proposed approximation can be used for higher Thiele modulus values for almost the entire time scale.

(21) Model due to Liao and Shiau (2000, June):

Liao and Shiau [51] formulated an axial dispersion model for the operation of a fixed bed adsorber with a linear adsorption isotherm.

According to the investigators, for 1-D plug flow, the unsteady state mass balance equation for a fixed bed tubular adsorber can be written as

$$R_d \partial c / \partial t = -u \partial c / \partial z + D_e \partial^2 c / \partial z^2, \quad 0 < z < L, \quad t > 0.$$

R_d , the retardation coefficient (dimensionless) is given by

$$R_d = 1 + \rho_s K_d (1 - \epsilon) / \epsilon.$$

Here, ρ_s = bulk density of adsorbent (kg / m^3);

K_d = parameter of linear adsorption isotherm.

D_e , the effective dispersion coefficient (m^2 / s) is defined as

$$D_e = D_v + D_L.$$

Initial Condition is

$$c(z,0) = C_i, \quad 0 \leq z \leq L.$$

Boundary conditions are

$$c(0,t) = C_s, \quad t > 0.$$

$$\partial c / \partial z = 0, \quad z = L, \quad t > 0.$$

The investigators solved the model analytically using the method of separation of variables. The asymptotic solution for a large Peclet number and / or a small operation time was also obtained using two limiting cases. Influence of both, the Peclet number and the retardation coefficient on the operation of a fixed bed adsorber was also studied. As an example, the axial dispersion model was applied to the experimental data of the removal of Phenol from the solution in the activated carbon and the Amberlite resin XAD-4 fixed bed adsorbers.

The investigators observed that the axial dispersion model is somewhat better than the solid diffusion and combined diffusion models that do not take into account the dispersion effect.

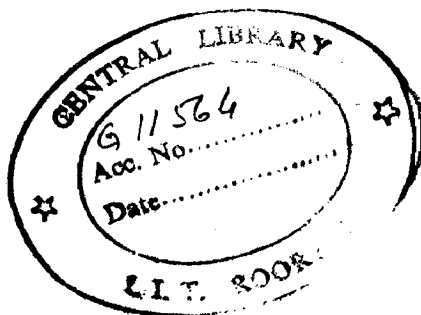
2.2 Conclusions

In this chapter up-to date review of mathematical models relating to displacement washing or similar systems with or without adsorption or dispersion is made. The models developed very recently for some other systems (quite similar to pulp fibers) are also presented.

It is found from the literature that there is abundant of information regarding steady state models mainly required for the material balances for the macroscopic evaluation of the design estimates. However, there is little information about the interaction of various time dependent operational parameters for control purposes. Very few investigators have attempted to throw light on these aspects. Majority of the investigators have concentrated on displacement washing studies though in normal practice the process is related to dilution and extraction and also with displacement. Many investigators did not take into account the parameters related to diffusion, dispersion, adsorption, desorption, multiporosity values for inter particle and intra particle voids and reinforced parameters like temperature, pressure drop and consistency. Although some mathematical models are available in literature limited studies are carried out for pulp washing under the influence of longitudinal dispersion coefficient, mass transfer coefficients and solute accumulation capacity of pulp fibers. Many works are also applicable to only nonporous solids. Though these are fantastic in their approach and the corresponding solution

techniques, these are not truly applicable to porous adsorptive beds like pulp mat. Besides, there are significant variations noted among the models of many investigators in their adsorption desorption isotherm equations. The solution techniques (either analytical or numerical or quasi-analytical or statistical) are also remarkably different. No investigator has ever compared the results evolved out by assuming different adsorption isotherms that too for different boundary conditions with mill practice values. Very few workers applied the results of simulation with displacement washing data to brown stock washer operation in rotary vacuum filter equipment in a very concise form but it lacks clarity. From design point of view these are of little relevance.

The solution of partial differential equation can also be possible with numerical techniques which is not very complex yet preserving the required accuracy for evaluating an industrial system. The system equation must address the issues of practical significance. It therefore demands a rational approach for interlinking the output data from a mathematical problem and the parameters normally known to the practicing engineers of a pulp and paper industry.



CHAPTER-3

DEVELOPMENT OF MATHEMATICAL MODELS

3.1 Principles

The mathematical model can be initiated through the equation of continuity showing conservation of mass. This in turn can be further extended to the flow of fluid through a pulp mat—a typical porous media. The equation is again coupled with the equation of mass transfer i.e. Fick's second law of diffusion and the sorption equilibrium isotherm. The role of adsorption–desorption dynamics can be briefly outlined

3.2 Role of dispersion-diffusion

While deriving a model one has to characterize initially ideal flow pattern within the equipment (BSW). However, because of non-ideal behaviour of flow of black liquor or wash liquor in real situation the parameters influencing the non-ideality have to be considered. In the present problem of pulp washing, first of all, ideal plug flow of wash water is considered which also sometimes called steady state slug flow, piston flow, rod like flow or ideal tubular or unmixed flow. It is characterized by the fact that the flow of fluid through the elements of the equipment is orderly with no element of fluid overtaking or mixing with any other element ahead or behind. In actual practical situation there may be lateral mixing of fluid in a plug flow. However, there must be no mixing or diffusion along the flow path. The necessary and sufficient condition for the plug flow is for the equal residence time for all elements of fluid, which can be established only by using the second law of thermodynamics. It is supposed that some degree of backmixing or intermixing is superimposed, the magnitude of which is independent of position within the element of the equipment (in this case Brown Stock Washer for a paper mill).

The condition implies that there exist no stagnant pockets and no gross bypassing or short-circuiting of fluid in the vessel. This is called dispersed plug flow model or simply the dispersion model. This is visualized in Figs. 3.1a and 3.1b.

Figures showing dispersion of flow:

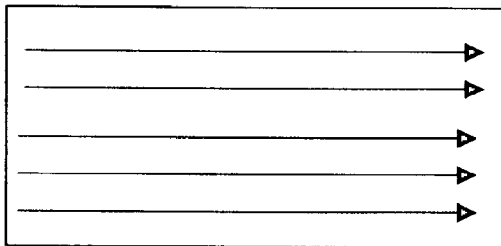


Fig. 3.1a Streamline Flow

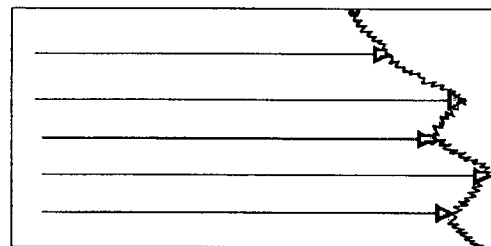


Fig. 3.1b Dispersed Flow

It is interesting to note that with varying intensities of turbulence or intermixing the prediction of this model should range from plug flow at one extreme to mixed flow at the other.

In pulp washing system, the diluted black liquor flows in z direction. The wash liquor, though at initial stage, pushes like piston the weak black liquor which disperse through the pulp matrix in the washing zone of brown stock washer. In absence of adsorption-desorption and contribution of the convective transport, the equation of dispersed flow can be written in the similar way as for molecular diffusion.

The equation of dispersed flow can be written as follows:

$$\frac{\partial c}{\partial t} = D_i \frac{\partial^2 c}{\partial z^2}$$

The D_i indicates the coefficient of longitudinal dispersion or axial dispersion uniquely characterizing the degree of backmixing during flow. It is called axial dispersion just to distinguish from the mixing in the lateral or the radial directions.

If $i = v$, this leads to the equation for molecular diffusion uniquely characterizing the process.

For complete plug flow there is a flat velocity profile whereas in dispersed plug flow there are fluctuations due to different flow velocities molecular and turbulent diffusion. The basic

governing differential equation representing the above dispersion model (without considering the adsorption-desorption etc.) in the z direction and following Fick's law can be written as

$$\frac{\partial c}{\partial t} = (D_L / uL) \frac{\partial^2 c}{\partial z^2} - \frac{\partial c}{\partial z}$$

D_L / uL is defined as vessel dispersion number, popularly known as Bodenstein Number (Bo), the reciprocal of which is called the Peclet Number (Pe).

The above stipulated conditions can be analytically represented as under.

If $D_L / uL \rightarrow 0$ or $uL / D_L \rightarrow \infty$ then negligible dispersion, hence plug flow occurs.

If $D_L / uL \rightarrow \infty$ or $uL / D_L \rightarrow 0$ then large dispersion, hence mixed flow occurs and the beds behave like a perfect mixing vessel.

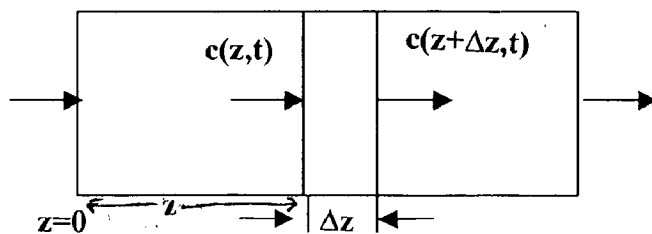
Where D_L / uL is termed as vessel dispersion number or simply dispersion number, the reciprocal of dispersion number is called Peclet number (Pe) according to many investigators^[407] or Bodenstein number(Bo) according to Gra^[23]. Modified Peclet number for flow through beds can also be defined as:

$$Pe_m = Lu / D_L \epsilon$$

3.3 Mathematical modeling of the physical problem

A section of a pulp pad of finite thickness L in the washing zone of a brown stock washer as shown in Fig. 3.2 is considered with a differential element of thickness Δz at a distance z from the origin.

Fig. 3.2 Simple Shell Balance



However the origin is supposed at the surface of the cake or pulp pad. The equation of continuity can be applied for the various species being transported through this section. Before

arriving at the equation of continuity, it is prudent to describe the models regarding two important parameters pertaining to the differential equation. These are models for average porosity (ϵ_{av}) and permeability (K), though these two variables are connected to each other. These are detailed in subsequent sections concerning parameter estimation.

With the above models of porosity and permeability one can proceed for developing the equation of continuity as follows:

3.4 Equation of continuity

Rate of Mass of solute in + Rate of Mass production by chemical reaction = Rate of Mass out + Rate of Mass Accumulation in the liquid phase + Rate of Mass Accumulation in the solid phase due to Adsorption-Desorption.

If A is the area of the bed, ϵ , the total average porosity (sum of porosities in the displaceable liquid ϵ_d and in the immobile phase ϵ_s), u, the velocity of the liquor in the mat, c, the concentration in the liquid phase, the equation in one dimension can be written as

$$A\epsilon u c \Big|_{z,t} = A\epsilon u c \Big|_{z+\Delta z,t} + A\epsilon \Delta z \frac{\partial c}{\partial t} + A(1-\epsilon) \Delta z \frac{\partial n}{\partial t} \quad \dots(3.1)$$

$$\lim_{\Delta z \rightarrow 0} (A\epsilon u c \Big|_{z,t} - A\epsilon u c \Big|_{z+\Delta z,t}) / \Delta z = A\epsilon \frac{\partial c}{\partial t} + A(1-\epsilon) \frac{\partial n}{\partial t},$$

where $z < \bar{z} < z + \Delta z$.

If ϵ and A are assumed to be constant, one can obtain the following expression

$$-\epsilon c (\partial u / \partial z) = \epsilon u (\partial c / \partial z) + \epsilon (\partial c / \partial t) + (1-\epsilon) (\partial n / \partial t). \quad \dots(3.2)$$

(I) (II) (III) (IV)

Term (IV) is related to adsorption-desorption, term (III) to dispersion and diffusion, term (II) shows concentration gradient and the velocity gradient appears in the term (I).

Using Fick's second law of diffusion, i.e.

$$-c (\partial u / \partial z) = (D_L + D_V) (\partial^2 c / \partial z^2) \quad \dots(3.3)$$

the following equation is obtained.

$$(D_L + D_V) (\partial^2 c / \partial z^2) = u(\partial c / \partial z) + (\partial c / \partial t) + [(1-\epsilon) / \epsilon] (\partial n / \partial t) \quad \dots(3.4)$$

Putting the values of various porosities in the intrafiber and interfibre masses, the above equation can be further rewritten as

$$(D_L + D_V) (\partial^2 c / \partial z^2) = u \partial c / \partial z + \partial c / \partial t + (1 - \epsilon_s - \epsilon_d) / (\epsilon_s + \epsilon_d) (\partial n / \partial t) \quad \dots(3.5)$$

The above equation is non-homogeneous, linear, first degree, second order parabolic partial differential equation.

Furthermore ϵ , u and D_L are functions of z whereas c and n are functions of z and t .

Writing in form of functional dependence of ϵ , D_L and u on z , the equation can be remodeled as

$$-\epsilon(z)c(z,t)\partial u(z)/\partial z = \epsilon(z)u(z)\partial c(z,t)/\partial z + u(z)c(z,t)\partial \epsilon(z)/\epsilon(z)\partial c(z,t)/\partial t + [1-\epsilon(z)] \partial n(z,t)/\partial t \quad \dots(4.6)$$

Replacing the left hand side term of the product of concentration and velocity gradient as shown in Eq.(3.3), the Eq.(3.6) can be simplified as under.

$$(D_L + D_V)\partial^2 c / \partial z^2 = u(z)\partial c(z,t)/\partial z + u(z)c(z,t)/\epsilon(z)\partial \epsilon(z)/\partial z + \partial c(z,t)/\partial t + \{[1-\epsilon(z)]/\epsilon(z)\} \partial n(z,t)/\partial t \quad \dots(3.7)$$

Expanding Eq.(3.7) in terms of ϵ_d , the porosity of the displaceable liquor and ϵ_s , the same for immobile liquor, the detailed equation can be formulated as follows

$$\begin{aligned} \epsilon_d(D_L + D_V)\partial^2 c / \partial z^2 + \epsilon_s(D_L + D_V)\partial^2 c / \partial z^2 &= \epsilon_d u(z)\partial c(z,t)/\partial z + \epsilon_s u(z)\partial c(z,t)/\partial z \\ + u(z)c(z,t)\partial \epsilon_d / \partial z + u(z)c(z,t)\partial \epsilon_s / \partial z + \epsilon_d \partial c(z,t) / \partial t + \epsilon_s \partial c(z,t) / \partial t + (1 - \epsilon_d - \epsilon_s) \partial n(z,t) / \partial t \end{aligned} \quad \dots(3.8)$$

Considering no dispersion in the stagnant layer and replacing the concentration c by c_{st} for the same layer (which is reasonable to assume), D_L in the second term on the left hand side can be neglected and the equation takes the form

$$\begin{aligned} \epsilon_d(D_L + D_V)\partial^2 c(z,t) / \partial z^2 + \epsilon_s(D_V)\partial^2 c_{st}(z,t) / \partial z^2 &= \epsilon_d u(z)\partial c(z,t) / \partial z + \epsilon_s u(z)\partial c_{st}(z,t) / \partial z + \\ u(z)c(z,t)\partial \epsilon_d / \partial z + u(z)c(z,t)\partial \epsilon_s / \partial z + \epsilon_d \partial c(z,t) / \partial t + \epsilon_s \partial c_{st}(z,t) / \partial t + (1 - \epsilon_d - \epsilon_s) \partial n(z,t) / \partial t \end{aligned} \quad \dots(3.9)$$

Effect of Tortuosity factor, τ on the mass transfer within intrafibre pores and the mobile layer can be introduced only in the case when diffusion is important compared to dispersion.

D_v , the effective diffusion coefficient in the stagnant layer and the fibres can be considered as

$D_v = \varepsilon_s/\tau$. Now Eq.(3.9) stands as:

$$\begin{aligned} \varepsilon_d(D_L + D_v)\partial^2 c(z,t)/\partial z^2 + \varepsilon_s(D_v\varepsilon_s/\tau)\partial^2 c_{st}(z,t)/\partial z^2 = \varepsilon_d u(z)\partial c(z,t)/\partial z + \varepsilon_s u(z)\partial c_{st}(z,t)/\partial z \\ + u(z)c(z,t)\partial \varepsilon_d/\partial z + u(z)c_{st}(z,t)\partial \varepsilon_s/\partial z + \varepsilon_d \partial c(z,t)/\partial t + \varepsilon_s \partial c_{st}(z,t)/\partial t + (1-\varepsilon_d-\varepsilon_s) \partial n(z,t)/\partial t \end{aligned} \quad \dots(3.10)$$

Eq.(3.10) requires the expression for $u(z)$ in terms of pressure drop ($-\Delta P$), equilibrium relationship for adsorption-desorption isotherm, and porosity in terms of measurable parameters. In addition to the above stipulation its solution also demands initial and boundary conditions. These are described as follows:

Substituting Darcy's equation connecting pressure drop $u = u_0/\varepsilon = (1/\varepsilon)(K/\mu) \partial P/\partial z$ in the above equation, it becomes

$$\begin{aligned} \varepsilon_d(D_L + D_v)\partial^2 c(z,t)/\partial z^2 + \varepsilon_s(D_v\varepsilon_s/\tau)\partial^2 c_{st}(z,t)/\partial z^2 = \varepsilon_d(1/\varepsilon)(K/\mu)(\partial P/\partial z)\partial c(z,t)/\partial z + \varepsilon_s(1/\varepsilon) \\ (K/\mu)(\partial P/\partial z)\partial c_{st}(z,t)/\partial z + (1/\varepsilon)(K/\mu)(\partial P/\partial z)c(z,t)\partial \varepsilon_d/\partial z + (1/\varepsilon)(K/\mu)(\partial P/\partial z)c_{st}(z,t)\partial \varepsilon_s/\partial z + \\ \varepsilon_d \partial c(z,t)/\partial t + \varepsilon_s \partial c_{st}(z,t)/\partial t + (1-\varepsilon_d-\varepsilon_s)\partial n(z,t)/\partial t \end{aligned} \quad \dots(3.11)$$

Now to express Eq.(3.11) in terms of Peclet Number, dimensionless length, concentrations of solute, time and pressures as detailed below,

$$Z = z/L, T = ut/L, C = (c-C_s)/(C_i-C_s), N = (n-C_s)/(C_i-C_s), C^* = (c_{st}-C_s)/(C_i-C_s),$$

$$P_0 = \text{Pressure at } z = 0$$

$$P^* = (P-P_0) / \Delta P_c,$$

$$P_e = uL/D_L = (1/\varepsilon)(K/\mu)(\partial P/\partial z)(L/D_L)$$

$$= (1/\varepsilon)(K/\mu)(\Delta P_c/L)(\partial P^*/\partial Z)(L/D_L) = (1/\varepsilon)(K/\mu)(\Delta P_c/D_L)\partial P^*/\partial Z$$

$$\partial c/\partial t = (\partial c/\partial C)(\partial C/\partial T)(\partial T/\partial t) = [u(z)/L] (C_i-C_s)\partial C/\partial T$$

$$\partial c/\partial z = (\partial c/\partial C)(\partial C/\partial Z)(\partial Z/\partial z) = [(C_i - C_s)/L] \partial C/\partial Z$$

$$\partial^2 c/\partial z^2 = [(C_i - C_s)/L^2] \partial^2 C/\partial Z^2$$

$$\begin{aligned} \partial n/\partial t &= (\partial n/\partial N)(\partial N/\partial T)(\partial T/\partial t) = [u(z)/L](C_i - C_s) \partial N/\partial t \quad \partial c_{st}/\partial z = (\partial c_{st}/\partial C)(\partial C/\partial Z)(\partial Z/\partial z) \\ &= [(C_i - C_s)/L] \partial C/\partial Z \end{aligned}$$

$$\begin{aligned} \partial c_{st}/\partial t &= (\partial c_{st}/\partial C)(\partial C/\partial T)(\partial T/\partial t) = [u(z)/L](C_i - C_s) \partial C/\partial T \quad \partial P/\partial z \\ &= (\partial P/\partial P^*)(\partial P^*/\partial Z)(\partial Z/\partial z) = [\Delta P_c/L] \partial P^*/\partial Z, \end{aligned}$$

one gets the following equation.

$$\begin{aligned} &\varepsilon_d(D_L + D_V)[(C_i - C_s)/L^2] \partial^2 C/\partial Z^2 + \varepsilon_s(D_V \varepsilon_s/\tau)[(C_i - C_s)/L^2] \partial^2 C'/\partial Z^2 \\ &= \varepsilon_d(P_e D_L/L^2)(C_i - C_s) \partial C/\partial Z + \varepsilon_s(P_e D_L/L^2)(C_i - C_s) \partial C'/\partial Z + (P_e D_L/L^2)C(z,t) \partial \varepsilon_d/\partial Z \\ &+ (P_e D_L/L^2)C_{st}(z,t) \partial \varepsilon_s/\partial Z + \varepsilon_d(P_e D_L/L^2)(C_i - C_s) \partial C/\partial T + \varepsilon_s(P_e D_L/L^2)(C_i - C_s) \partial C'/\partial T \\ &+ (1 - \varepsilon_d - \varepsilon_s)(P_e D_L/L^2)(C_i - C_s) \partial N/\partial T = 0, \end{aligned} \quad \dots(3.12)$$

Rearranging the above, one gets

$$\begin{aligned} &\varepsilon_d[(D_L + D_V)/Pe D_L](\partial^2 C/\partial Z^2) + \varepsilon_s(D_V \varepsilon_s/\tau Pe D_L) \partial^2 C'/\partial Z^2 - \varepsilon_d \partial C/\partial Z - \varepsilon_s \partial C'/\partial Z \\ &- (C/C_i - C_s) \partial \varepsilon_d/\partial Z - (C_{st}/C_i - C_s) \partial \varepsilon_s/\partial Z - \varepsilon_d \partial C/\partial T - \varepsilon_s \partial C'/\partial T - (1 - \varepsilon_d - \varepsilon_s) \partial N/\partial T = 0 \end{aligned} \quad \dots(3.13)$$

Replacing the $(1 - \varepsilon_d - \varepsilon_s)$ by λC_F , one can get the resulting equation as under:

$$\begin{aligned} &\varepsilon_d[(D_L + D_V)/(Pe D_L)](\partial^2 C/\partial Z^2) + \varepsilon_s(D_V \varepsilon_s/\tau Pe D_L) \partial^2 C'/\partial Z^2 - \varepsilon_d \partial C/\partial Z - \varepsilon_s \partial C'/\partial Z \\ &- [C/(C_i - C_s)] \partial \varepsilon_d/\partial Z - [C_{st}/(C_i - C_s)] \partial \varepsilon_s/\partial Z - \varepsilon_d \partial C/\partial T - \varepsilon_s \partial C'/\partial T - \lambda C_F \partial N/\partial T = 0 \end{aligned} \quad \dots(3.14)$$

where $\lambda = 6.80 \times 10^{-4}$.

The model developed above with various assumptions can lead to the models proposed by Grahs [24], Brenner [6], Kuo [42], Sherman [88], Viljakainen [105], Perron and Lebeau [75], Pellett [71], and Lapidus & Amundson [48] etc. as special cases.

3.5 For stagnant layer

$$\varepsilon_s \partial c_{st}/\partial t = k_1 c + k_3 n - k_2 c_{st} - k_4 c_{st} \quad \dots(3.15)$$

In a special case, $k_1 = k_4$ and $k_2 = k_3$

$$\varepsilon_s \partial c_{st}/\partial t = k_1(c - c_{st}) - k_2(c_{st} - n) = k_1 a_1(c - c_{st}) - k_2 a_2(c_{st} - n) \quad \dots(3.16)$$

3.6 For fibers

$$C_F(z)\partial n/\partial t = k_2 a_2 (c_{st} - n) \quad \dots(3.17)$$

Where $n = f(c_{st}^*)$, c_{st}^* being the equilibrium concentration of any solute on the fibres due to adsorption.

3.7 Adsorption-desorption isotherm for various species of black liquor

The Adsorption-Desorption isotherm dynamics are unfortunately not clearly known for Na^+ and lignin. Therefore both non-linear (Langmuir or Guggenheim) adsorption isotherm which obey Gibbs adsorption concept or finite linear type or Freundlich model can be used. These equations are either a first order differential equation or a linear / non-linear algebraic equation. Therefore judicial decision has to be purported during actual application of the adsorption-desorption isotherm for the species under examination. In the present investigation suitability of various possible adsorption-desorption isotherm equations will be attempted.

3.7.1 Adsorption-desorption isotherm equations

The following adsorption-desorption equilibrium equations are available in literature. These can be applied for Na^+ , and lignin species also. Only the values of constant coefficients, variable coefficients and mass transfer coefficients will vary from species to species.

Equations for various adsorption isotherms:

$$\partial n/\partial t = k_1 c - k_2 n \quad \dots(3.18)$$

$$\partial n/\partial t = K(c-n) \quad \dots(3.19)$$

$$n = kc \quad \dots(3.20)$$

3.8 Boundary condition for Langmuir type

$$uc_{in} = uc(0+) - D_L (\partial c/\partial z)_0 + (\partial c/\partial z)_{z=L} = 0.$$

$$c = c_{st} = c_i = c_0; n = n_0 \text{ for all } z \text{ at } t = 0.$$

In the present problem, D_L is substituted by $(D_L + D_v)$.

3.9 Equation in terms of Na^+ and lignin

As the brown stock washing involves complicated phenomena of Adsorption-Desorption Dynamics and Dispersion –Diffusion of multiple solutes or ions, the exact mathematical model building of large number of solutes pertinent to the pulp washing system becomes practically impossible. Therefore in the present problem the equation for single and double species consisting of group of constituents are developed and attempted to solve for Na^+ and lignin only. The model thus gives us a system of differential and algebraic equations which in turn needs several initial and boundary conditions relevant to the real (practical) system of washers in terms of individual species.

3.10 Corollaries from the developed model

As already indicated that the model developed in the present study is a general case. All the models developed or studied by previous investigators can be obtained from this model by neglecting certain terms which are irrelevant to the system studied or which are not playing significant role in the system.

(1) Model due to Edeskurty and Amundson

In this study pore-diffusion model is considered. Thus the porosity and D_L are not taken into consideration. Neglecting c_{st} and adjusting $K/\mu \partial P/\partial z$ to become $2/z$, the model developed in this study reduces to the model of Edeskurty and Amundson [14].

(2) Model due to Lapidus and Amundson

Neglecting D_L , c_{st} , ε_s and $\partial \varepsilon_d/\partial z$ the model developed in the present study reduces to the model considered by Lapidus and Amundson [48].

(3) Model due to Kuo

Neglecting D_L , D_v , ε_s , C_{st} and considering porosity as constant, the model developed in the present study reduces to the model considered by Kuo [42].

(4) Model due to Brenner

Neglecting D_v , c_{st} , ϵ_s , $\partial\epsilon_d/\partial z$ and $\partial n/\partial t$, the model developed in the present study reduces to the model considered by Brenner [6].

(5) Model due to Sherman

Neglecting D_v , c_{st} , ϵ_s and $\partial\epsilon_d/\partial z$, the model developed in the present study reduces to the model considered by Sherman [88].

(6) Model due to Pellett

Neglecting D_v , c_{st} , ϵ_s and $\partial\epsilon_d/\partial z$ and replacing the term n , concentration of solute in solid phase by Q , the accumulation capacity of particles for solute, the model developed in the present study reduces to the model considered by Pellett [71].

(7) Model due to Grah

Neglecting D_L , D_v , ϵ_s , C_{st} and $\partial\epsilon_d/\partial z$ and using C_F for $(1 - \epsilon_d - \epsilon_s)$ the model developed in the present study reduces to the model considered by Grah [24].

(8) Model due to Perron and Lebeau

Neglecting the terms D_L , D_v , c_{st} , $\partial\epsilon_d/\partial z$ and considering ϵ_s in place of $(1 - \epsilon_d - \epsilon_s)$ as multiple of $\partial n/\partial t$, the model developed in the present study reduces to the model considered by Perron and Lebeau [75].

(9) Model due to Rasmuson and Neretnieks

Neglecting the terms D_v , c_{st} , ϵ_s and $\partial\epsilon_d/\partial z$ and replacing concentration in solid phase n by volume averaged concentration in particles \bar{n} , the model developed in the present study reduces to the model considered by Rasmuson and Neretnieks [82].

(10) Model due to Gren and Strom

Expressions taken by Gren and Strom to make the concentration in liquid phase dimensionless is same as taken in the present study. Therefore, the model studied by Gren and Strom [28] is analogous to the model studied in the present study.

(11) Model due to Viljakainan

Neglecting the terms D_v , c_{st} , ϵ_s and $\partial\epsilon_d/\partial z$ the model developed in the present study reduces to the model considered by Viljakainan [105].

(12) Model due to Wong and Reeve

Neglecting the terms D_v , c_{st} , ϵ_s , $\partial\epsilon_d/\partial z$, $\partial c/\partial z$ and $\partial n/\partial t$ the model developed in the present study reduces to the model considered by Wong and Reeve [107].

(13) Model due to Teruo Takahashi, Takashi Korenaga and Fenghua Sen

Model of Fenghua Sen is similar to model developed in present study. The change is due to the change in system. Model of Fenghua Sen et. al. [18] is for two dimensional system.

(14) Model due to Farooq and Ruthven

Neglecting the terms D_v , c_{st} , ϵ_s , $\partial\epsilon_d/\partial z$, the model developed in the present study reduces to the model considered by Farooq and Ruthven [17].

(15) Model due to Lai and Tan

Model considered by Lai and Tan [45] is a three dimensional model developed for non linear adsorption in a packed bed adsorber. the basic idea is same as of present model.

(16) Model due to Sun and Levan

Model considered by Sun and Levan [95] is not exactly but very much similar to the present model in dimensionless form.

(17) Model due to Westerterp, Dil'man and Kronberg

Model considered by Westerterp et.al.[108] is almost similar to the present model except the change due to the nature of laminar flow studied by the investigators.

(18) Model due to Potucek

Neglecting the terms D_v , c_{st} , ϵ_s , $\partial\epsilon_d/\partial z$ and $\partial n/\partial t$ the model developed in the present study reduces to the model considered by Potucek [81].

(19) Model due to Kukreja

Neglecting the terms D_v , c_{st} , ε_s , and $\partial\varepsilon_d/\partial z$, the model developed in the present study reduces to the model considered by Kukreja [40].

(20) Model due to Miroslaw K. Szukiewicz

Model considered by Miroslaw K. Szukiewicz [96] is same as equation (3.4) in the development of the present model with some modifications necessary for the system under consideration.

(21) Model due to Liao and Shiau

Model considered by Liao and Shiau [51] is same as equation (3.4) in the development of the present model. The deviation is due to the fact that adsorption is not considered and $\partial c/\partial t$ is multiplied by a retardation coefficient.

3.11 Simplification of the present model

The mathematical models developed through transport phenomena principles as depicted from equations (3.1) to (3.14) and the equations of isotherms (3.18) to (3.20) given in Section 3.7.1 with various boundary and initial conditions are attempted to solve through finite difference method. The equation (3.14) is however extremely intricate in nature, bewildered and practically appears to be unsolvable even by using sophisticated numerical techniques. Besides, it is expected that solution of the equation needs enormous computer time for achieving accuracy, which is not required really for simulation of a real life problem for industrial design. Using some approximation, by neglecting certain terms one does not demerit the solution of the problem provided almost the same level of accuracy is attained. As a matter of fact, most of the practical problems are expressed in comparatively simplified form avoiding cumbersome calculations, yet they give acceptable accuracy. Therefore, an attempt has been made in this investigation to neglect some of the unimportant terms in equation (3.14) as shown below.

3.12 Simplification of the transport phenomena model derived in equation (3.14)

Equation (3.14) contains D_v , the volumetric diffusion coefficient and D_L , the axial or longitudinal dispersion coefficient both having the same units. According to Sherman [88] the dispersion coefficient in beds of granular and synthetic fibrous media is of the order of $10^{-6} \text{m}^2 \text{s}^{-1}$ for the displacement velocities normally encountered in practice, while the diffusion coefficient is of the order of $10^{-9} \text{m}^2 \text{s}^{-1}$ for the diffusion controlled mixing at a planar interface between dilute aqueous solutions according to Lee [50]. This indicates that $D_L / D_v \cong 1000$ times. In this situation, D_v can be neglected even in the case of adsorption-desorption dynamics prevalent in the pulp washing system.

Neglecting D_v , $\partial \epsilon_s / \partial Z$, $\partial \epsilon_d / \partial Z$, $\partial C' / \partial Z$ the following equation results

$$D_L \partial^2 C / \partial Z^2 = Pe (\partial C / \partial Z + \partial C / \partial T + \mu \partial N / \partial T) \quad \dots(3.21)$$

If the effect of dispersion coefficient D_L is also not taken into account, the equation reduces to

$$\partial C / \partial Z + \partial C / \partial T + \mu \partial N / \partial T = 0. \quad \dots(3.22)$$

It is known that for obvious reasons, in any partial differential equation solution, the parameters are expressed in dimensionless form.

Isotherms taken in dimensionless form are

$$\partial N / \partial T = G(H + KC - N) \quad \dots(3.23)$$

$$\partial N / \partial T = G(C - N) \quad \dots(3.24)$$

$$N = H + K C \text{ or, } \partial N / \partial T = K \partial C / \partial T \quad \dots(3.25)$$

Table (3.1): Different models considered in the present investigation

| Sl. No. | Transport Equation | Adsorption Isotherm |
|---------|--|---|
| 1. | $D_L \frac{\partial^2 C}{\partial Z^2} = Pe (\frac{\partial C}{\partial Z} + \frac{\partial C}{\partial T} + \mu \frac{\partial N}{\partial T})$ | $\frac{\partial N}{\partial T} = G (H + K C - N)$ |
| 2. | $D_L \frac{\partial^2 C}{\partial Z^2} = Pe (\frac{\partial C}{\partial Z} + \frac{\partial C}{\partial T} + \mu \frac{\partial N}{\partial T})$ | $\frac{\partial N}{\partial T} = G (C - N)$ |
| 3. | $\frac{\partial C}{\partial Z} + \frac{\partial C}{\partial T} + \mu \frac{\partial N}{\partial T} = 0$ | $\frac{\partial N}{\partial T} = G (H + K C - N),$ |
| 4. | $\frac{\partial C}{\partial Z} + \frac{\partial C}{\partial T} + \mu \frac{\partial N}{\partial T} = 0$ | $\frac{\partial N}{\partial T} = G (C - N)$ |
| 5. | $D_L \frac{\partial^2 C}{\partial Z^2} = Pe (\frac{\partial C}{\partial Z} + \frac{\partial C}{\partial T} + \mu \frac{\partial N}{\partial T})$ | $N = H + K C$ or, $\frac{\partial N}{\partial T} = K \frac{\partial C}{\partial T}$ |
| 6. | $\frac{\partial C}{\partial Z} + \frac{\partial C}{\partial T} + \mu \frac{\partial N}{\partial T} = 0$ | $N = H + K C$ or, $\frac{\partial N}{\partial T} = K \frac{\partial C}{\partial T}$ |

In models (1) and (3), $K = k_1 / k_2$, $G = k_2 L / u$ and $H = (K - 1) C_s / (C_i - C_s)$.

In models (2) and (4), $G = K L / u$, where $K = (k_1 + k_2) / 2$.

In models (5) and (6), $K = k_1 / k_2$ and $H = (K - 1) C_s / (C_i - C_s)$.

Boundary and initial conditions considered are considered as same for all the models.

The values of $N(Z,0)$ are calculated from Langmuir Adsorption Isotherm with the assumption that initial concentration of solute in the bed will be the same as the concentration of solute in the vat. Only first four models could be solved in this study using the values of parameters as given by Grah [25] for simulation. Model no. (5) and (6) could not give satisfactory results for all the difference schemes tried.

The various models developed for Brown Stock Washing now will be subjected to Boundary and Initial conditions given in the following table.

Table (3.2): Boundary and Initial Conditions

| B.C.& I.C. | B.C.& I.C. (in dimensionless form) |
|--|---|
| $c(z,0) = C_i$ | $C(Z,0) = 1$ |
| $c(0,t) = C_s$ | $C(0,T) = 0$ |
| $u c - D_L \partial c / \partial z = u C_s, t > 0$ | $\partial C / \partial Z = Pe C (Z = 0+, T > 0)$ |
| $n(z,0) = n_i$ | $N(Z,0) = 0.4, \text{ for Sodium}$ $0.008, \text{ for lignin}$ |

3.13 Conclusions:

In this investigation mathematical models are derived for washing zone of a rotary vacuum washer from basic equation of continuity in one dimensional form for flow through porous media, Fick's law of diffusion and dispersion with adsorption and desorption isotherm equations for two species namely Na^+ and lignin. The equations are coupled with many other fluid mechanical parameters and thus general in nature.

For solving the models varying initial and boundary conditions applicable to rotary vacuum brown stock washer is proposed.

The developed models can be reduced to various earlier proposed models using simplifying assumptions and neglecting certain terms. These are clearly depicted.

As the developed models are mathematically complex to solve, these are simplified for further investigation in order to compare some of the models proposed by Grah [24], Brenner [6], Sherman [88] and Kukreja [40] but with different numerical techniques.

Four set of models differing in adsorption isotherm with same initial and boundary conditions are proposed to solve through finite difference method. In fact earlier investigators did not attempt to use this simple technique.

CHAPTER-4

SOLUTION TECHNIQUE

In Chapter-3 it has been found that the model concerned with the unsteady state operation of brown stock washing leads to a system of partial differential equations. The solution technique depends on what kind of partial differential equation is developed? Homogeneous / non-homogeneous, linear / non-linear or quasi-linear? What are the order and degree? Further, it is parabolic, elliptic or hyperbolic or a mixed type- Tricomi form? Is it a difference-differential or integro-differential type? To answer these questions it is an imperative necessity to go in to details of the genesis of the differential equation? While the answers to few questions are straightforward, some are difficult to answer. In this section the model developed is defined to what category it belongs? Thereafter solution technique is sought for.

Approximation methods, whether analytical or numerical in character, are the only means of solution. Analytical approximation methods often provide extremely useful information concerning the character of the solution for critical values of the dependent variables but tend to be more difficult to apply and requires application of advanced mathematical methods than the numerical methods. On the other hand, it is generally easier to produce sufficiently approximate solutions by simple and efficient numerical methods. Several numerical methods have been proposed for the solution of partial differential equations. Of the numerical approximation methods available for solving partial differential equations, finite element methods (Orthogonal collocation, Galerkin, Sub-domain, Method of Moments and Ritz method etc.) and finite difference methods are more frequently used and more universally applicable than any other method. Finite difference methods are approximate in the sense that derivatives at a point are approximated by difference quotients over a small interval, i.e., $\partial\phi / \partial x$ is replaced by $\delta\phi / \delta x$ where δx is small while the other

independent variable y is constant, but the solutions are not approximate in the sense of being crude estimates. The data of the problems of technology are invariably subject to errors of measurement, besides which, all the arithmetical work is limited to a finite number of significant figures and contains rounding errors, so even analytical solutions provide only approximate numerical answers. Finite difference methods generally give solutions that are either as accurate as the data warrant or as accurate as is necessary for the technical purpose for which the solutions are required. In both cases a finite difference solution is as satisfactory as one calculated from an analytical formula. Out of the above mentioned methods only the finite-difference methods have become popular and are more gainfully employed than others.

Problems involving time t as one independent variable lead usually to parabolic or hyperbolic equations.

The simplest parabolic equation, $\partial u/\partial t = k \partial^2 U/\partial x^2$, derives from the theory of heat conduction and its solution gives, for example, the temperature U at a distance x units of length from one end of a thermally insulated bar after t seconds of heat conduction. In such a problem the temperatures at the ends of a bar of length l (say) are often known for all time. In other words, the boundary conditions are known. It is also usual for the temperature distribution along the bar to be known at some particular instant. This instant is usually taken as zero time and the temperature distribution is called the initial condition. The solution gives U for values of x between 0 and l and values of t from zero to infinity. Hence the area of integration S in the x - t plane is the infinite area bounded by the x -axis and the parallel lines $x = 0$ and $x = l$. This is described as an open area because the boundary curves marked C do not constitute a closed boundary in any finite region of the x - t plane. Applications of finite-difference methods of solution to parabolic equations are no different from their application to elliptic equations in so far as the integration of the differential equation over S is approximated by the solution of algebraic equations. The structure of the algebraic equations is

different however in that they propagate the solution forward from one time row to the next in a step-by-step fashion.

Hyperbolic equations generally originate from vibration problems, or from problems where discontinuities can persist in time, such as with shock waves, across which there are discontinuities in speed, pressure and density. The simplest hyperbolic equation is the one-dimensional wave equation $\partial^2 u / \partial t^2 = c^2 \partial^2 U / \partial x^2$, giving, for example, the transverse displacement U at a distance x from one end of a vibrating string of length l after a time t . As the values of U at the ends of the string are usually known for all time (the boundary conditions) and the shape and velocity of the string are prescribed at zero time (the initial conditions), it is seen that the solution is similar to that of a parabolic equation in that the calculation of U for a given x and t , ($0 \leq x \leq l$), entails integration of the equation over the open area S bounded by the open curve C . Although hyperbolic equations can be solved numerically by finite difference methods, those involving only two independent variables, x and t say, are often dealt with by the method of characteristics, specially if the initial conditions and/or boundary conditions involve discontinuities. This method finds special curves in the x - t plane, called characteristic curves, along which the solution of the partial differential equation is reduced to the integration of an ordinary differential equation. This ordinary equation is generally integrated by numerical methods.

In conclusion, it is worth noting that whereas changes to the shape of the area of integration or to the boundary and initial conditions of partial differential equations often make their analytical solutions impossible, such changes do not fundamentally affect finite difference methods although they sometimes necessitate rather complicated modifications to the methods.

On the basis of above we conclude that the finite difference methods are applicable to a wide class of problems and usually the most convenient for a computer solution. It can converge within reasonable time, fairly stable and does not consume much CPU. We will therefore restrict

ourselves to the treatment with the finite-difference methods. Working of the method is explained as follows.

The general second-order partial differential equation is of the form

$$A \frac{\partial^2 u}{\partial x^2} + 2B \frac{\partial^2 u}{\partial x \partial y} + C \frac{\partial^2 u}{\partial y^2} - F(x, y, u, \frac{\partial u}{\partial x}, \frac{\partial u}{\partial y}) = 0.$$

If A, B and C are functions of x, y, u, $\frac{\partial u}{\partial x}$ and $\frac{\partial u}{\partial y}$, then this equation is called quasilinear partial differential equation. When A, B and C are functions of x and y and F is a linear function of u, $\frac{\partial u}{\partial x}$ and $\frac{\partial u}{\partial y}$ then the equation is called linear. A linear partial differential equation may be written as

$$A \frac{\partial^2 u}{\partial x^2} + 2B \frac{\partial^2 u}{\partial x \partial y} + C \frac{\partial^2 u}{\partial y^2} + D \frac{\partial u}{\partial x} + E \frac{\partial u}{\partial y} + F u + G = 0,$$

Where A, B, C, D, E, F and G are constants or functions of x and y only. This equation is homogeneous if $G = 0$, otherwise inhomogeneous.

This equation can be classified with respect to the sign of the discriminant, $\Delta_s = B^2 - AC$.

If $\Delta_s = 0$, then the equation is said to be of parabolic type, if $\Delta_s < 0$, then elliptic type and if $\Delta_s > 0$, then hyperbolic type.

Parabolic Equations:

$$\frac{\partial^2 u}{\partial x^2} = F_1(x, y, u, \frac{\partial u}{\partial x}, \frac{\partial u}{\partial y}).$$

or,

$$\frac{\partial^2 u}{\partial y^2} = F_2(x, y, u, \frac{\partial u}{\partial x}, \frac{\partial u}{\partial y}).$$

Elliptic Equations:

$$\frac{\partial^2 u}{\partial x^2} + \frac{\partial^2 u}{\partial y^2} = F_3(x, y, u, \frac{\partial u}{\partial x}, \frac{\partial u}{\partial y}).$$

Hyperbolic Equations:

$$\frac{\partial^2 u}{\partial x \partial y} = F_4(x, y, u, \frac{\partial u}{\partial x}, \frac{\partial u}{\partial y}).$$

or,

$$\frac{\partial^2 u}{\partial x^2} - \frac{\partial^2 u}{\partial y^2} = F_5(x, y, u, \frac{\partial u}{\partial x}, \frac{\partial u}{\partial y}).$$

Here x and y are the independent variables in all the three cases.

To solve a partial differential equation or a system of partial differential equations with initial and boundary conditions, the differential equation is replaced with a finite-difference equation by replacing the derivatives with central-difference quotients. The interval is subdivided into a suitable number of equal subintervals, and the difference equation at each point is written where the value of the function is unknown. When the initial or boundary value conditions involve derivatives, the domain will have to be extended beyond the interval. The derivative initial or boundary conditions are utilized to write difference quotients that permit the elimination of the fictitious points outside the interval.

The system of equations so created is solved to obtain approximate values for the solution of the differential equation at discrete points on the interval. If the original differential equation is non-linear, the system of equations will also be non-linear. In such situations, some other method will normally be preferred. This can be exemplified with a simple parabolic equation of the form

$$\partial u / \partial t = \partial^2 u / \partial x^2,$$

in an arbitrary region $R \times [0, T]$ with suitable boundary conditions, where $R = (a \leq x \leq b)$ and $0 \leq t \leq T$. We superimpose on $R \times [0, T]$ a rectilinear grid with grid lines parallel to the coordinate axes with spacing h and k in space and time directions, respectively.

The points of intersection of these families of lines are called mesh points, lattice points, nodal points or grid points. In finite difference methods the solution is approximated numerically at a number of discrete points, called “mesh, lattice, nodal or grid points”.

The grid points on $R \times [0, T]$ are given by

$$t_n = nk, \quad n = 0, 1, 2, \dots, N$$

$$x_m = a + mh, \quad m = 0, 1, 2, \dots, M$$

where $x_0 = a$, $x_M = b$, $M = (b-a)/h$. The space nodes on the n th time grid usually constitute the n th layer or level. Let the solution value $u(x_m, t_n)$ be denoted by $U(m, n)$ and its approximate value by $u(m, n)$. The differential equation at the node (m, n) becomes

$$\partial u / \partial t (x_m, t_n) = \partial^2 u / \partial x^2 (x_m, t_n).$$

The construction of the difference scheme for the considered differential equation will be based on the approximation to the partial derivatives in this equation.

The simple approximations to the first derivative in the time direction are given by

$$\begin{aligned} \partial u / \partial t (x_m, t_n) &= (U(m, n+1) - U(m, n)) / k + O(k) \\ &= (U(m, n) - U(m, n-1)) / h + O(k) \\ &= (U(m, n+1) - U(m, n-1)) / 2k + O(k^2) \end{aligned}$$

where $U(m, n+1) = u(x_m, t_{n+1})$. Next, approximation to the second derivative $\partial^2 u / \partial x^2$ in the space direction can be written as

$$\partial^2 u / \partial x^2 (x_m, t_n) = (U(m-1, n) - 2u(m, n) + U(m+1, n)) / h^2 + O(h^2).$$

Substituting these approximations into the equation considered, we obtain

$$\begin{aligned} (U(m, n+1) - U(m, n)) / k &= (U(m-1, n) - 2u(m, n) + U(m+1, n)) / h^2 + O(k + h^2) \\ \text{or, } (U(m, n) - U(m, n-1)) / h &= (U(m-1, n) - 2u(m, n) + U(m+1, n)) / h^2 + O(k + h^2) \\ \text{or, } (U(m, n+1) - U(m, n-1)) / 2k &= (U(m-1, n) - 2u(m, n) + U(m+1, n)) / h^2 + O(k^2 + h^2). \end{aligned}$$

The terms $O(k + h^2)$ and $O(k^2 + h^2)$ denote the order of the local truncation error and is also known as the order of the method. Neglecting the truncation errors and simplifying we obtain the difference equations

$$\begin{aligned} U(m, n+1) &= (1-2\lambda) u(m, n) + \lambda (u(m-1, n) - u(m+1, n)) \\ \text{or, } u(m, n-1) &= -\lambda u(m-1, n) + (1+2\lambda) u(m, n) - \lambda u(m+1, n) \\ \text{or, } u(m, n+1) &= u(m, n-1) + 2\lambda (u(m-1, n) - 2u(m, n) + u(m+1, n)), \end{aligned}$$

where $\lambda = k / h^2$ is called the mesh ratio parameter.

It can be shown that this formula is valid only for $0 < \lambda \leq 1/2$.

The equation obtained will give the value of the variable u at a grid point if the values at the neighbouring points are known.

4.1 Solution of the problem through MATLAB

What are the pre-requisites of MATLAB?

As the model developed is a system of equations containing transport equation coupled with adsorption isotherm together with two initial and two boundary conditions, to solve it through programming is a lengthy and time consuming job as the equations are inter-linked and looped. It seemed to be more creditable to use some suitable software in the present era of software development, when these are already available. Since we have used the discrete method for solving the partial differential equations of two variables, i.e. of two dimensions, there was dependency of variables in loop of the type $F(x,y) = f_1(x,y) + f_2(x,y) + G(x,y)$ and $G(x,y) = f_3(x,y) + f_4(x,y) + F(x,y)$. So the iterative method of solution what we have used seems to be one of the best methods keeping the condition of convergence in consideration. MATLAB is a very powerful tool for matrix manipulation and also it is easy to simulate there therefore the problem under consideration have been solved with the help of this software. But each software has its limitations and can't be used to solve any problem even when it is made to solve that type of problems. To overcome such a situation one has to solve one's problem with the help of the software by making program of the problem readable to the software.

The solution of the above models have been done with the help of MATLAB by introducing specially prepared computer program in C++ language so that MATLAB software can accept the program and thereby solve the inter-linked and looped partial differential equations equipped with suitable initial and boundary conditions. In the present investigation, the transport equation for

flow through porous media (the fiber bed in brown stock washer) demanded looping with the adsorption isotherm equation.

The above procedure is followed for specifically Sodium and lignin species what are predominantly pertinent constituents in same form or the other in black liquor.

As the two species are characteristically different, Na^+ being highly alkaline ionic species of low molecular weight whereas lignin is organic non-ionic species of high molecular weight, lignin is slightly charged with other components in aqueous black liquor medium. As a result both the species must display different adsorption-desorption dynamics at any condition of the brown stock washer. However, the mathematical form of the transport equation remains the same. It is a fact that these two species display different behaviour because of difference in values of dispersion, diffusion and mass transfer coefficients.

CHAPTER-5

PARAMETER ESTIMATION, DATA ANALYSIS AND VALIDITY OF MODELS

After developing mathematical models and finding out the solution technique, it is required to estimate the parameters demanded by the model solutions. The parameters are hydrodynamic, or process or design related. Where equations are not available, experimental data reported by different investigators are used. While using data, correlations or models equation it is very important to assess the accuracy and range of their applicability. In this chapter, various models of hydrodynamic parameters are reviewed. Appropriate equations are selected for model solution.

5.1 Review of modeling of fluid –mechanical parameters

5.1.1 Properties of pulp bed-porosity and permeability

Porosity is defined as the ratio of volume available for flow to the total volume of the bed. Porosity of the pulp mat is an important factor as the hydrodynamics of the filtrate is highly influenced by the porous path through which the fluid will move. The models presented for various applications are enumerated below.

5.1.1.1 Models due to Tiller and Cooper

Tiller and Cooper [97] investigated the role of porosity in filtration under constant pressure condition. They demonstrated that ordinary differential equation, describing flow through a porous compressible solid, can be represented by partial differential equation in a better way. They further explained in detail the role of porosity under constant pressure filtration by analyzing the variation of porosity as a function of the distance from the medium or surface and also with dimensional parameter z / L in various graphical representations. As the pressure drop across the cake increases, the porosity at the medium decreases and eventually reaches a minimum value equal to the porosity determined by the maximum applied pressure. It can also be evident that the porosity

decreases with time at any point. The average porosity over the entire bed has been formulated by Tiller et. al.[97] in the following manner.

$$\epsilon_{av} = (1/L) \int_0^L \epsilon(z) dz. \quad \dots(5.1)$$

Changing the variable of integration, one obtains

$$\epsilon_{av} = (1/L) \int_0^{p-p_1} \epsilon (dz/dp_s) dp_s \quad \dots(5.2)$$

The term dz/dp_s can be obtained from the basic empirical equation

$$- g_c dp_z/dz = g_c dp_s/dz = \alpha_x \mu \rho_s (1-\epsilon) q, \quad \dots(5.3)$$

describing flow through a porous and compressible solid.

On substituting the appropriate expression for dz/dp_s from this equation in the previous equation, one obtains

$$\epsilon_{av} = (g_c / \mu \rho_s q) (1 / L) \int_0^{p-p_1} \epsilon / \{ \alpha_x (1-\epsilon) \} dp_s. \quad \dots(5.4)$$

Where g_c , μ , ρ_s , q , p , p_1 , α_x and p_s , indicate conversion factor, viscosity, true density of solids, rate of flow of liquid in cake at distance z from surface, applied filtration pressure, pressure at interface of medium and cake, value of specific resistance at distance z from surface of cake where solid compressive pressure is p and solid compressive pressure at distance z from surface of cake respectively.

The thickness of the cake can be found by integrating dz from zero to L as follows:

$$\int_0^L dz = L = (g_c / \mu \rho_s q) \int_0^{p-p_1} 1 / \{ \alpha_x (1 - \epsilon) \} dp_s. \quad \dots(5.5)$$

Substituting for L from this equation in the previous one, one obtains

$$\epsilon_{av} = \int_0^{p-p_1} \epsilon / \{ \alpha_x (1 - \epsilon) \} dp_s / \int_0^{p-p_1} 1 / \{ \alpha_x (1 - \epsilon) \} dp_s \quad \dots(5.6)$$

$$\text{or, } \epsilon_{av} = 1 - \int_0^{p-p_1} (1 / \alpha_x) dp_s / \int_0^{p-p_1} 1 / \{ \alpha_x (1 - \epsilon) \} dp_s \quad \dots(5.7)$$

The integration needs the functional dependence of ϵ on p , p_1 , p_s , q , α etc.

5.1.1.2 Walker's compressibility model for drainage of pulp suspension

While deriving a model for sheet forming process, Walker [106] found the decrease in the average porosity of a pulp bed when the initial driving force was increased during wet end of paper forming. The result implies that porosity of a given layer in the bed will be dependent on the driving force as the layer is formed. The existence of a porosity gradient in the wet paper sheet has been confirmed by many investigators, noticeably by Sherratt [89] and Szikla & Paulapuro [c.f.86].

Walker developed a model to describe the porosity of the bed as a compressibility model of the porosity with some assumption and can be applied mostly for a system where suspension is tending to a final mat. It is expressed as following.

If $h = h_0$, then $\epsilon = \epsilon_{\min}$ and if $h = 0$, then $\epsilon = \epsilon_{\max}$.

Here, h is head of flowing fluid and h_0 is initial head of flowing fluid.

The porosity of layers formed at a given head of flowing fluid must be a function of that head such that $\epsilon = \epsilon_{\max} - f(h/h_0)$ when $h = h_0$ and then $f(h/h_0) = \epsilon_{\max} - \epsilon_{\min}$ (5.8)

Thus $\epsilon = \epsilon_{\max} - [(\epsilon_{\max} - \epsilon_{\min}) g(h/h_0)]$, where $g(h/h_0)$ is a function such that $g(1) = 1$ (5.9)

While a porosity gradient is suggested, the nature of the gradient is unknown. To allow all feasible cases to be considered, a power term is introduced, and $g(h/h_0)$ is remodeled as $(h/h_0)^r$. This yields the final form of the compressibility model of porosity as

$$\epsilon = \epsilon_{\max} - [(\epsilon_{\max} - \epsilon_{\min}) (h/h_0)^r]. \quad \dots (5.10)$$

The parameter r fixes the parameter ϵ_{\min} .

The working range of r and hence of ϵ_{\min} can be calculated by considering the material balance of the system.

If L is the depth of the bed then the differential material balance for the solids of the system can be expressed as

$$(1 - \varepsilon) dL = -(1 - \varepsilon_{\max}) dh. \quad \dots(5.11)$$

If no solids are lost through the forming wire, the integral form of this equation can be expressed as

$$(1 - \bar{\varepsilon}) L_{\max} = - (1 - \varepsilon_{\max}) (h_0 - h_f), \quad h_f \text{ being the final head of flowing fluid.} \quad \dots(5.12)$$

The mean porosity is defined in the usual way as

$$(1 - \bar{\varepsilon}) = \frac{\int_0^{L_{\max}} (1 - \varepsilon) dL}{\int_0^{L_{\max}} dL}. \quad \dots(5.13)$$

A differential equation has been solved using Simpson's rule integration technique. Effect of the pore size distribution has also been included.

Study of flow through immiscible porous media was also carried out by Higgins and Young [c.f.86] and confirmed the effect of pore size distribution and the orientation of the fibers.

However, the above work is related to dilute suspension only.

5.1.1.3 Kozeny-Carman model for packed bed of any materials

Sampson et al. [86] used Kozeny-Carman model for explaining the resistance to water removal on a Fourdrinier wire and subsequent the mat formed in the process.

$$V = K \Delta P / \mu L \text{ and } K = (c / S_0^2) \varepsilon^3 / (1 - \varepsilon)^2, \quad \dots(5.14)$$

where the constant c, has a typical value 0.18 for paper.

The above equation has been used by Corte [c.f.86] and Coulson et.al.[c.f.86]. The permeability constant or its equivalent term has been defined by Scheidegger [c.f.86], Emersleben [c.f.86] and Iberall [c.f.86]. Higgins and deYoung [c.f.86] rederived Iberall's [c.f.86] theory assuming all fibers to be oriented at right angles to the direction of flow and defined as

$$k = \varepsilon d_f^2 (2 - \ln(d_f v_s \rho / \mu \varepsilon)) / 16 (1 - \varepsilon). \quad \dots(5.15)$$

Foscolo et al. [20] extended the Kozeny- Carman model to account for the tortuous nature of the flow path as

$$T(\varepsilon) = 1/\varepsilon. \quad \dots(5.16)$$

The final expression arrived at gives the pressure drop across a packed bed of spheres

$$\Delta P = 17.3 \mu v_s L (1-\epsilon) / d_p^2 \epsilon^{4.8} \quad \dots(5.17)$$

The exponent 4.8 was arrived at by assuming that the drag forces on a single particle approach those for unhindered settling at high porosities. If this assumption is not made and we consider our system to be hindered in some way, then we can refer to the previous stage in the derivation, shown as

$$\Delta P = k_h \mu v_s L (1-\epsilon) / d_p^2 \epsilon^{4.8}, \quad \dots(5.18)$$

where $k_h = 72$ for a packing of spheres.

Permeability value has been applied to estimate the amount of water immobilized by the swollen fiber where the permeability has been defined as the empirical constant, K in Darcy's law for unidirectional flow in porous media.

5.1.1.4 Lindsay's model

One key characteristic that has received little attention in the past is the flow porosity, defined as the fraction of the total pore space that is open to fluid flow. It is a matter of fact that much of the pore space in pulp mat or paper and other porous media is generally inaccessible to fluid flow in the presence of hydraulic pressure gradient. This is especially important in this particular case of vegetable fibers originated from wood, bamboo, bagasse etc. In this case, many lumens may be closed to flow, micro-pores in the cell wall generally offer too much flow resistance for significant flow and the geometric arrangements for the fibers and fines may lead to dead end pores that are open only at one end. By definition, the total pore space includes everything that is not cellulose or other solids and also includes water that is chemically bound or otherwise immobilized. Therefore, in water saturated pulp mat, the flow may be restricted by physical and chemical absorption and mechanical obstruction (isolated or dead end pores). This aspect is concerned with different zones of a brown stock washer. This is especially applicable in the filtration zone and washing zone. In

partially saturated pulps, i.e. in both the first and second dewatering zones, surface tension effects may further hinder fluid flow through the mat or the sheet. For an improved understanding of many practical processes in fibrous media, it will be useful to know what fraction of the pore space is available to fluid flow. In the case of penetration by an immiscible phase (air) in the two dewatering zones in displacement dewatering of pulp, two phase partitioning and relative permeability effect also become important. In this case gas is used to displace liquid water / dilute black liquor from the mat matrix. The amount of dilute black liquor removal will be affected by the amount of water in pores open to flow.

The above concepts and the terms related to porosity have been advocated by Lindsay [52]. This is given in the following table (5.1).

Table (5.1): Different type of porosities

| Term | Definition |
|---|--|
| Total porosity, ϵ | Fraction of total volume occupied by pores or 1-volume fraction of solid. |
| Effective flow porosity, ϵ_{eff} | Fraction of total volume occupied by pores open to flow. |
| Relative flow porosity, $\epsilon_{rw} = \epsilon_{eff} / \epsilon$ | Fraction of total pore space that is open to Flow. |
| Extrafiber porosity, ϵ_0 | Fraction of total volume occupied by pore space Between fibers or 1-volume fraction of fibers. |

The relative flow porosity has possible values between 0 and 1 and is important in two dewatering zones of BSW where two fluids are involved.

Lindsay further used the Kozeny–Carman model by replacing ϵ by ϵ_0 and the value of Kozeny constant k , also called shape factor that accounts for effects of channel shape (shape of the pores

and the ratio of the tortuous length that liquid traverses in passing through the bed to the actual thickness of the bed) and orientation. For fibrous media (for randomly packed bed) a value 5.55 is a widely used value showing no apparent variation with porosity . though values in general may lie between 3 to 7 for porosities less than 0.8. Potucek [81] has emphasized that the value 5.55 can be valid even within the range of 0.45 to 0.86. The use of ϵ_0 is justified as the pore space considered in the derivation is the extrafiber pore space. The water trapped in the cell wall presumably does not contribute to flow and, in effect, increases the apparent volume of the solid (immobile) phase.

The well known Kozeny-Carman equation can be obtained as

$$K = (1 / k S_0^2) \epsilon_0^3 / (1 - \epsilon_0)^2, S_0 \text{ being the surface area per unit volume of solid material. } \dots(5.19)$$

One may assume that ϵ_0 approximates ϵ_{eff} . The effective volume of the swollen fibers is defined as α with units of cm^3/g . At a concentration of $c \text{ g/cm}^3$, the extrafiber porosity is

$$\epsilon_0 = 1 - \alpha c. \dots(5.20)$$

Substituting this expression for ϵ_0 and assuming $k = 5.55$, the above equation becomes

$$K = (1 / 5.55 S_0^2) (1 - \alpha c)^3 / \alpha^2 c^2. \dots(5.21)$$

If S is the flow-exposed surface area of the fibers per unit mass, commonly called the specific surface area, then $\alpha S_0 = S$(5.22)

Incorporating this idea and rearranging, one obtains

$$(Kc^2)^{1/3} = (1 / 5.55 S^2)^{1/3} (1 - \alpha c). \dots(5.23)$$

If one assumes $\epsilon_{\text{eff}} = \epsilon_0$, then

$$\epsilon_{\text{rel}} = \epsilon_0 / \epsilon = (1 - \alpha c) / \epsilon = 1 - \alpha \rho_s (1 - \epsilon) / \epsilon. \dots(5.24)$$

This equation shows that ϵ_{rel} is a function of ϵ for several typical values of specific volume. This also depicts that α decreases with compression.

5.1.1.5 Kyan's Geometrical model

Kyan et. al.[44] derived expressions for relative porosity based on geometrical considerations for a structure composed of cylindrical fibers arrayed in a regular pattern. The derivation assumes that all the pore space behind a fiber in a representative cell of the fibrous structure is stagnant and makes other simple assumptions about the geometry of the fibrous medium. The derived expression for effective flow porosity is:

$$\varepsilon_{\text{eff}} = N_e^2 (1 - \varepsilon) (0.5 / \pi), \text{ where } N_e \text{ is the effective porosity number:} \quad \dots(5.25)$$

$$N_e = (\pi / 0.5 (1 - \varepsilon))^{1/2} - 2.5. \quad \dots(5.26)$$

The investigator observed that these formulae give relative porosity values $\varepsilon_{\text{eff}} / \varepsilon$ much less than unity, e.g. a fibrous web with a porosity of 50 % would have $\varepsilon_{\text{rel}} = 0.174$.

5.1.1.6 Roux and Vincent and later Lindsay model

Roux and Vincent [c.f.52] expressed effective porosity as

$$\varepsilon_{\text{eff}} = \varepsilon_0 = \varepsilon - \text{WRR} (\rho_s / \rho_L) (1 - \varepsilon), \quad \dots(5.27)$$

where WRR is water retention ratio (also called water retention value, WRV) of pulp, reported as grams of water per gram of dry fiber, a measure of the water still held by the fibers after centrifugal dewatering. ρ_s is the dry solid density and ρ_L is the liquid density.

If all extra fiber pores were open to flow, the relative porosity would be

$$\varepsilon_{\text{rel}} = 1 - \text{WRR} (\rho_s / \rho_L) (1 - \varepsilon) / \varepsilon. \quad \dots(5.28)$$

The total porosity can also be determined from sheet thickness under compression and basis weight as under:

$$\varepsilon = 1 - \text{BW} / \rho_c L \quad \dots(5.29)$$

where BW is the sheet basis weight, ρ_c is the matrix density (the density of pure cellulose in filler free sheets) and L is the sheet thickness.

5.1.1.7 Grah's model for total overall porosity

Grah [24] correlated ε_t with fiber consistency C_F through an empirical equation

$$\varepsilon_t = 1.00 - 6.80 \times 10^{-4} C_F, \quad \dots(5.30)$$

where, C_F is expressed in kg / m^3 .

This model predicts the actual values within an error of 1%. It is true for any zone provided two phase flow does not exist. Therefore for the formation zone it is perfectly true and within reasonable accuracy during washing zone. However, it may deviate for dewatering zone.

$$\text{Grah has expressed } \varepsilon_d \text{ as } \varepsilon_d = 1.00 - 1.75 \times 10^{-3} C_F. \quad \dots(5.31)$$

$$\text{For any zone, however, } \varepsilon_t = \varepsilon_d + \varepsilon_s. \quad \dots(5.32)$$

5.1.1.8 Model for overall porosity (ε_t)

The porosity has been modeled based on average consistency of mat during the cake formation zone. The effect of air on porosity has not been considered because the saturation of cake is approximately 1 in the cake formation zone. Porosity of the pulp suspension varies from position to position during rotation of the drum. Local total porosity can be defined as

$$\varepsilon_t = \rho_f (1 - C_y) / [\rho C_y + \rho_f (1 - C_y)]. \quad \dots(5.33)$$

$$\text{Alternatively, } \varepsilon_t = 1 - C_{yi} \rho_{sus} / \rho_f \quad \dots(5.34)$$

$$\text{Where, } \rho_{sus} = (1 - \varepsilon_t) \rho_f + \varepsilon_t \rho. \quad \dots(5.35)$$

$$\text{Also, } \rho_{sus} = \rho \rho_f / [\rho C_y + \rho_f (1 - C_y)]. \quad \dots(5.36)$$

5.1.1.9 Permeability Model due to Kozeni

Permeability is a factor which influences the flow of fluid through a porous media and is a function of porosity and specific surface area. It is also a strong function of size, shape and orientation of the particles.

The permeability K is evaluated using the Kozeni's model.

$$K = \varepsilon_t^3 / [k_1 S_0^2 (1 - \varepsilon_t)^2]. \quad \dots(5.37)$$

The value of k_1 equal to 2 has been used by many systems. Experimental measurements indicate that the theoretical formula can be improved if the 2 in the denominator is changed to a value somewhere between 4 and 5. Analysis of a great deal of data has led to a value 25/6.

For cellulose fibers Kozeny's constant k_1 is assumed to be on the order of 5.55. In pulp washing, porosity value is usually vary high and is of the order of $\epsilon_t > 0.8$. As a matter of fact the solids (fibers) are cylindrical in shape and compressible in nature. For higher porosity values ($\epsilon_t > 0.8$) the above equation gives poor agreement with the experimental data.

5.1.1.10 Resistance due to cake and Specific cake resistance α , and the filtration medium resistance R_m , Compressibility parameter s Specific Volume, Specific surface area S_0 and Permeability Constant K .

The resistance due to cake can be represented as $m_c \alpha / A$ where m_c , the mass of dry cake obtained after washing the cake free of soluble material and drying, A the area and α the specific resistance of cake. α is a function of pressure drop, and can be expressed as:

$$\alpha = k_1 (1 - \epsilon) (S_p / v_p)^2 / \epsilon^3 \rho_s = k_1 (1 - \epsilon) (S_0)^2 / \epsilon^3 \rho_s = 1 / [K \rho_s (1 - \epsilon)] \quad \dots(5.38)$$

The mean specific cake resistance can also be expressed given as under:

$$\alpha = 2 A^2 g_c (-\Delta P) (1 - m w) / \rho C \mu w, \quad \dots(5.39)$$

where w is the weight fraction of solid in the slurry; m the ratio of wet cake to dry cake and C is the dimensional constant [111].

Xie Lai Su [109] has determined the specific resistance of pulp mat as a function of Schopper Riegler drainage degree as

$$\alpha = k [(^{\circ}SR - 4) / (100 - ^{\circ}SR)]^n, \quad \dots(5.40)$$

where k is a constant and n is an index. In normal test conditions, $k = 4.8 \times 10^9$ and $n = 1$.

The filter medium resistance R_m, m^{-1} is defined as

$$R_m = \rho (C_y / 100) \alpha V_f / A (1 - m C_y / 100), \quad \dots(5.41)$$

Where $m = m_f / m_c$.

The value of R_m increases with increasing filtration–pressure resistance for a given material. The empirical observation has been made that R_m is numerically equal to 0.05–0.1 times the mean specific cake resistance for the test and a numerical value of $R_m \cong 0.1 \cdot \alpha$ has been suggested as sufficiently accurate for most practical filtration calculations unless very thin cakes are to be handled.

Compressibility and specific volume can be considered as parameters for describing the structure of the fiber wall and the specific surface as a parameter for describing the fiber shape. The compressibility is a measure of the volume change of a system subject to compressive stress. The volume change of a system can be seen by changes in the pulp consistency, kg / m^3 .

In compressible filter cakes (mat), the porosity and specific resistance vary through the depth of the deposited mat. Therefore it is important to determine the effect of the mechanical–pressure stress on the porosity and specific resistance of compressible cakes having uniform porosity throughout the depth.

Ingmanson et. al.[34] and later Cheng [9] defined compressibility using parameters M and N, which can be solved through the following Equation:

$$C = M P^N, \quad \dots(5.42)$$

where C is the pulp mat consistency in kg / m^3 , M is compressibility coefficient in $\text{kg} / \text{m}^3 / \text{Pa}^N$, P is the applied pressure in Pa and N is the compressibility exponent. This equation is also widely used to define the correlation between the consistency of the fiber mat and the applied pressure.

The values of M and N for different pulp samples at 60°C are given in Table (5.3) in Appendix-I.

When the cake is compressible, the specific cake resistance is given as a function of pressure drop through empirical equations as under:

$$\alpha = \alpha_0 (-\Delta P)^s \text{ or } \alpha = \alpha_0 [1 + \beta (-\Delta P)^s] \quad \dots(5.43)$$

where α , α_0 , β , s are empirical constants.

The former is more widely used as it involves only two constants and is easier to use though it is not appropriate at low pressure drops as it indicates a zero resistance at zero ΔP . s , called compressibility coefficient, is a measure of compressibility. It is zero for incompressible sludges and positive for compressible ones. In most industrial filtration the value of s lies between 0.1 and 1.0, the large values applying to more compressible sludges.

If the specific resistance of cake α is known, the value of K can be simply written as follows:

$$K = 1 / (\alpha \rho_s (1 - \epsilon_t)) \text{ where } \alpha \text{ ,the mean specific cake resistance and the instantaneous value, } \alpha_p \text{ as}$$

$$\alpha = \Delta P_c / \int^{\Delta P_c} P_c / \alpha_p \quad \dots(5.44)$$

McCabe has reported two equations. In one model α has been related to pressure drop across the cake, ΔP_c as

$$\alpha = \alpha_0 (-\Delta P_c)^s \text{ where } s \text{ is the compressibility factor} \quad \dots(5.45)$$

5.1.1.11 Davis model for Permeability

For high porosity range Kozeni's model was modified by Davis [13]. The following equation is applicable to any system of cylindrical geometry such as natural and synthetic fibers.

$$K = [K_1 S_0^2 (1 - \epsilon_t)^{3/2} \{1 + K_2 (1 - \epsilon_t)^3\}]^{-1} \quad \dots(5.46)$$

For fibers of vegetable origin like wood, bamboo and bagasse straw, the value of constants K_1 and K_2 differ. Average values of all these pulp making fibers have been experimentally determined by Ingmanson et.al.[34] as 3.5 and 57 respectively.

Xie has found empirically the permeability through pulp mat in terms of °SR as follows:

$$K = 2.08 \times 10^{-13} [(100 - \text{°SR}) / (\text{°SR} - 4)] \quad \dots(5.47)$$

5.1.2 Equations for filter design parameters

Before estimating the process parameters for brown stock washer, one requires to estimate the relationship between wash ratio and the time of washing. The wash liquor flow in turn needs filtration rate. This demands a derivation from basic filtration theory. These are elaborated as follows:

$$\text{Total pressure drop} = -\Delta P = -\Delta P_c - \Delta P_m = \mu u / g_c [m_c \alpha / A + R_m] \quad \dots(5.48)$$

Putting $m_c = Vc$ and $u = dV / A dt$, one can get the filtration rate.

5.1.2.1 Filtration Rate

$$(dV / dt) = A (-\Delta P) g_c / \mu [\alpha c V / A + R_m] \quad \dots(5.49)$$

$$(dt/dV) = \mu [\alpha c V / A + R_m] / A (-\Delta P) g_c = K_p V + B \quad \dots(5.50)$$

$$\text{where } K_p = \mu \alpha c / A^2 (-\Delta P) g_c \text{ and } B = \mu R_m / A (-\Delta P) g_c \quad \dots(5.51)$$

c can be calculated as follows:

$$c = c_s / [1 - \{(m_F / m_c) - 1\} c_s / \rho] \quad \dots(5.52)$$

One can get by integration

$$t = K_p V^2 / 2 + BV \quad \dots(5.53)$$

If $R_m = 0$ (when filter medium resistance is neglected for continuous filtration i.e. rotary vacuum filter operation), $B = 0$, the volume of filtrate in relation to t as under filtration in relation becomes as follows.

5.1.2.2 Volume of filtrate V and filtration time relationship

$$V = (2 t / K_p)^{0.5} \quad \dots(5.54)$$

Using $t = f t_c$ and compressibility relationship $\alpha = \alpha_0 (-\Delta P)^s$ one can arrive at

$$V / A t_c = u = [2 f (-\Delta P)^{1-s} g_c / \mu \alpha_0 c t_c]^{0.5} \quad \dots(5.55)$$

Area of the filter can thus be calculated as follows.

5.1.2.3 Area of a Rotary Vacuum Filter

$$A = (V / t_c) [\mu \alpha_0 c t_c / 2 f (-\Delta P)^{1-s} g_c]^{0.5} \quad \dots(5.56)$$

Wash rate can be represented as follows.

5.1.2.4 Washing Rate

$$(dV / A dt)_w = (-\Delta P) g_c / \mu \alpha c V / A \quad \dots(5.57)$$

$$V_w / A = t_w * (dV / A dt)_w = [(-\Delta P) g_c / \mu \alpha c V / A] * t_w = [(-\Delta P)^{1-s} g_c / 2 f t_c \mu \alpha_0 c]^{0.5} * t_w \quad \dots(5.58)$$

5.1.2.5 Wash Ratio

The equations given in Section 5.1.2.4 is now expressed in terms of wash ratio

$$WR = V_w / A / V_1 / A \quad \dots(5.59)$$

$$V_1 / A = k_2 [2 (-\Delta P)^{1-s} g_c f t_c / \mu \alpha_0 c]^{0.5} \quad \dots(5.60)$$

5.1.2.6 Wash Ratio and Washing Time relationship.

$$\text{Thus } WR = t_w / 2 f t_c k_2 = k_3 t_w \quad \dots(5.61)$$

Where k_2 and k_3 are constants.

If the value of washing time is known the wash ratio can be estimated. The proportionality constant k_3 can be easily estimated. The wash liquor ratio, WR has been varied between 0.8 to 1.0 by Edwards, Peyron and Minton [15a] with range of Peclet number 0 to 16.

The above equations are now used for parameter estimation and simulation.

If the filter medium resistance is not neglected, one can show the volume of filtrate, V as

$$V = -R_m A / c \alpha + A [R_m^2 / c^2 \alpha^2 + g_c (-\Delta P) t / c \mu \alpha]^{0.5} \quad \dots(5.62)$$

After finding the volume of filtrate one can proceed in the same way as above.

5.2 Displacement washing data

After development of models it is essential to validate them either through data obtained from laboratory or pilot plant or from full scale plant or from various correlations already developed for

this purpose. Most of the data available in this regard is based on displacement washing of kraft pulp.

In this section the relevant data from different investigators are compiled from their experimental results reported for model verification, interpretation of findings of present investigation and finally putting conclusive remarks. Table (5.2) given in Appendix-I presents a snapshot view of operational conditions of displacement washing. Where data are not available, the data are extrapolated from graphs, or estimated from the mathematical equations available. These are discussed in the following paragraphs.

5.2.1 Interpretation of data from displacement washing

It is observed from the Table that the ranges for bed thickness, mat consistency, velocity of liquor, temperature and solute concentration are found wide. Most of them may not be applicable for brown stock washing in rotary vacuum filter. This is because of the reasons that displacement washing is quite different from vacuum filter washing. Therefore, data required for washing calculation have to be modified accordingly as suggested by Grah [25].

In addition to above, a detailed review has also been done on rational definitions of parameters pertinent to brown stock washing. The interrelations between the different parameters are also reported. This is an important area as these can help the designer and the practicing engineers to predict, to compare, to optimize and to design the washing systems and equipments for mill practice.

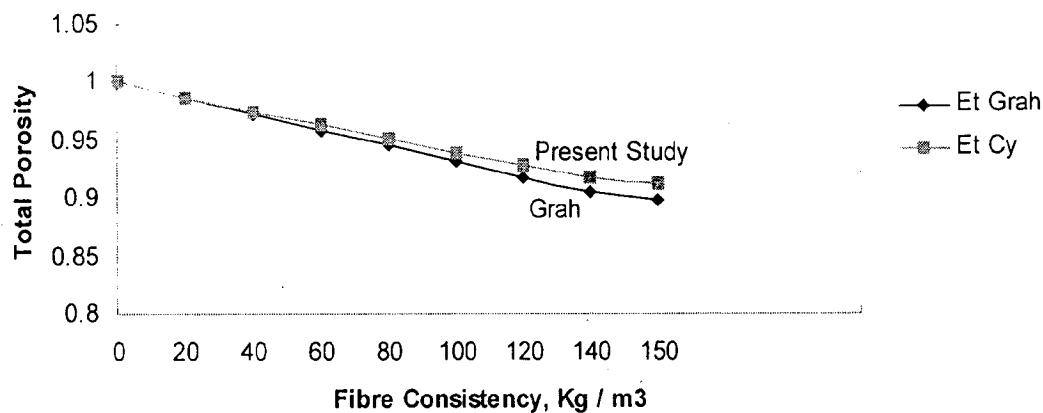
5.3 Estimation of data for various fibers and bed parameters used for simulation

5.3.1 Porosity

For estimation of porosities some of the equations given in Section 5.1 are used which cover all types of suspension concentration of fibers in pulp and paper mill including those for brown stock washing. The values calculated from different Equations are shown in Table (5.4). From the data it

is clear that the equation given by Grah [24] and the equation derived from material balance are quite comparable. The values are compared in Fig.5.1 as a function of fiber consistency. It is evident that there is no significance difference for total porosity values though the densities of liquor and water are assumed the same, at least for pulp washing system. Therefore any one of the equations can be employed to determine the total porosity values. For displaceable liquors Grah's experimental data can be used.

**Fig. 5.1. Total Porosity vs. Fibre Consistency
(Comparison of Grah's Eq. and Present Investigation)**

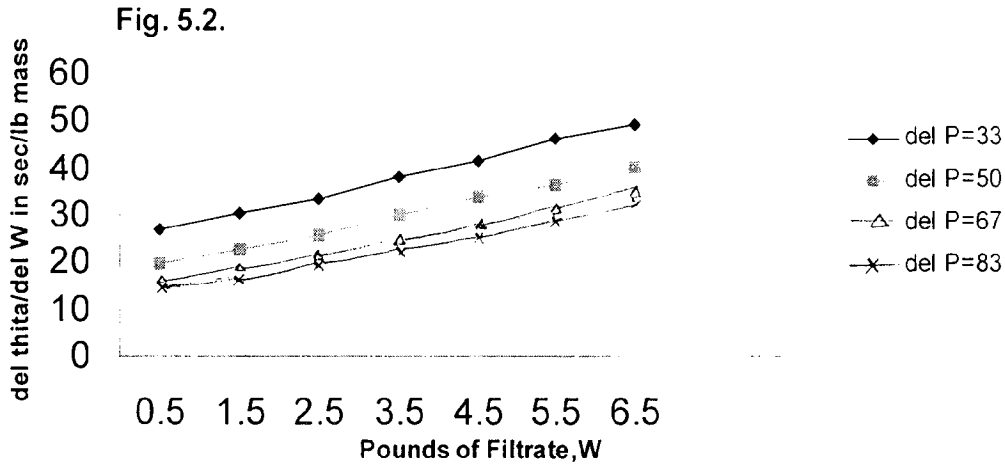


5.3.2 Estimation of Resistance due to Cake and Specific cake resistance α , and the filtration medium resistance R_m , and Compressibility parameter s Specific Volume, Specific surface area S_0 and Permeability Constant K

The value of specific cake resistance α , compressibility coefficient s and filter medium resistance R_m must need experimental data.

For pulp fibrous mat TAPPI has reported the variation of pressure drop as a function of mass of filtrate. The pressure however ranges from 1580 N / m² to 3974 N / m² with 15 % consistency

pulp. These values are plotted in Fig. 5.2. From the figure the slope, intercepts and the R_m values are calculated. The compressibility coefficient is found of the order of 0.78.



The values of α and filter medium resistance, R_m are given as follows:

| $\Delta P, N / m^2$ | $\alpha, m / kg$ | R_m, m^{-1} |
|---------------------|----------------------|----------------------|
| 1580 | 1.6798×10^8 | 8.333×10^8 |
| 2394 | 2.385×10^8 | 8.825×10^8 |
| 3208 | 2.8894×10^8 | 9.7769×10^8 |
| 3974 | 3.595×10^8 | 9.58×10^8 |

Though the pressure drop values are evaluated at slightly lower pressure, this can be employed by extrapolation to higher pressures applicable to vacuum washers.

Permeability constant, K are estimated based on both Kozeny-Carman Equation as well as modified Equation of Davis using various specific surface area values applicable for different pulp fibers obtained from literature and the total porosity values ϵ_r . These values are compared in Table (5.6) given in Appendix-II. As expected the Permeability constant is found to be always higher in case of long fiber pulp (pine) though the specific surface area values are always lower than non

wood based pulp. Another important feature is that the K values estimated from Davis Equation predicts lower magnitude (almost 50%) than those estimated from Kozeny Carman Equation. The relations of S_0^2 or S_0 with K are shown in Figs. 5.3a and 5.3b. It is evident from the figures that with the increase in S_0^2 or S_0 the value of K decreases.

Fig. 5.3a. Permeability Constant vs. Square of Specific Surface Area

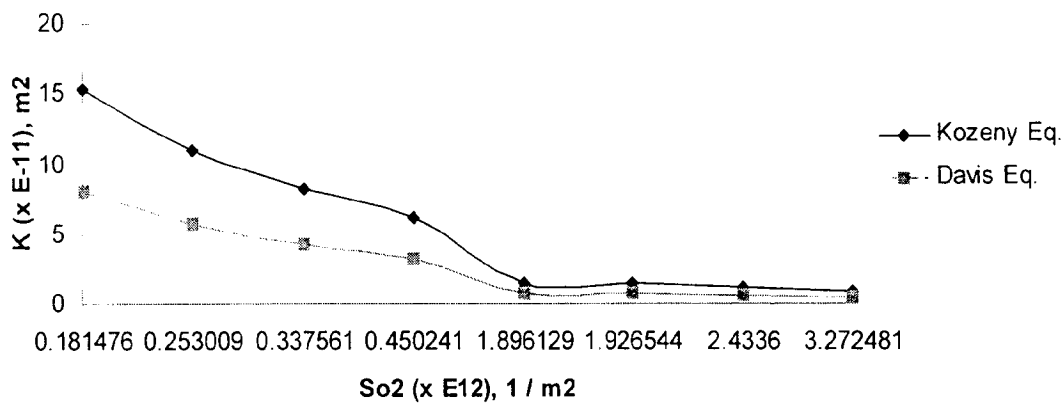
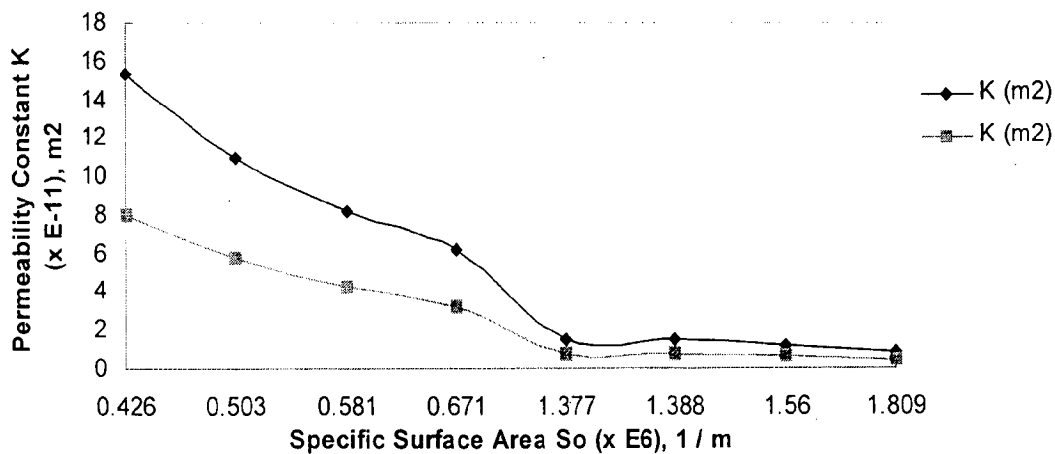


Fig. 5.3b. Permeability Constant vs. Specific Surface Area



5.3.3 Other bed parameters (bed length, velocities through bed, Mass transfer coefficients)

Grah [25] has experimentally determined various bed parameters with a specific set of variables such as bed length, fiber consistency, volumetric flow rate of wash liquid, dispersion coefficient, mass transfer coefficients, velocity through bed and the concentration values of original liquor and

wash liquor for simulation purposes. The conditions of experiment and the data obtained of washing the packed bed of a pine sulphate pulp having a kappa number of 49.7 are given in the Table (6.1) shown in Appendix-IV. The Table also depicts two sets of data indicating the influence of the nature of species, namely Na^+ and lignin which are species of our main interests in the present investigation.

5.3.4. Sodium, Soda and lignin loss by adsorption:

The phenomena of sorption effects of sodium and lignin on pulp fibers is well known. Pekkanen and Norden [70] have summarized the earlier works on sorption effects. Day [c.f.70] claimed the total amount of absorbed alkali to be 7.5- 12.5 kg Na_2SO_4 per tonne air dry pulp. Many widely differing figures (between 0.5 and 15 kg Na_2SO_4 per tonne air dry pulp) have since been given for the total sorbed sodium on pulp, but only after only after Fogelberg and Fugleberg [c.f.49] and Rosen [84] published their works was a more fundamental understanding of sorption possible. Fogelberg and Fugleberg [c.f.49] proposed that the Langmuir isotherm be used to correlate the amount of sodium sorbed on fibers with the concentration of sodium in the liquid around fibers. Later many other workers used the Langmuir isotherm to correlate the sorption data. Results of mill measurements for sodium loss due to sorption was around 40% of the total loss were presented by Rosen [84]. The parameters for the Langmuir isotherm have been determined by Hartler and Rydin [33] for sodium, lignin and BOD and Grah [24], Norden & Viljakainen [65] and Hakamaki and Kovasin [30] for sodium.

Laxen [49] indicated that depending upon wood species, Kappa number and pH values the amount of adsorbed sodium lies somewhere between 1.2 and 2.2 kg / tp which is equivalent to 3.5 to 7 kg / tp Na_2SO_4 (determined at a pH = 9.5).

In all the above works stipulated that the loss due to the sorption is significant and the calculated loss is much too small when sorption is ignored. That makes it essential to include sorption effects in calculations when efficient washing systems are studied.

In the present investigation the sorption values are calculated using non-linear adsorption isotherm which is of Langmuir type for estimation of Na⁺ / soda loss and lignin. The constants A and B compiled from different experimental findings are shown in Tables (5.5 a, b, c and d). The tables are shown in Appendix-I. To bring uniformity the parameters are tabulated in the same units as follows:

The amounts adsorbed (both Na⁺ and lignin) as a function of initial concentration or kappa number of pulp are shown in Table (5.7a) through (5.7e) given in Appendix-II. The amount adsorbed, kg / ton of pulp = $A B C_i / (1 + B C_i)$, where A is in kg / ton, B is in $l / g = m^3 / kg$ and C_i is concentration of Na / lignin in liquor in gm / liter i.e. in kg / m³. The amount of Na⁺ adsorbed, soda loss as Na₂SO₄ as a function of kappa number at various initial concentration of Na⁺, the same at a fixed kappa number are shown in Figs. 5.4a, b and c.

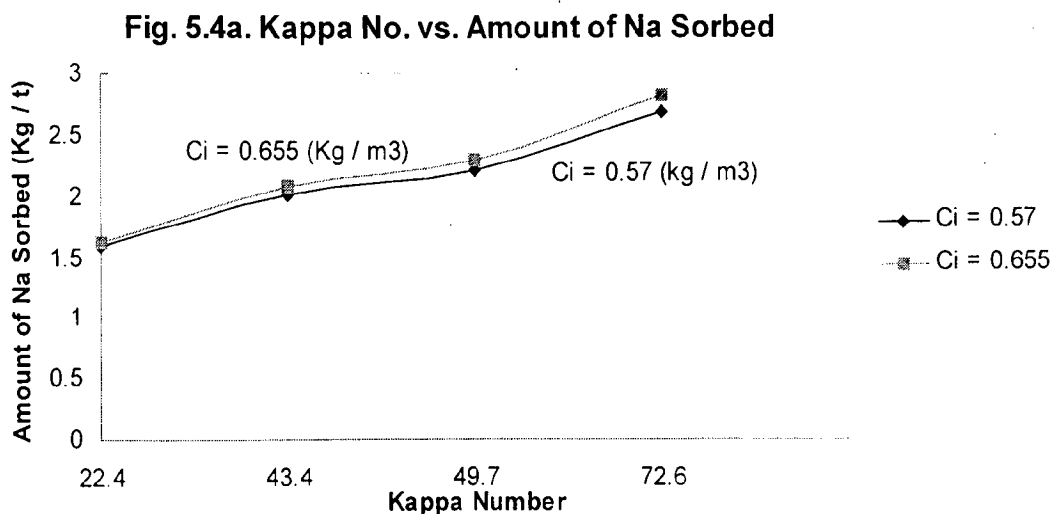


Fig. 5.4b. Kappa No. vs. Amount of Soda Loss Sorbed as Na₂SO₄

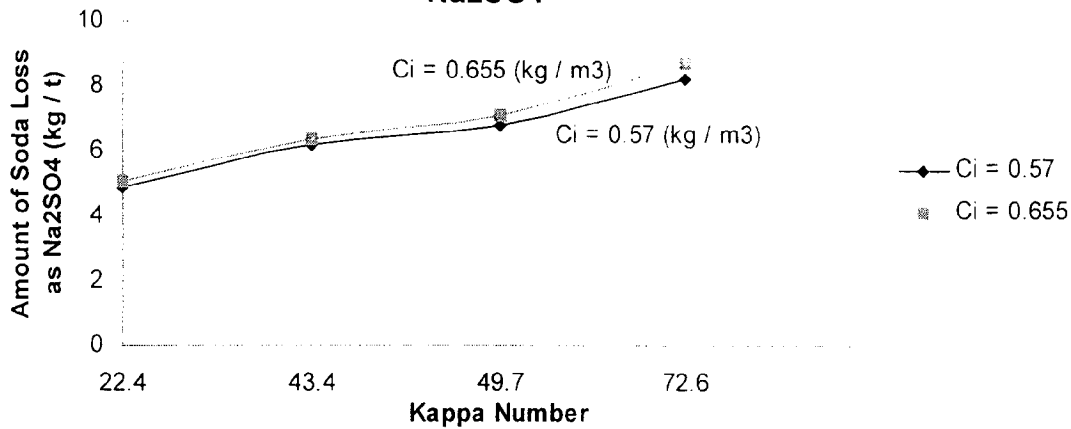
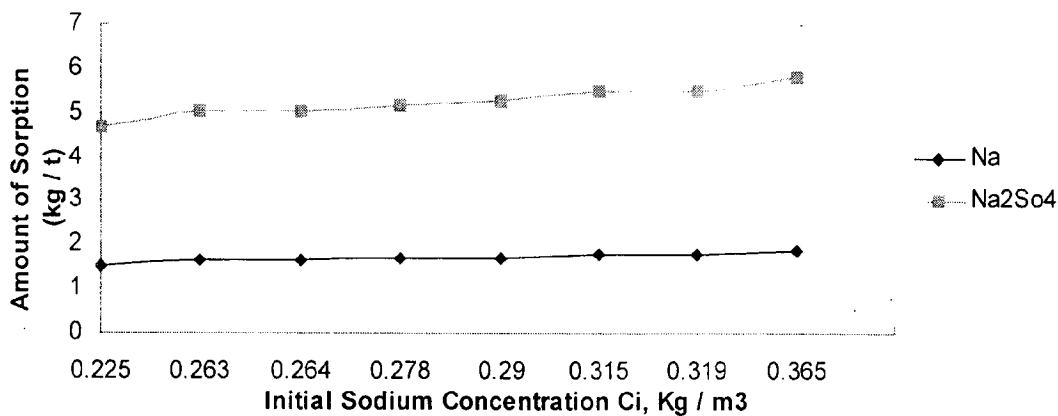


Fig. 5.4c. Initial Sodium Concentration vs. Na Sorbed and Soda Loss Sorbed at Kappa No. 49.7



It is reflected from the figures that

- Higher the initial concentration, higher is the adsorption and higher is the soda loss at a fixed kappa number. At practical values of kappa number for bleachable grade kraft pulp, the adsorption of Na⁺ and soda loss will be on the order of 1.5-1.75 kg / t and 4.8-5.5 kg / t respectively.
- Higher the kappa number, higher is the adsorption in a nonlinear manner.

Figs. 5.5a, b and c are drawn to show the effect of kappa number, initial concentration for various pulps on lignin adsorption. It is important to mention that Hartler & Rydin [33] have shown the value of Langmuir constants for lignin for a particular type of pulp to be zero, thereby no lignin

absorption. Grah [25] also reported negligible lignin adsorption. Therefore it is important to estimate these values from available adsorption-desorption isotherm.

Fig. 5.5a. lignin Adsorbed vs. Initial Concentration at Various Kappa Numbers for Pine Craft Pulp

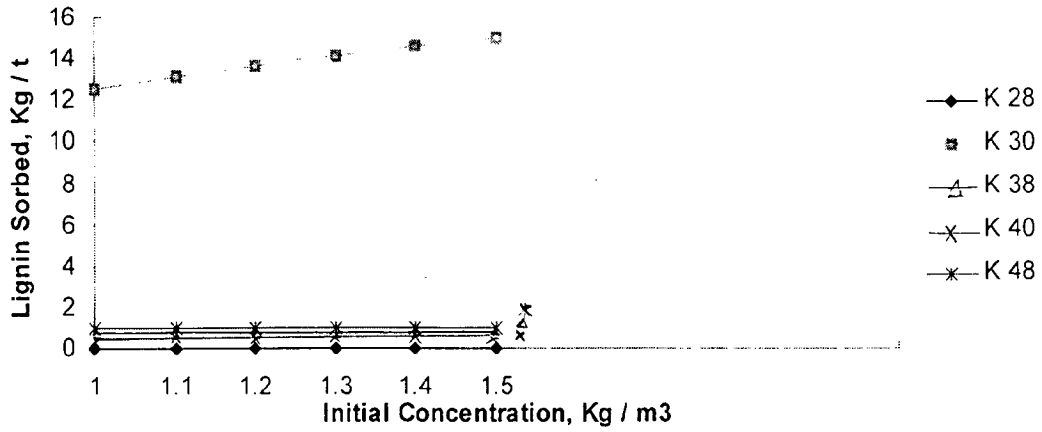


Fig. 5.5b. lignin Sorbed vs. Initial Concentration at Various Kappa Numbers for Birch Kraft Pulp

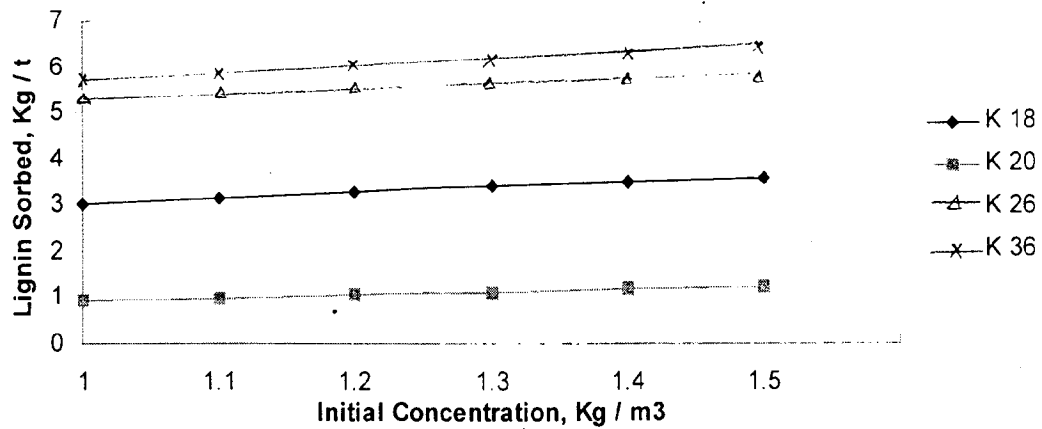
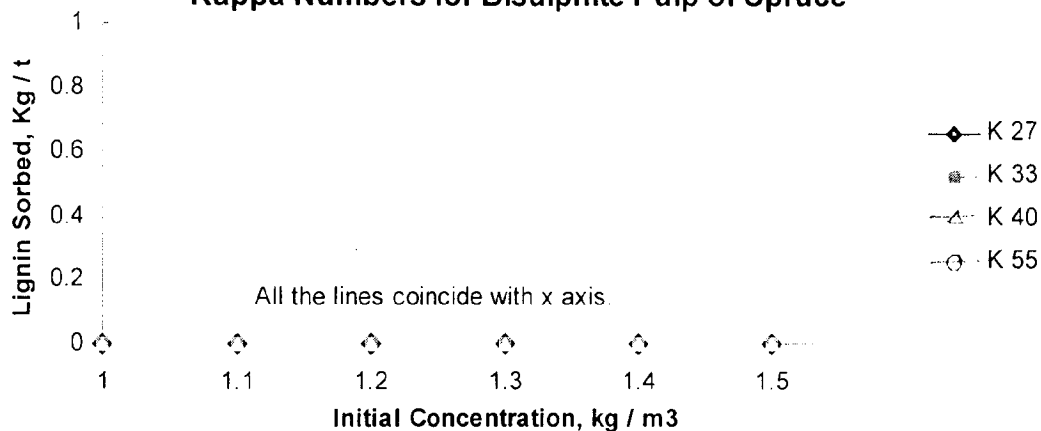


Fig. 5.5c. lignin Sorbed vs. Initial Concentration at Various Kappa Numbers for Bisulphite Pulp of Spruce



The figures reveal the following:

- Higher the kappa number, higher the lignin sorption. At kappa number admissible for bleachable grade pulp the amount of lignin sorption will be on the order of 3 kg / t to 5.5 kg / t.
- Higher the initial concentration, the sorbed lignin increases linearly but very slowly.
- Comparisons of Na⁺ and lignin are made in Figs. 5.6a, b and c as a function of initial concentration with kappa number as a parameter.

Fig. 5.6a. Sorption of Na and lignin vs. Kappa Number for Pine Kraft Pulp

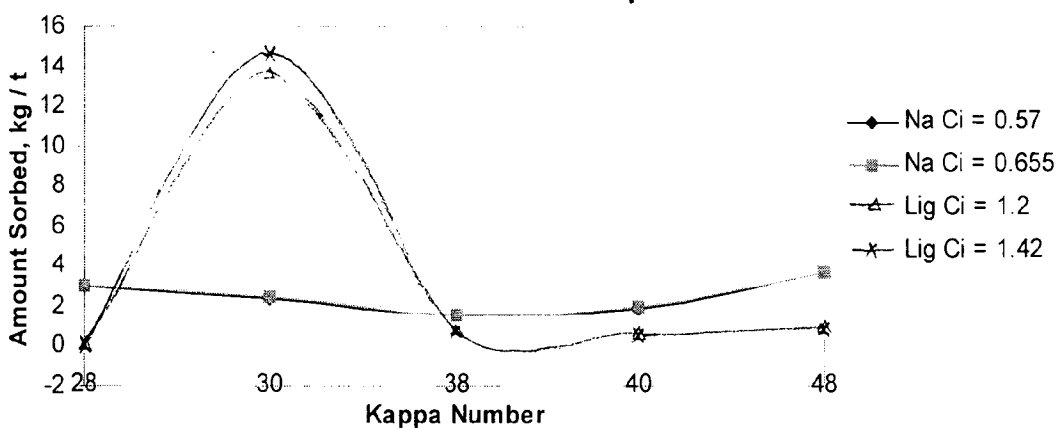


Fig. 5.6b. Sorption of Na and lignin vs. Kappa No. for Birch Kraft Pulp

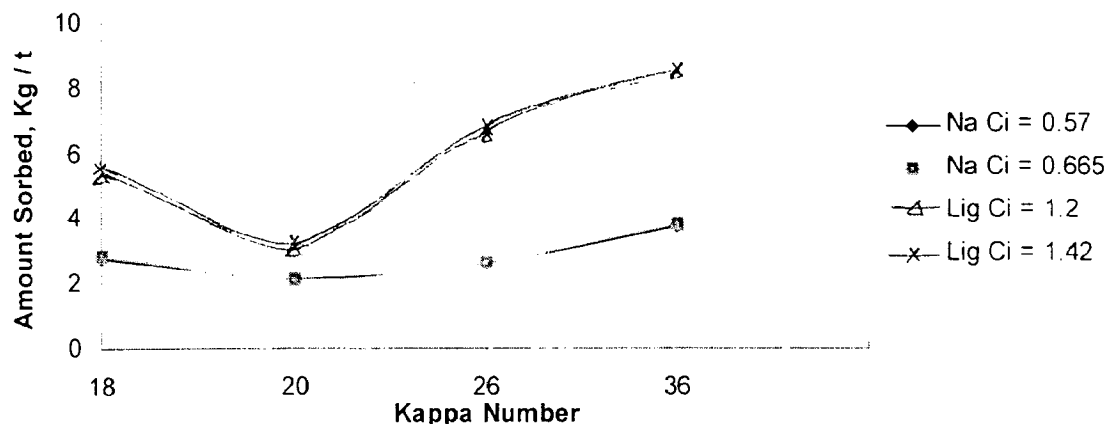
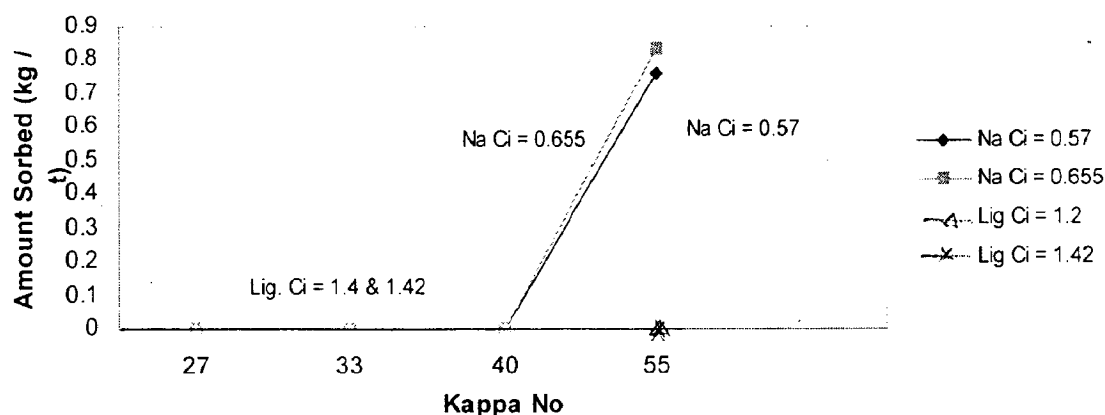


Fig. 5.6c. Amount Sorbed of Sodium, Soda Loss and lignin vs. Kappa Nos. for Bisulphite Pulp of Spruce



The figures reveal the following:

- The adsorption of lignin on pulp is much higher than those of Na^+ for their respective concentration values. For lignin the curve displays an adsorption peak at near kappa number near 30. It increases initially very sharply, reaching the peak, then decreases with the increase of kappa number and there is an increasing trend thereafter. Fig. 5.6b shows the same trend for Na^+ but the lignin variation with kappa number shows quite opposite profile. It decreases at first unlike Na^+ , minimum at kappa number 20 and then increases beyond. However, in the former case the pulp was pine kraft with kappa number 28 to 48 but the later is meant for Birch kraft pulp with kappa number 18 to 36. This behavior might be due to species variation and pulp quality.

This aspect needs further thorough investigation.

5.3.5 Peclet number, dispersion coefficient D_L and the algorithm for its estimation

As varying flow conditions can be assumed in different parts of the pulp bed, an average value of the dispersion coefficient is required to be estimated. This is important as various authors simulated with various ranges of Peclet number though the pulp quality remains almost the same. As for example Potucek [81] used very low Pe (1.0-11.3) for pulp fibers and high for glass fibers following Brenner [6], whereas Grah [25], Poirier [79], Crotagino [10] used high ranges (generally 80-100) though the data of Table (5.8) indicates also some value nearing 13. Poirier et. al.[79] categorically mentioned that displacement efficiency decreases below Pe number 20 and therefore one expect inconsistencies in the profiles. An order of estimate values of Pe therefore should be predicted. As washing efficiency has been expressed by Potucek [81] as a function of Pe, it becomes more relevant to evaluate for washer performance study. The modified Peclet number, Pe_m and modified dispersion coefficient D_{Lm} are then calculated as

$$Pe_m = u L / D_L \epsilon \text{ and } D_{Lm} = u L / Pe_m. \quad \dots(5.63)$$

The algorithmic procedure for estimation of D_L is given in Appendix-III.

From the concentration c , time t data from this present investigation for all the models, Peclet number is estimated approximately avoiding iterative calculations and considering open vessel.

Table (5.8): The calculated values based on the data reported by various investigators for displacement washing are shown in the following table

| Investigators | $U/D_L, 1/m$ | Pe | U / D_L | Pe | Comments |
|---------------|--------------|--------|--------------------|------------------|----------------------|
| Grah | 2277.78 | 378.11 | 678.703 (Na^+) | 71.26 (Na^+) | Displacement washing |
| Grah | 1200 | 199.2 | 527.70 (Lignin) | 55.43 (Lignin) | Displacement washing |

| | | | | | |
|----------------|----------|--------|---------------------------|---------------------------------------|----------------------|
| Grah | 1493.33 | 185.17 | 536.06 (Na ⁺) | 55.75 (Na ⁺) | Displacement washing |
| Grah | 1300.275 | 161.23 | 564.84(Lignin) | 58.74 (Lignin) | Displacement washing |
| Grah | 1333.766 | 165.39 | 1617.5 | 168.22 | Displacement washing |
| Grah | 957.14 | 98.58 | 2201.96 | 224.6 | Displacement washing |
| Edwards et al. | - | 4.0 | Potucek | 1.0-209 (Lignin) | Displacement washing |
| Han & Edwards | 130 | 3.835 | Edwards et al. | 0-16 | Displacement washing |
| Han & Edwards | 130 | 6.643 | Turner et. al. | U/D _L =130 (cons.),Pe=3.25 | Pulp washer |

Table (5.9): On estimating the Pe number by approximating to low degree of dispersion and avoiding the Laan [c.f.118] equation the values obtained at the bed exit point are as follows

| Parameter | Model I | | Model II | Model III | Model IV |
|----------------|-----------|----------|--------------|--------------|---------------|
| | A | B | | | |
| Peclet No, Pe | 4.23 (Na) | 4.31(Na) | 4.22765(Na) | 4.57437(Na) | 4.57522 (Na) |
| | 4.25(L) | 4.30(L) | 4.25428(L) | 4.57379(L) | 4.57383(L) |
| Dispersion No. | 0.24(Na) | 0.23(Na) | 0.236530(Na) | 0.218609(Na) | 0.218569 (Na) |
| | 0.235(Na) | 0.23(L) | 0.235058(L) | 0.218637(L) | 0.218635(L) |

A indicates the Peclet number used by Grah as 27 for Na^+ and 20 for lignin whereas B indicates the same at $\text{Pe} = 100$. The low value tally with Han and Edwards, Edwards et. al. and Potucek. The value will be higher at other locations and assuming closed vessel conditions. The data indicates that the approximately estimated Pe (or dispersion number) numbers are for model 1 and model 2 whereas the models 3 and 4 predict the same value. Practically there is no difference of Pe numbers for Na^+ and lignin components.

5.4 Model Validation and Simulation

For simulation purpose Eqs. (3.21) to (3.25) are used in various combinations as shown in the Table (3.1).

In all the cases the boundary and initial conditions are used as given in Table (3.2).

However, the values of adsorption parameter $N(Z,T)$ have been chosen from the practical values of both Sodium (Na^+) and lignin. The value of $N(Z,0)$ however have been found out by Langmuir adsorption isotherm equation and the parametric values experimentally determined by Grah [25], Rudin [33] and some other workers. The calculated values for adsorption are shown in Tables (5.7a through 5.7e) as shown in Appendix-II.

There are many other forms of isotherms possible. Before simulation, it is an imperative necessity to validate the present models with some known simulation work. This comparison will dictate about the accuracy of the proposed solution. It is important to mention that the problem with its simplified version has been solved analytically by Brenner [6], numerically using Orthogonal Collocation by Grah [23] and present investigation is based on finite difference method. In a similar manner the models can also be compared with those of Kukreja [40], Perron and Lebeau [75], Potucek [81], Edwards and Rydin [15], Sherman [88], Kuo and Barratte [43]. Most of these works have however, attempted to simulate a rotary vacuum brown stock washer using some data

from displacement washing study with suitable modification. These comparisons will be shown during actual simulation of washer in a pulp mill using practical data.

For the above comparison Grah [23] has considered with a specified parameter; Peclet Number, collocation points M & N and the time step input $\Delta\tau$ for Na^+ species.

In the present investigation, therefore for the same species as finite difference method has been used, the comparison can be made with only at the different practicable Peclet numbers (Pe).

However, this present study has focussed attention for all the models considering both the situations, namely with or without dispersion.

5.4.1 Comparison of results with those due to Grah [23], Brenner [6] and present investigation

Using $Pe = 100$, $N = 4$, $M = 13$ and dimensionless time step = 0.025, Brenner and Grah solved the differential equation. A comparison of the data is shown below:

Table (5.10): Comparison of an Analytical solution due to Brenner, Numerical solution due to Grah and present investigation using the simplified equation (Eq. 3.21).

| | Analytical Solution | Num. Sol. (Ortho. Collo.) | Num. Sol. (Finite Difference) Model 1 (Pe = 100) | Num. Sol. (Finite Difference) Model 2 (Pe = 100) | Num. Sol. (Finite Difference) Model 3 (Pe = 100) | Num. Sol. (Finite Difference) Model 4 (Pe = 100) |
|----------|----------------------------|----------------------------------|---|---|---|---|
| T | C | C | C | C | C | C |
| 0.5 | 1.0000 | 0.9993 | 0.9107 | 0.9107 | 0.9651 | 0.9652 |
| 0.6 | 0.9998 | 1.0004 | 0.8253 | 0.8253 | 0.9119 | 0.9120 |
| 0.7 | 0.9935 | 0.9931 | 0.7148 | 0.7149 | 0.8264 | 0.8265 |
| 0.8 | 0.9361 | 0.9361 | 0.5914 | 0.5915 | 0.7141 | 0.7142 |

| | | | | | | |
|-----|--------|--------|--------|--------|--------|--------|
| 0.9 | 0.7521 | 0.7521 | 0.4683 | 0.4683 | 0.5873 | 0.5874 |
| 1.0 | 0.4721 | 0.4724 | 0.3558 | 0.3559 | 0.4602 | 0.4604 |

The comparison of solution of equations as a function of t/z is shown in Table (5.10) and in Fig.5.7 for $Pe = 100$. For better clarity absolute differences between numerical and analytical solution for $Pe = 27$ and 100 have also been plotted in Figs. 5.8-5.9 The comparison between all the four models are depicted therein.

The former one represents a breakthrough curve C vs. t/z and the later describes the absolute difference as a function of t/z .

Fig. 5.7. C vs T Profiles For Na At Z = 1 For Analytic Sol., Num. Sol. Due To Grah And For All The Four Models

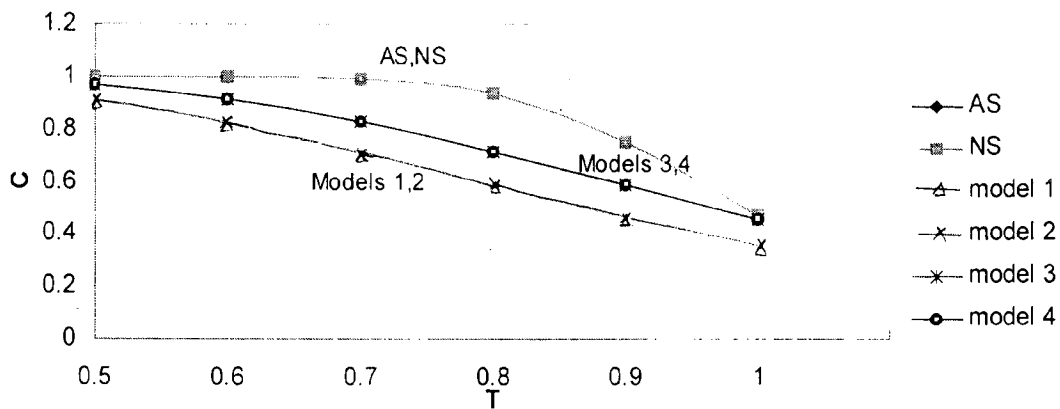


Fig. 5.8. Comparison of absolute differences between numerical solutions in the present study at $Pe = 27$ and analytical solution due to Brenner (For Na)

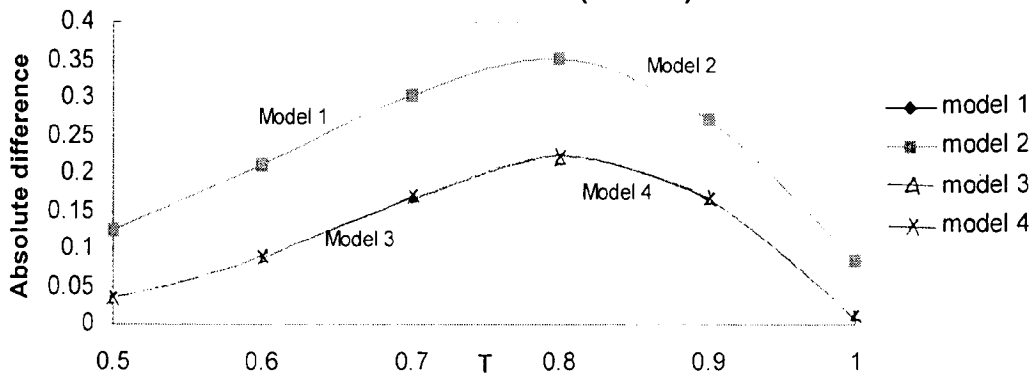
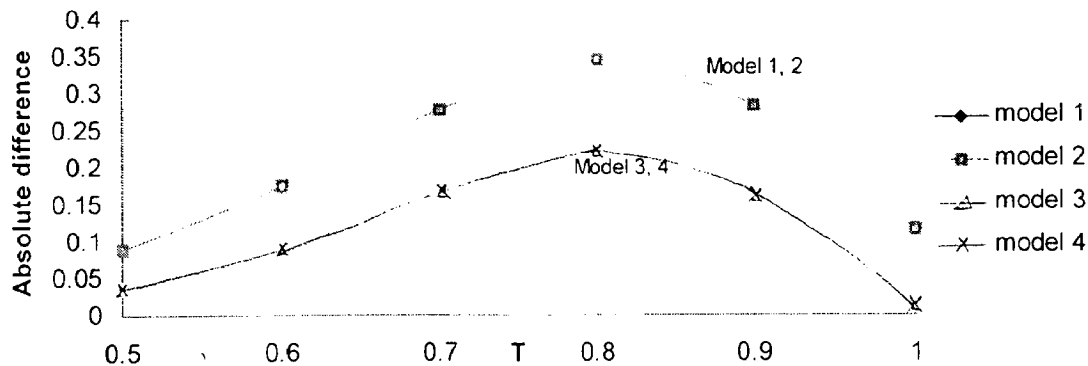


Fig. 5.9. Comparison of absolute differences between numerical solutions in the present study at $Pe = 100$ and analytical solution due to Brenner (For Na)



Above graphs and Tables amply clears out that the magnitudes of error obtained near about $T = 0.7-0.9$ are of the order of maximum 37.73 % (for model 1 and model 2) and 23.72 % (for model 3 and model 4) and minimum 8.93 % (for model 1 and model 2) and 2.52 % (for model 3 and model 4) at $T = 1$, and 3.5 % at $T = 0.5$ (for model 3 and model 4) deviation respectively from the analytical solution. The order of deviation from Grah's Orthogonal Collocation is the same. The percentage error introduced due to use of finite difference method is not very significant from $T = 0.0$ to 0.6 and $T = 1$ (nearly) and therefore can be acceptable for practical purposes. This further indicates the accuracy of the models for predicting data. However, the solution of Grah is superior to the present solution as it is well known that solution by Orthogonal Collocation leads to better accuracy when compared to the present finite difference method.

One very interesting point observed is that while the Orthogonal Collocation method used by Grah gives an increasing oscillation up to $\tau = 1.5$ and thereafter the amplitude stated decreasing. This is contrary to the analytical solution of Brenner which shows a continuous decreasing trend from 1.0 to 0.0853 with the value of $T = 0.5$ to $T = 1.2$. The present investigation follows the same trend like the analytical solution indicating the stability of the solution. Hence the finite difference

approach can claim better than that due to orthogonal collocation results employed by Grah at least in this respect.

On comparing the various models the model 3 and model 4 (without dispersion) both coincides and give lower degree of deviation from analytical solution of Brenner and numerical solution by Orthogonal Collocation by Grah. On the other hand models 1 and model 2 again coincides with each other and deviates to a slightly greater extent though the values are not very significant.

5.5 Conclusions

- The various models for parameters like porosity, permeability, specific cake resistance, filter medium resistance, compressibility constants, design equations for filtration are reviewed in detail. Various porosity terms are clearly defined. The equation given by Grah [24] and the equation derived from material balance are quite comparable without any significant difference for total porosity values though the densities of liquor and water are assumed the same at least for pulp washing system. Therefore, any one of the equations can be employed to determine the total porosity values. For displaceable liquors Grah's experimental data can be used.
- A relationship between washing time and volume of filtrate as well as wash ratio is developed for further use for simulation of practical brown stock washing in rotary vacuum filters.
- The ranges for bed thickness, mat consistency, velocity of liquor, temperature and solute concentration are found widely different among various investigators. Most of them may not be applicable for brown stock washing in rotary vacuum filter. This is because of the reasons that displacement washing is quite different from vacuum filter washing. Therefore, data required for washing calculation have to be modified accordingly as suggested by Grah [25].
- As expected the Permeability constant is found to be always higher in case of long fiber pulp (pine) though the specific surface area values are always lower than non-wood based pulp.

Another important feature is that the K values estimated from Davis Equation predicts lower magnitude (almost 50%) than those estimated from Kozeny Carman Equation

- In the present investigation the sorption values are calculated using non-linear adsorption isotherm which is of Langmuir type for estimation of Na⁺, soda loss and lignin. The constants A and B are however compiled from different experimental findings
- Higher the initial concentration, higher is the adsorption and higher is the soda loss at a fixed kappa number. At practical values of kappa number for bleachable grade kraft pulp, the adsorption of Na⁺ and soda loss will be on the order of 1.5-1.75 kg / t and 4.8-5.5 kg / t respectively.
- Higher the kappa number, higher is the adsorption with an nonlinear manner.
- Higher the kappa number, higher the lignin sorption. At kappa number admissible for bleachable grade pulp the amount of lignin sorption will be on the order of 3 kg / t to 5.5 kg / t.
- Higher the initial concentration, the sorped lignin increases almost linearly but very slowly.
- The adsorption of lignin on pulp is much lesser than those of Na⁺ for their respective concentration values.
- The low value of Pe number tallies with those of Han and Edwards, Edwards et al. and Potucek for open vessel conditions. The value will be higher at other locations and if one assumes closed vessel conditions. The data indicates that the approximately estimated Pe numbers (or dispersion number) are some for model 1 and model 2 whereas the model 3 and 4 predicts the same value but of different magnitude. Practically there is no difference of Pe numbers for Na and lignin components
- The present models (four models) are validated with those of Grah based on numerical technique (Orthogonal Collocation) and Brenner with analytical methods with same species and Pe numbers estimated by Grah.

- The magnitudes of error obtained near about $T = 0.7-0.9$ are of the order of maximum 37.73% (for model 1 and model 2) and 23.72% (for model 3 and model 4) and minimum 8.93% (for model 1 and model 2) and 2.52% (for model 3 and model 4) at $T=1$. The lowest value of deviation is observed at $T=0.5$ and is 3.5% (for model 3 and model 4) from the analytical solution. The order of deviation from Grah's results using Orthogonal Collocation presents the same order of deviation. The percentage error introduced due to use of finite difference method is not very significant from $T = 0.0$ to 0.6 and at nearly $T = 1$ and therefore can be acceptable for practical purposes. This further indicates the accuracy of the models for predicting data. However, the solution of Grah is superior to the present solution as it is well known that solution by Orthogonal Collocation leads to better accuracy when compared to the present finite difference method.
- One very interesting point observed is that while the orthogonal collocation method used by Grah gives an increasing oscillation up to $\tau = 1.5$ and thereafter the amplitude starts decreasing. This is contrary to the analytical solution of Brenner which shows a continuous decreasing trend from 1.0 to 0.0853 with the value of $T = 0.5$ to $T = 1.2$. The present investigation follows the same trend like the analytical solution of Brenner indicating the stability of the solution. Hence the finite difference approach can claim better than that due to Orthogonal Collocation results employed by Grah at least in this respect.
- On comparing the various models the model 3 and model 4 (without dispersion) both coincides and give lower degree of deviation from analytical solution of Brenner and numerical solution by Orthogonal Collocation by Grah. On the other hand models 1 and model 2 again coincides with each other and deviates to a slightly greater extent though the values are not very significant.

CHAPTER-6

RESULTS AND DISCUSSION OF THE MODELS

After satisfactory validity of the model attempt is now made in this section to compute data of various inputs and output parameters, first for displacement washing for finding out concentration-time profiles and then extending them for estimating the washing efficiency for washing. This is then compared with the data from a real industrial filter (Brown stock washer) used for pulp and paper mill. In order to achieve the above goal one needs some data for the fiber, fiber bed, kraft black liquor concentration such as, cake thickness, pulp pad consistencies, velocities through bed, various porosity values, dispersion coefficient, Peclet number, area of the packed bed, and mass transfer coefficients. For simulating an industrial system in turn further requires the knowledge of concentration values in both input and output streams from the washer. The above values must be determined experimentally. Grah [25] has determined a set of data for the displacement washing simulation. In absence of any other reliable data these values given in Table (6.1) shown later in Appendix-IV has been used for the basis of simulation. Some data quoted by Grah [25], however further verified from the respective models given in Section 5.1. The computed parameters in terms of C vs. T (dimensionless concentration in liquid phase vs. dimensionless Pseudo time) and N vs. T (dimensionless concentration in solid phase vs. dimensionless pseudo time) from various models through MATLAB are now interpreted in terms of various characteristic graphs. For simulation purpose the data of Table (6.2) is used.

Table (6.2). Parameters of displacement washing and their ranges for Simulation:

Dependent profiles: C vs. Z , \bar{N} vs. Z , C vs. T and N vs. T ; Species: Na^+ and Lignin

| Independent parameters and their range | Ranges |
|--|--------|
|--|--------|

| | | | |
|---------------|---------------|--------------|-----------------------|
| Pe | Dimensionless | (for sodium) | 20 to 110 |
| Pe | Dimensionless | (for lignin) | 20 to 110 |
| D_L | m^2 / s | (for sodium) | 0.59e-006 to 5.9e-007 |
| D_L | m^2 / s | (for lignin) | 0.81e-006 to 8.1e-007 |
| u | m / s | (for sodium) | 0.008 to 0.026 |
| u | m / s | (for lignin) | 0.008 to 0.026 |
| ε | Dimensionless | (for sodium) | 0.1 to 0.95 |
| ε | Dimensionless | (for lignin) | 0.1 to 0.95 |
| k_1 | 1 / s | (for sodium) | 5.0e-3 to 500e-3 |
| k_1 | 1 / s | (for lignin) | 5.0e-3 to 500e-3 |
| k_2 | 1 / s | (for sodium) | 0.0002e-3 to 2e-3 |
| k_2 | 1 / s | (for lignin) | 2e-100 to 6e-100 |

From plethora of data four sets of graphs obtained from four models considered using Pe number 27 for Na^+ and 20 for lignin taken from table (for the models with dispersion) have been drawn for both the species namely Na^+ and lignin. These are interpreted below.

6.1 Effect of various input parameters on concentration

6.1.1 Effect of dimensionless distance Z on dimensionless solute concentration C of Sodium in wash liquor

To examine the effect of z, one has to get small increment of depth from top to bottom i.e. $L = \sum \Delta z$. In this investigation the bed depth has been divided into 10 equal parts and then the influence of z on c is estimated. Figs. 6.1a–6.1d are drawn to show the effect of dimensionless distance, $Z (= z / L)$ on dimensionless concentration, $C \{= (c - C_s) / (C_i - C_s)\}$ of the solute in the filtrate from

Fig.6 1a. C vs.Z Profile for Na+ at T = 1 for Model # 1

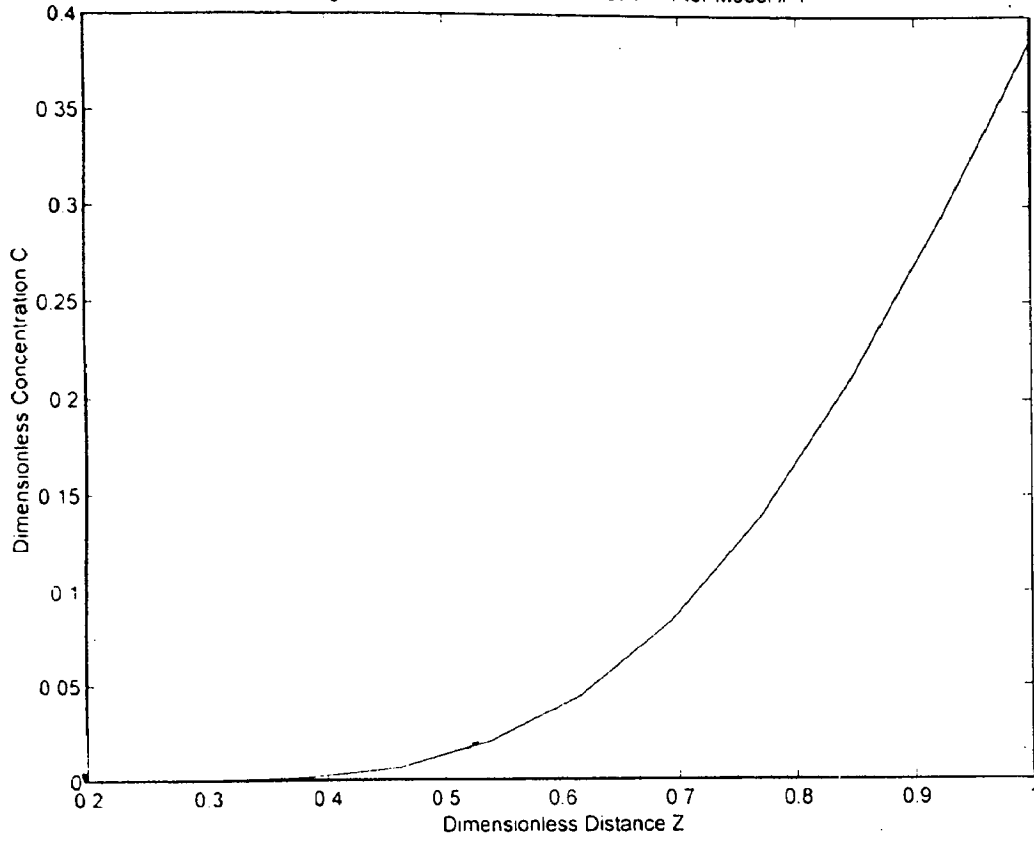


Fig.6.1b. C-Z Profile for Na+ at T = 1 for Model 2

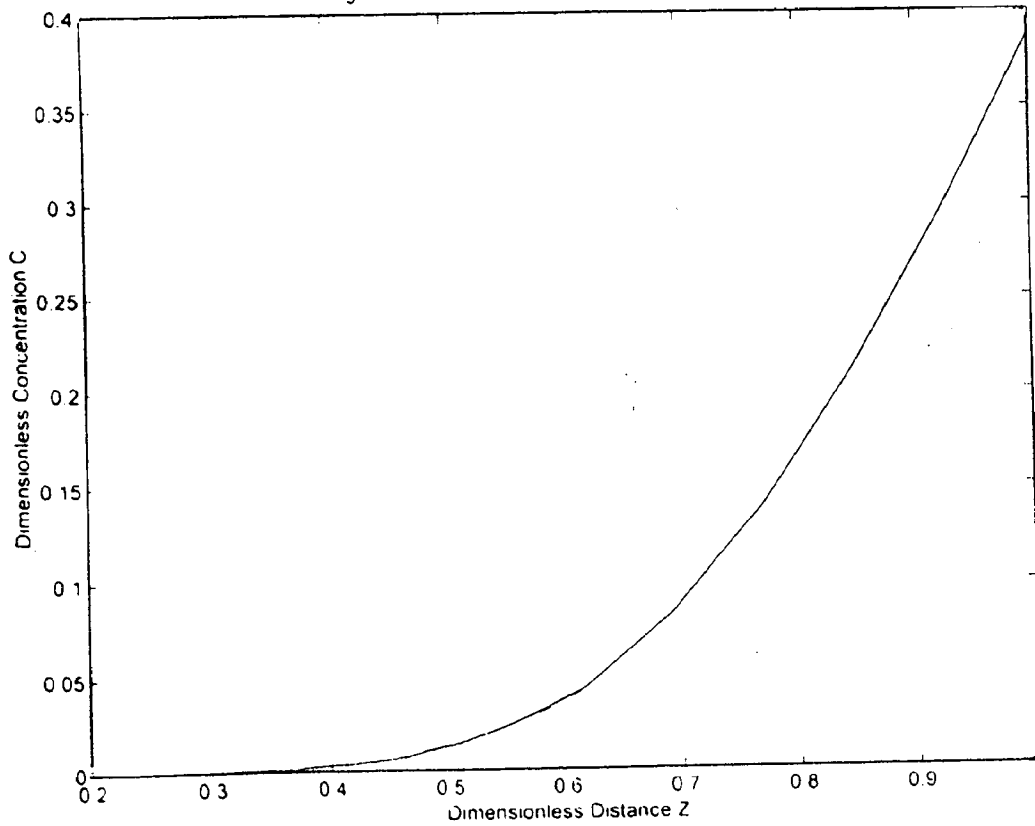


Fig 6.1c. C-Z Profile for Na⁺ at T = 1 for Model 3

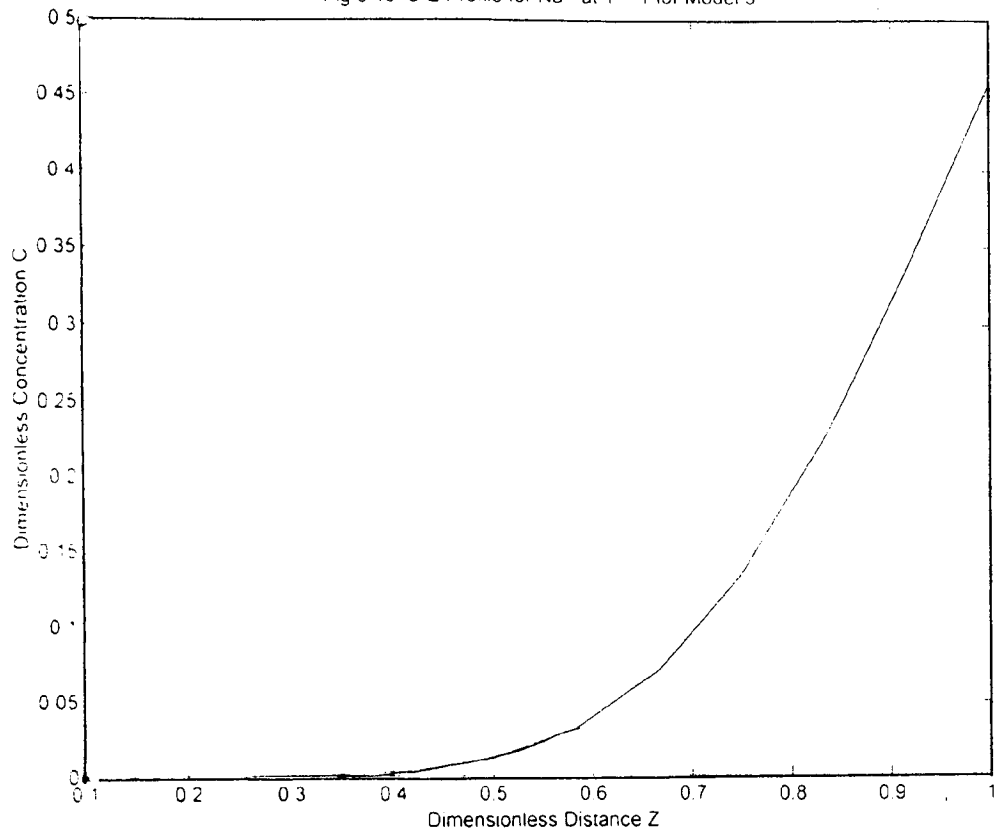
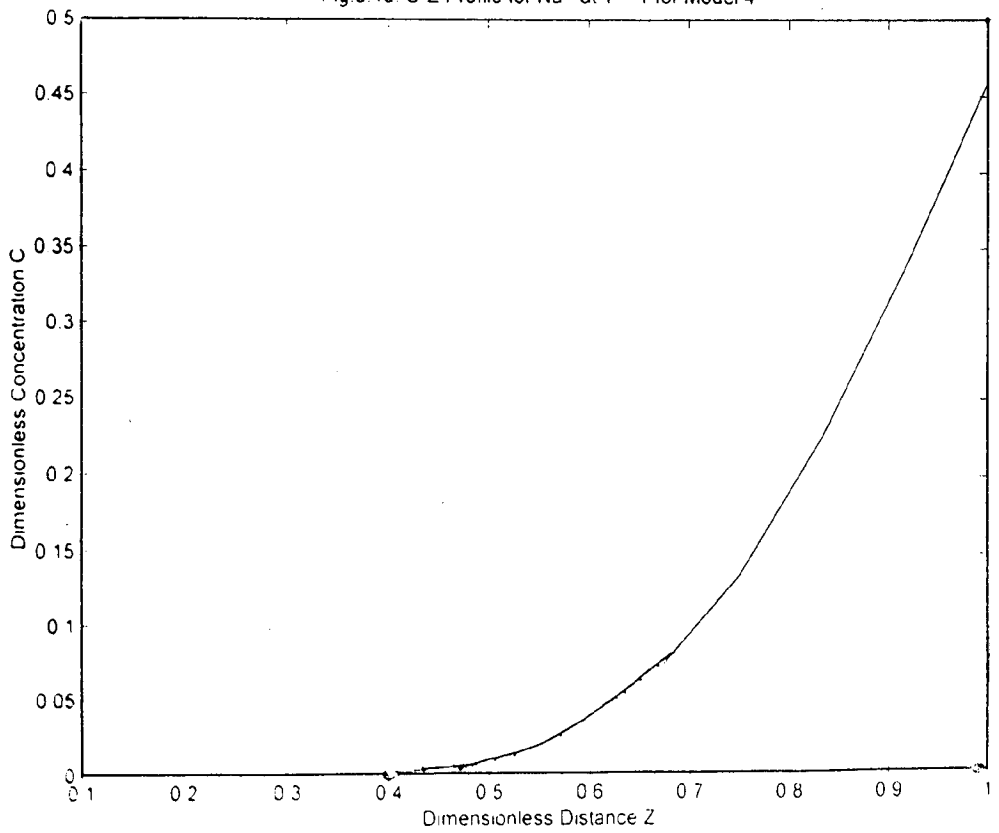


Fig 6.1d. C-Z Profile for Na⁺ at T = 1 for Model 4



washing zone at $T (= u t / L) = 1$ for models 1 through 4 respectively. This is important to show how c , i.e. solute concentration increases with the increase of bed depth (z) i.e. mat thickness.

As expected, it is evident that there is a nonlinear increase of C with Z . This is verified from the fact that the dimensionless concentration C , zero at the top layer will give maximum values at the bottom layer.

The figures have also been drawn for the other layers at different depths. It is further evident that deeper bed gives the higher washing efficiency. The conclusion excellently agrees with the findings of Grah [24], Grah and Gren [27], Gren & Strom [28] and Trinh et. al.[100].

6.1.2 Comparison of models for the nature of the species i.e. Na^+ on C-Z profiles

Fig. 6.2. C vs Z Profiles at T = 1.0 For Na For All The Four Models (Pe = 27)

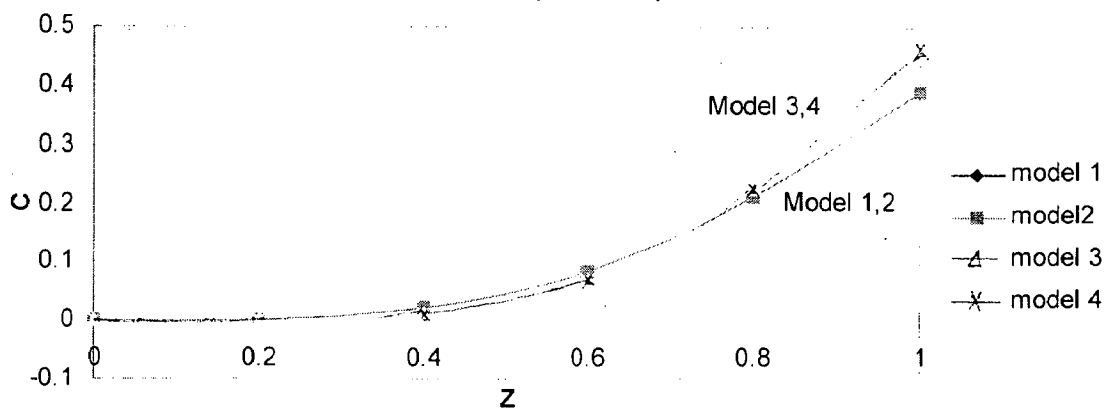


Fig.6.2 shows comparison of effect of dimensionless bed depth on dimensionless solute concentration of Na^+ in liquid phase. Initially the profiles for all the four models coincide upto $Z = 0.2$ and show that the concentration of solute in the liquor is equal to the concentration of the wash liquor in the upper layers. The concentration increases with the increase of bed depth. Models 1 and 2 show greater concentration from $Z = 0.2$ to $Z = 0.7$ than models 3 and 4. Thereafter the situation reverses. At bed exit point ($z = L$) the concentration of solute in the liquor is shown

Fig. 6.3a. C-Z Profile for lignin at T=1 for Model 1

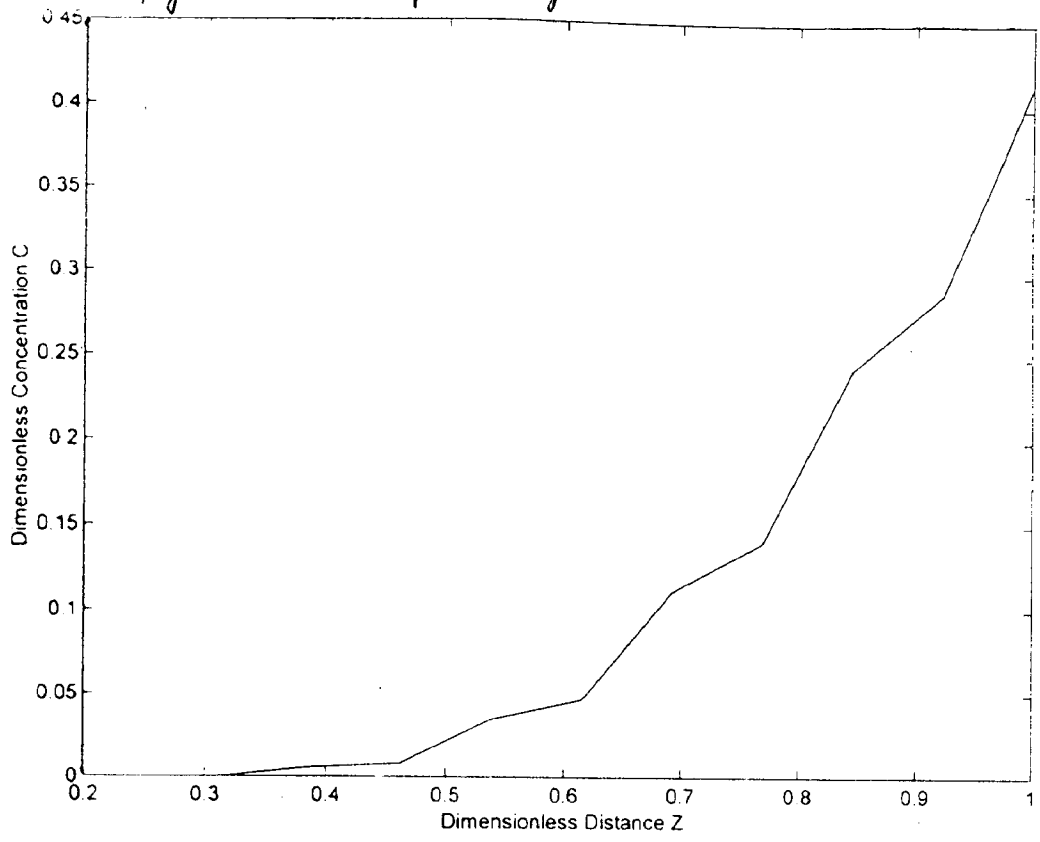


Fig. 6.3b. C-Z Profile for lignin at T = 1 for Model 2

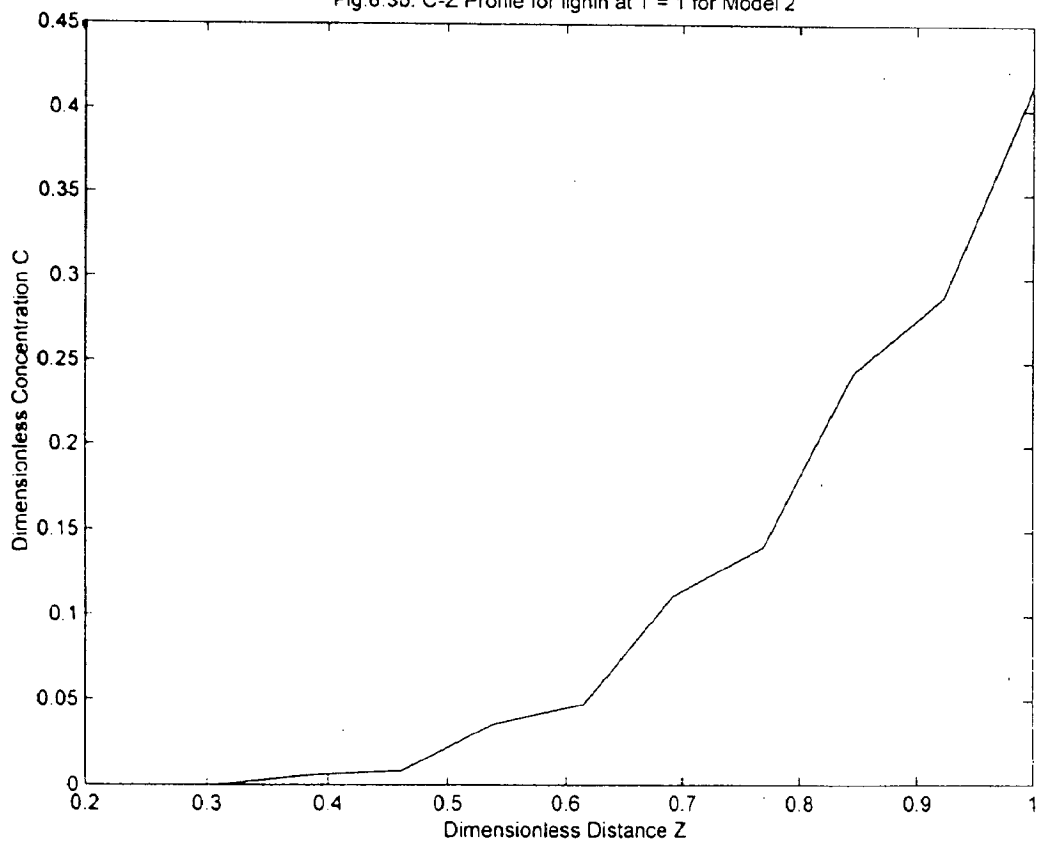


Fig. 6.3c C-Z Profile for lignin at T = 1 for Model 3

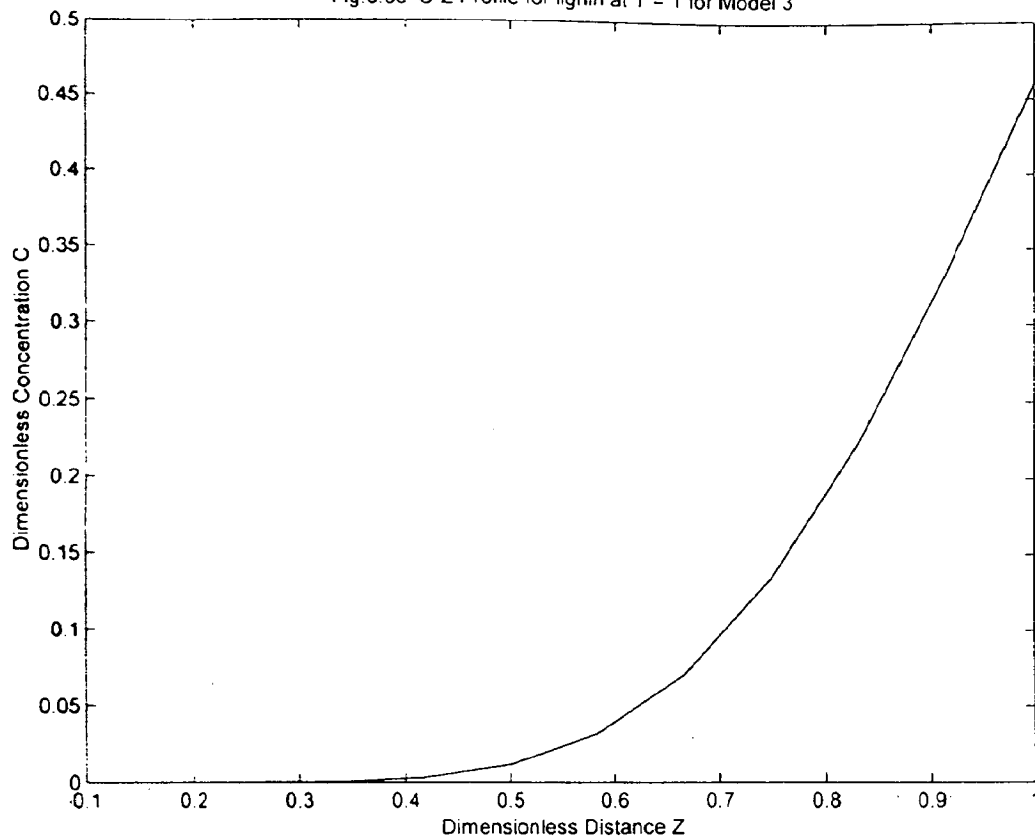
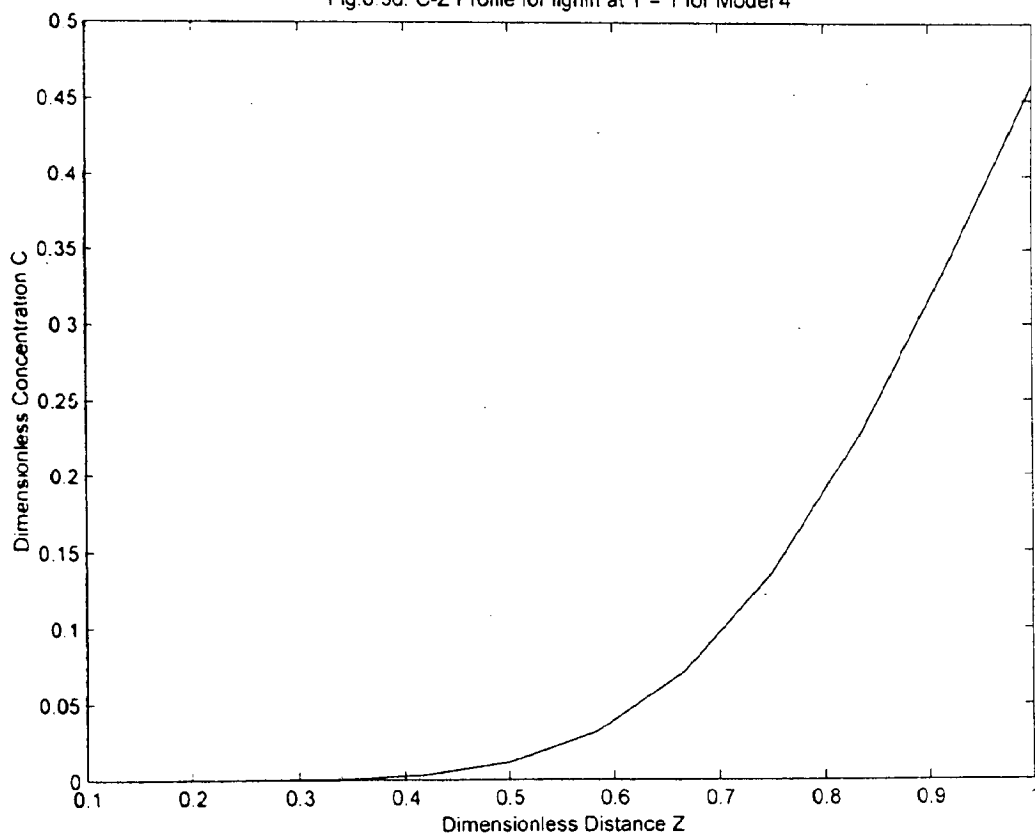


Fig. 6.3d. C-Z Profile for lignin at T = 1 for Model 4



somewhat more by models 3 and 4 i.e. by the models having transport equation without dispersion than by models 1 and 2 involving the dispersion.

6.1.3 Effect of dimensionless distance Z on solute concentration C of lignin in wash liquor

Figs. 6.3a-6.3d are drawn to show the effect of dimensionless distance, $Z (= z / L)$ on dimensionless concentration, $C \{= (c - C_s) / (C_i - C_s)\}$ of the solute in the fibers (solid phase) from washing zone at $T (= u t / L) = 1$ for models 1 through 4 respectively..

The profiles are having the same trend as that for Sodium. This is also verified from the fact that the dimensionless concentration of lignin also, increases as we move towards the bottom layer starting from the top layer where the dimensionless concentration of lignin is zero. .

6.1.4 Comparison of the models for the nature of the species i.e. lignin on C-Z profiles

Fig. 6.4. C vs Z At T = 1 For lignin For All The Four Models (Pe = 20)

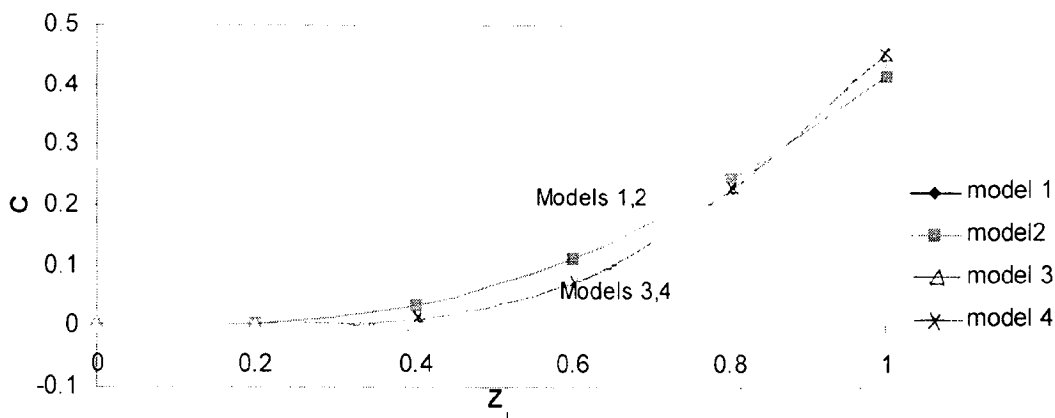


Fig. 6.4 shows comparison of effect of dimensionless bed depth on dimensionless solute concentration of lignin in the liquid phase. Like C-Z profiles for Na^+ for all the four models the same for lignin also show the similar behavior but with little change in slopes. The concentration in bed is that of wash liquor in the first layer. The profiles of the model coincide at $z = 0.83$ and then the position reverse as shown in Fig. 6.4.

6.1.5 Effect of dimensionless distance Z on solute concentration N of Sodium in solid phase

Fig 6 5a. N vs. Z Profile for Na+ at T = 1 for Model # 1

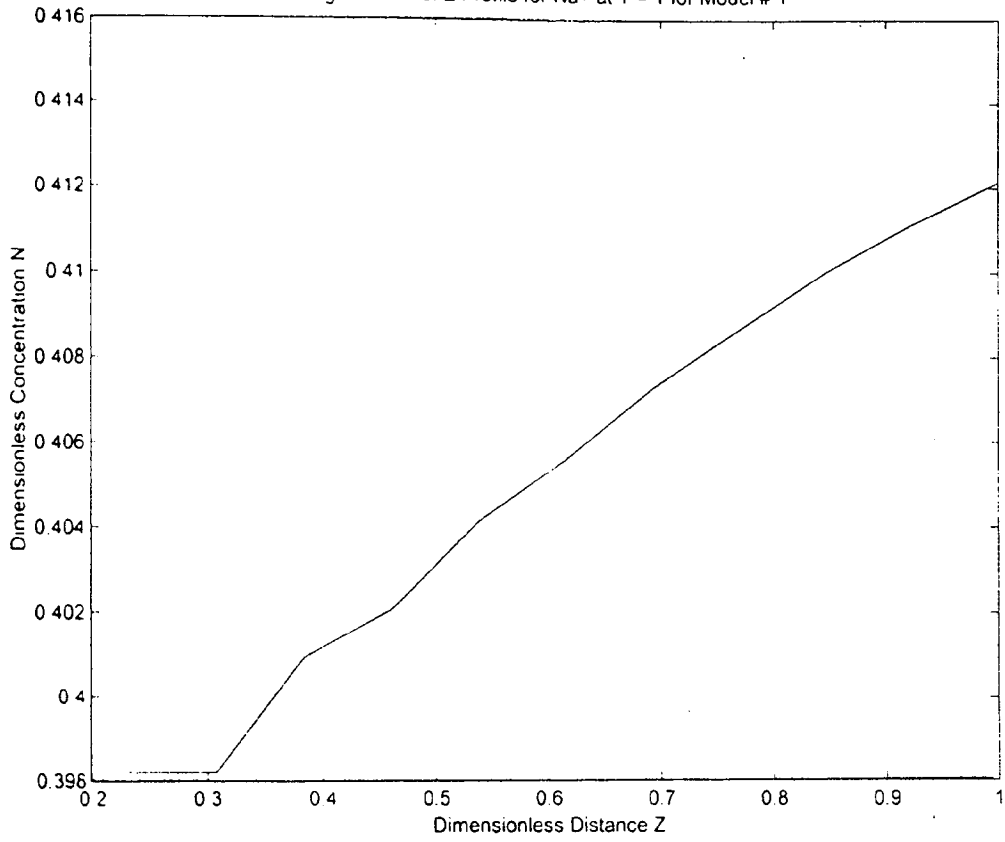


Fig 6 5b. N-Z Profile for Na+ at T = 1 for Model 2

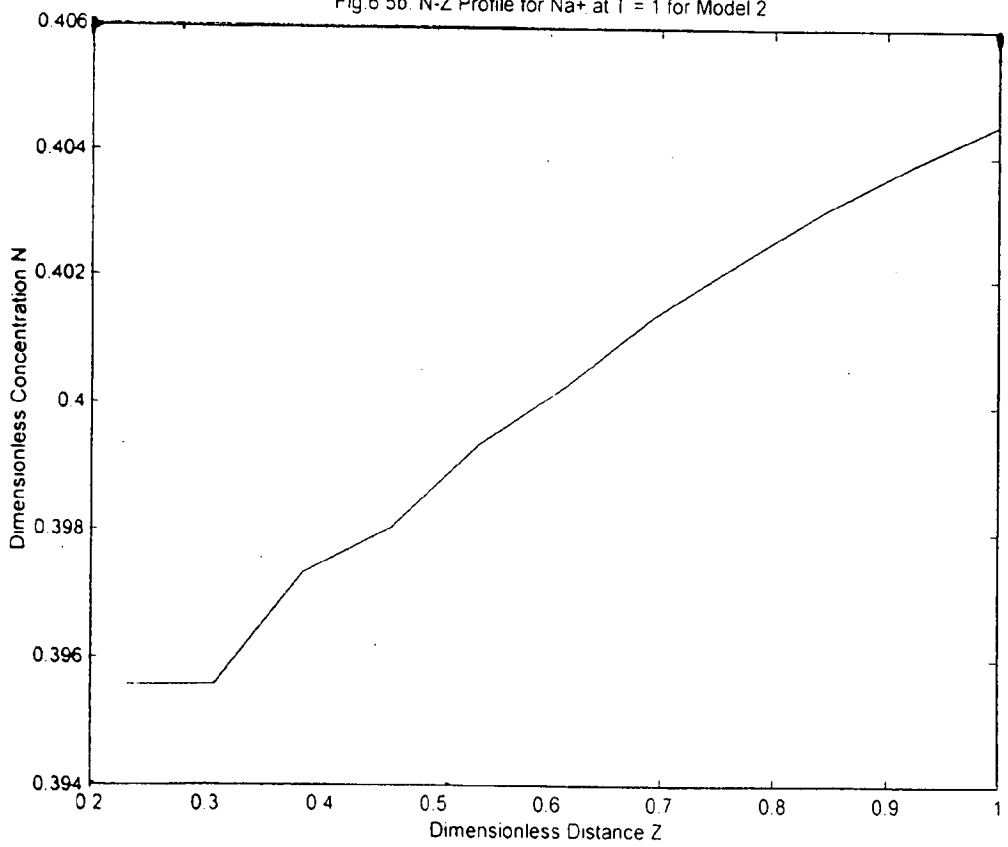


Fig 6.5c N-Z Profile for Na+ at T = 1 for Model 3

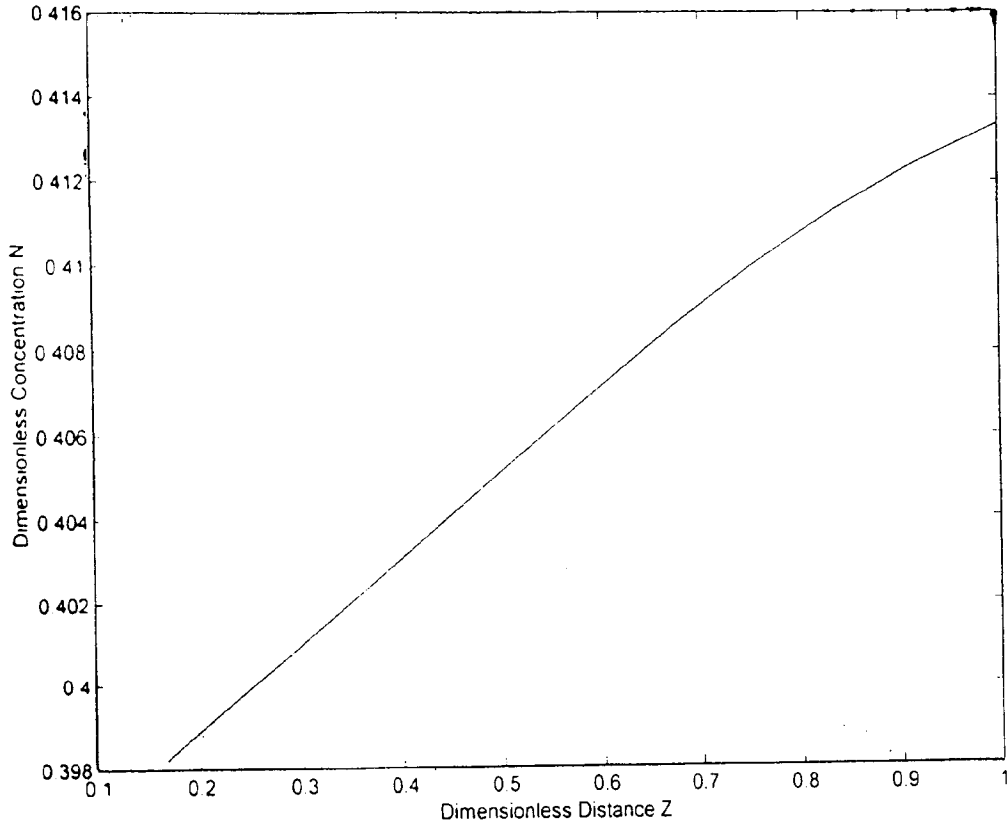
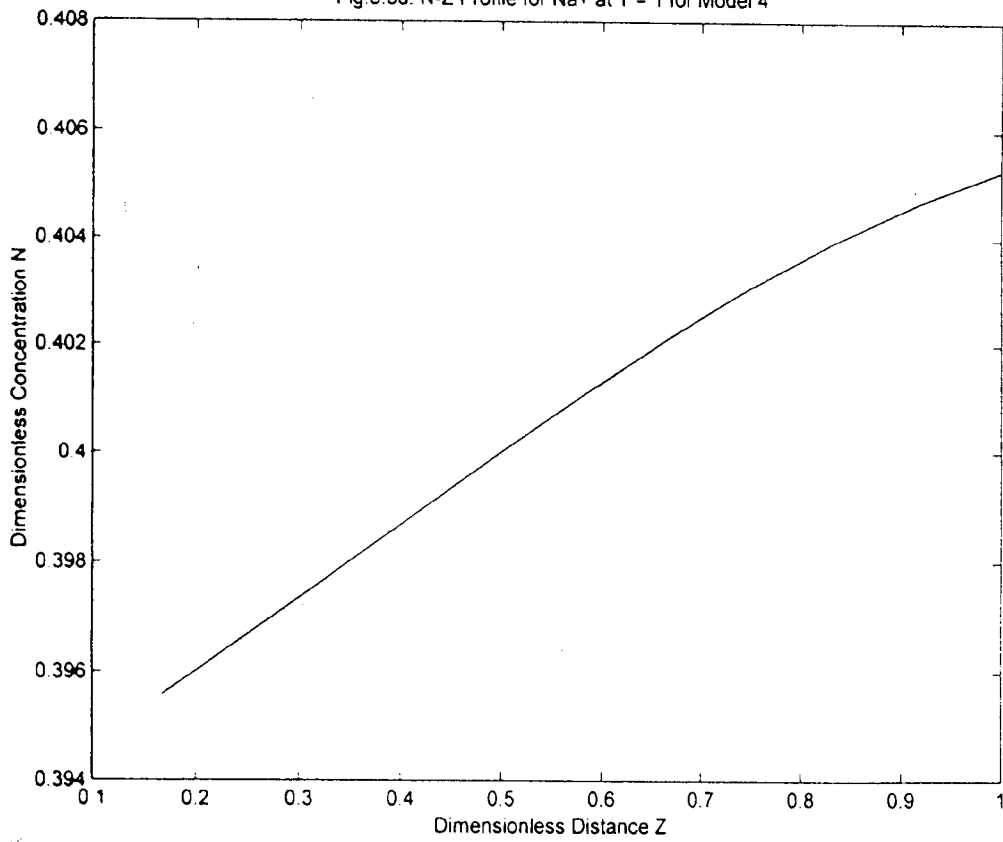


Fig.6.5d. N-Z Profile for Na+ at T = 1 for Model 4



Figs. 6.5a–6.5d are similarly drawn for sodium species to represent dimensionless concentration N $\{= (n - C_s) / (C_i - C_s)\}$ of solute in solid phase as a function of Z . The figures show that from the topmost layer there is no significant change in N upto $Z = 0.3$ approximately. Thereafter there is increasing trend of N with further increase of Z . It is an expected behavior as adsorbed N will be higher for higher concentration. This is verified by Trinh & Crotofino [98] through their large scale of experiments. This can be explained by the fact that as c (also C) increases with bed depth, n (thus N) will also follow the same trend as both are related through an equilibrium relationship.

6.1.6 Comparison of the models for the nature of the species of Na^+ on N - Z profiles

Fig. 6.6. N vs Z Profiles at $T = 1$ For Na For All The Four Models ($Pe = 27$)

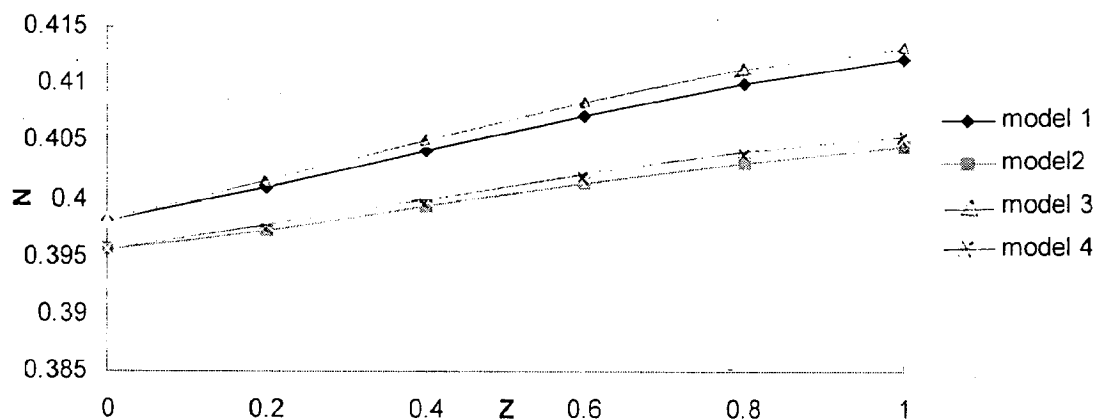
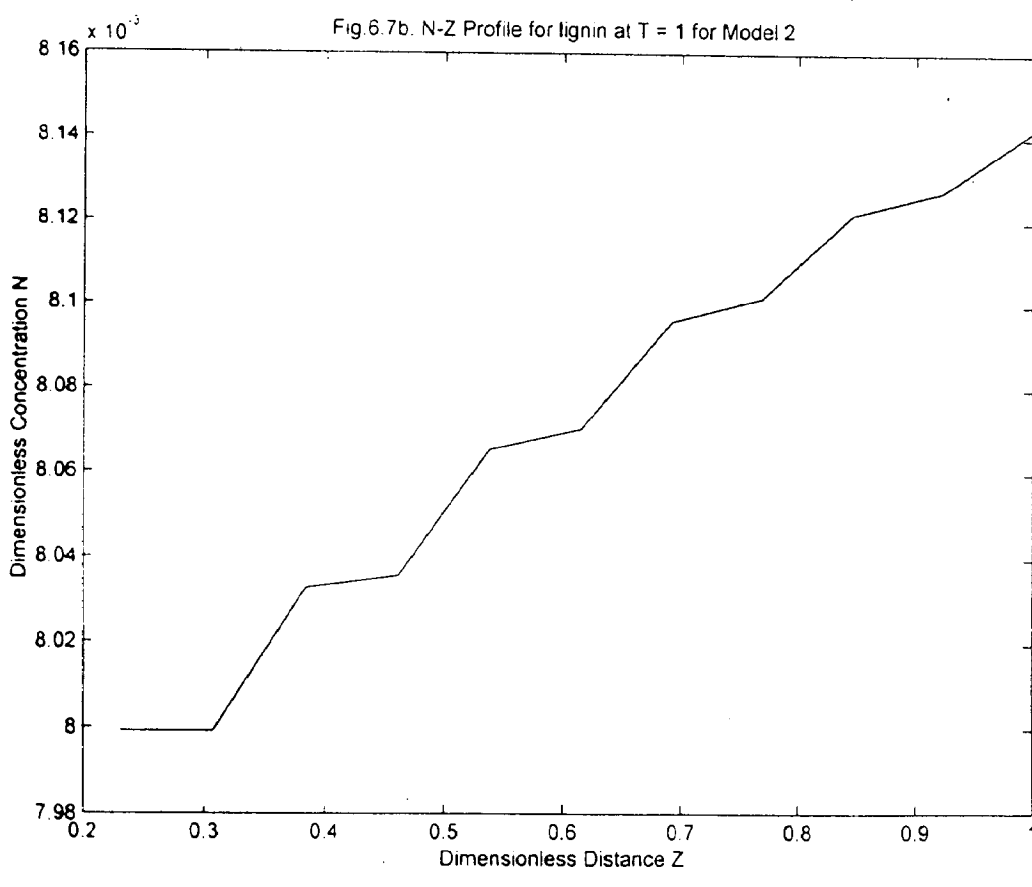
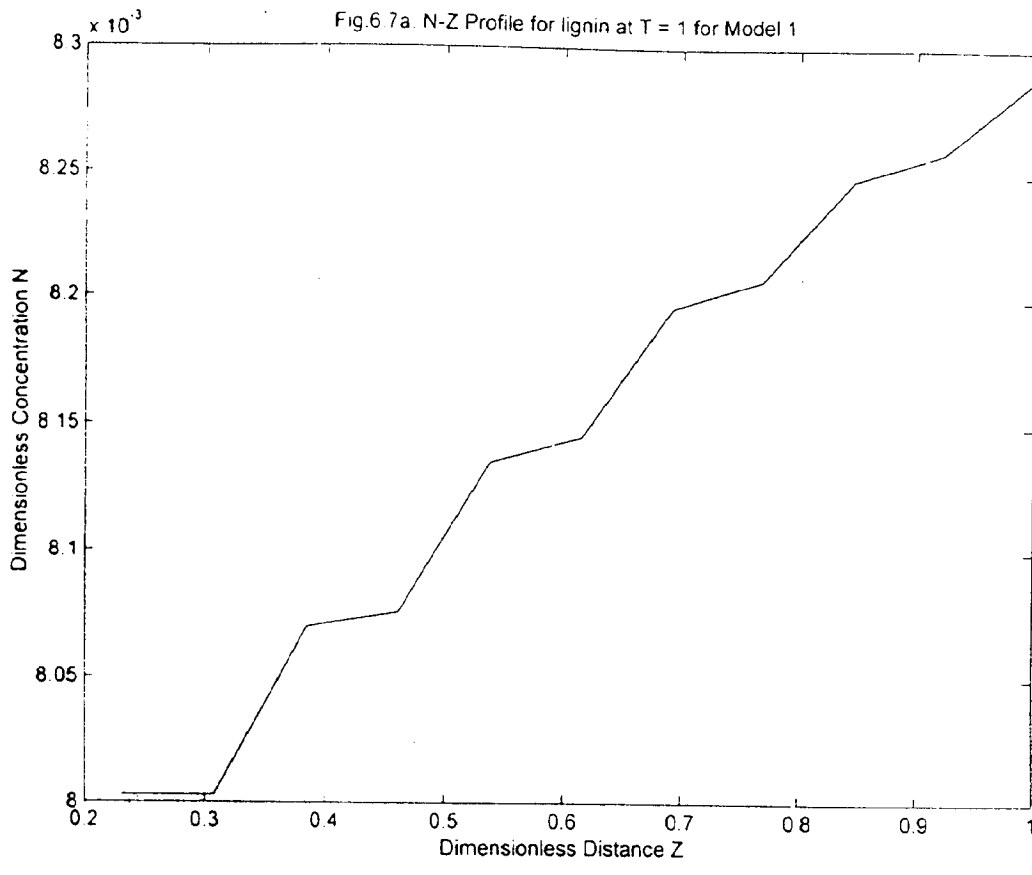
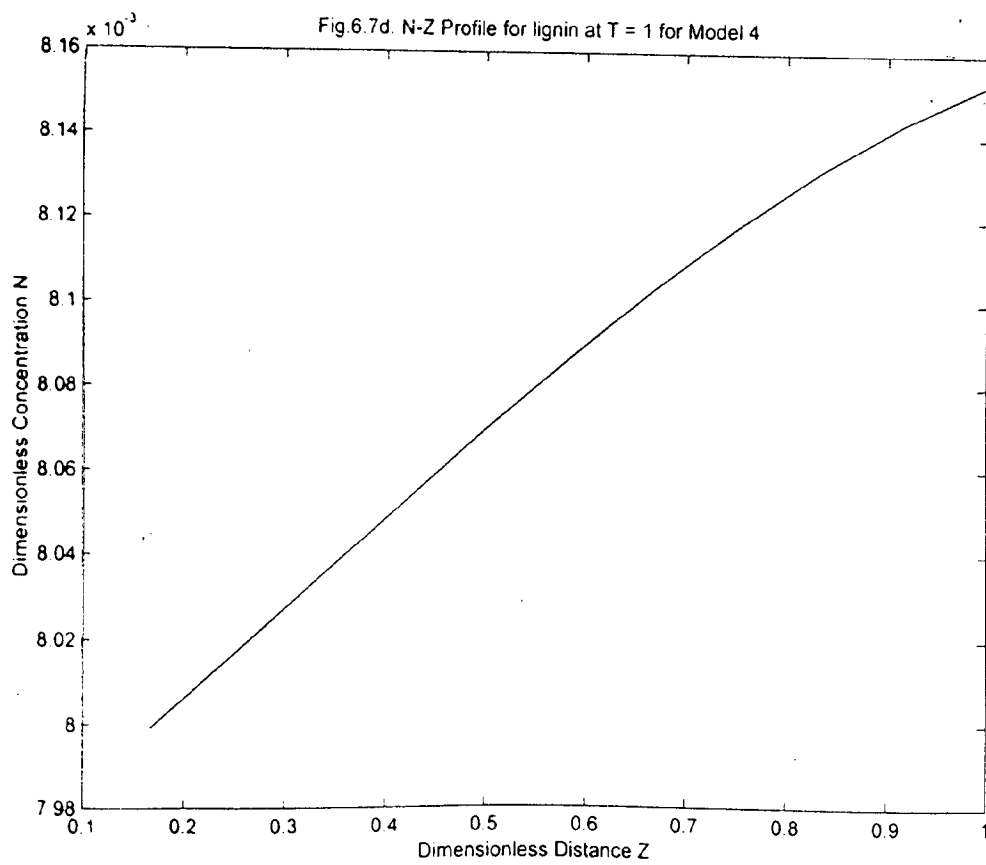
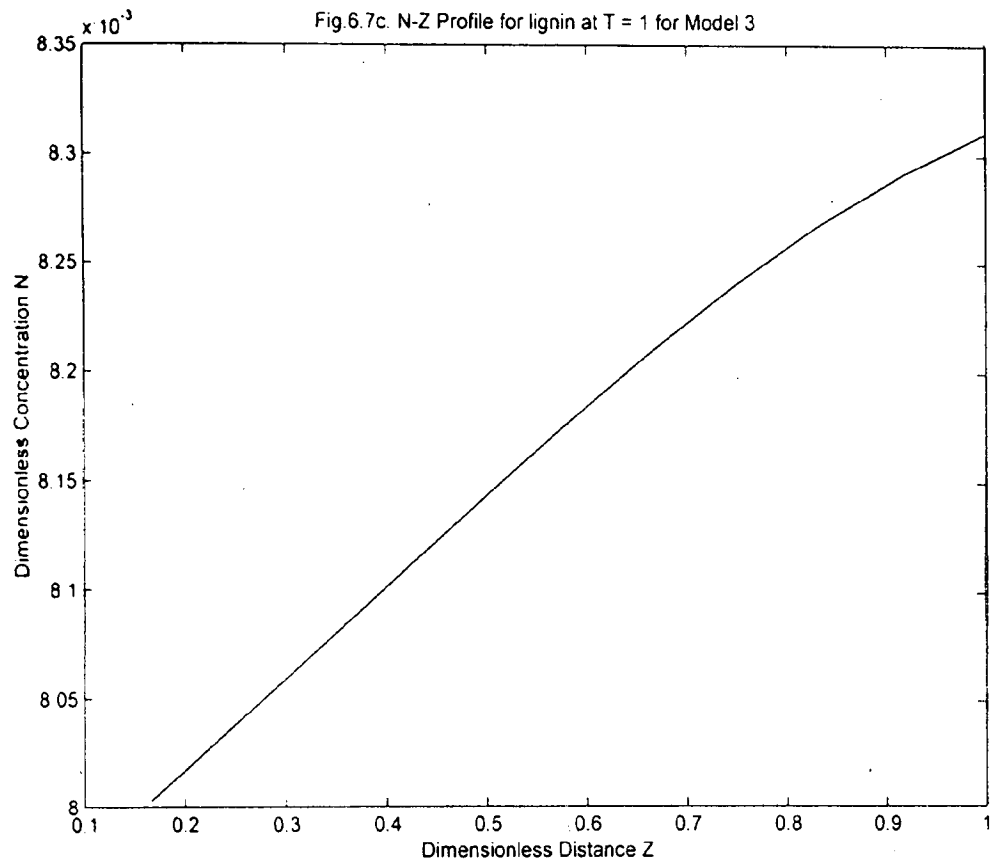


Fig. 6.6 shows N - Z profiles for Na^+ for all the four models at $T = 1$. The figure shows that the adsorption is more at lower layers in comparison to upper layers. It is also evident that the models 3 and 4 i.e. the models without dispersion show more adsorption compared to the model 1 and model 2. This is attributed to dispersion effects in the models 1 and 2 which affect adsorption on the solid phase.

6.1.7 Effect of distance Z on solute concentration N of lignin in solid phase

Fig. 6.7a-6.7d are similarly drawn for lignin species to represent dimensionless concentration N $\{= (n - C_s) / (C_i - C_s)\}$ of solute in solid phase as a function of Z . The figures show that from the





topmost layer there is no significant change in N values observed upto approximately $Z = 0.3$ for models 1 and 2 and up to $Z = 1.5$ for models 3 and 4. Thereafter there is an increasing trend of N with further increase of Z. This is valid for all the models. It is an expected behavior as adsorbed amount N will be higher for higher concentration of solutes(C) in solution. The concentration C in fact, as earlier explained increases with bed depth, hence the value of N. The adsorption at bed exit is shown slightly higher by models 1 and 3 compared to models 2 and 4. It shows that adsorption-desorption isotherm plays more significant role than dispersion in case of lignin species thus deviating the results from the earlier predicted ones.

6.1.8 Comparison of the models for nature of the species i.e. lignin on N-Z profiles

Fig. 6.8. N vs Z Profiles At T = 1 For lignin For All The Four Models (Pe = 20)

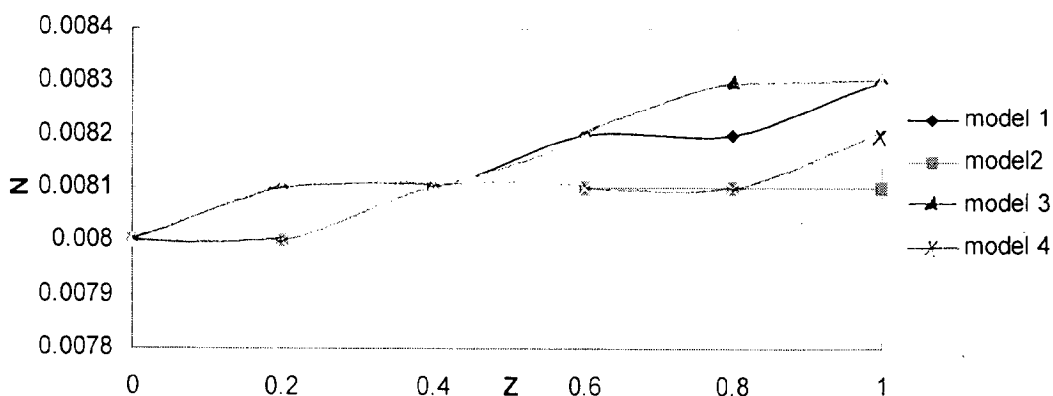


Fig. 6.8 shows N-Z profiles for lignin for all the four models at T = 1. The figure shows that upto $Z = 0.6$ the profiles of the models 1 and 3 coincide and those from the models 2 and 4 also coincide with each other, profiles of models 1 and 3 being above than those of models 2 and 4. However, all the four profiles coincide at $Z = 0.4$. From $Z = 0.6$ to $Z = 0.8$ the profiles of models 3, 1, 4 and 2 are arranged from larger extent to smaller extent of adsorption. This type of cross-over is not uncommon in this type of system. To understand this phenomena further investigation is required.

Fig. 6.9a. C vs. T Profiles for Na+ at Various Bed Depths for Model # 1

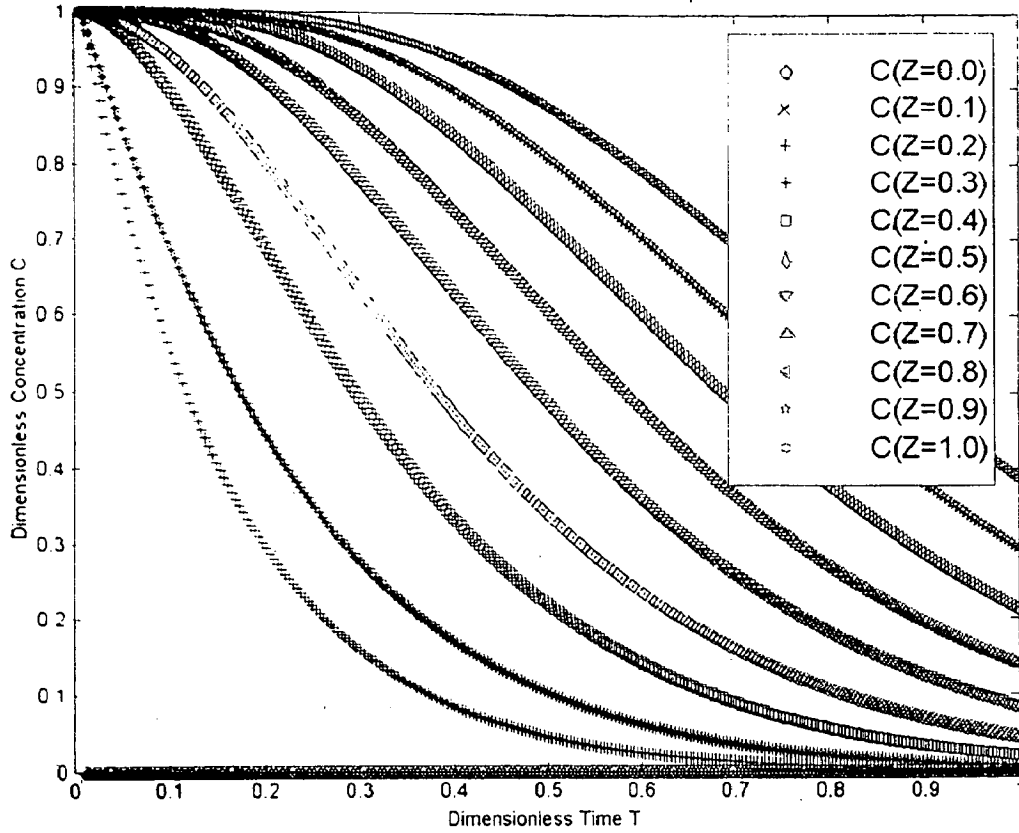


Fig. 6.9b. C-T Profiles for Na+ at Various Bed Depths for Model 2

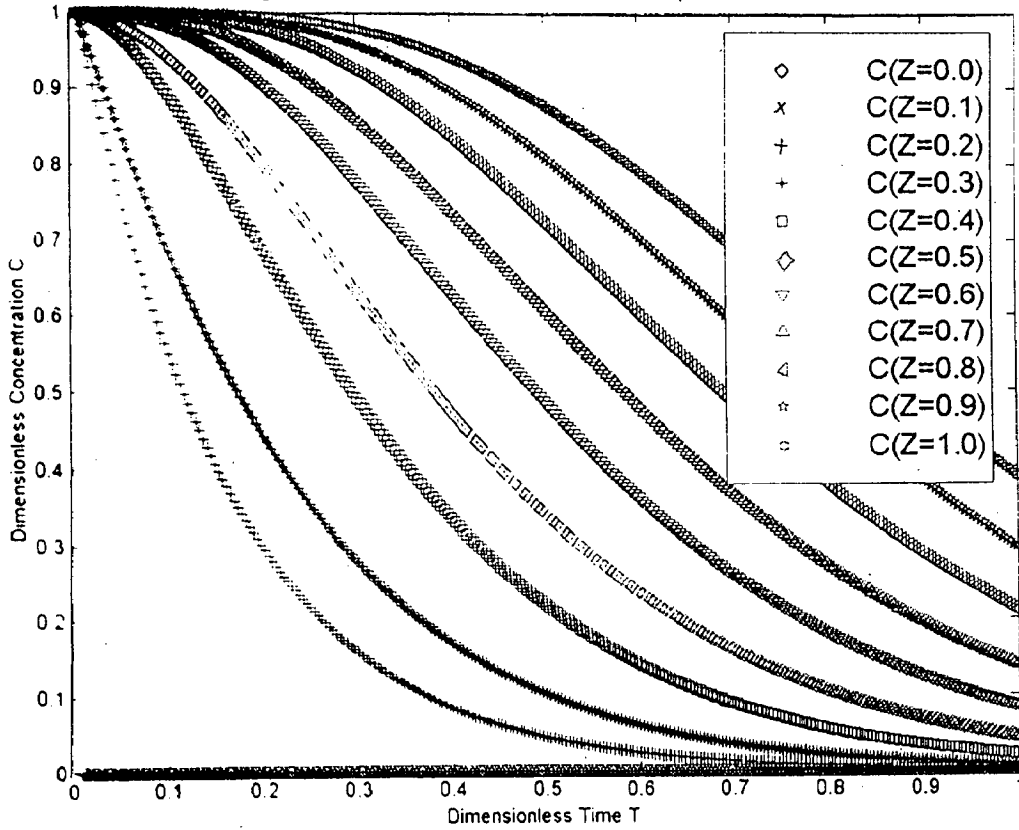


Fig.6.9c. C-T Profiles for Na⁺ at Various Bed Depths for Model 3

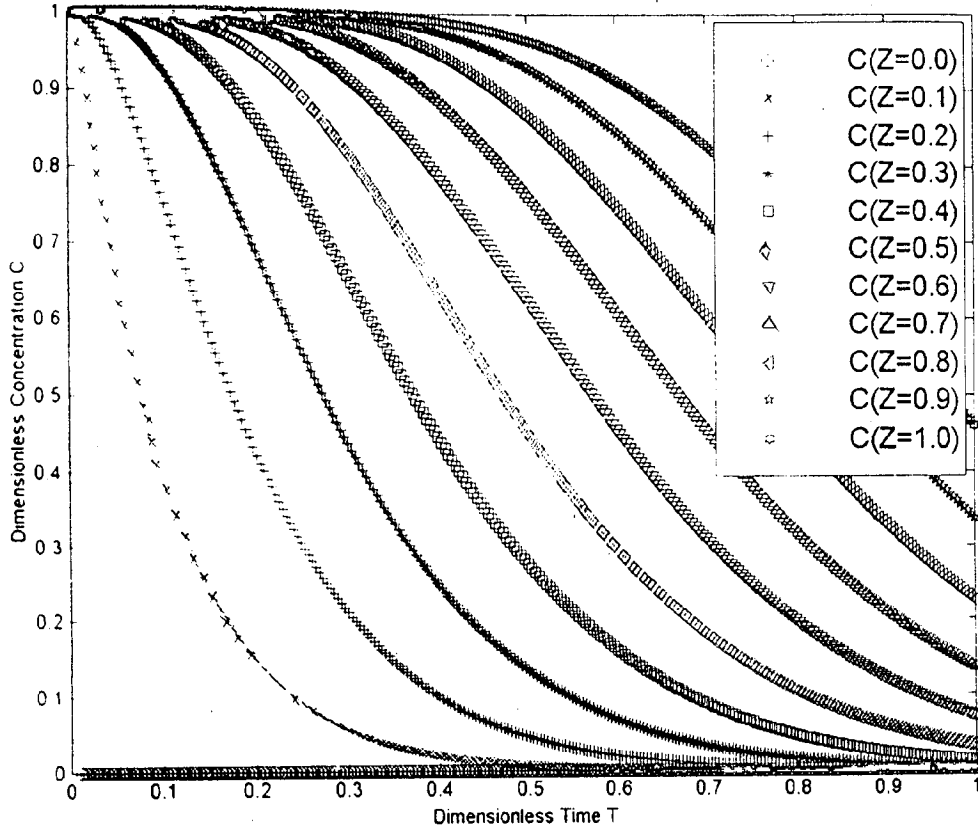
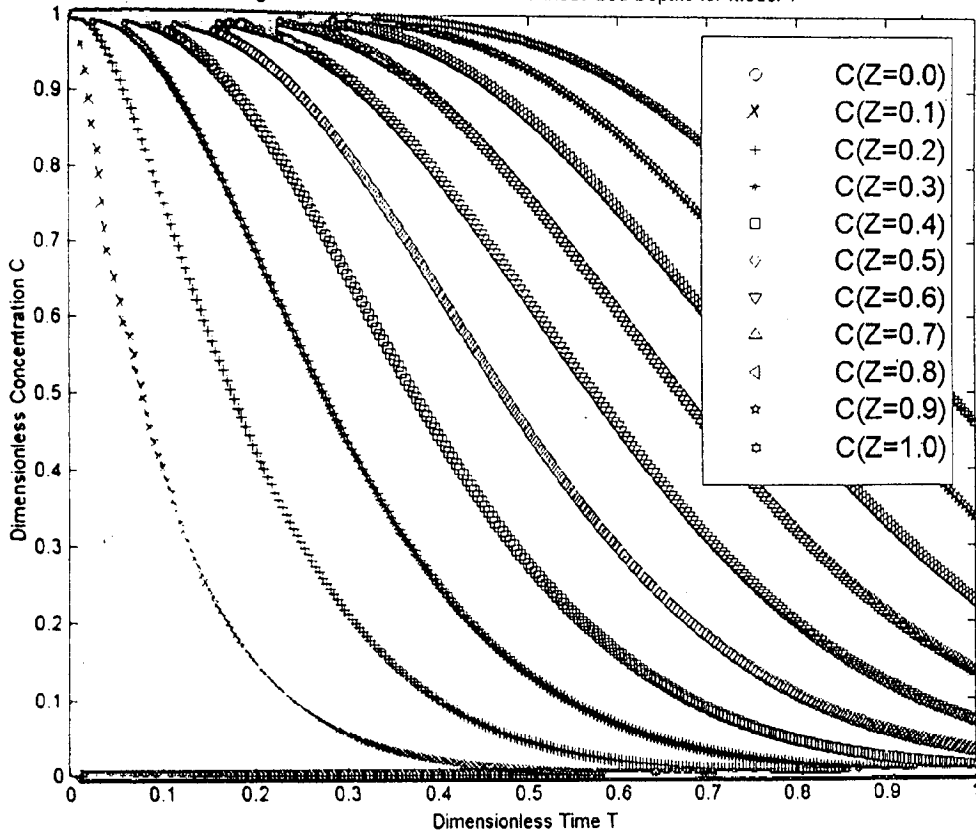


Fig.6.9d. C-T Profiles for Na⁺ at Various Bed Depths for Model 4



6.1.9 Effect of T on C of Sodium in wash liquor

Fig. 6.9a-6.9d show C as a function of T for Na^+ at various bed depths for all the four models 1 through 4 respectively. The depth has been divided into 10 equal parts. C, as usual, reflects the dimensionless solute concentration of sodium species whereas T is the dimensionless pseudo time. The variabilities in concentration at the top two layers become insignificant whereas for the bottommost layer C shows a typical breakthrough curve. Lowering the bed depth (from top to bottom), the shape of the breakthrough curves change to a non-linear curve which is practically an asymptotic in nature.

These curves show that there is insignificant contribution of displacement wash whereas the diffusional and dispersion washing become more predominant. This is in agreement with those of Grah [24], Poirier et. al.[78], Potucek [81] etc. This is attributed to the dispersion- diffusion becoming more predominant after few layers from the top.

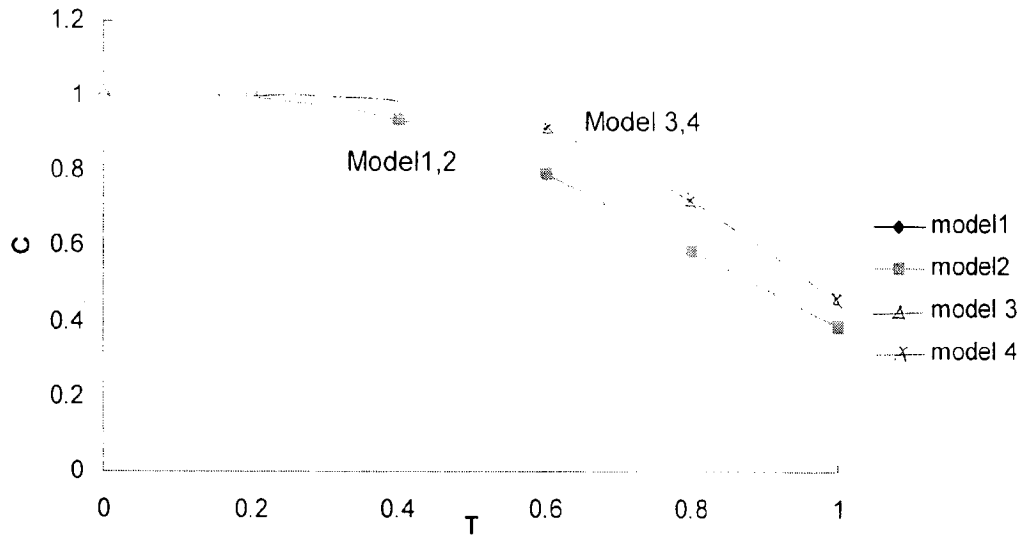
The profiles of the curves surprisingly display the same characteristic as shown by Kukreja [40] for pulp washing problem and also by Kuo [42] and Kuo & Barrett [43]. The later however used the system- calcium carbonate cake containing ammonium chloride solute with water as washing medium.

6.1.10 Comparison of the models for the nature of the species i.e. Na on C-T profiles

Fig. 6.10 represents a comparison among all the models at $Z = 1$ for $Pe = 27$. The figure indicates a longer displacement step followed by a sharp diffusional step. The extent of displacement is found lower for models 1 and 2 compared to models 3 and 4. Upto $T = 0.2$ the profiles of all the four models merge each other. Thereafter the merging of profiles from models 1 and 2 continue. The profiles from the models 3 and 4 deviates from those of models 1 and 2 though they are also merged each other. The latter models (models 3 and 4) however provide higher values of C than

those from the former (models 1 and 2). This is caused as earlier indicated by the dispersion which hampers adsorption.

Fig. 6.10. C vs T Profiles at Z = 1 For Na For All The Four Models (Pe = 27)



6.1.11 Effect of dimensionless pseudo time T on dimensionless solute concentration C of lignin in wash liquor

Figs. 6.11a-6.11d show C as a function of T for lignin at various bed depths for all the four models 1-4 respectively. Like Na⁺, the variations of concentration at the top two layers become insignificant whereas the same at the bottom most layer (at the bed exit point) shows a typical breakthrough curve. Lowering the bed depth (from top to bottom), the shape of the breakthrough curves analogous to Na, again change to a non-linear asymptotic curve for lignin.

6.1.12 Comparison of the nature of the species of lignin on C-T profiles

Fig. 6.12 shows C-T profiles at Z = 1.0 for lignin for all the four models for Pe = 20. Like the profiles for Na⁺, the profiles for lignin also have a decreasing trend. All the profiles coincide upto T = 0.2. After that models 3 and 4 show higher values of concentration than those from models 1 and 2 at any fixed time T. The graphs indicate that at a fixed position, concentration of solute

Fig.6.11a. C-T Profiles for lignin at Various Bed Depths for Model 1

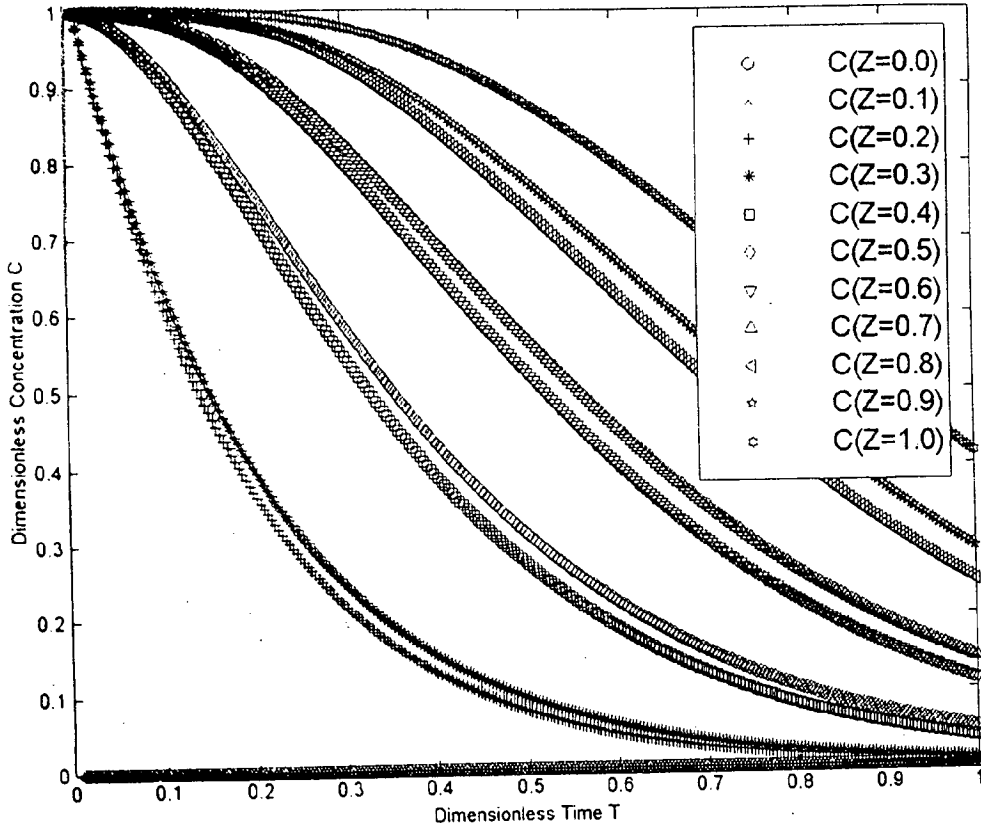


Fig.6.11b. C-T Profiles for lig at Various Bed Depths for Model 2

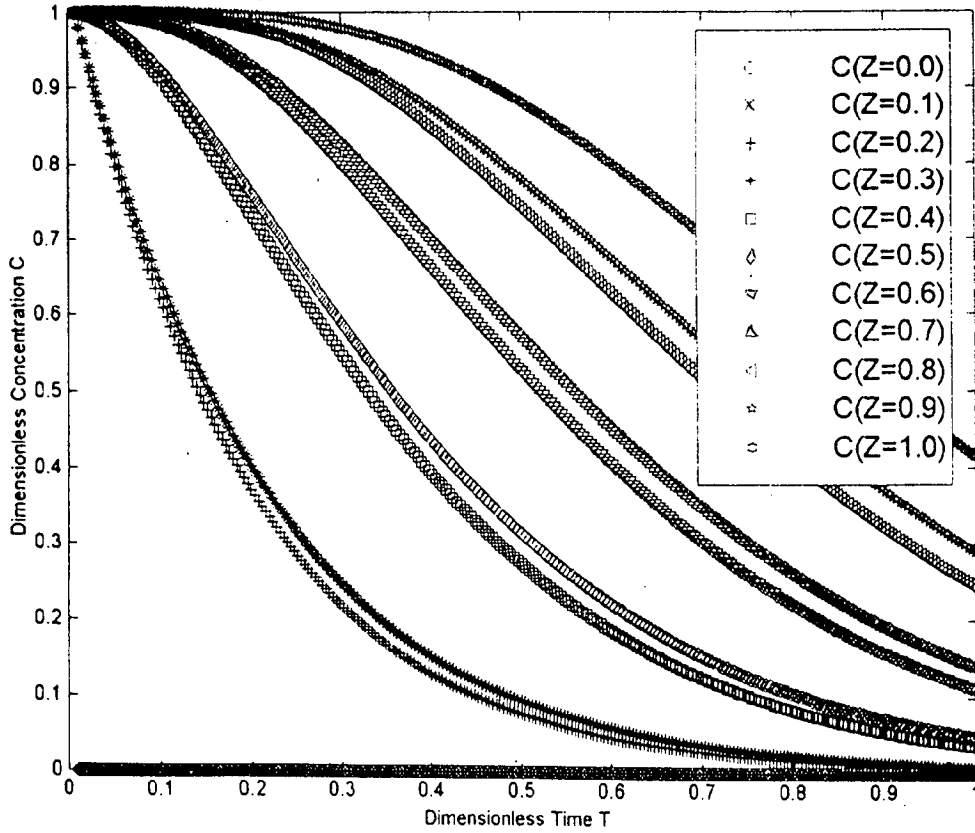


Fig.6.11c. C-T Profiles for lig at Various Bed Depths for Model 3

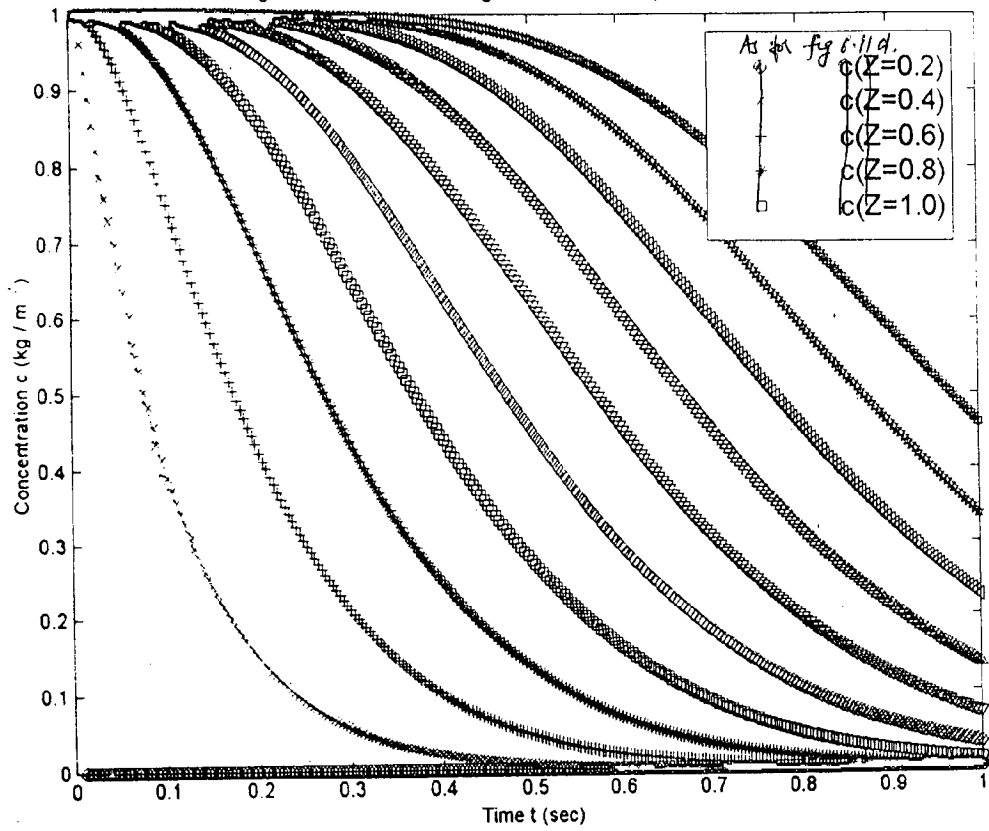
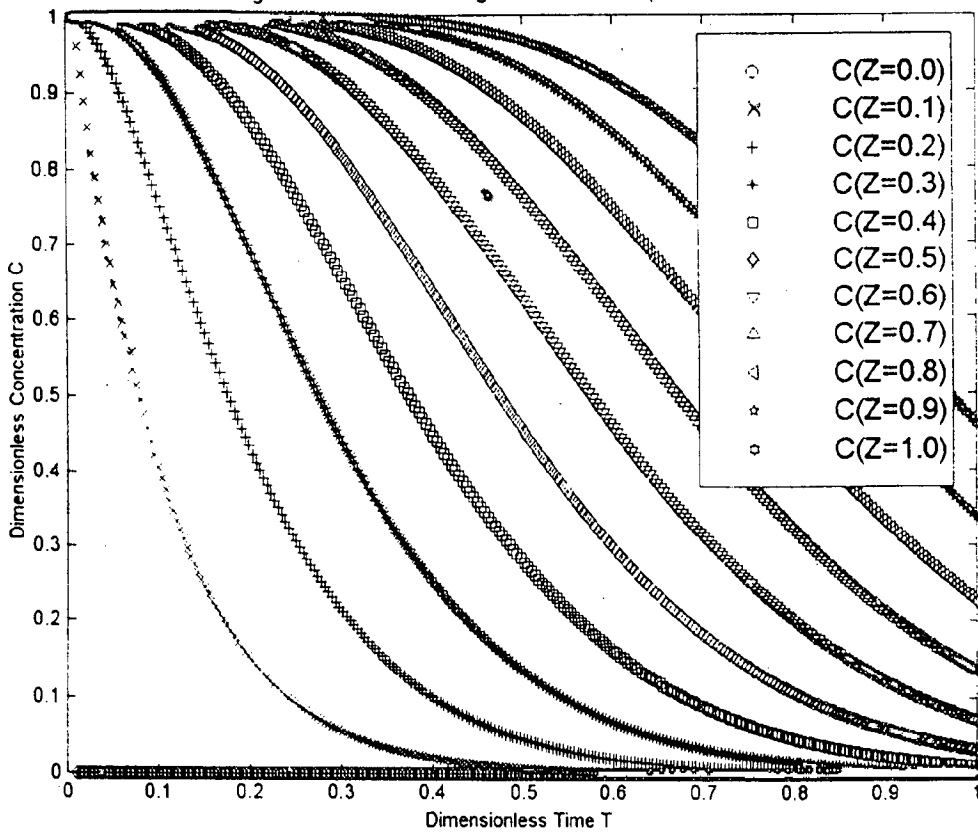
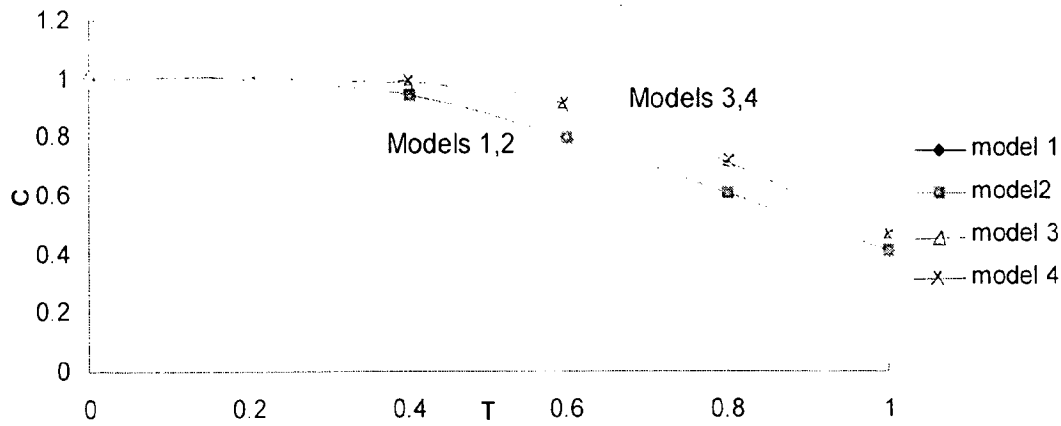


Fig.6.11d. C-T Profiles for lig at Various Bed Depths for Model 4



decreases with time, extent of decrease being less in the models without dispersion i.e. models 3 and 4.

Fig. 6.12. C vs T Profiles At Z = 1 For lignin For All The Four Models (Pe = 20)



6.1.13 Effect of T on adsorption-desorption dynamics of Sodium

The concentration of Na^+ adsorbed on pulp fibers were plotted for N against the dimensionless pseudo time T in Figs. 6.13a-6.13d at various bed depths (ten equally spaced segments) for models 1-4 respectively.

It is interesting to note that unlike the breakthrough curves for C vs. T, the value of N increases shortly originating from a point at 0.4 in the N axis with the increase of T at Pe equal to 27. It increases very fast to a certain time, becomes slower beyond that value and remains constant thereafter at the larger values of T. With the increase of bed depth the N – T profile become constant at a much higher value of T. The point of constancy for the bottommost layer may be beyond 1 which is hypothetical one.

The above observations, dealing with pulp black liquor washing system, seem to have not been reported so far in any publication. Kukreja [40], Kuo [42], Kuo and Barrett [43], and Perron and Lebeau [75] also dealt with this aspect but instead of concentration in solid phase they have considered the concentration in stagnant liquor inside the pores. As a result they have obtained

Fig. 6.13a N vs. T Profiles for Na⁺ at Various Bed Depths for Model # 1

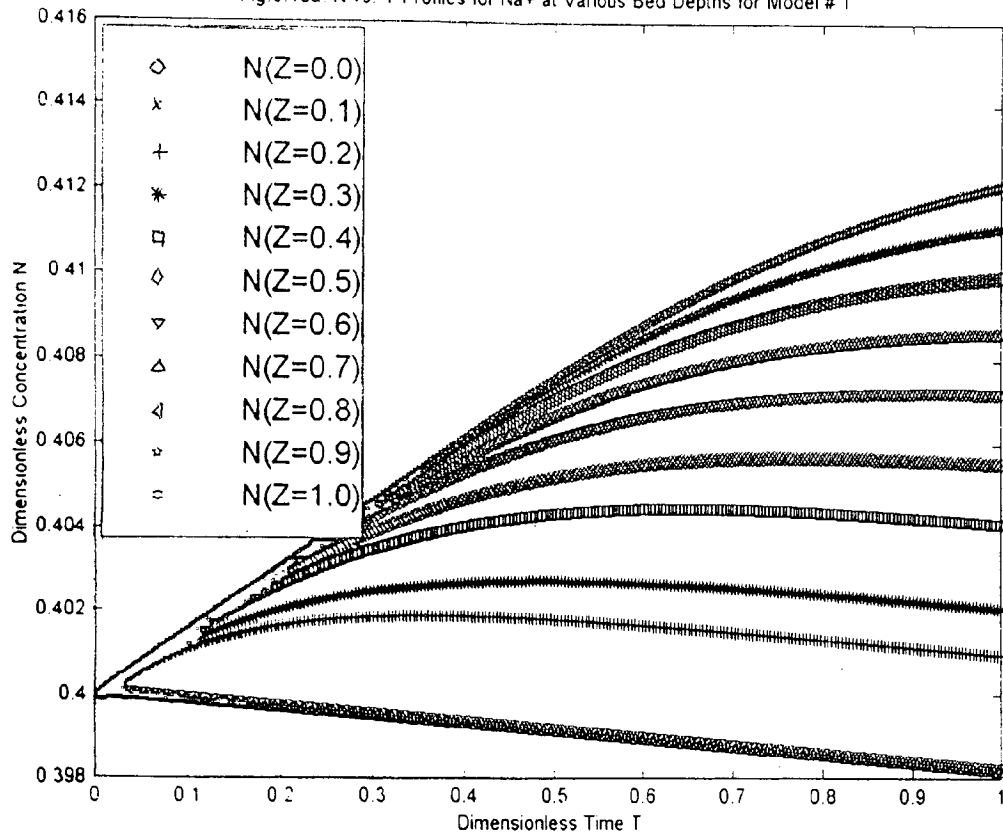


Fig. 6.13b N-T Profiles for Na⁺ at Various Bed Depths for Model 2

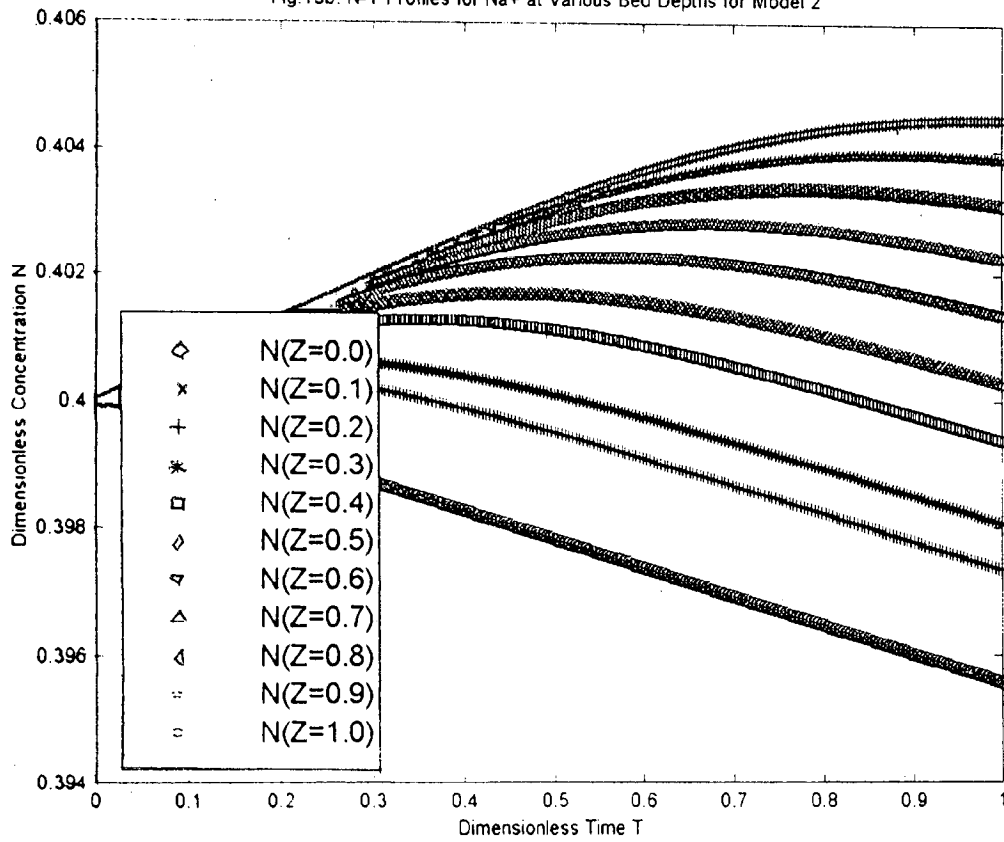


Fig.6.13c. N-T Profiles for Na+ at Various Bed Depths for Model 3

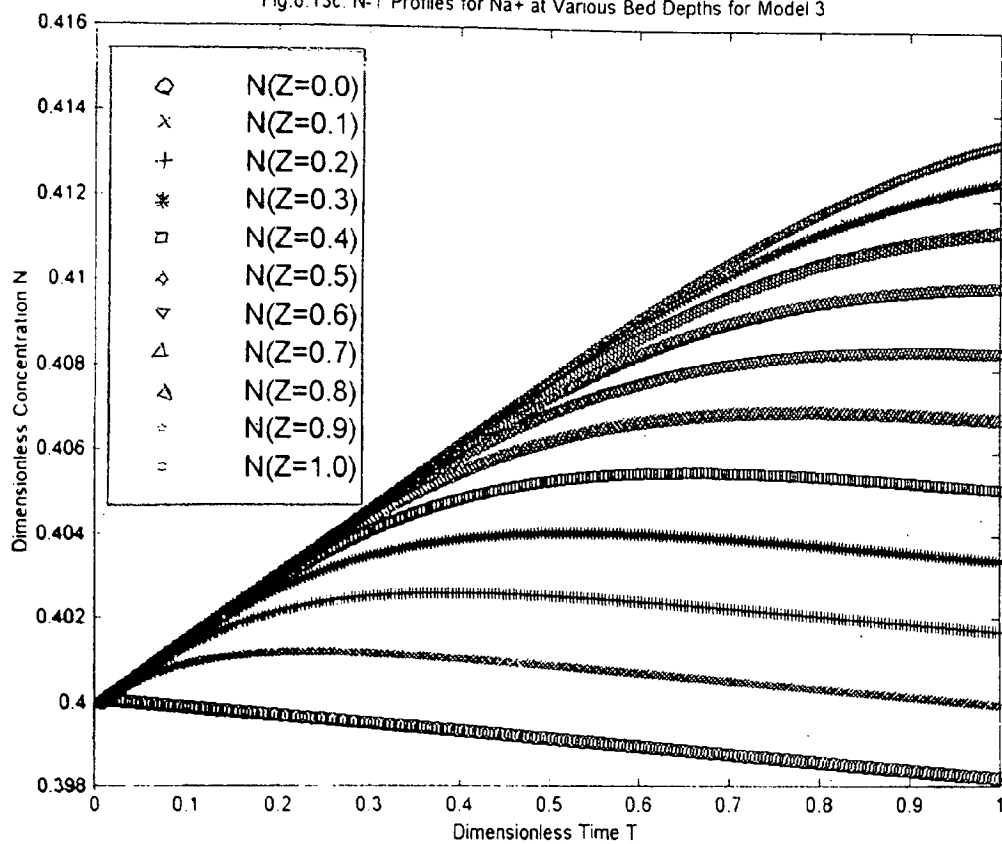
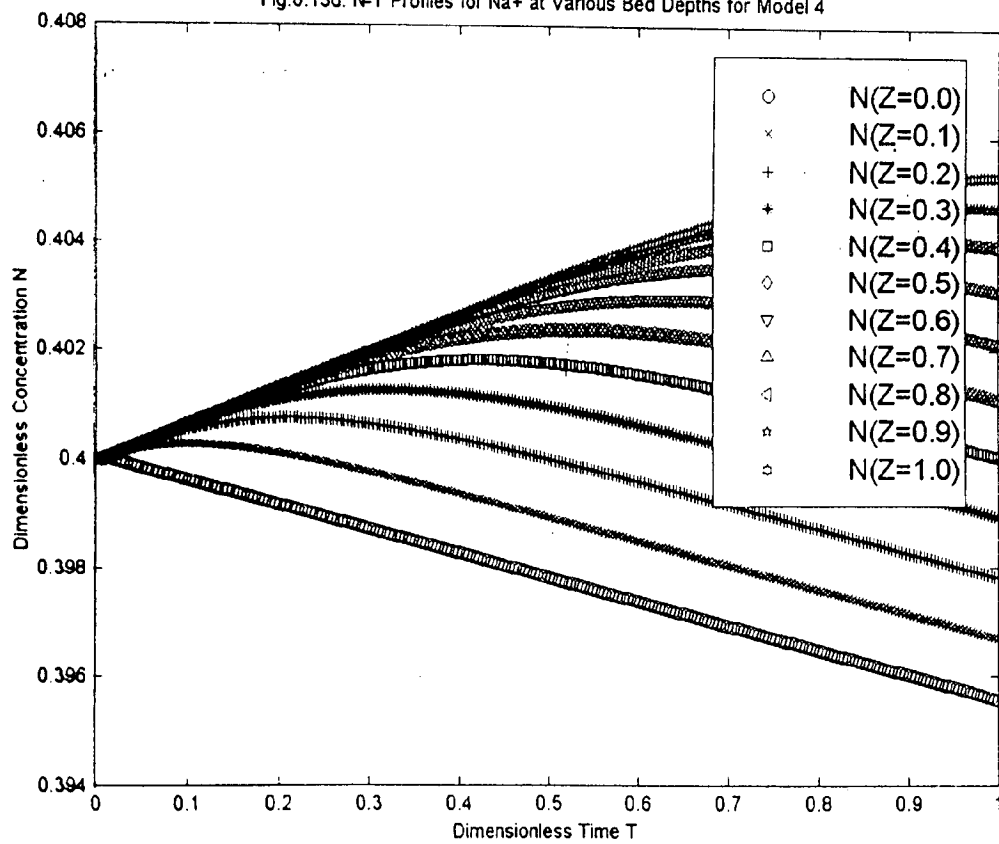


Fig.6.13d. N-T Profiles for Na+ at Various Bed Depths for Model 4



breakthrough curve with opposite trend. This is an expected behavior as the concentration in the solid phase is inversely proportional to that in liquid phase based on material balance concepts. However our study using solid phase as a basis closely agree with recent investigations of Liao & Shiau [51], where they developed a similar axial dispersion model for the operation of a fixed bed adsorber with a linear adsorption isotherm using the experimental data for the removal of phenol from the solution of activated carbon and the Amberlite resin XAD-4. These are valid for both large (10-60) and small Peclet numbers (0.1-5) and also for various retardation coefficients defined by the authors. It is important to mention that large value of Peclet number gives plug flow.

The model is further verified from the results of Lai & Tan [45] who has used a pore diffusion model assuming both the quartic profile and parabolic profile of exit concentration as a function of dimensionless time T . The adsorption rate has been assumed to much faster than the diffusion rate so that equilibrium exists at every location. The nature of the curve is found tallying very well with the present investigation.

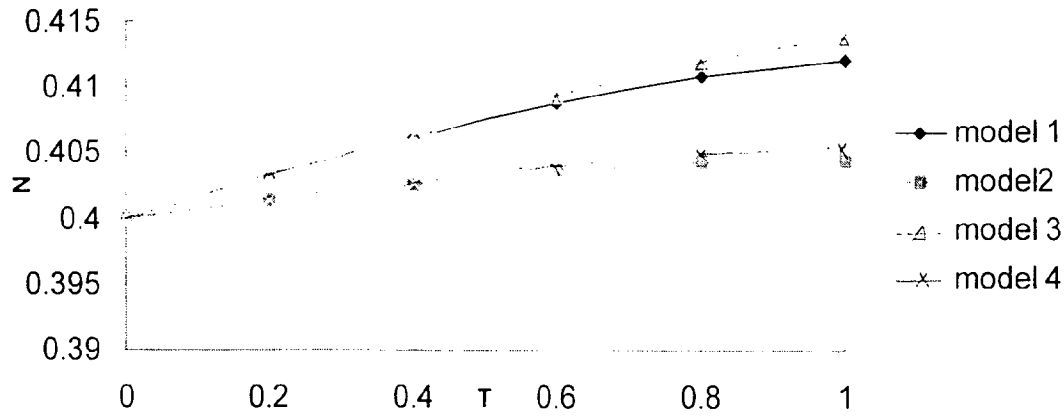
The model is also verified with the recent results of Sridhar [92] who has developed a model based on the isothermal sorption of a single solute in dispersed plug flow through a packed column of mono-dispersed porous particle and applied one point orthogonal collocation method to solve the model. The results of the present model are found also in close agreement of the results of the Sridhar [92].

The observations are also similar to those for a linear isotherm as pointed out by Do & Rice [c.f.45] and Rasmuson and Neretnieks [82].

Therefore the behavior displayed by the Na^+ during pulp washing in a paper mill in this present study must likely to occur. These findings claim a new dimension in the area of pulp and paper research and practices.

6.1.14 Comparison of the models for the nature of the species i.e. sodium on N-T profiles at bed exit

Fig. 6.14. N vs T Profiles At Z = 1 For Na For All The Four Models (Pe = 27)



For more clarity, the N–T profiles for all the models have been drawn for the Na^+ species at bed exit in Fig. 6.14. A comparison is made for all the models at $Z = 1$ and at $Pe = 27$.

Models 2 and 4 coincide at all the lower range of values of T but diverge as T becomes higher. The same is found true for models 1 and 3. The values from the later models are found to be higher than those predicted by models 2 and 4. The profiles depict that adsorption increases with time at bed exit. Models 3, 1, 4 and 2 show the adsorption of solute on pulp fiber in decreasing order at any fixed point after $T = 0.4$.

6.1.15 Effect of dimensionless pseudo time T on the adsorption-desorption dynamics of lignin

The concentration of lignin adsorbed on pulp fibers were plotted for N against the dimensionless pseudo time T in Figs. 6.15a-6.15d at various bed depths (ten equally spaced segments) for models 1-4 respectively. The nature of profiles in this case also is the same as that of the profiles for Sodium. The reasons are well explained above.

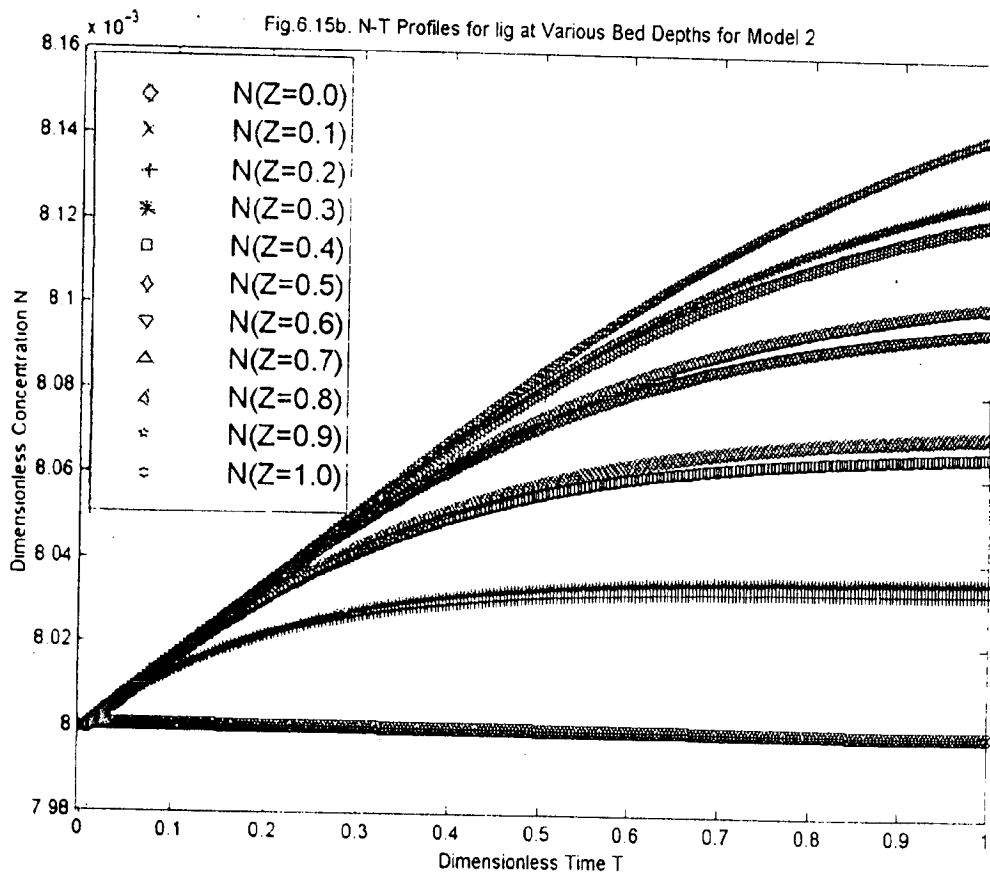
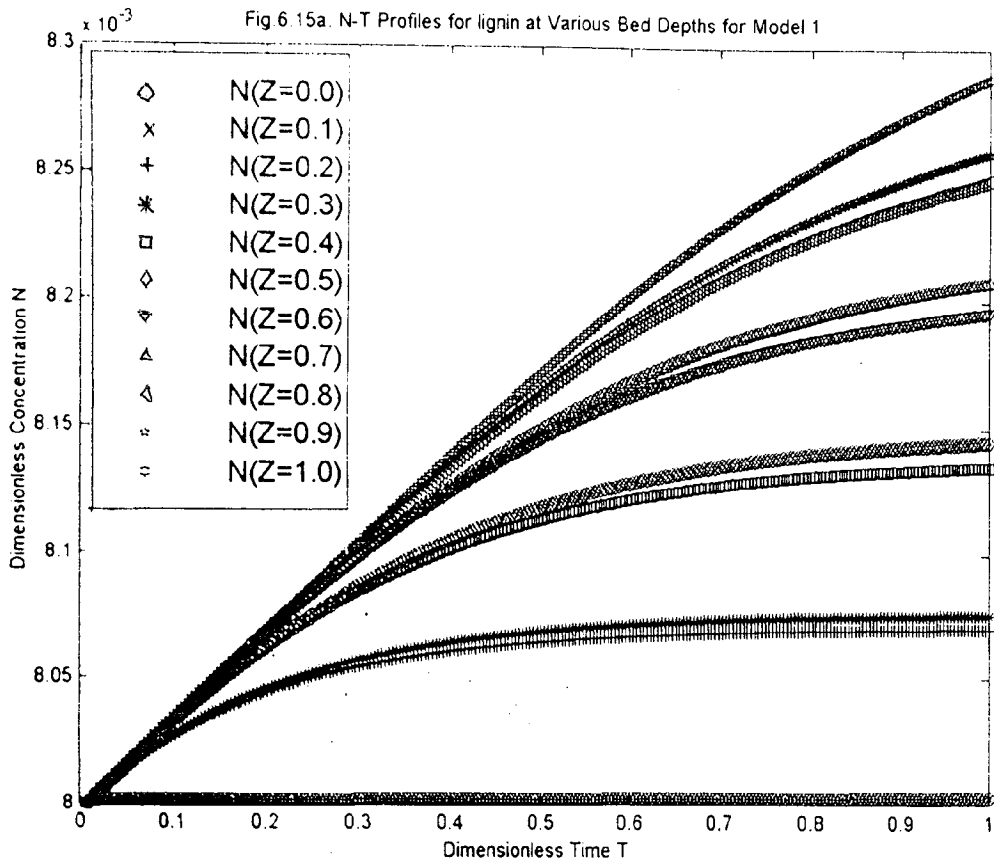


Fig.6.15c. N-T Profiles for lig at Various Bed Depths for Model 3

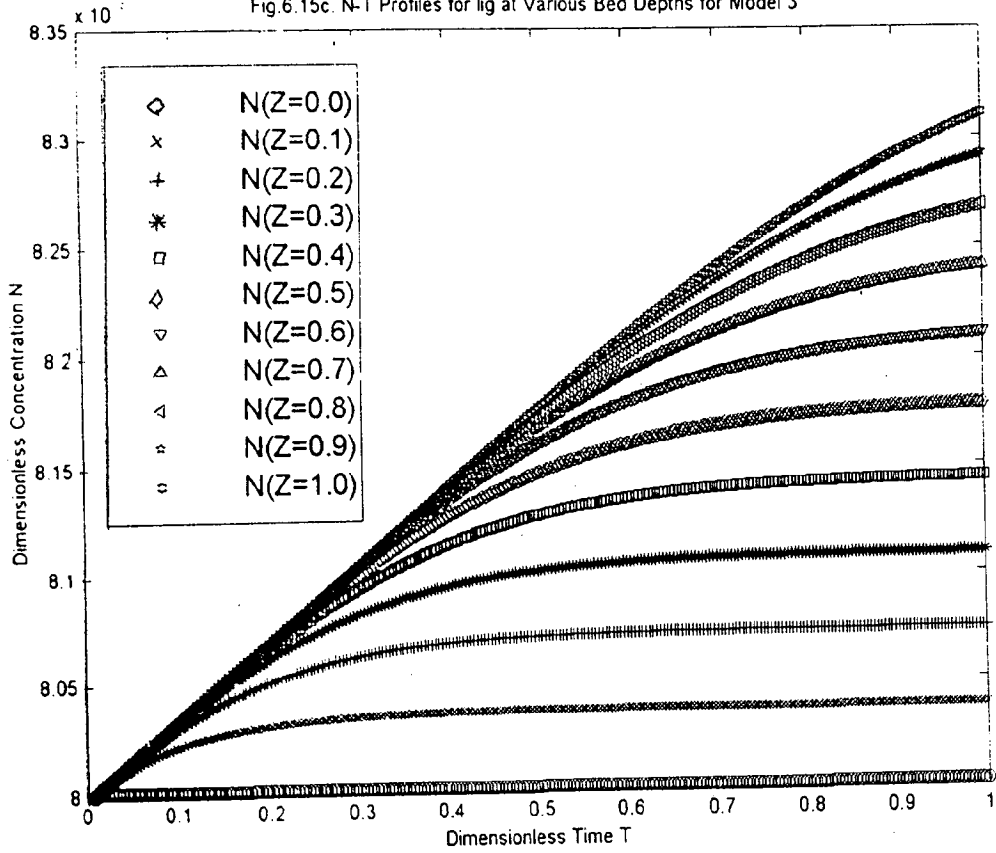
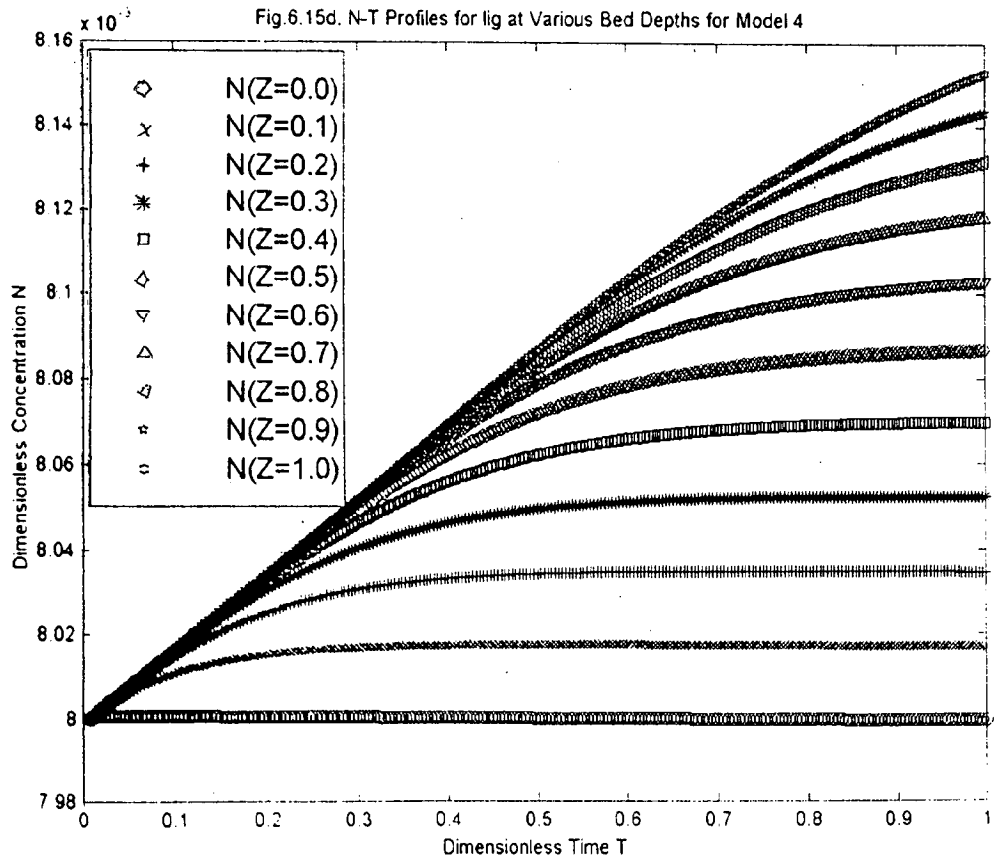
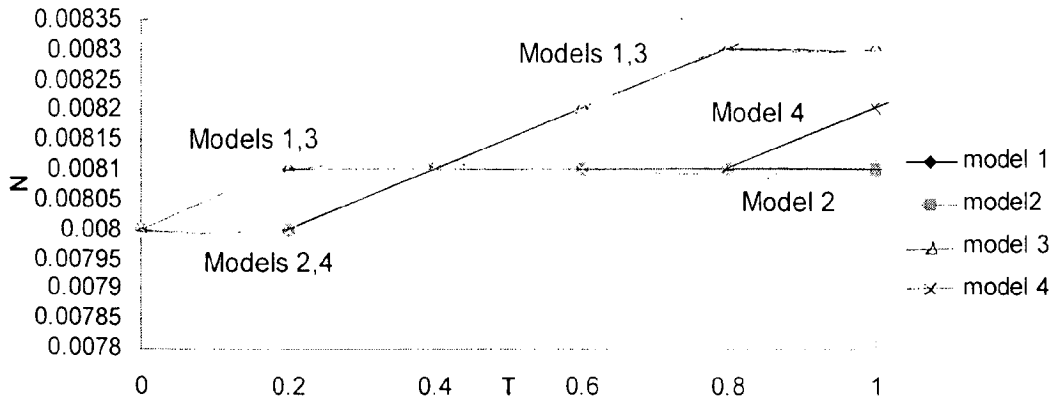


Fig.6.15d. N-T Profiles for lig at Various Bed Depths for Model 4



6.1.16 Comparison of models for the nature of the species of lignin on N-T profiles at bed exit

Fig. 6.16. N vs T Profiles At Z = 1 For lignin For All The Four Models (Pe = 20)



For more clarity, the N-T profiles for all the models have been drawn for the lignin species at bed exit in Fig. 6.16. A comparison is made for all the models at $Z = 1$ and at $Pe = 20$.

Upto $T = 0.2$ models 1 and 3 show more adsorption than models 2 and 4. The trend remains the same continuously till $T = 1$. The most interesting point to note is that the models with a particular type of adsorption-desorption isotherm show more adsorption than the model with another type of adsorption-desorption isotherm. The type of adsorption isotherm is thus playing a definite role.

6.1.17 Effect of T on C for Sodium at various values of ϵ at mid points of cake thickness

The effect of porosity on C-T profiles of the break through curves has been shown in Figs. 6.17a-6.17d for Na^+ species at mid points of the cake thickness. The porosity values have been varied from 0.1 (strictly valid for almost non-porous solids) to 0.95 (generally valid for fibrous mats in brown stock washer) within the range of both C and T (0 to 1). These assumed ranges can also be applicable for highly waterous pulp suspension such as in Fourdrinier wire in case of paper formation at the wet end to compact pulp mat under wet pressing operation. The values of porosity for the above system are explained earlier and are in conformity with the various models proposed for porosity given in Section 5.1 of chapter 5.

Fig 6 17a C-T Profiles for Na⁺ for Various Values of Porosity at the Mid of Cake Thickness for Model 1

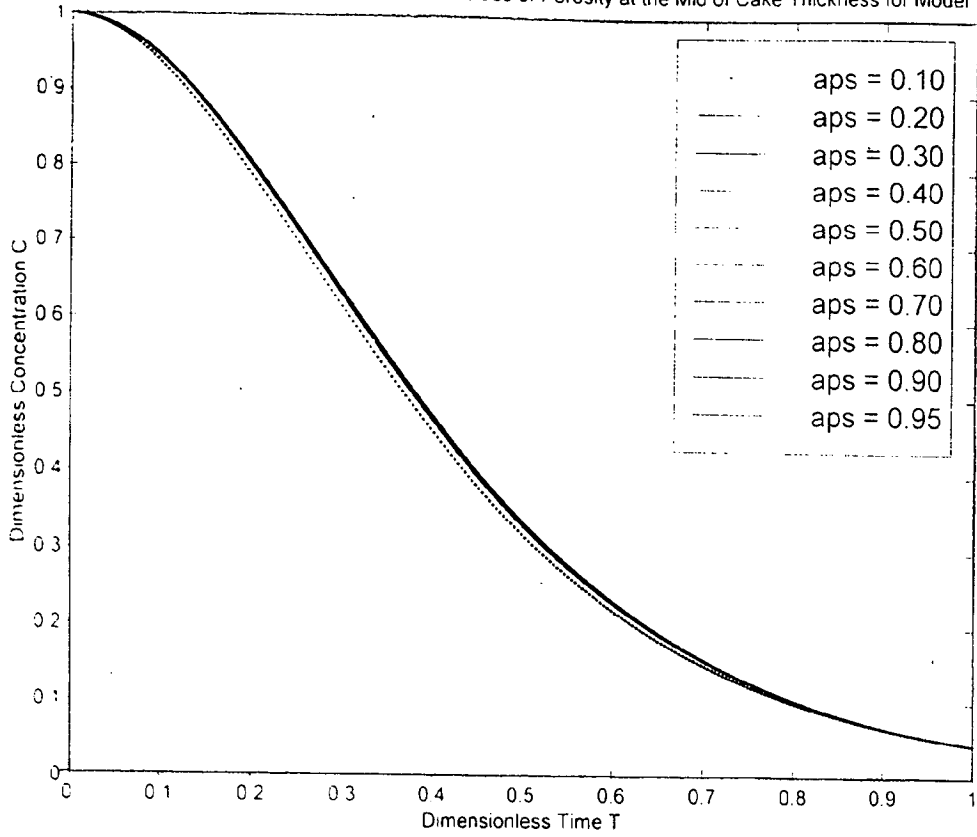


Fig 6 17b C-T Profiles for Na⁺ for Various Values of Porosity at the Mid of Cake Thickness for Model 2

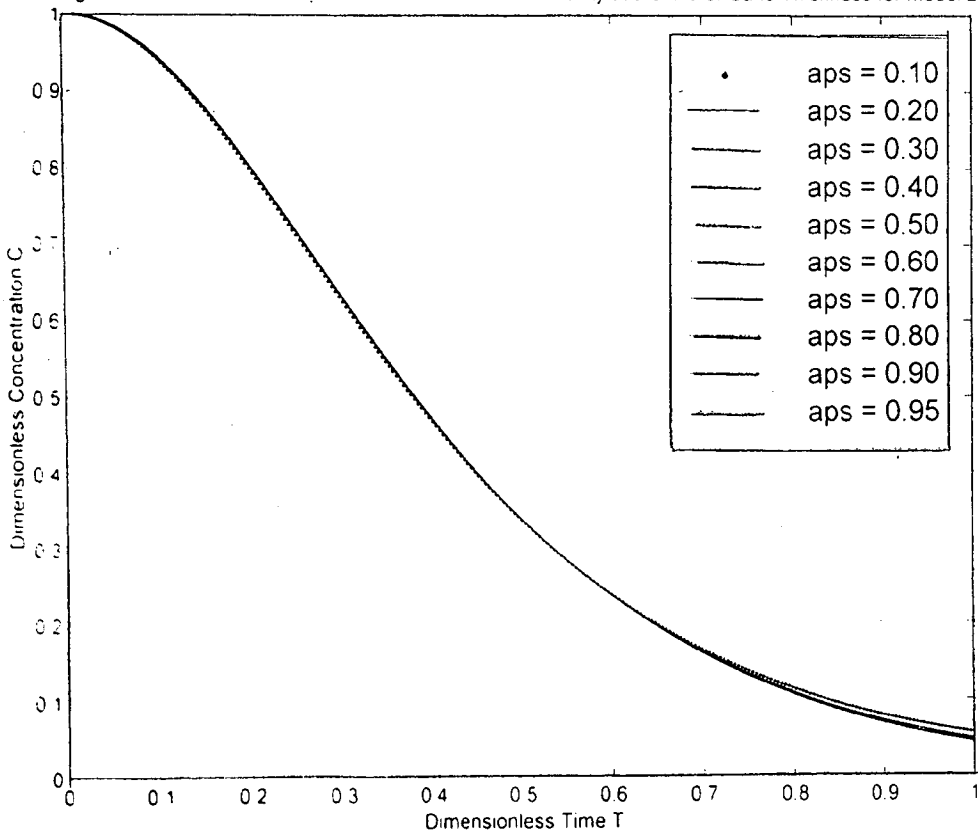


Fig 6. 17c. C-T Profiles for Na+ for Various Values of Porosity at Mid of Cake Thickness for Model 3

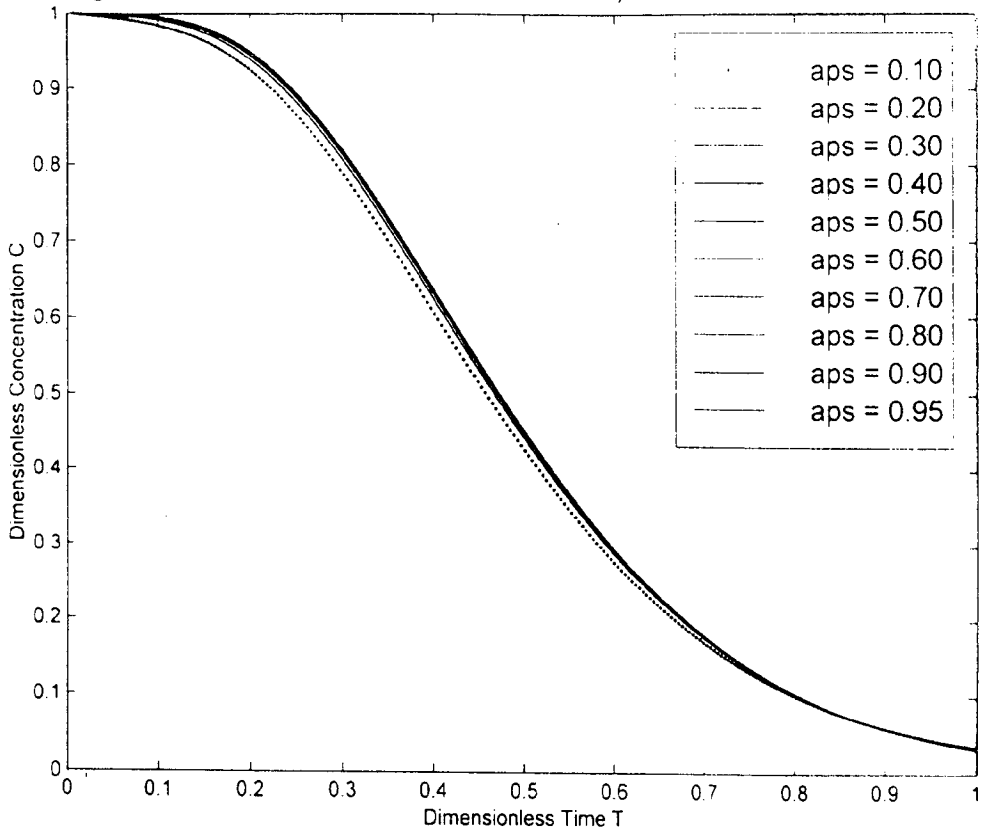
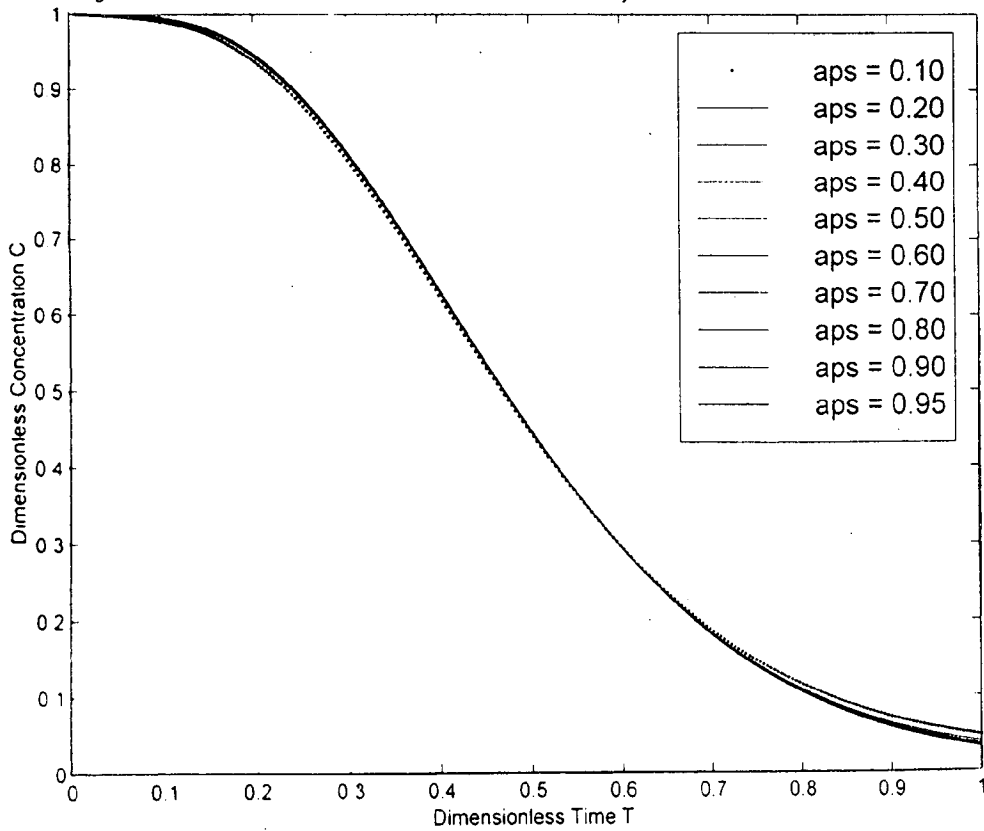


Fig 6 17d. C-T Profiles for Na+ for Various Values of Porosity at Mid of Cake Thickness for Model 4



There is no noticeable change of the C–T profiles with ϵ ranging from 0.4 to 0.95. However there is small change observed if one attempts to use very low consistency pulp. This deviation can be ignored in engineering practice. This fact is in agreement with many earlier investigators [24,28]. This might be due to the fact that for medium to high porosity values the effect is shrouded by the concomitant effect of longitudinal dispersion coefficient, tortuosity and local flow velocity. The longer range is considered to cover not only the entire range of suspension hebetated by the stock in paper making process in practice but also to cover the porosity value of the flowing zone (0.7 to 0.85), the same for stagnant zone (0.1 to 0.2) and total mean porosity values above 0.90.

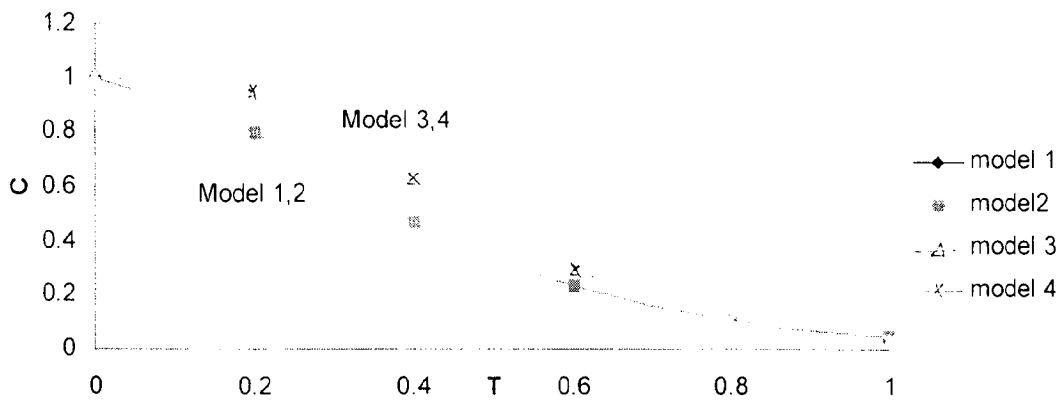
Similar type of plots can be shown for models 2, 3 and 4. It is important to mention that models 1 and 2 involve dispersion whereas models 3 and 4 have neglected this aspect.

Further, the models 1 and 3 have similar adsorption-desorption dynamics, distinctly different from models 2 and 4. It is interesting to note that the diversions from coincidental lines for low porosity values are more in models 1 and 3, whereas the diversion almost disappears in models 2 and 4. This is valid upto the point of 80 % porosity. A more interesting point is also found that beyond $T = 0.75$, models 1 and 3 coincide without any deviation whereas for models 2 and 4 the deviation appears in appreciable amount if one uses the value upto $T = 1$. This might be attributed to the adsorption-desorption of Na^+ that interplay major role alongwith dispersion mechanism.

6.1.18 Comparison of C–T profiles for Sodium for constant ϵ for all the models at mid points of cake thickness

Fig. 6.18 shows a comparison of C–T profiles for sodium at mid points of cake thickness using a constant value of porosity ($\epsilon = 0.95$). Profiles of models with and without dispersion show different nature although the difference is very small. The profiles are found to be a break through type meeting at $T = 0.8$ and then diverging again.

**Fig. 6.18. C vs T At Z = 0.5 For Na For All The Four Models, $\epsilon = 0.95$
($Pe = 27$)**



6.1.19 Effect of T on C for lignin at various values of ϵ at mid points of cake thickness

The C–T profiles for lignin at various values of porosity as indicated in previous paragraph for sodium have been drawn in Figs.6.19a–6.19d for models 1–4 respectively. Unlike the sodium species, the C–T profiles remain the same for all porosity values with merging each other and also for all the models.

6.1.20 Comparison of C–T profiles of lignin for constant ϵ for all the models at mid points of cake thickness

The plots of C–T profiles have been drawn for lignin, a major component for the black liquor in Fig. 6.20 for models 1-4 at mid points of cake thickness using a constant value of porosity ($\epsilon = 0.95$). It is evident from the graphs that Models 1-2 (with dispersion) coincides and the same is true for models 3 and 4 (without dispersion). Virtually these are not distinguishable. The analysis of the data indicates the followings:

- Boundary conditions do not influence the shape of the profiles and the value of the concentration C.
- Adsorption-desorption dynamics has little role to play.
- The difference is mainly due to dispersion effects.

Fig 6. 19a. C-T Profiles for lig for Various Values of Porosity at Mid of Cake Thickness for Model 1

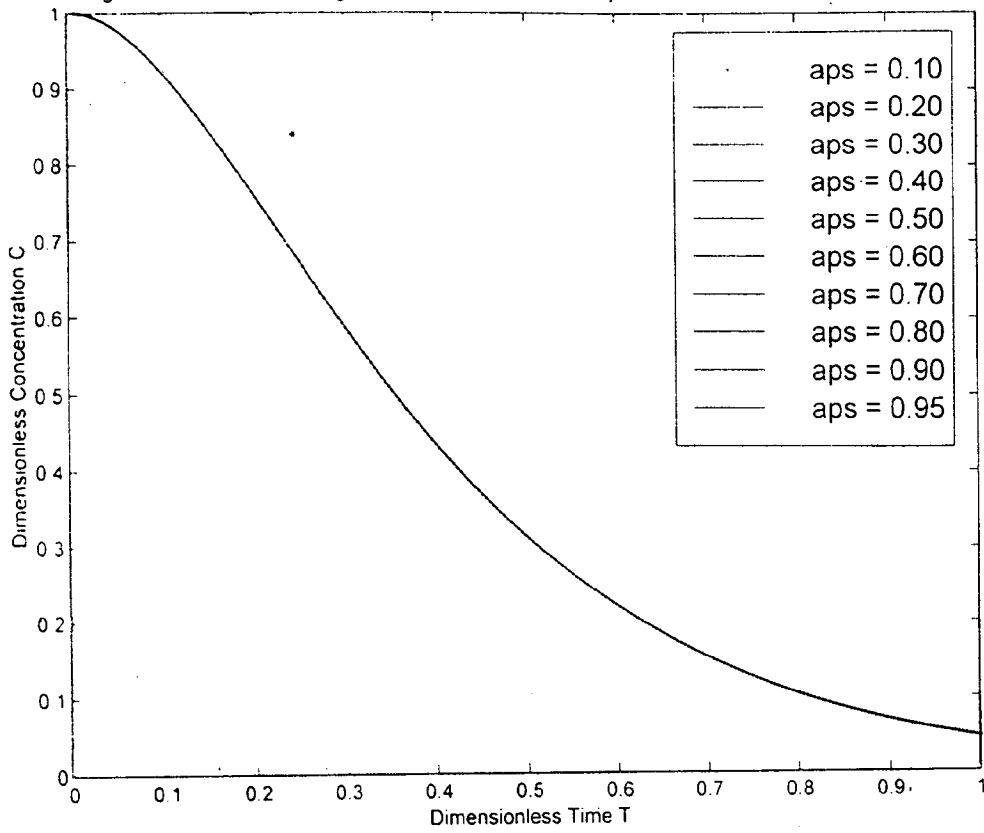


Fig 6. 19b. C-T Profiles for lig for Various Values of Porosity at Mid of Cake Thickness for Model 2

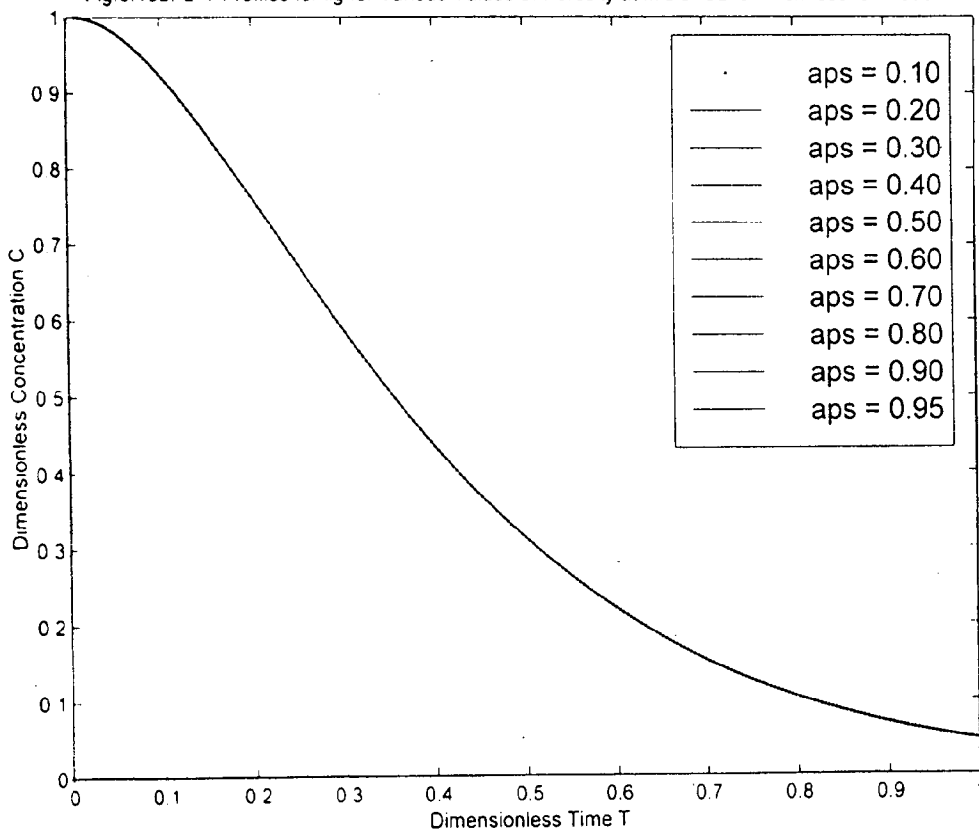


Fig 6.19c. C-T Profiles for lig for Various Values of Porosity at Mid of Cake Thickness for Model 3

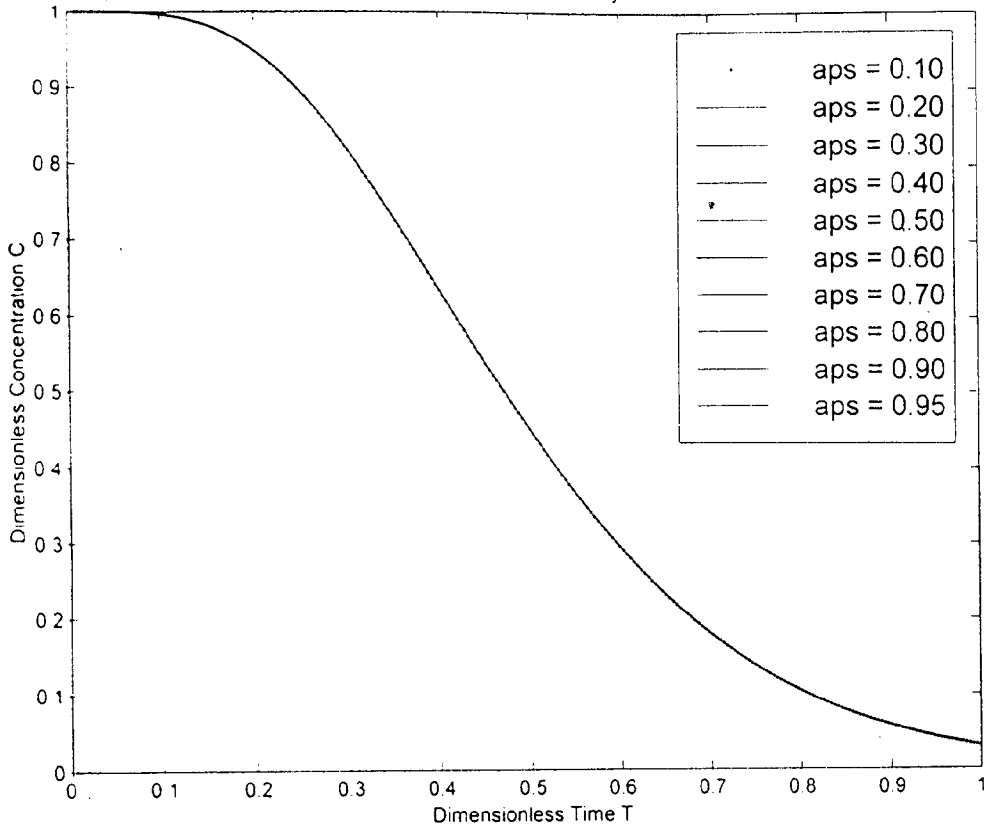
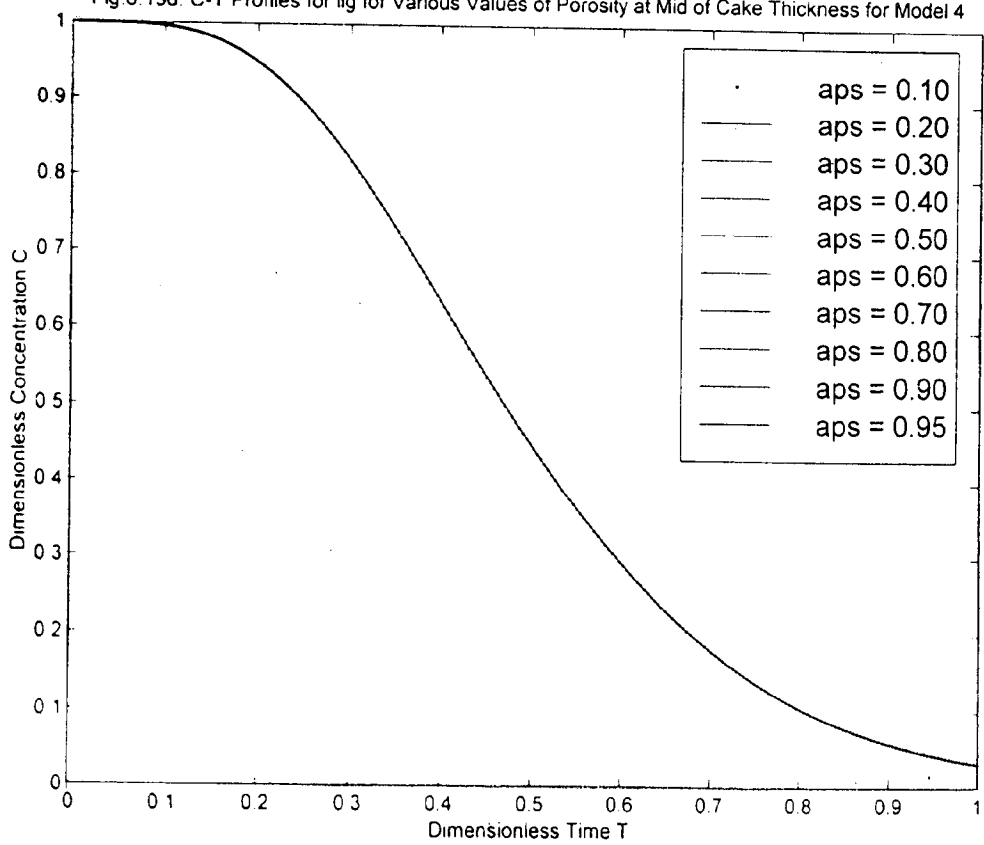


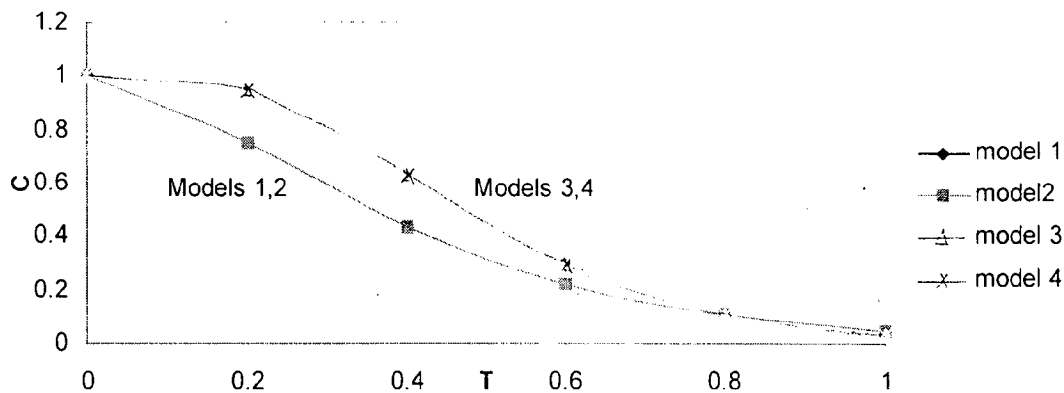
Fig 6.19d. C-T Profiles for lig for Various Values of Porosity at Mid of Cake Thickness for Model 4



- Model 1 and model 2 has no displacement part due to predominant effect of dispersion.
- The difference of the value of C at a fixed T is very significant between groups of models.

It is important to mention that lignin is a high molecular weight organic substance. Its molecular weight is much higher than that of the sodium. The rate of transfer is also very different for that of sodium because of mobility of lignin species is much smaller in magnitude than that of sodium species. Therefore it is expected that the performance of any given washing system with respect to lignin fragment removal must be quite different from its performance with respect to sodium removal.

Fig. 6.20. C vs T Profiles At Z = 0.5 For lignin For All The Four Models, $\alpha_{ps} = 0.95$ ($Pe = 20$)



6.1.21 N – T profiles for Sodium with porosity as a parameter at mid points of the cake thickness

Figs. 6.21a-6.21d are drawn for N–T profiles, with the porosity values as mentioned in Table 6.1, at mid points of the cake thickness for models 1–4 respectively. As expected the dimensionless concentration increases with the increase of T, at first very sharply, almost linearly till $T = 0.3$ and then becomes strongly non linear (parabolic in nature) between $T = 0.3$ and $T = 0.7$ and thereafter exhibits almost linear characteristics with decreasing trend. This behavior is displayed by the data from model 1 and model 3 where isotherm is assumed the same.

Fig 6 21a N-T Profiles for Na+ for Various Values of Porosity at the Mid of Cake Thickness for Model 1

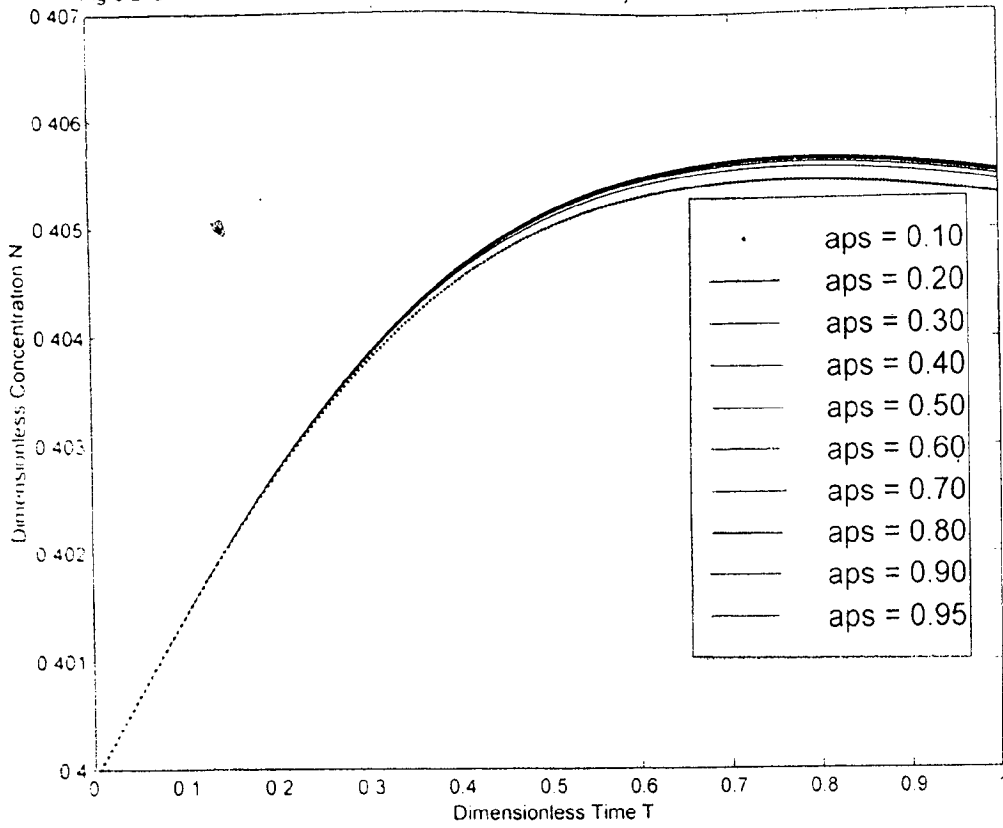


Fig 6 21b N-T Profiles for Na+ for Various Values of Porosity at the Mid of Cake Thickness for Model 2

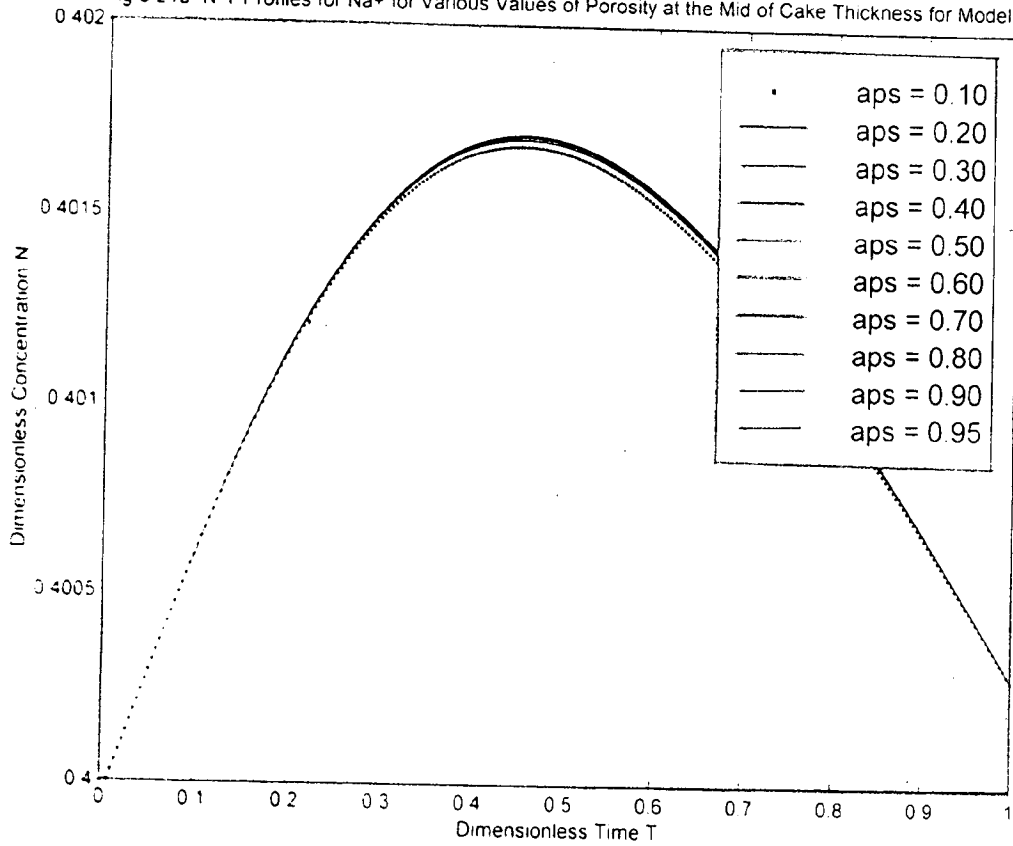


Fig 6 21c. N-T Profiles for Na+ for Various Values of Porosity at Mid of Cake Thickness for Model 3

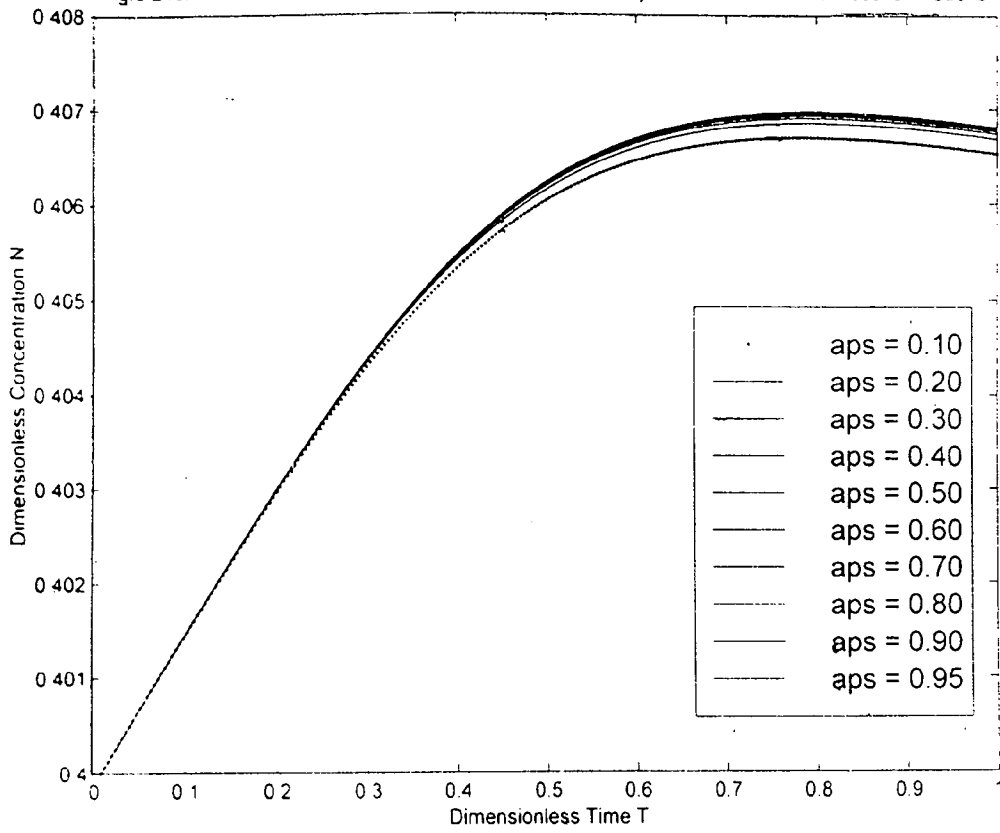
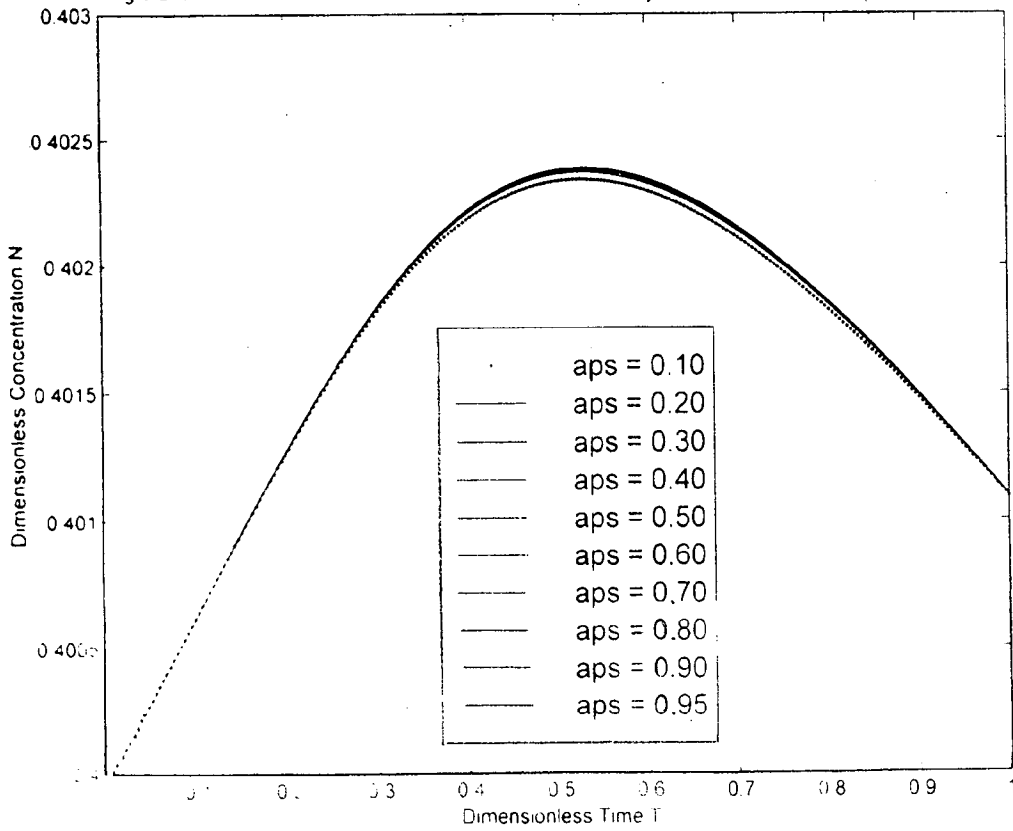


Fig 6 21d. N-T Profiles for Na+ for Various Values of Porosity at Mid of Cake Thickness for Model 4

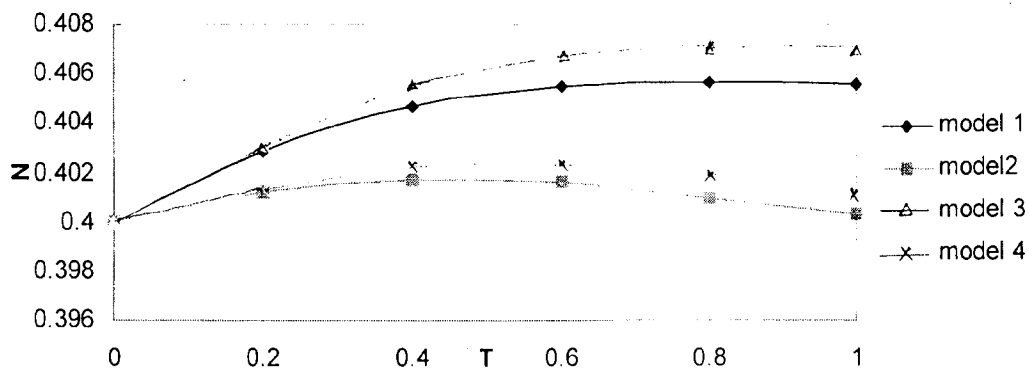


Though there is a difference of model building, it may be pointed out that model 1 contains dispersion term while model 3 does not. It is apparent therefore that dispersion has minor role compared to adsorption for N-T profiles. This is an established fact. It is also interesting to note that the porosity has no influence at a lower time values but deviates larger and larger for higher time values. For porosity values higher than 0.4, as earlier found, there is no difference noticed.

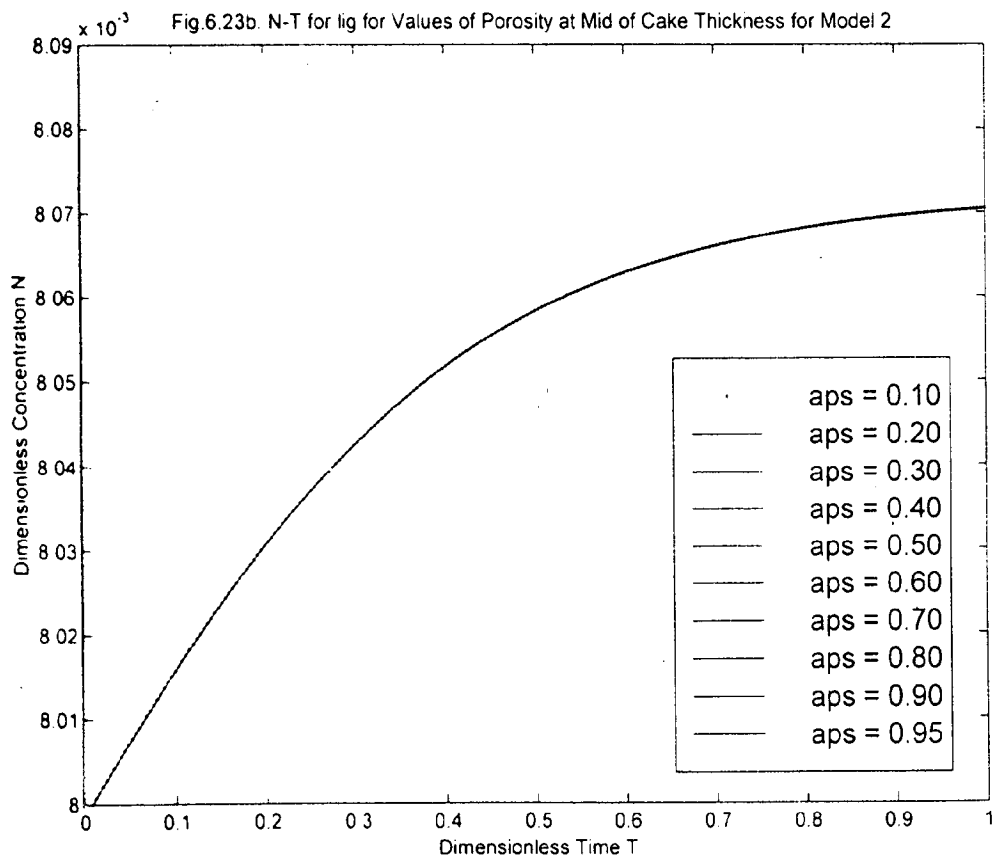
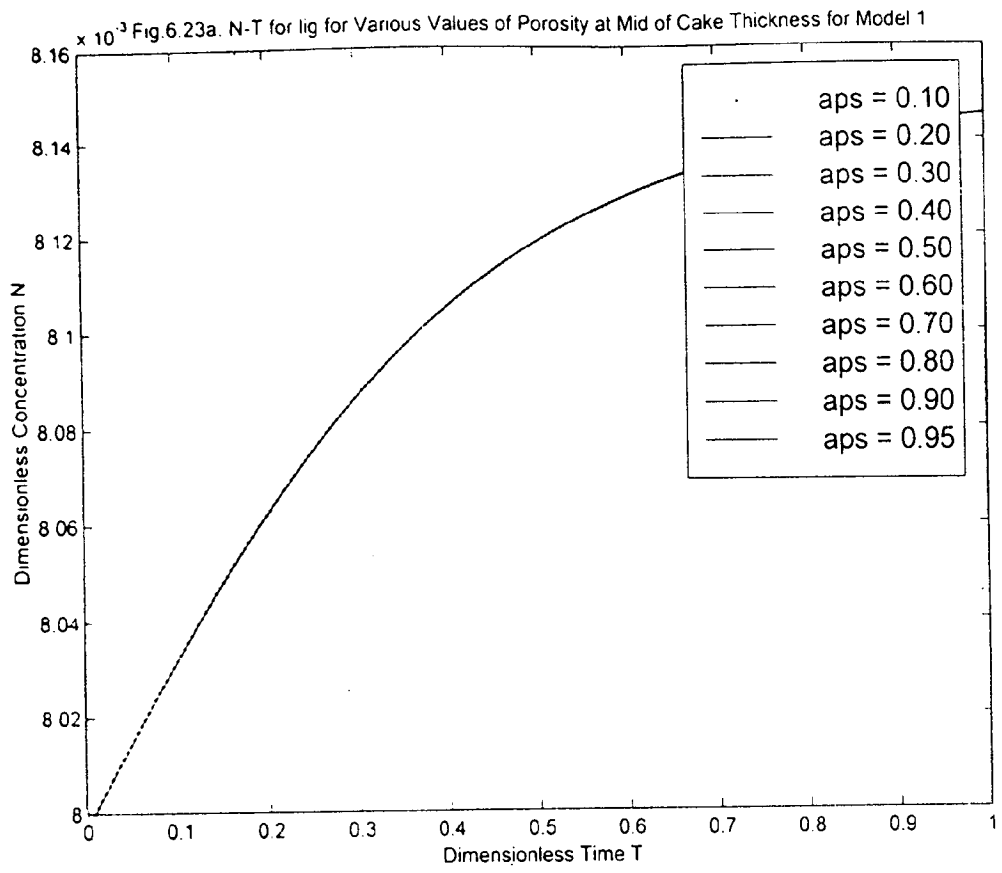
In sharp contrary to the above profiles (N-T profiles) of models 1 and 3, the profiles for models 2 and 4 exhibits a perfect parabola with change of vertices. Do and Rice [c.f.45] agrees with this type of behaviour. As earlier found there is no effect of porosity at the lower values of T, but deviation is observed somewhere between T = 0.3 and T = 0.7 and thereafter it again coincides for the time values greater than T = 0.7. The deviation however at the central part of time is limited to very low value of porosity. For higher porosity values above 0.3, there are insignificant changes.

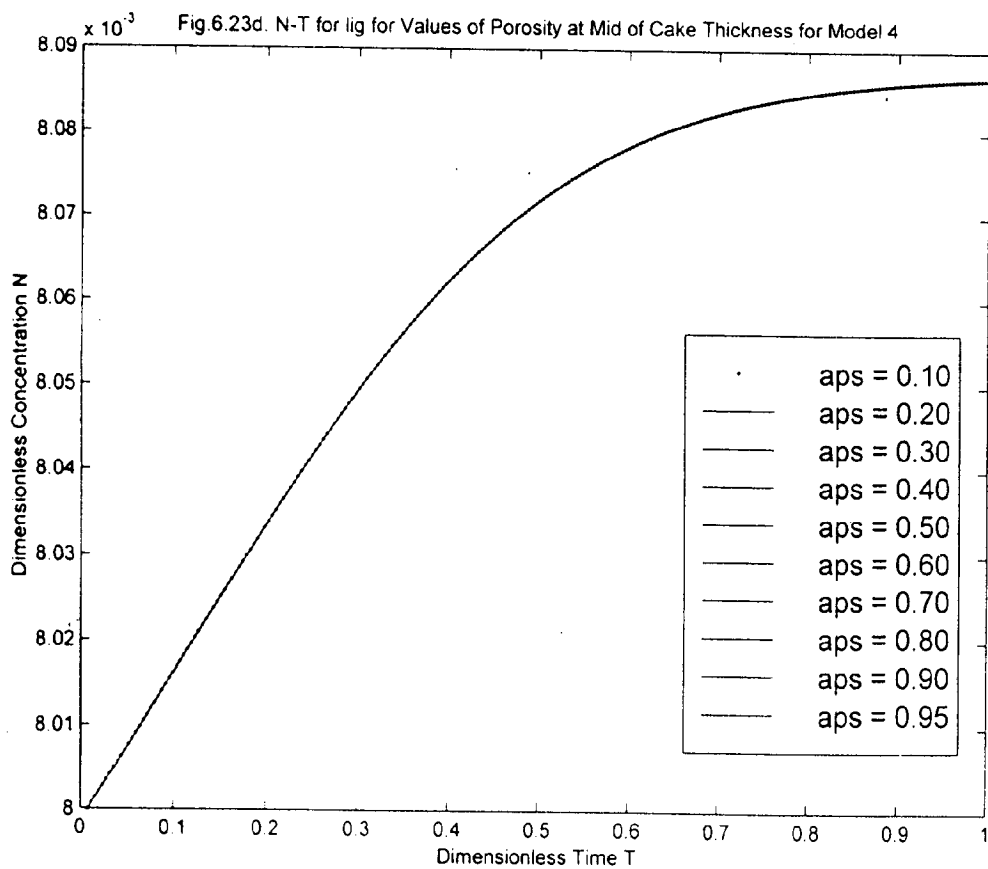
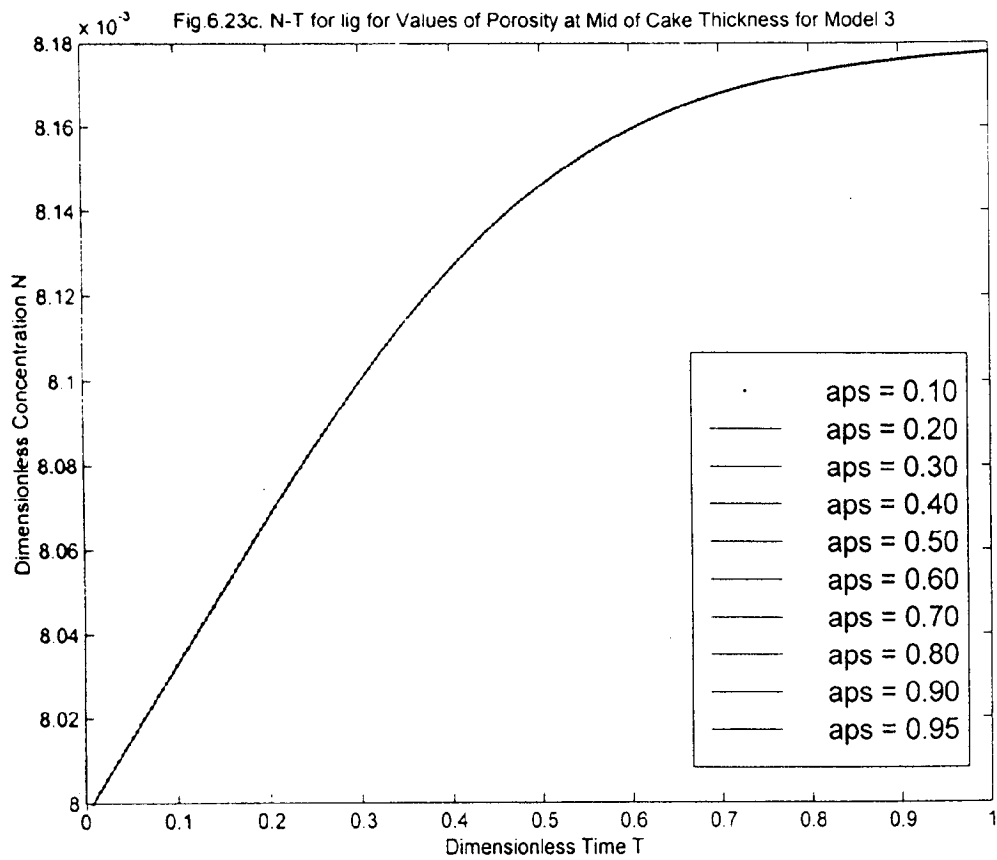
6.1.22 Comparison of N-T profiles for Sodium for constant ϵ for all the four Models

Fig. 6.22. N vs T At Z = 0.5 For Na For All The Four Models, $\epsilon = 0.95$ (Pe = 27)



The comparison of all the models (1-4) has been depicted in Fig.6.22 which has been drawn at Z = 0.5 at a fixed value of porosity ($\epsilon = 0.95$) with Pe number 27. It is clear from the figure that similar behavior is exhibited by all the models initially. The curves show increasing trend with a particular type of adsorption-desorption dynamics. The value of C is originated from 0.4 at T = 0 and





increases as T increases for models 1 and 3, though model 3 gives higher values than model 1. However for model 4 and model 2, though increases initially upto $T = 0.4$ then there is slight decreasing trend observed. In this later case also model 2 predicts lower value than model 4 upto $T = 0.6$. The increasing order of C values are as follows: $3 > 1 > 4 > 2$. These behavior need more detailed investigations

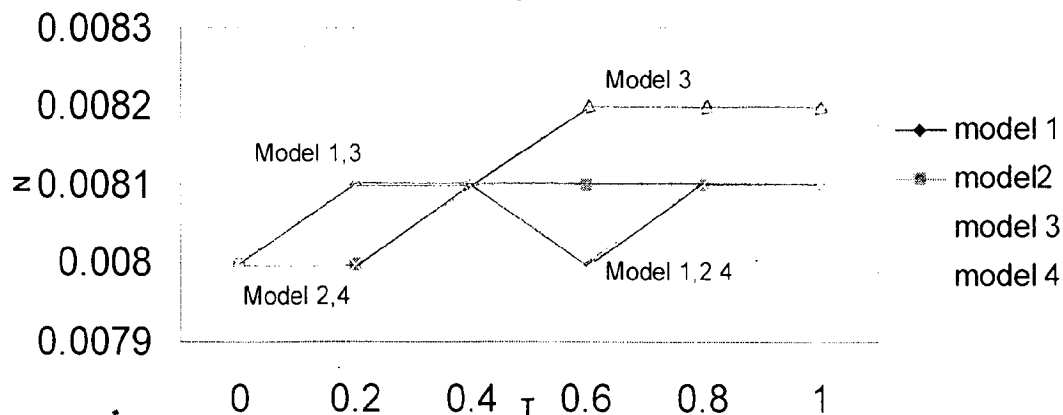
6.1.23 N–T profiles for lignin with porosity as a parameter at mid points of cake thickness

Figs. 6.23a–6.23d depict the N–T profiles for lignin species at various porosity values at mid points of the cake thickness for models 1–4 respectively.

Most striking difference is observed for lignin adsorption-desorption kinetics. All the models display the same curvilinear characteristics (half parabola) for all the models (1-4) and for all the porosity values (0.1-0.95) considered. All the curves originated from zero time i.e. at the start, go linearly upto $T = 0.4$ and then become slightly curvilinear, thereafter become linear for higher values of time T (0.7). However there is a change of slopes in all the four cases. It is clear from the graphs that neither dispersion nor adsorption influenced to a great extent. In fact earlier investigators assumed that adsorption of lignin can be considered negligible.

6.1.24 Comparison of N–T profiles for lignin for constant ε for all the four models

Fig. 6.24. N vs T profiles At $Z = 0.5$ For lignin For All The Four Models, $\alpha_{ps} = 0.95$ ($Pe = 20$)



A comparison is made for N-T profile for all the models namely models 1-4 in Fig. 6.24 at $Z = 0.5$ for lignin at a constant Peclet number ($Pe = 20$) and total porosity value of 0.95. It is evident from the figure that the models 1 - 4 coincide after $T = 0.4$. In sharp contrast the model 3 though departs apparently and but in terms of magnitude it is not very significant. The same explanation as given in Sec. 6.1.23 is also applicable in this case.

6.1.25 Effect of local average velocity on C vs. T profiles for Sodium and lignin at mid points of cake thickness

Effect of linear average velocity on C-T profiles for Sodium have been shown in Figs. 6.25a-6.25d at mid points of the cake thickness. It is evident that at all values of interstitial velocity u , ranging from 8 mm / s to 26 mm / s, the C-T profiles display the same characteristics. Most interesting point to mention is that at a certain dimensionless time T lying between 0.3 and 0.4, the profiles give point of inflexion. The profiles of the models with dispersion term becomes upside down beyond the inflexion point i.e. lower velocity profile will be at the upper side of the profiles. This is attributed to the combined effect of velocity which is changing from point to point in the porous bed and diffusion induced dispersion phenomena. In fact we have neglected the diffusion of solutes in the porous bed due to its much smaller magnitude compared to dispersion (Section 3). The profiles of the models without dispersion term coincide throughout the span.

Effect of linear average velocity on C-T profiles for lignin have been shown in Figs. 6.26a-6.26d at mid points of the cake thickness. Like the profiles for Sodium the profiles for lignin also give inflexion point at a certain dimensionless time T lying between 0.3 and 0.5 and exhibits the same characteristics. This is in excellent agreement with Grah [24]. The profiles of the models without dispersion term also coincide throughout the span.

Fig.6.25a C-T Profiles for Na+ for Various Values of u at the Mid of Cake Thickness for Model 1

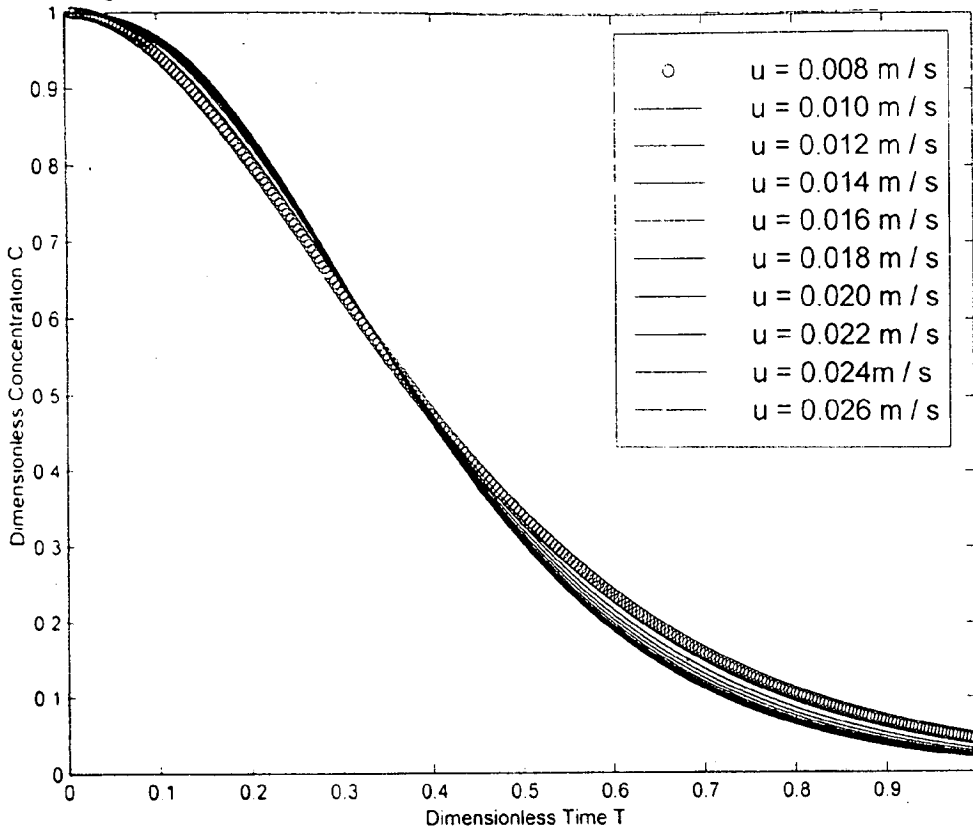


Fig.6.25b C-T Profiles for Na+ for Various Values of u at Mid of Cake Thickness for Model 2

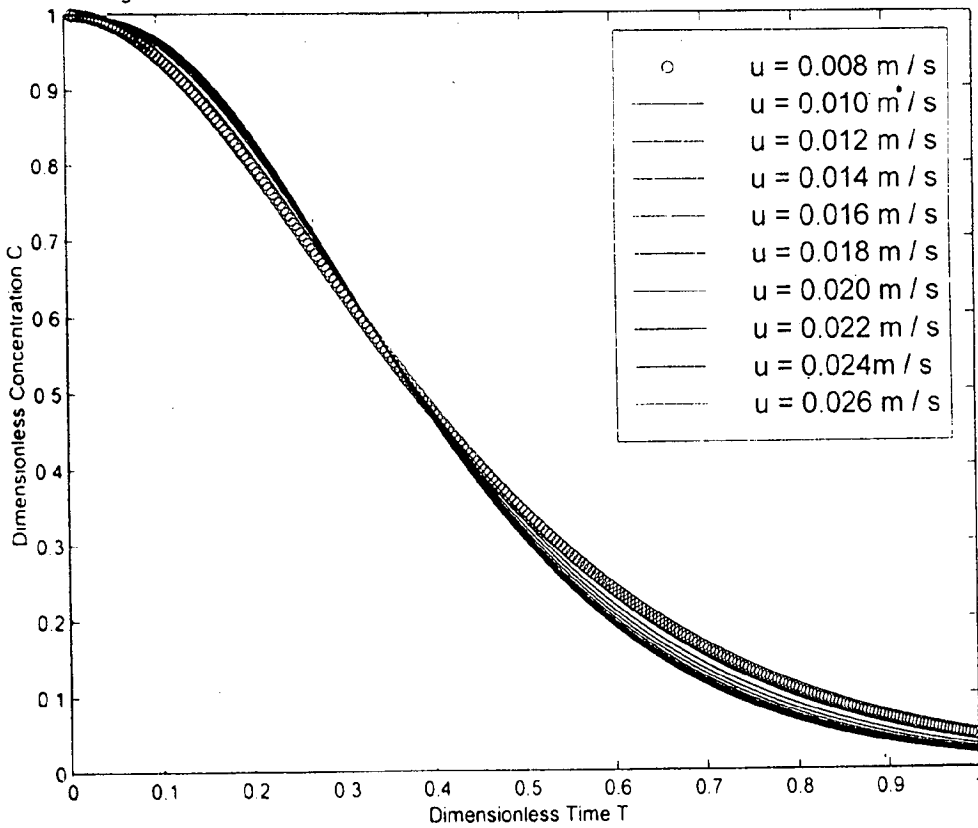


Fig.6.25c. C-T Profiles for Na+ for Various Values of u at Mid of Cake Thickness for Model 3

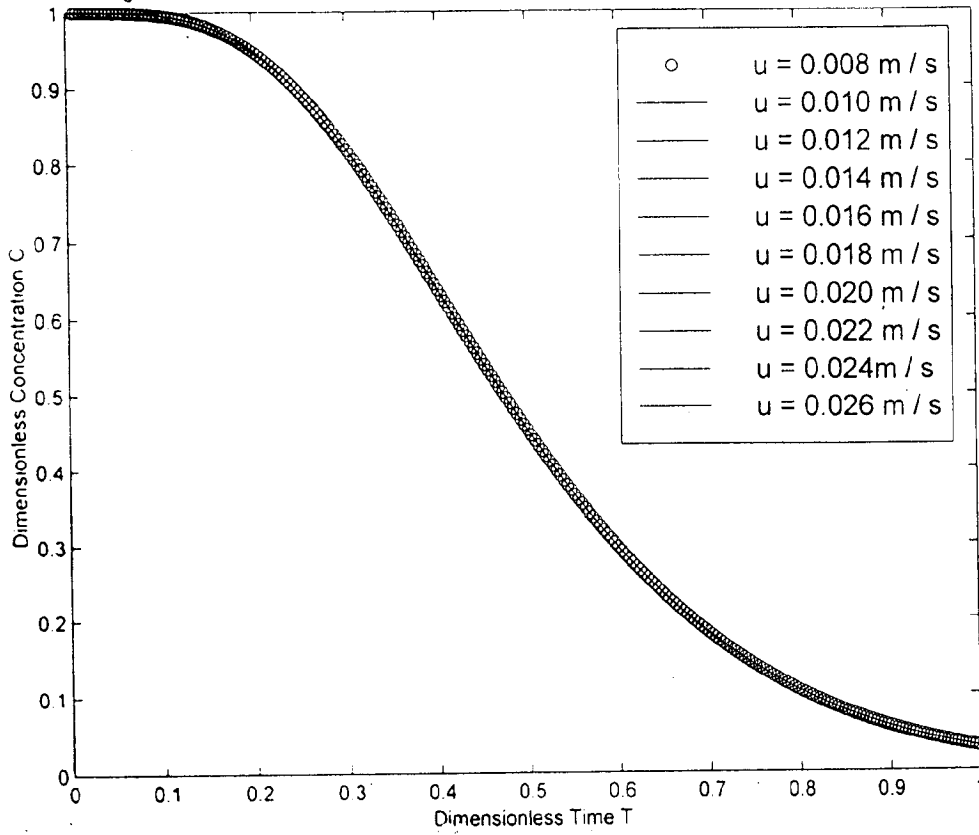


Fig.6.25d. C-T Profiles for Na+ for Various Values of u at Mid of Cake Thickness for Model 4

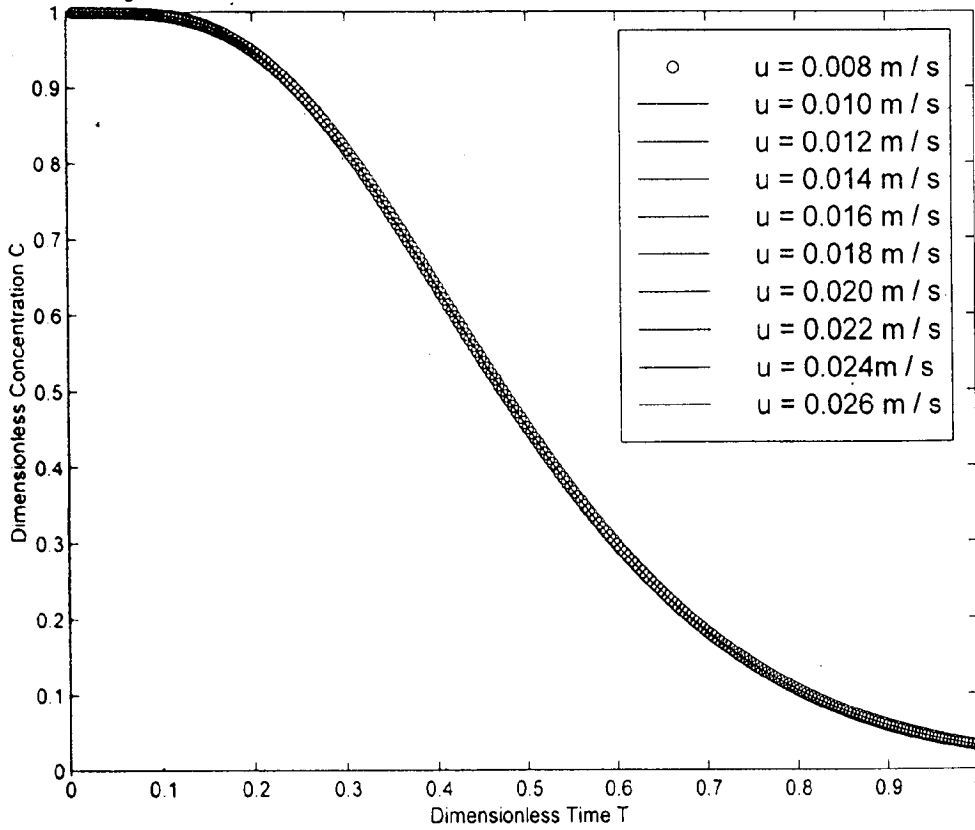


Fig.6.26a. C-T Profiles for lig for Various Values of u at Mid of Cake Thickness for Model 1

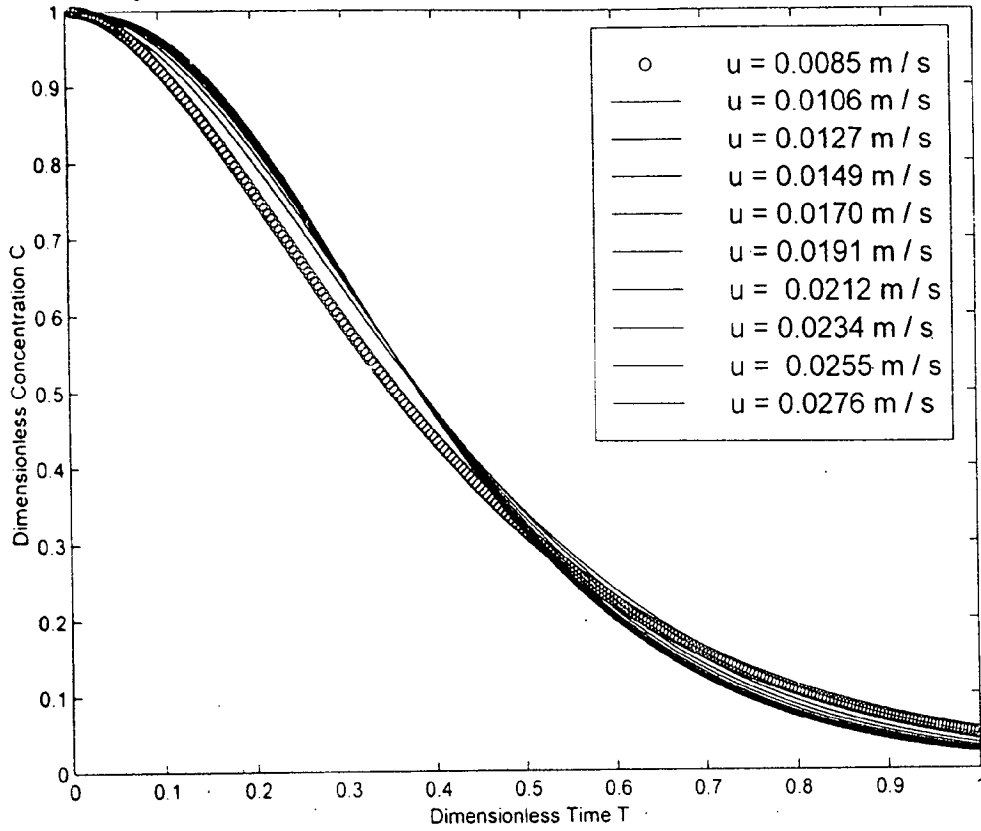


Fig.6.26b. C-T Profiles for lig for Various Values of u at Mid of Cake Thickness for Model 2

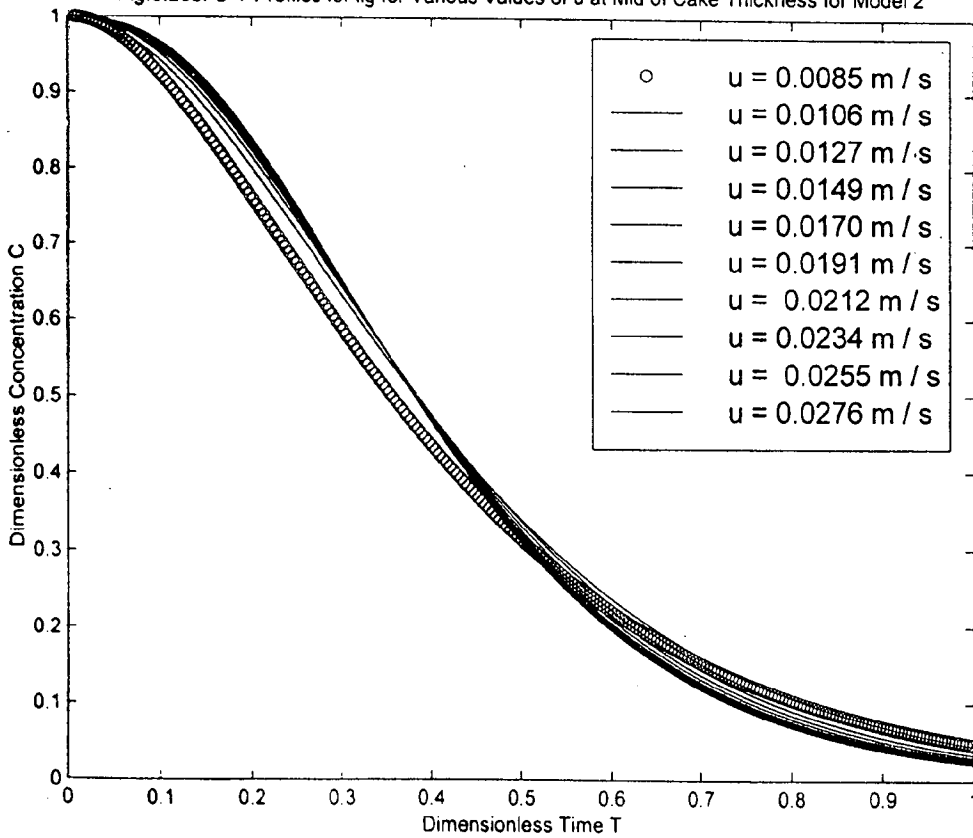


Fig.6.26c. C-T Profiles for lig for Various Values of u at Mid of Cake Thickness for Model 3

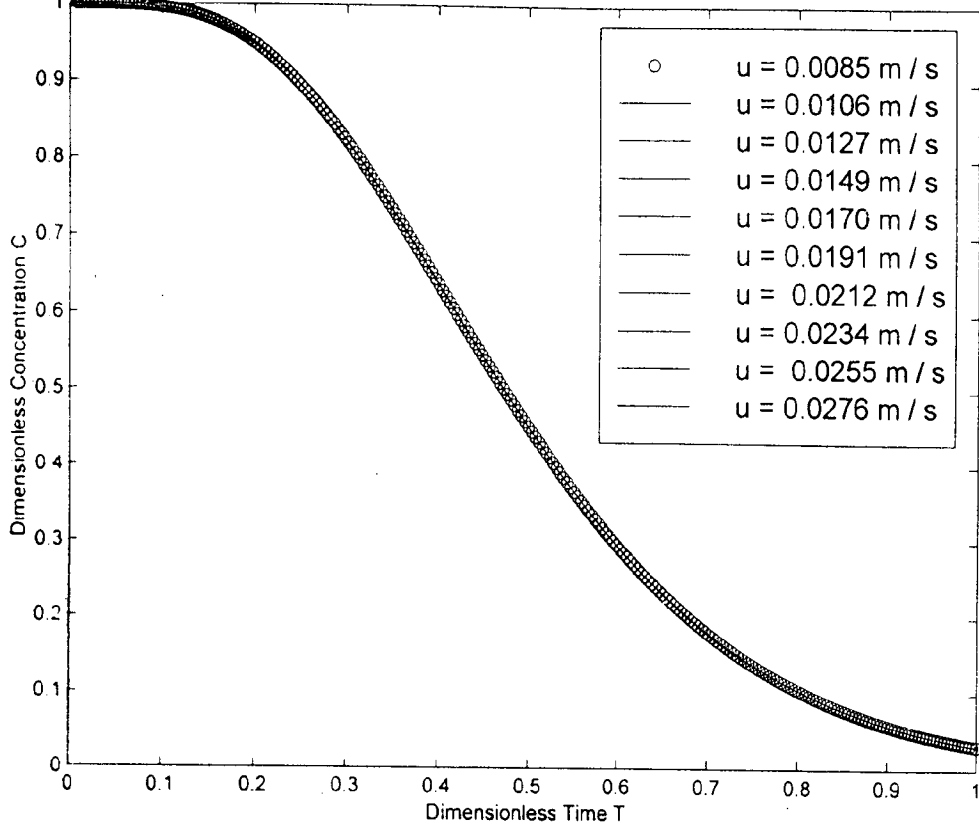


Fig.6.26d. C-T Profiles for lig for Various Values of u at Mid of Cake Thickness for Model 4

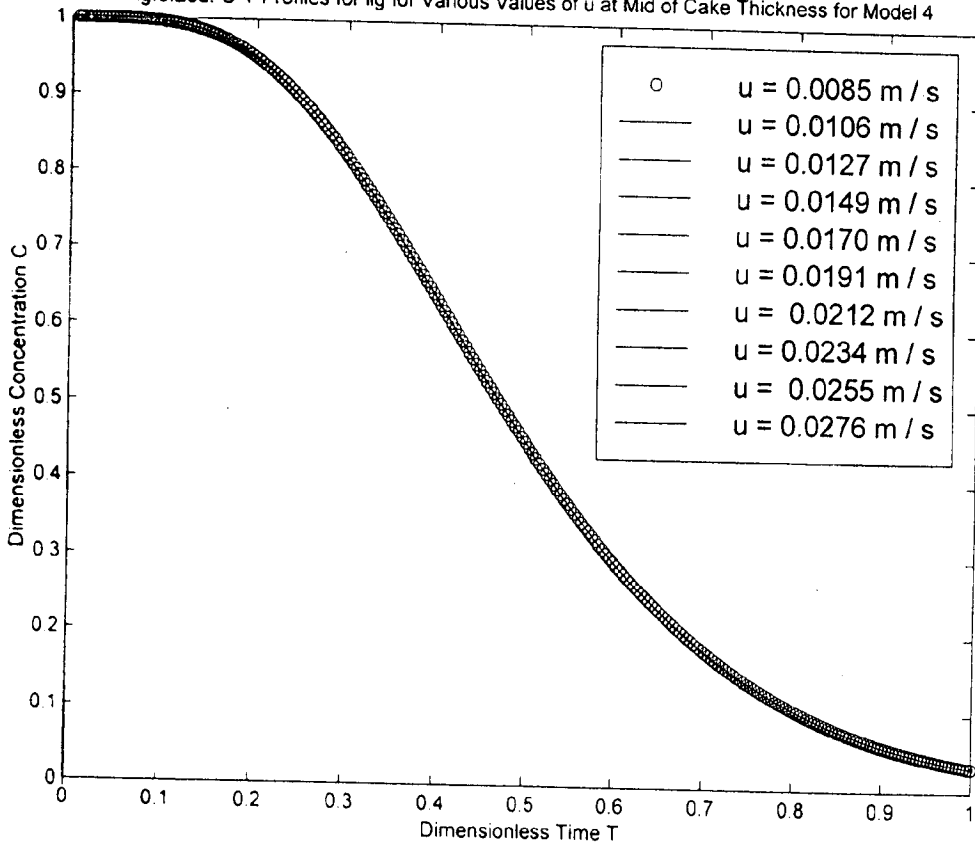


Fig.6.27a N-T Profiles for Na+ for Various Values of u at the Mid of Cake Thickness for Model 1

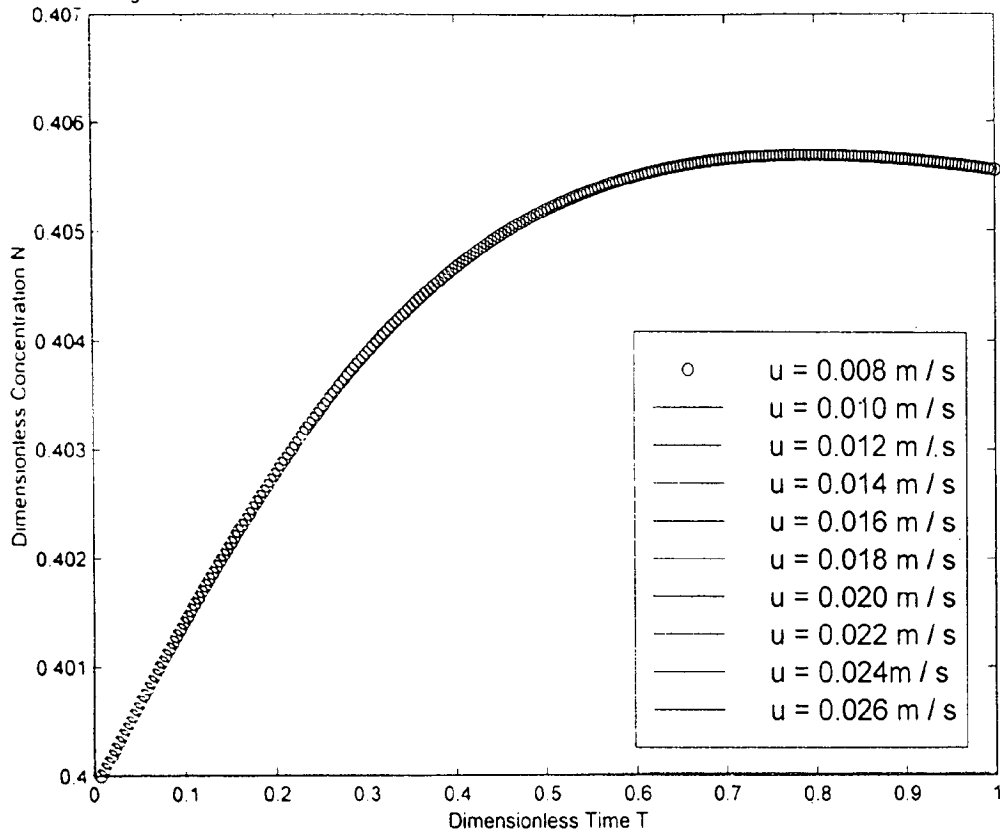


Fig.6.27b. N-T Profiles for Na+ for Various Values of u at Mid of Cake Thickness for Model 2

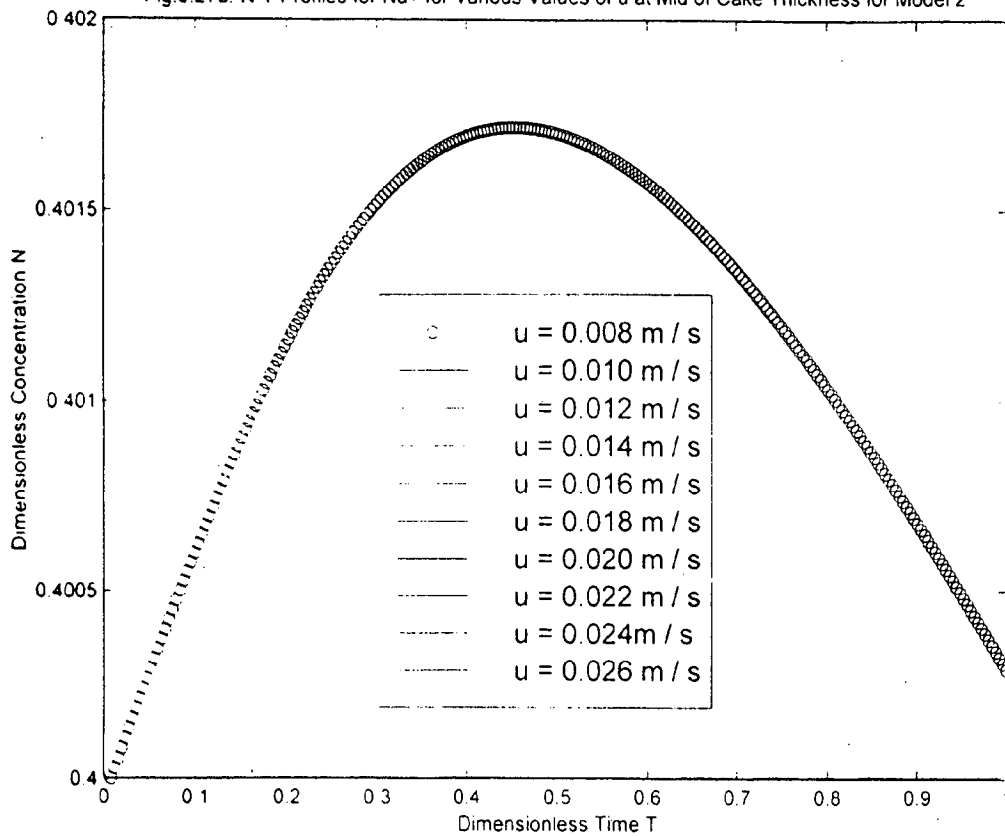


Fig.6.27c. N-T Profiles for Na+ for Various Values of u at Mid of Cake Thickness for Model 3

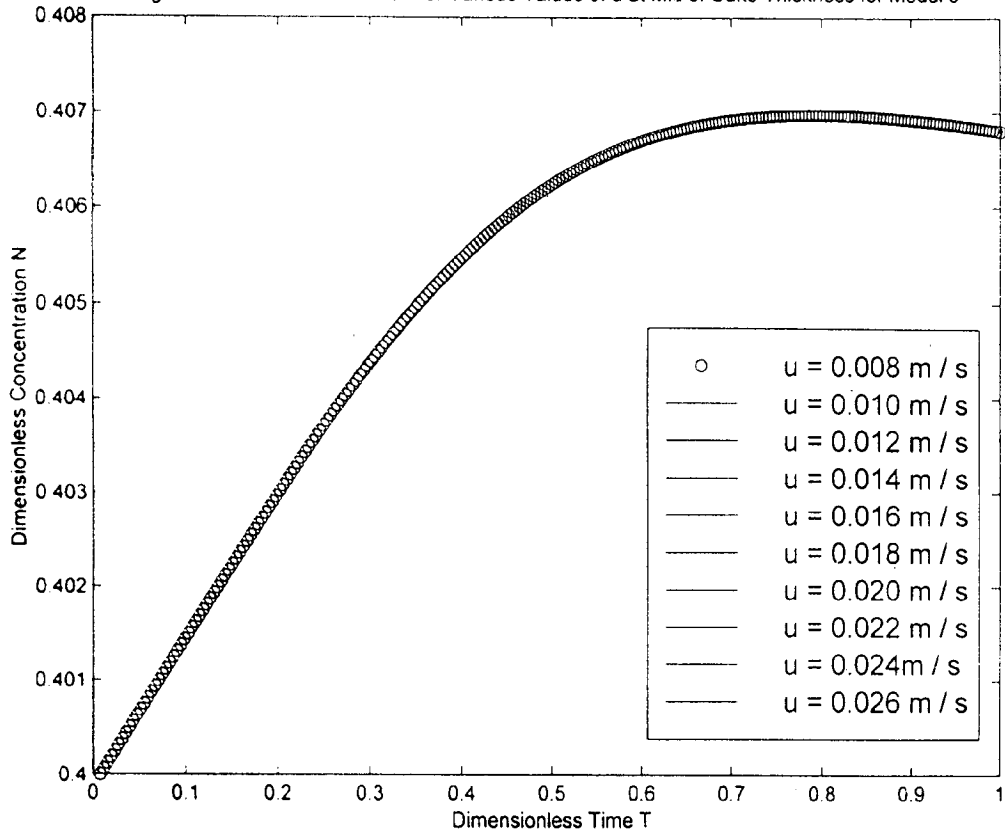
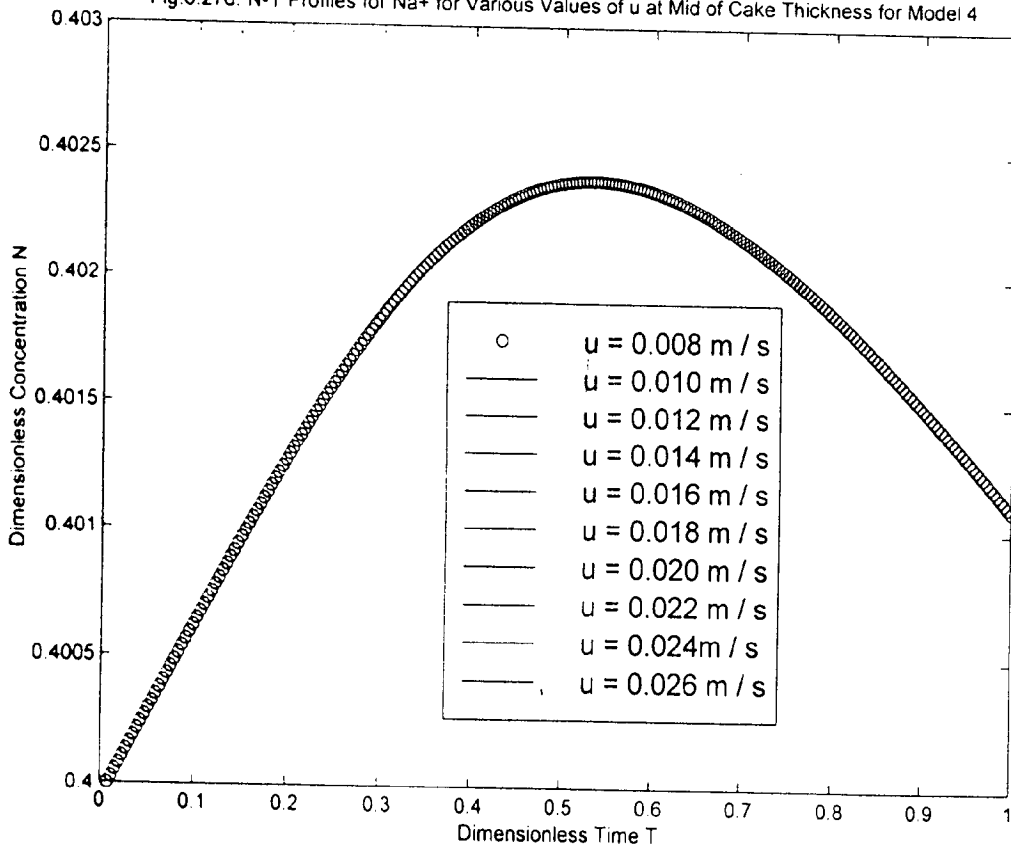
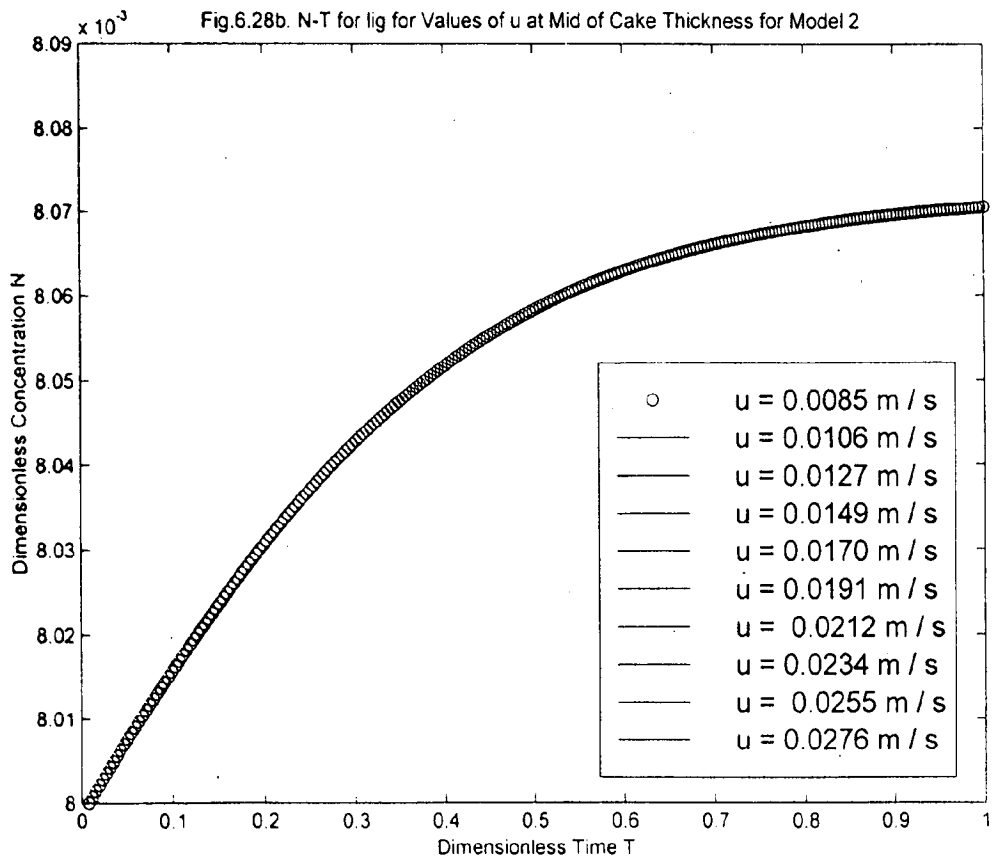
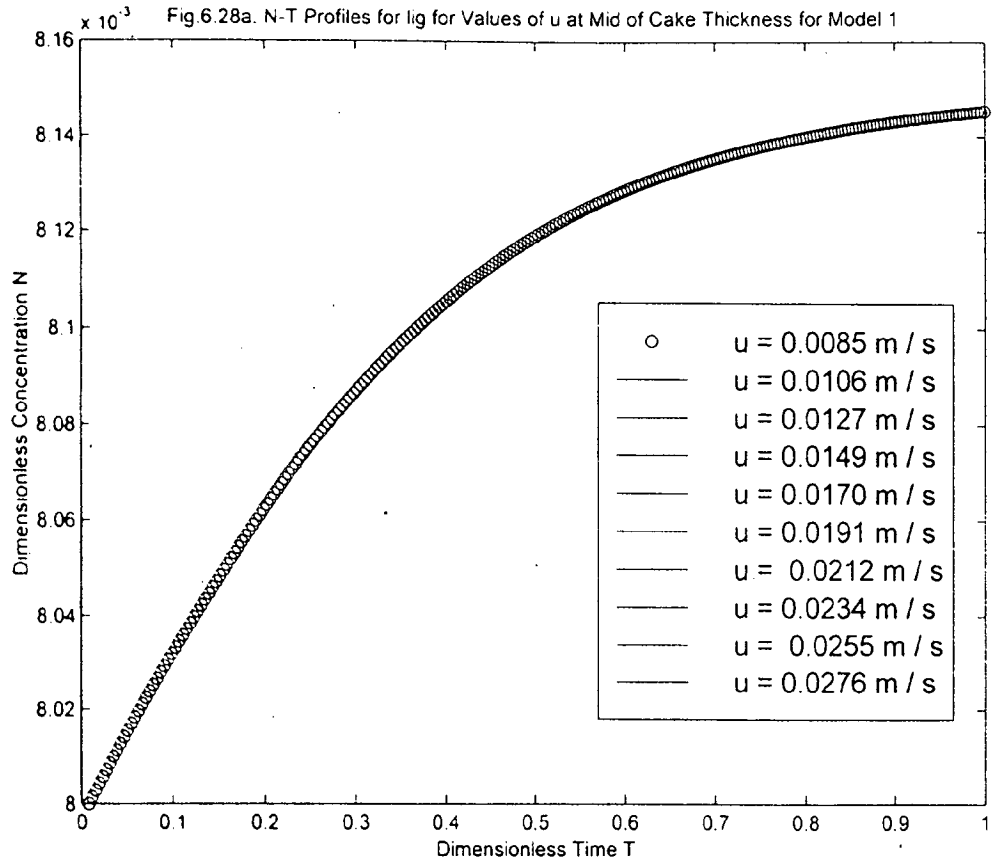
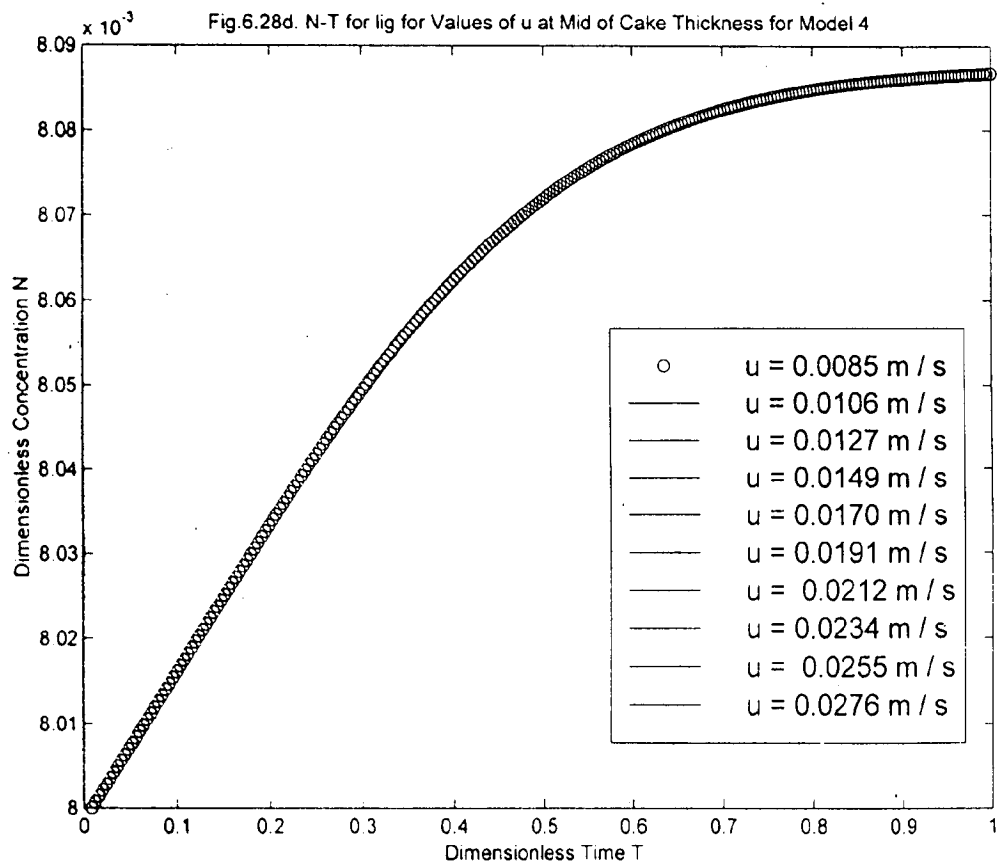
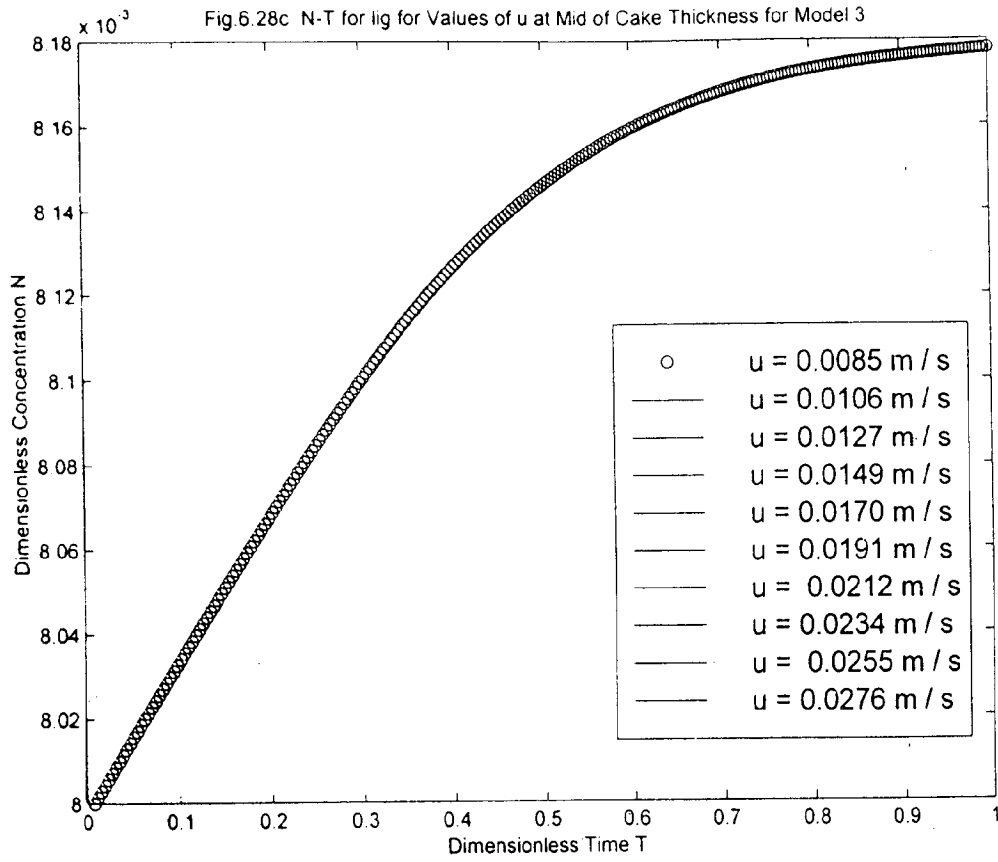


Fig.6.27d. N-T Profiles for Na+ for Various Values of u at Mid of Cake Thickness for Model 4







6.1.26 Effect of local average velocity on N vs. T profiles for Sodium and lignin at mid points of cake thickness

Figs. 6.27a-6.27d are drawn to show the effect of linear average velocity on N-T profiles for Sodium at mid points of the cake thickness. At a low value of linear velocity of the order of 8 mm / s, a distinct curve is appeared whereas with higher velocity the profiles coincide with the T axis.

Similarly Figs. 6.28a-6.28d are drawn for lignin. The nature of profiles is found the same as that of the profiles for Sodium. Similar conclusions can be drawn for lignin also.

6.1.27 Effect of dispersion coefficient D_L on C vs. T plot for Sodium and lignin with constant u at mid points of cake thickness

Effect of dispersion coefficient D_L on the C-T profiles for Sodium have been shown in Figs. 6.29a-6.29d at mid points of the cake thickness. The D_L is varied from 5.9×10^{-6} to $0.59 \times 10^{-6} \text{ m}^2/\text{s}$. Like the u values, it displays same characteristics as those of Grah [24]. There is also an appearance of an inflexion point between $T = 0.3$ and $T = 0.4$. Thereafter the profiles become reversed. This is also in excellent agreement with those of Grah [24]. The deviation is quite significant from $T = 0.1$ to 0.2 and from 0.6 to 0.8.

Effects of dispersion coefficient D_L on C-T profiles for lignin have been shown in Figs. 6.30a-6.30d at mid points of the cake thickness. The D_L is varied from $0.81 \times 10^{-6} \text{ m}^2/\text{s}$ to $8.1 \times 10^{-6} \text{ m}^2/\text{s}$. The characteristics for all the models for lignin are the same as those of Sodium.

The dispersion coefficient D_L increases when the rate of flow of liquor in the bed is increased. This is in agreement with the other investigators such as Pellett [71]. This is corroborated with the fact that the mean value of porosity in the zone of flowing liquor is increasing too when the liquor flow rate increases. That means that a larger part of the bed volume is used for liquor in motion when the flow rate is increased. A break through curve becomes less steep when the D_L value is increased as a consequence of elongated mixing zone in the bed.

Fig 6.29a C-T Profiles for Na+ for Various Values of DL at Mid of Cake Thickness for Model 1

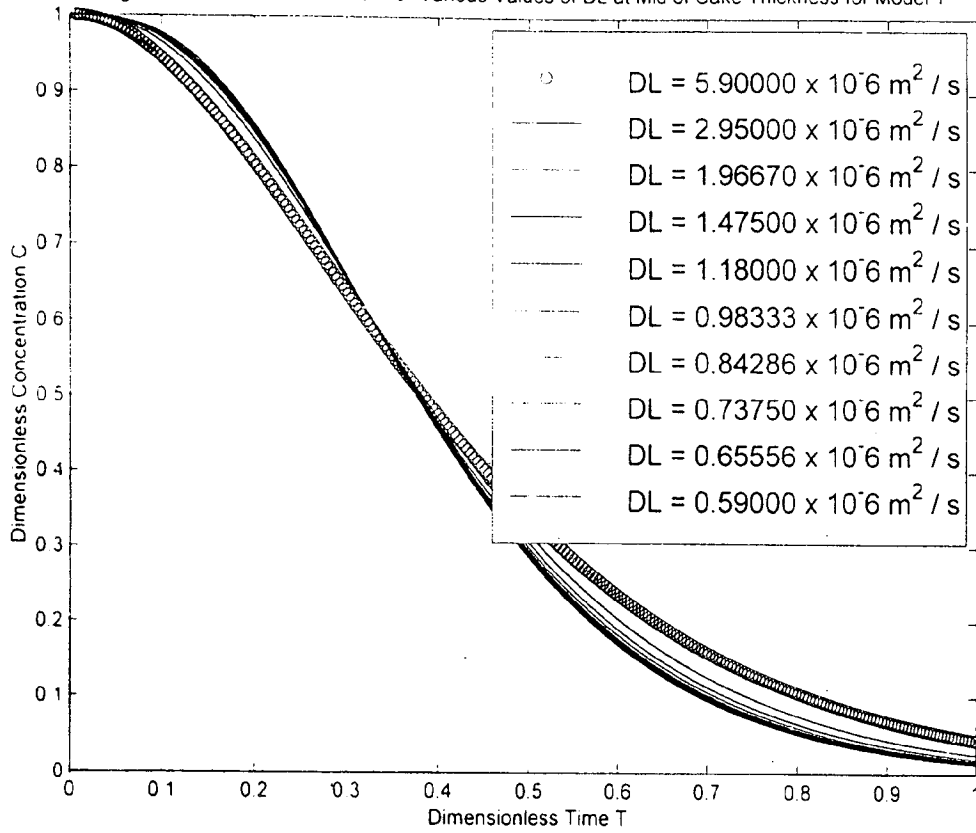


Fig 6.29b C-T Profiles for Na+ for Various Values of DL at Mid of Cake Thickness for Model 2

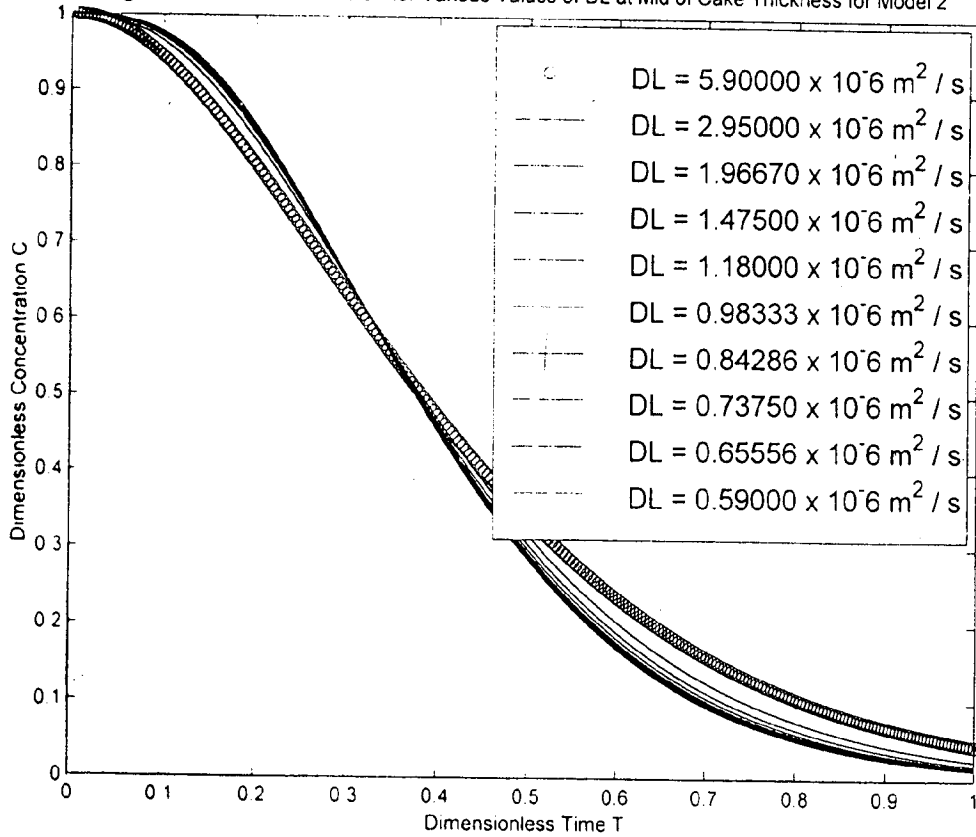


Fig.6.29c. C-T Profiles for Na⁺ for Various Values of DL at Mid of Cake Thickness for Model 3

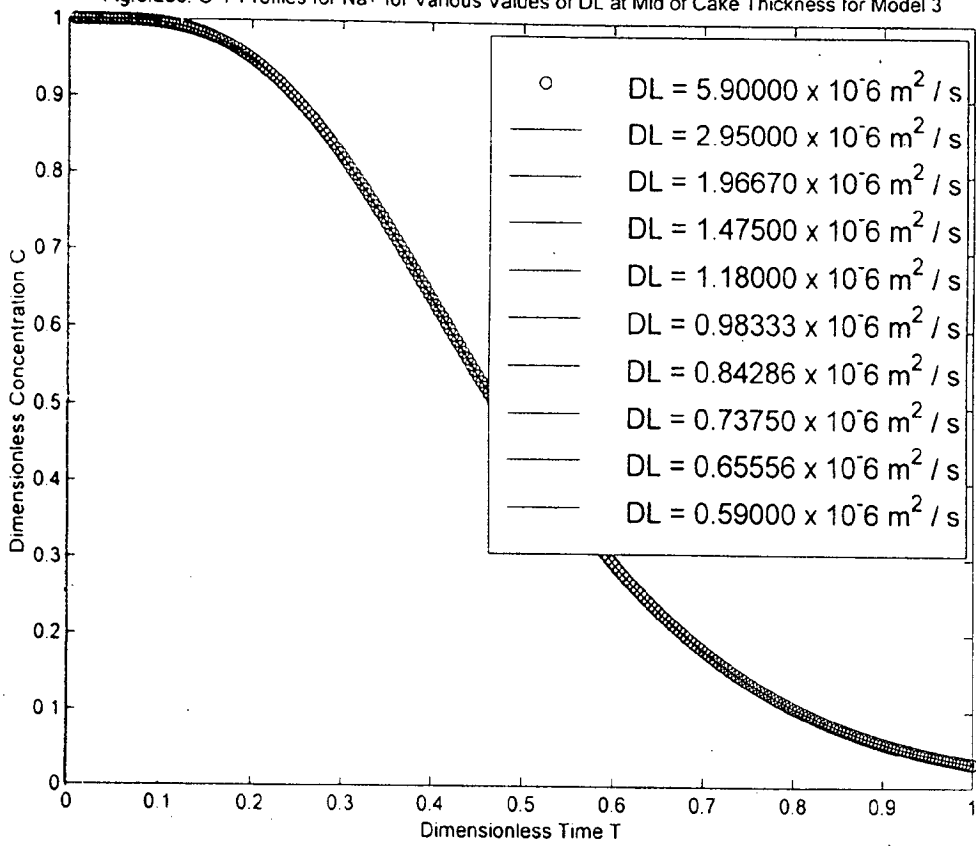


Fig.6.29d. C-T Profiles for Na⁺ for Various Values of DL at Mid of Cake Thickness for Model 4

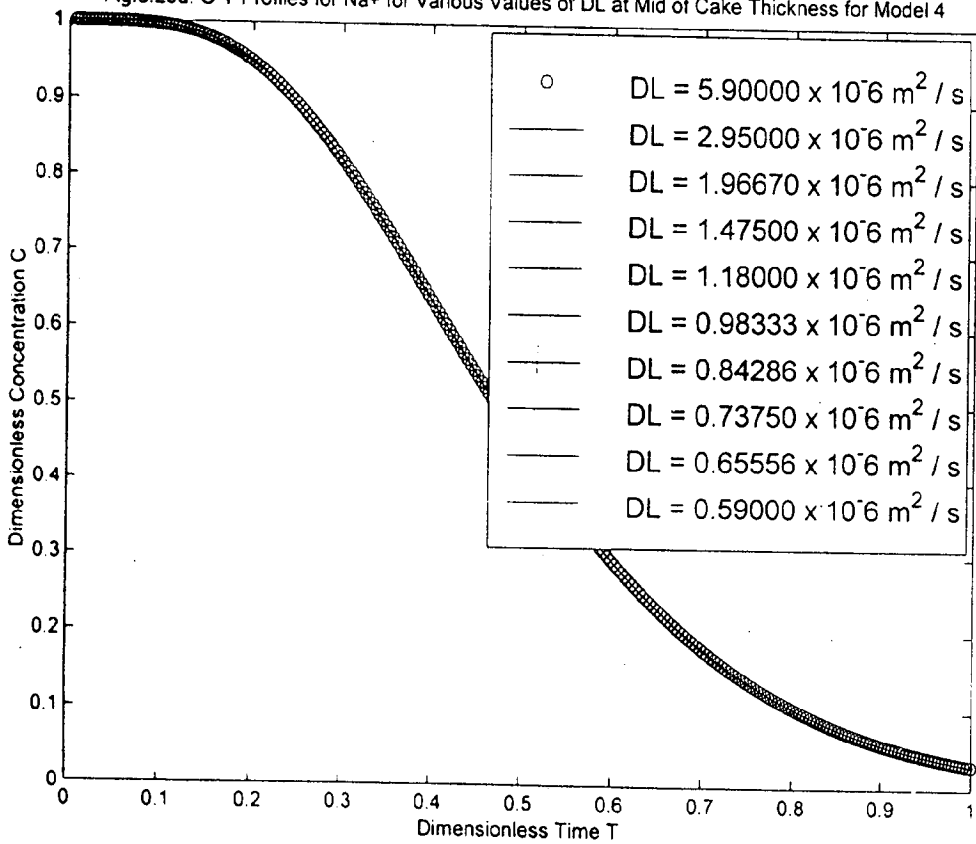


Fig.6.30a. C-T Profiles for lig for Various Values of DL at Mid of Cake Thickness for Model 1

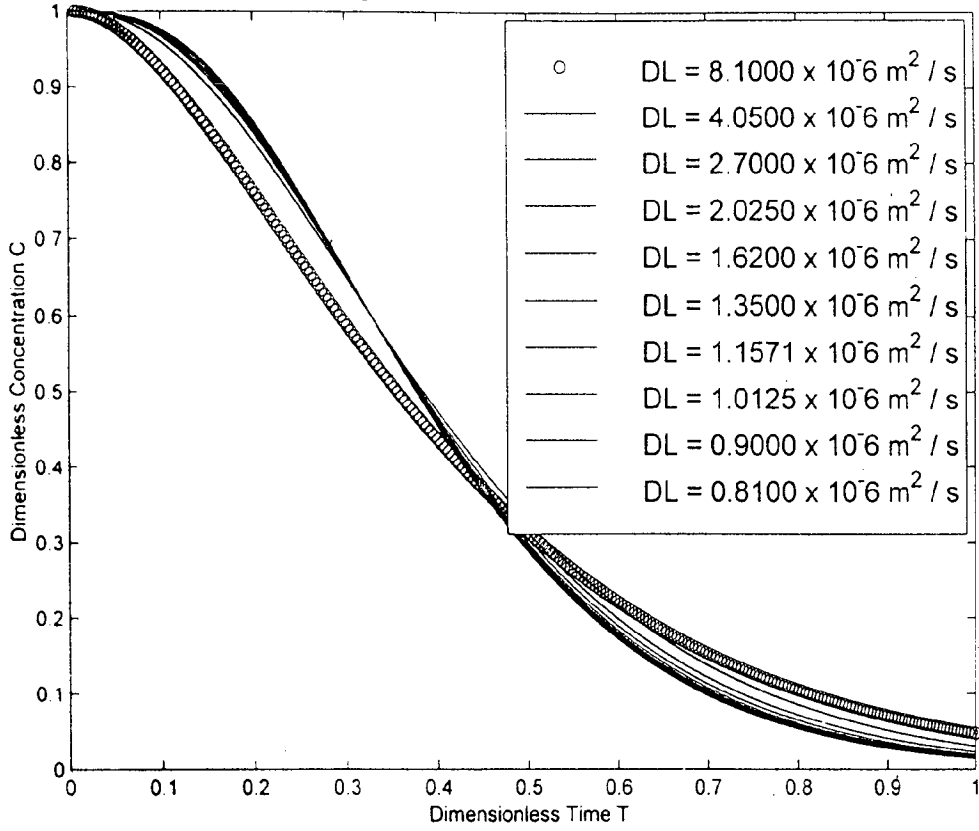


Fig.6.30b. C-T Profiles for lig for Various Values of DL at Mid of Cake Thickness for Model 2

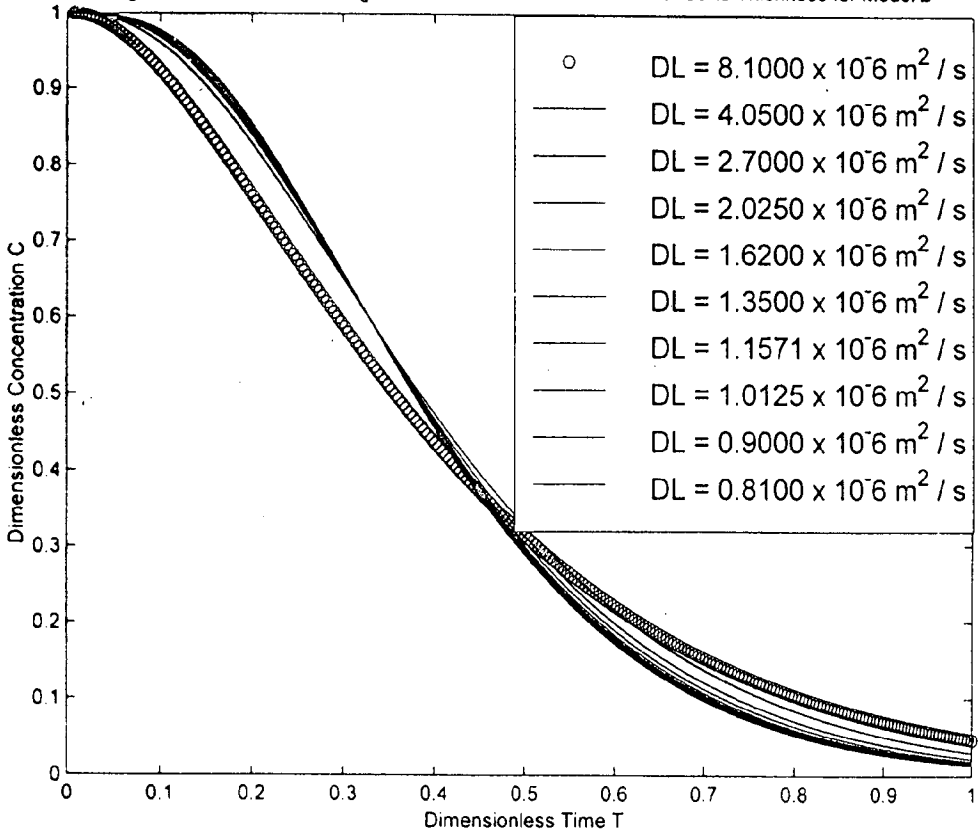


Fig 6.30c. C-T Profiles for lig for Various Values of DL at Mid of Cake Thickness for Model 3

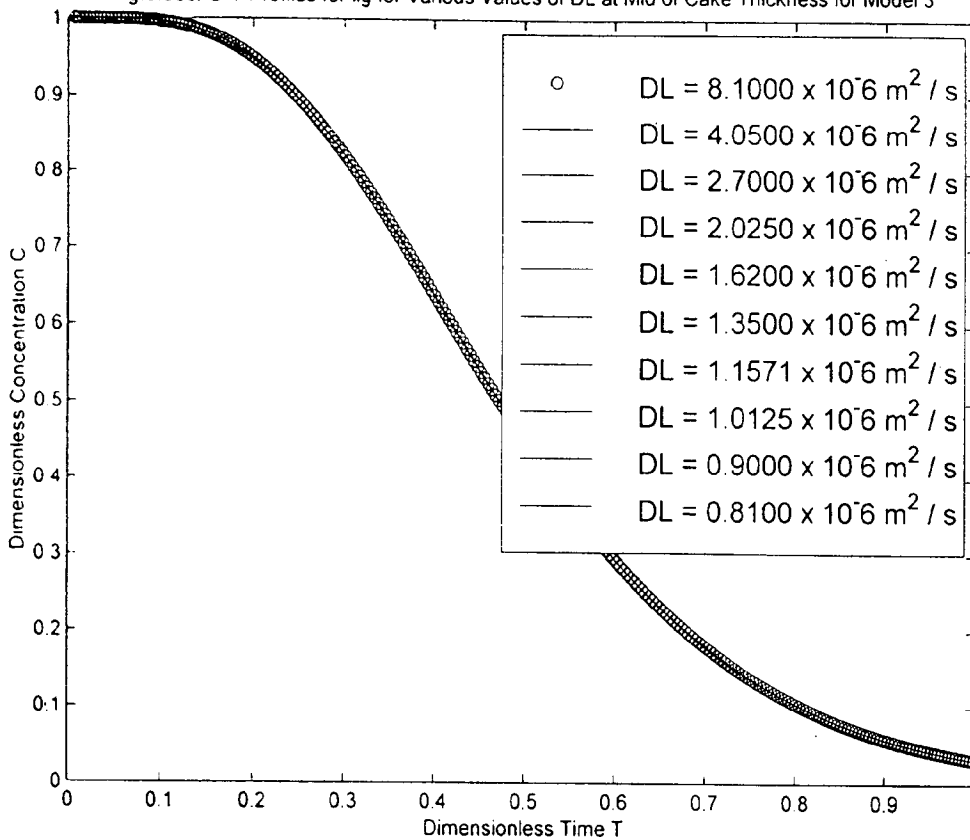


Fig 6.30d. C-T Profiles for lig for Various Values of DL at Mid of Cake Thickness for Model 4

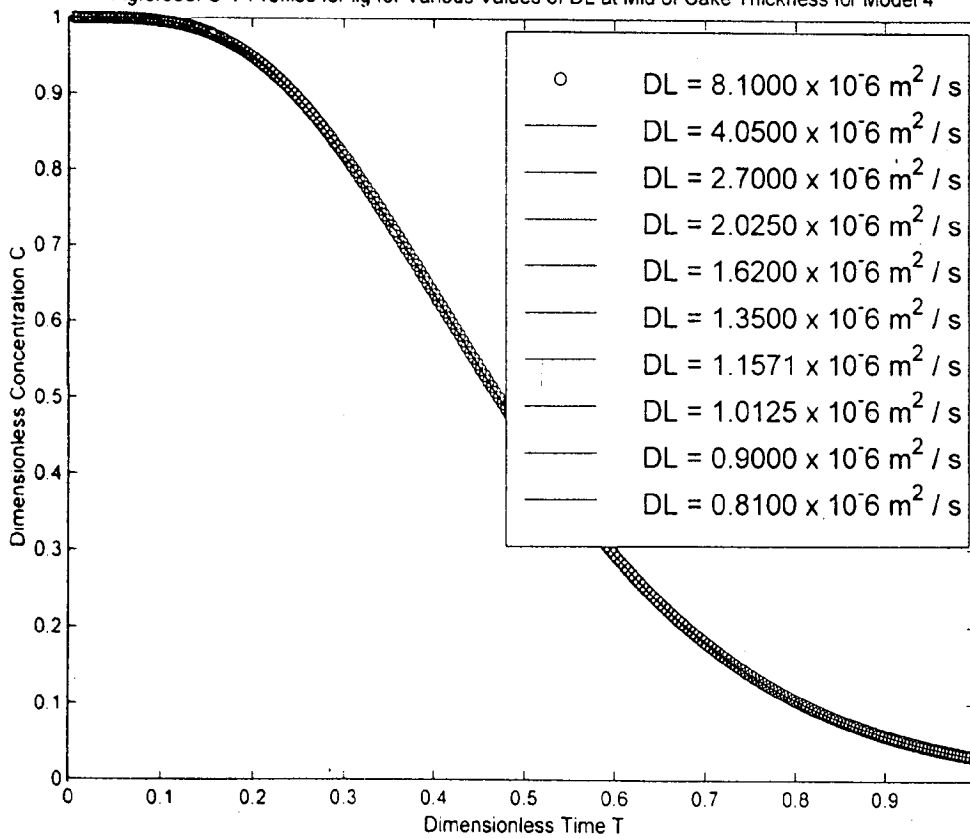


Fig.6.31a. N-T Profiles for Na+ for Various Values of DL at Mid of Cake Thickness for Model 1

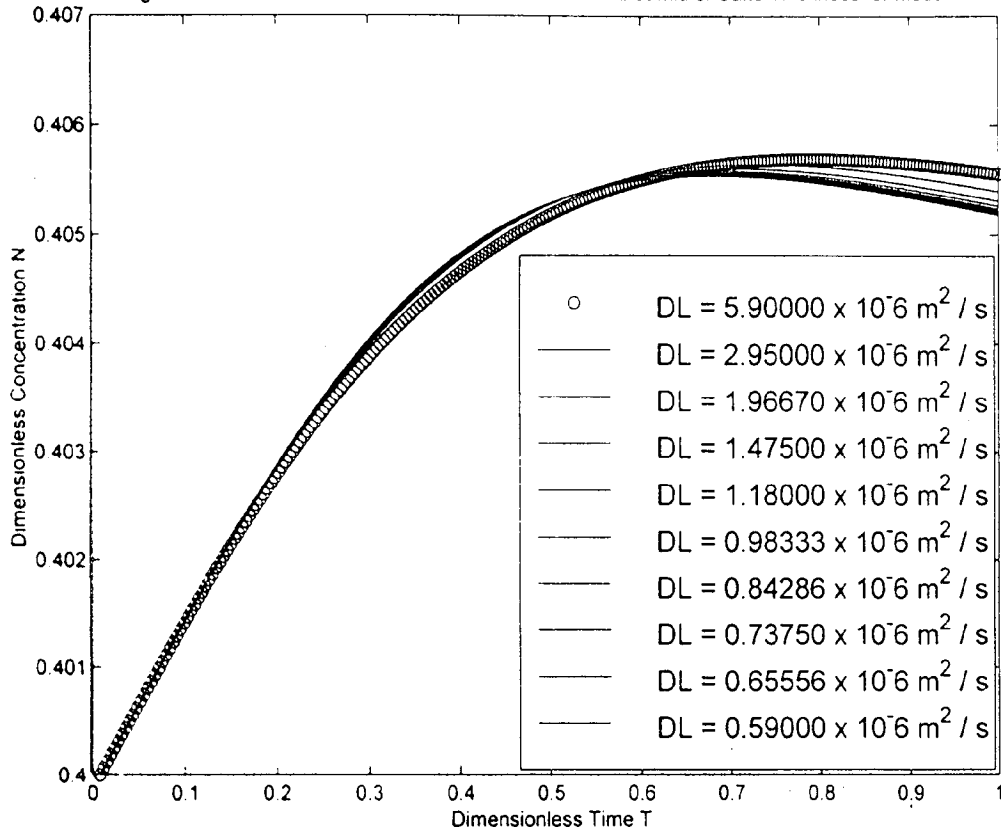


Fig.6.31b. N-T Profiles for Na+ for Various Values of $DL \times 10^6 \text{ m}^2 / \text{s}$ at Mid of Cake Thickness for Model 2

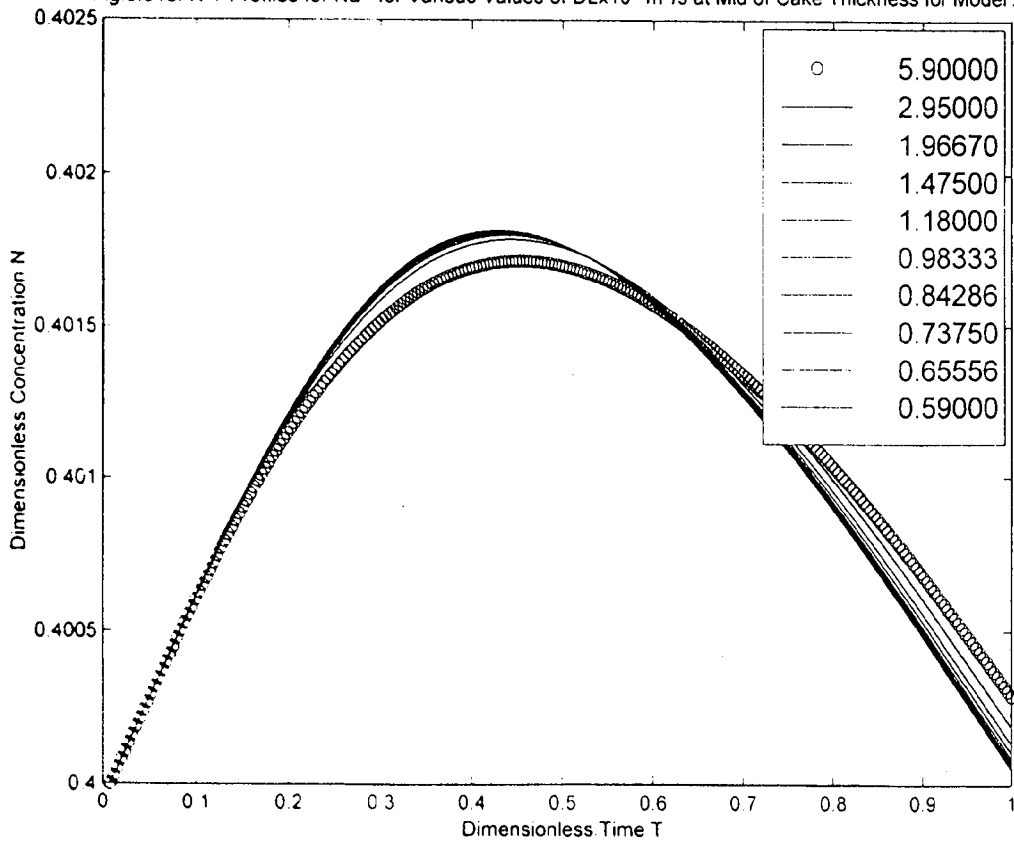


Fig 6.31c N-T Profiles for Na⁺ for Various Values of DL at Mid of Cake Thickness for Model 3

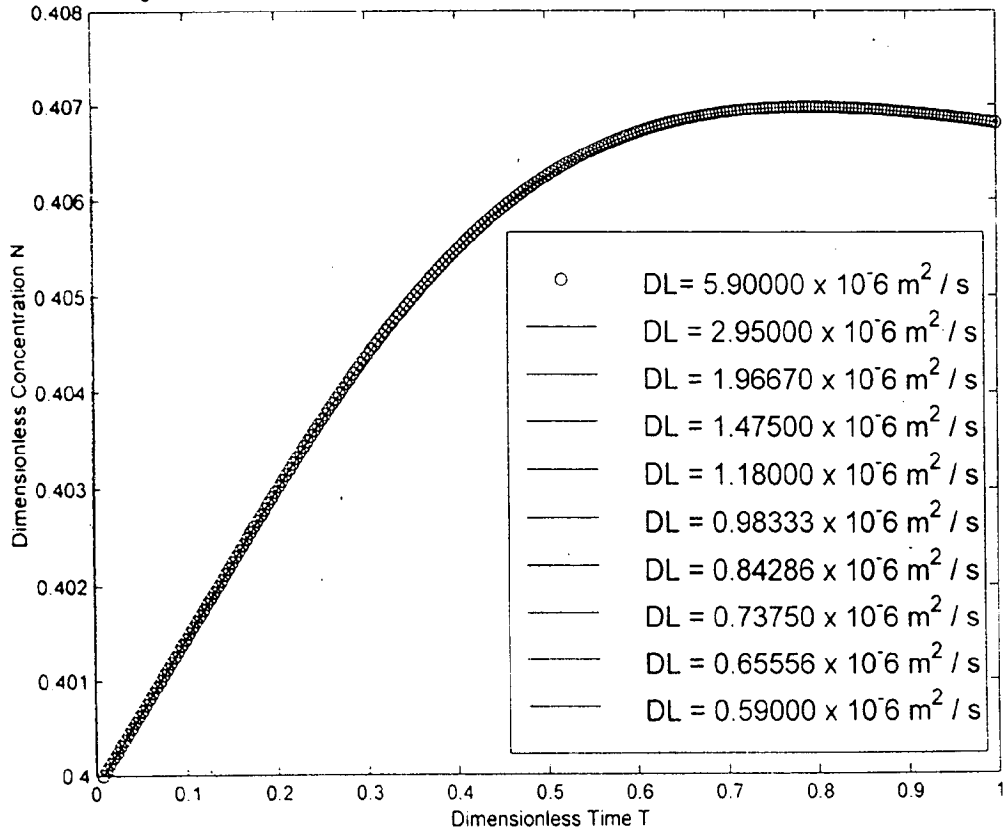
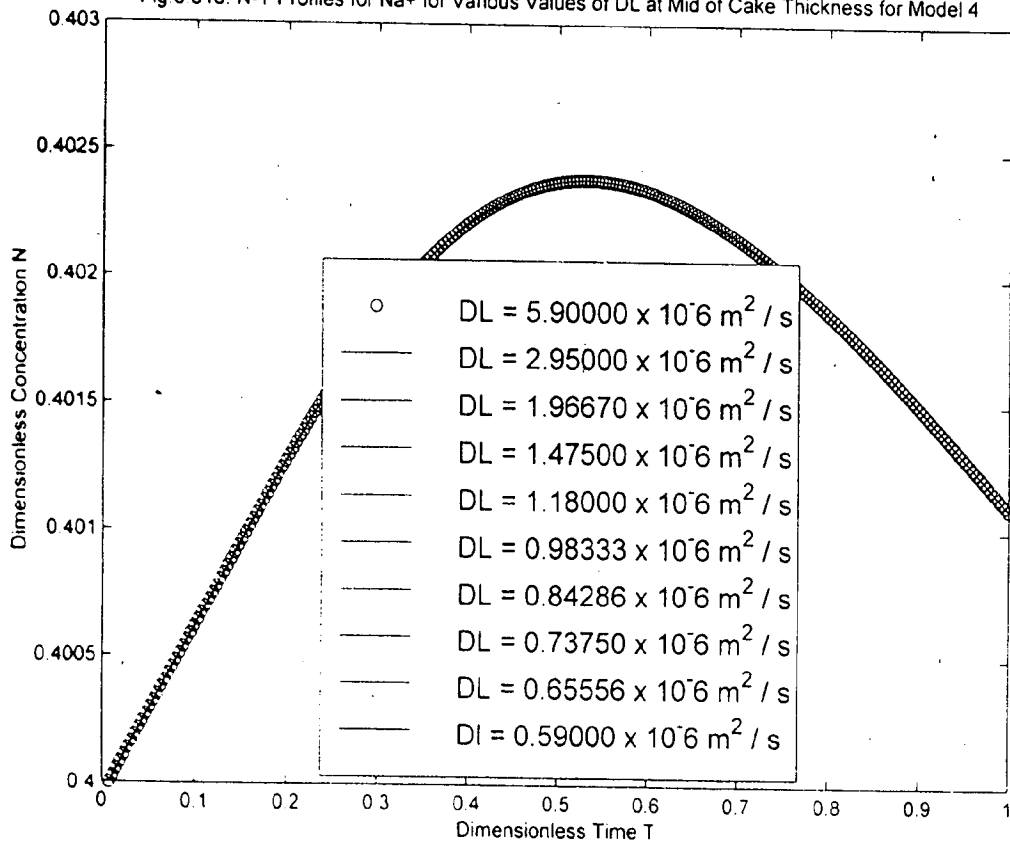
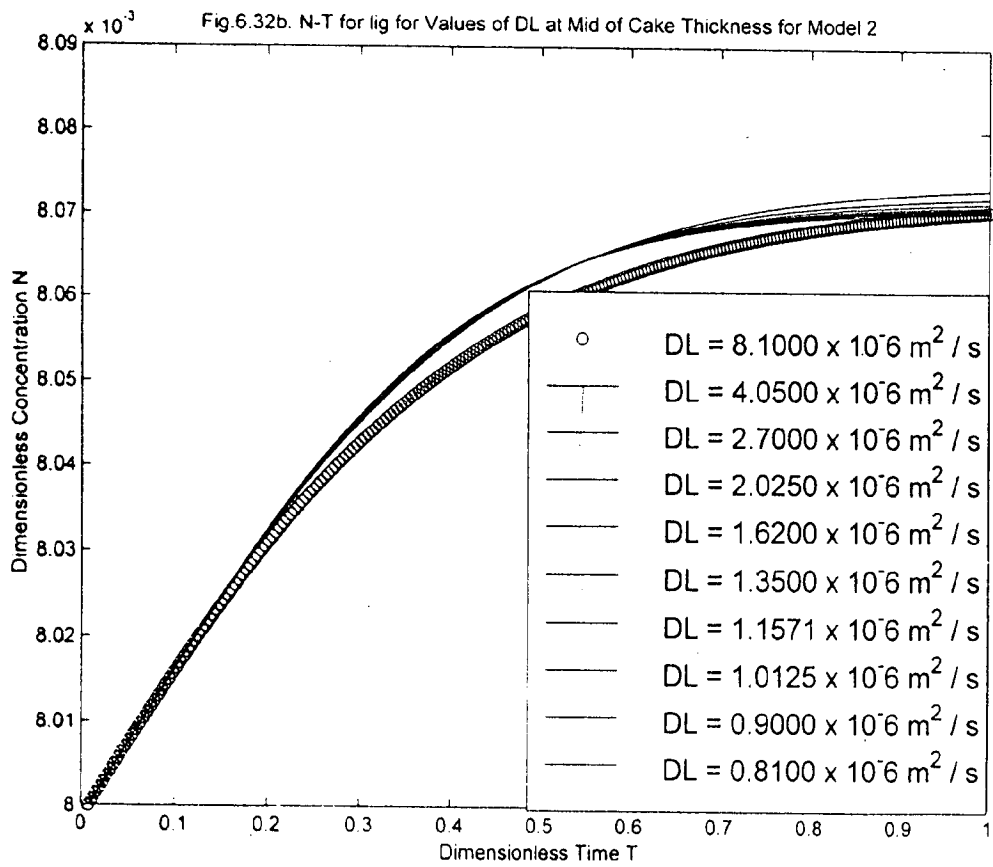
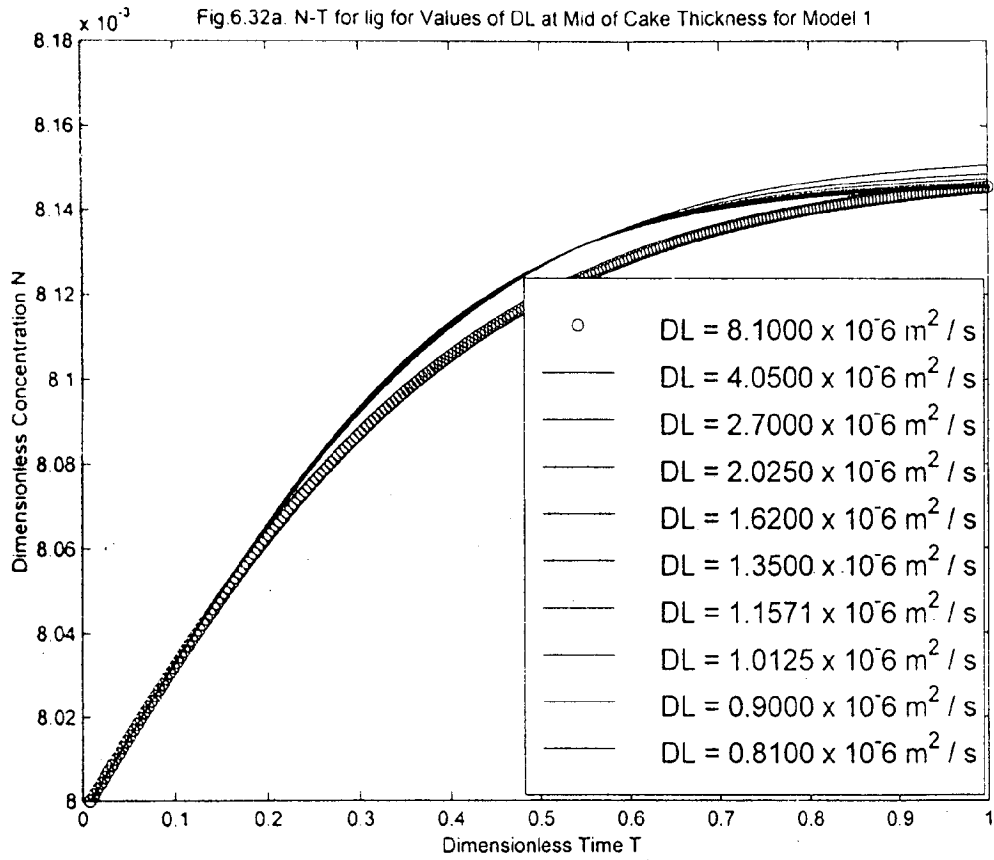
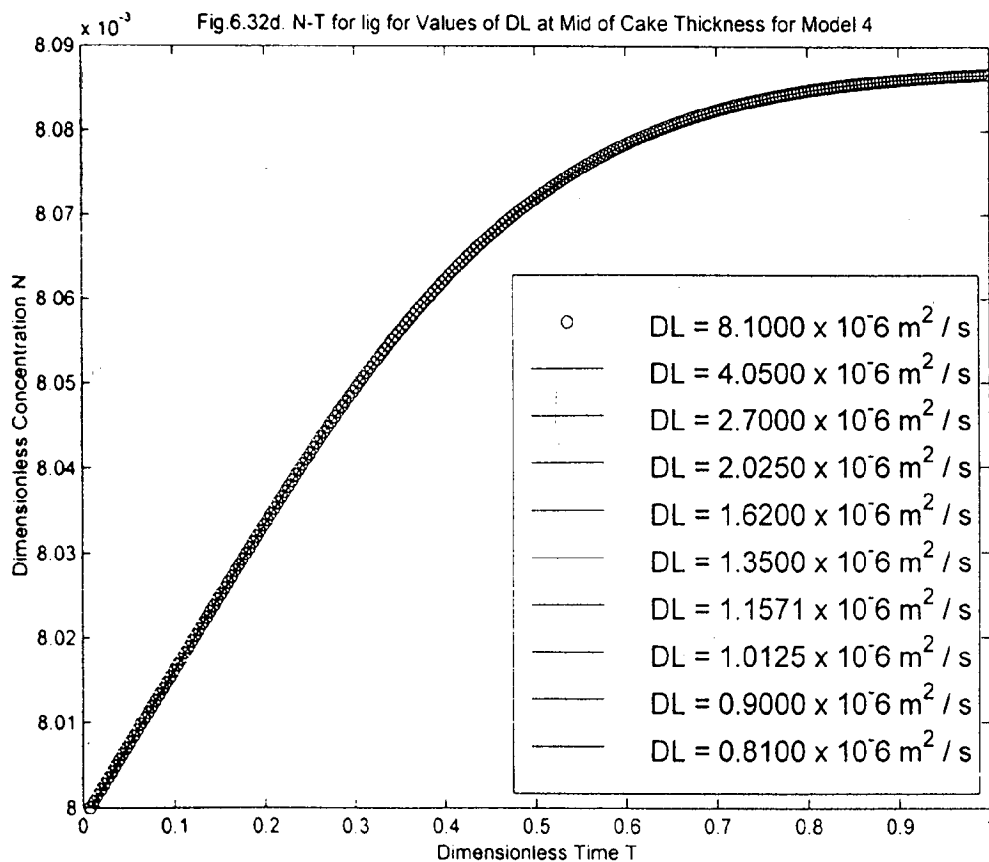
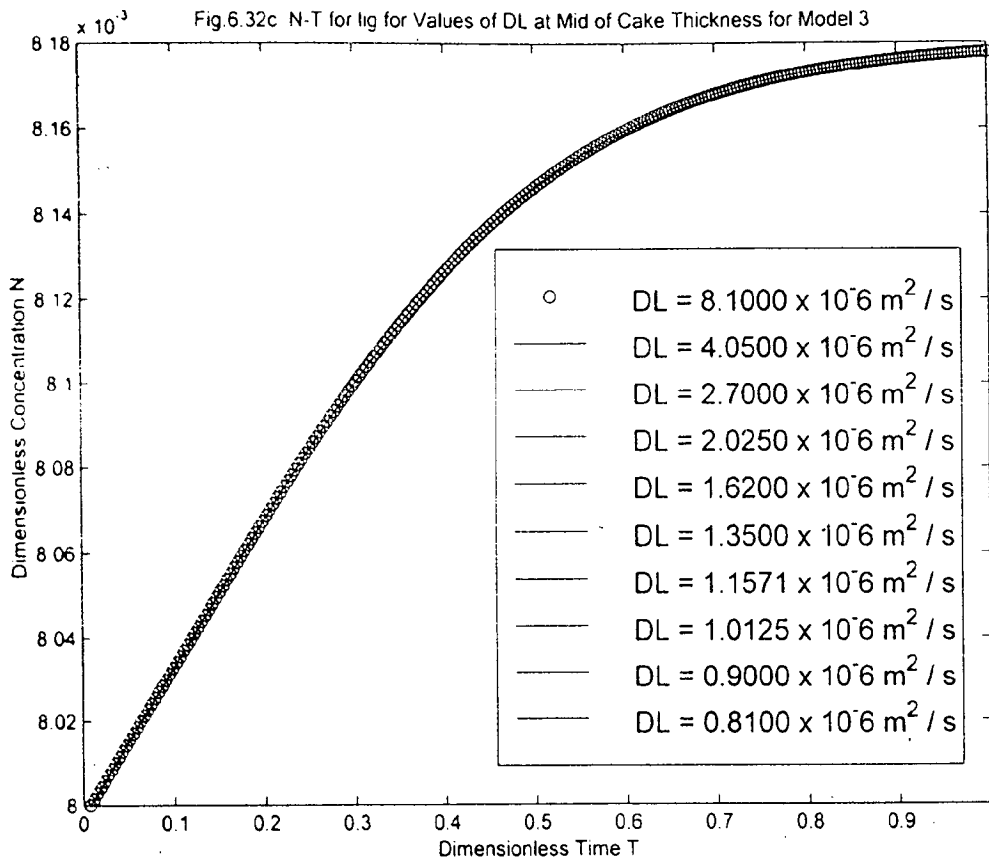


Fig 6.31d. N-T Profiles for Na⁺ for Various Values of DL at Mid of Cake Thickness for Model 4







The profiles of the models without dispersion term coincide throughout the span. It shows that there is no effect of dispersion coefficient on C-T profiles if the term Pe containing D_L is not present in the model.

6.1.28 Effect of dispersion coefficient D_L on N vs. T plot for Sodium and lignin with constant u at mid points of cake thickness

Figs. 6.31a-6.31d are drawn to show the effect of dispersion coefficient on N-T profiles for Sodium at mid points of the cake thickness. Similar behavior is exhibited as the C-T profiles except the nature of the curve. It means that there is an obvious point between $T = 0.6$ and $T = 0.7$, beyond which the profiles become reversed. At higher values of T there is a slight decreasing trend of the profiles at a much slower rate in case of the models with one type of adsorption-desorption isotherm while the decreasing trend is significant in case of models with another type of adsorption-desorption isotherm.

Figs. 6.32a-6.32d are drawn to show the effect of dispersion coefficient on N-T profile for lignin at mid points of the cake thickness. The nature of profiles is the same as that of the profiles for Sodium except that the trend is of increasing nature. The profiles coincide somewhere between $T = 0.5$ and 0.6 of the models with dispersion term except the profile with $D_L = 8.1 \times 10^{-6} \text{ m}^2 / \text{ s}$ which shows slightly decreasing trend. The profiles of the models without dispersion term coincide throughout the span as expected for both the cases of Na^+ and lignin.

6.1.29 Effect of mass transfer coefficient k_1 on C-T and N-T profiles for Sodium and lignin

Figs. 6.33a-6.33d are drawn to show C-T profiles for Sodium for five values of mass transfer coefficient k_1 varying from $5 \times 10^{-3} / \text{ s}$ to $500 \times 10^{-3} / \text{ s}$ for models 1-4 respectively. The profiles are of break through type having inflexional point between $T = 0.3$ and $T = 0.5$. The profiles show that there is no appreciable effect of varying value of k_1 on C-T profiles as all of them coincide with each other. This fact is found to be in agreement with Grah [24] who has mentioned the weak

Fig.6.33a C-T Profiles for Na+ for Various Values of k1 at Mid of Cake Thickness for Model 1

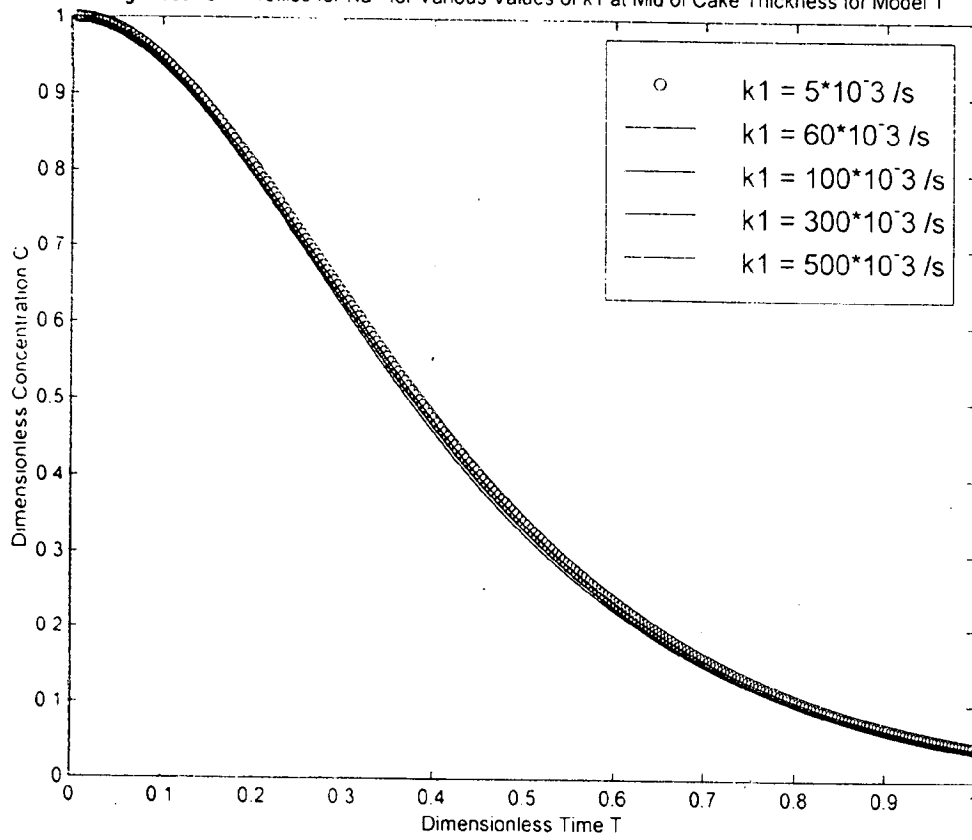


Fig.6.33b C-T Profiles for Na+ for Various Values of k1 at Mid of Cake Thickness for Model 2

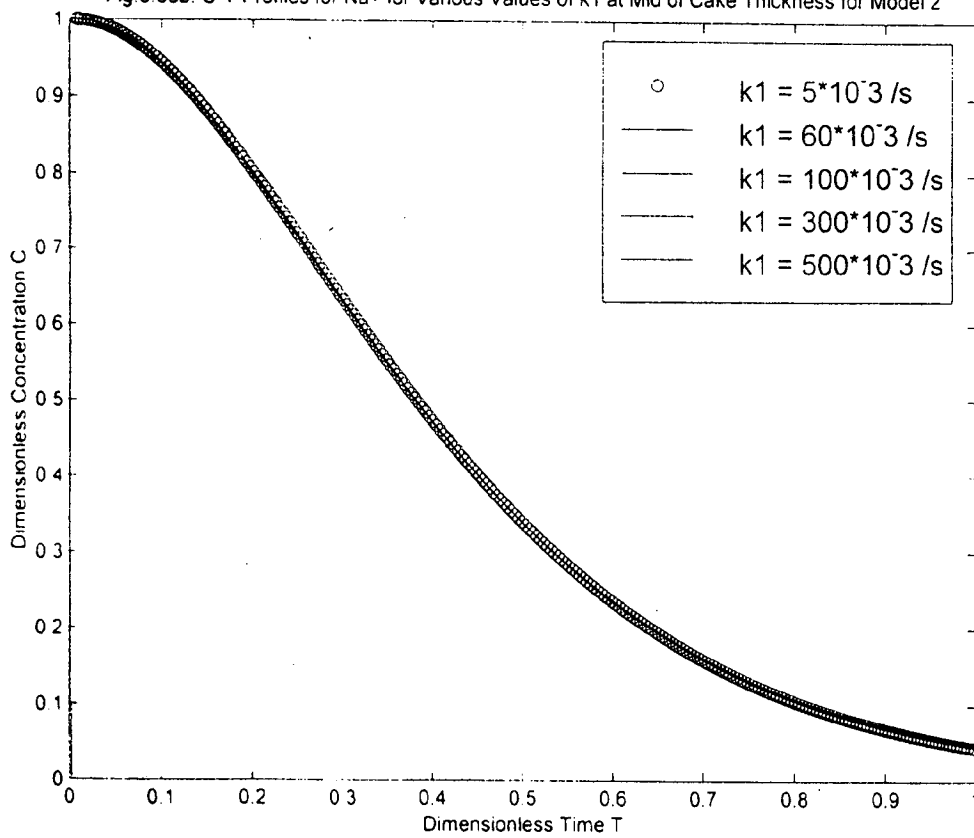


Fig 6.33c. C-T Profiles for Na+ for Various Values of k1 at Mid of Cake Thickness for Model 3

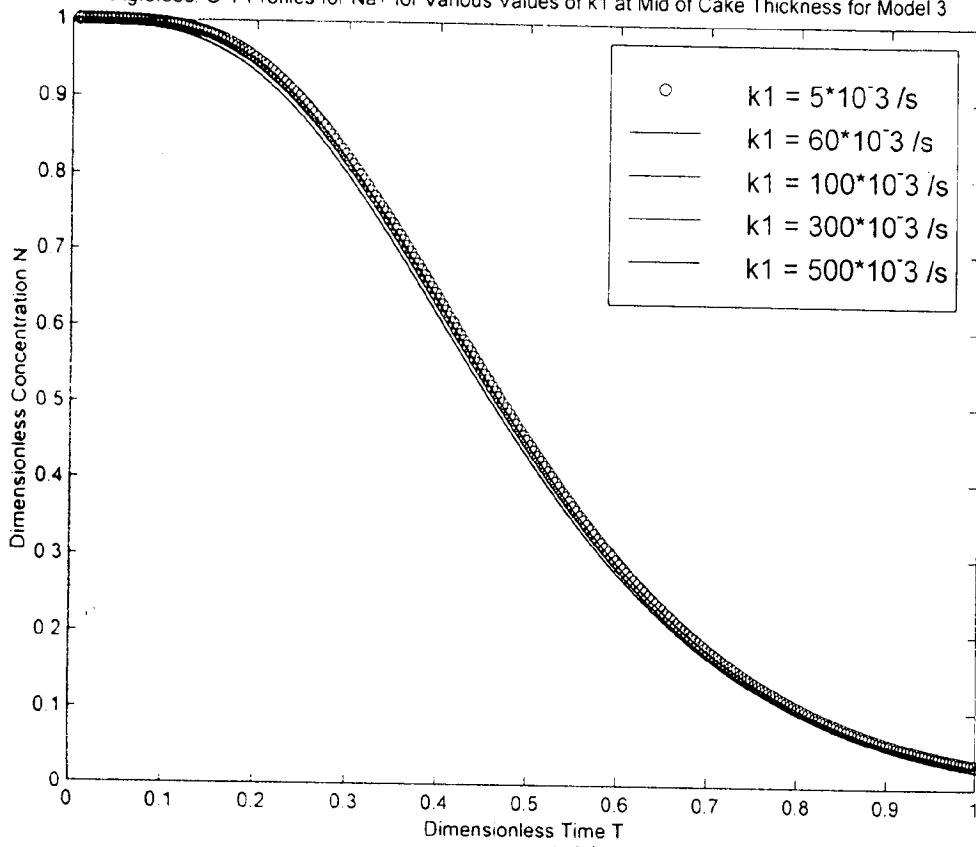


Fig.6.33d. C-T Profiles for Na+ for Various Values of k1 at Mid of Cake Thickness for Model 4

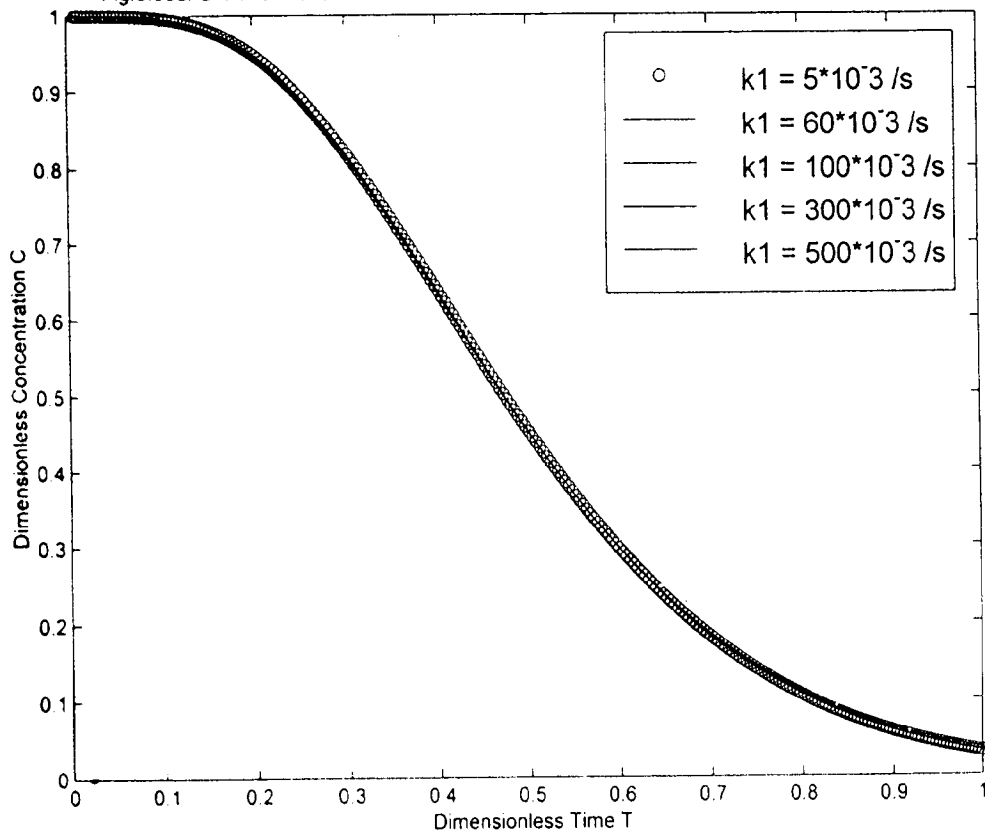


Fig.6.34a. C-T Profiles for lig for Various Values of k_1 at Mid of Cake Thickness for Model 1

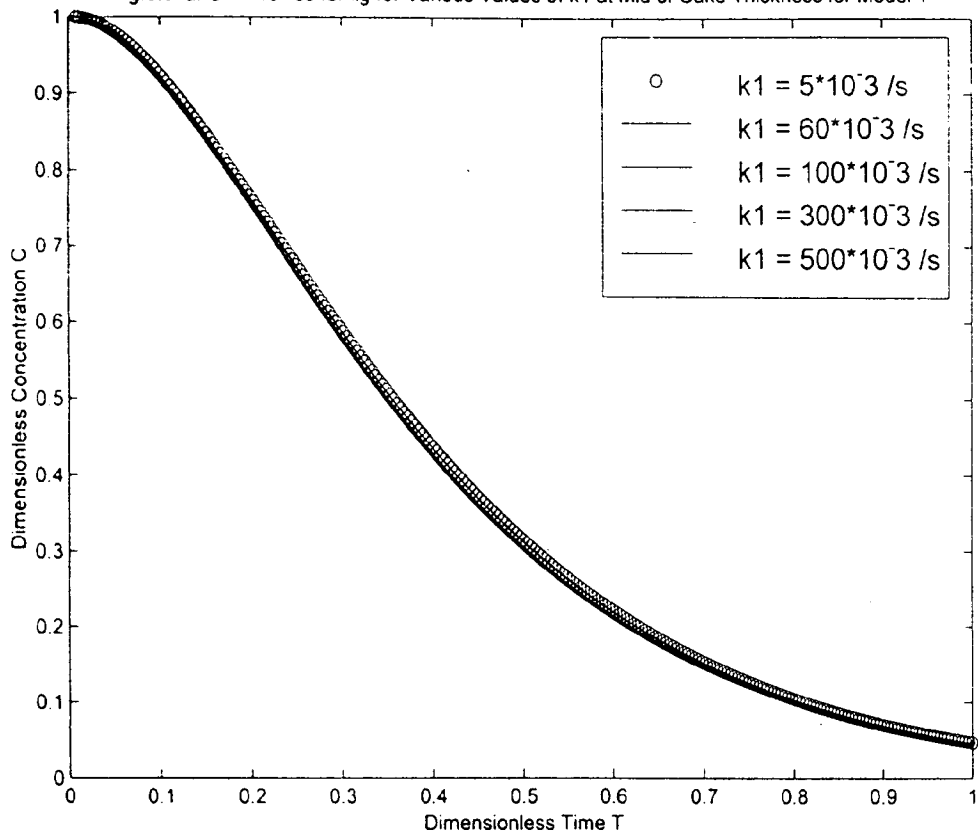


Fig.6.34b. C-T Profiles for lig for Various Values of k_1 at Mid of Cake Thickness for Model 2

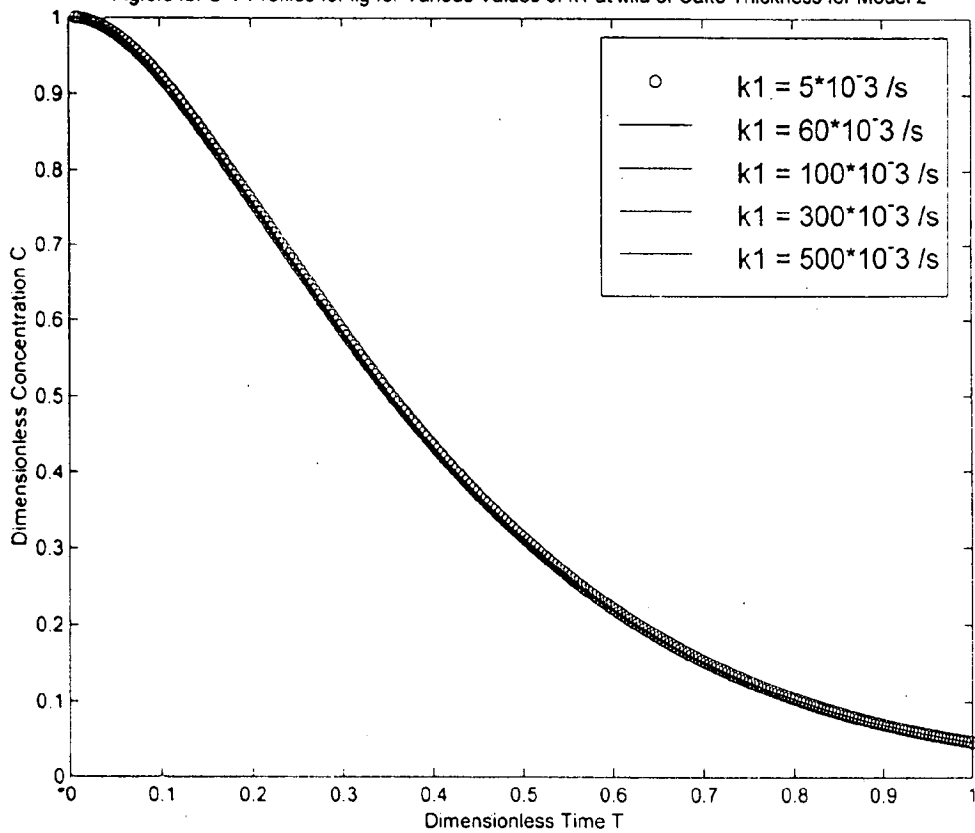


Fig.6.34c. C-T Profiles for lig for Various Values of k1 at Mid of Cake Thickness for Model 3

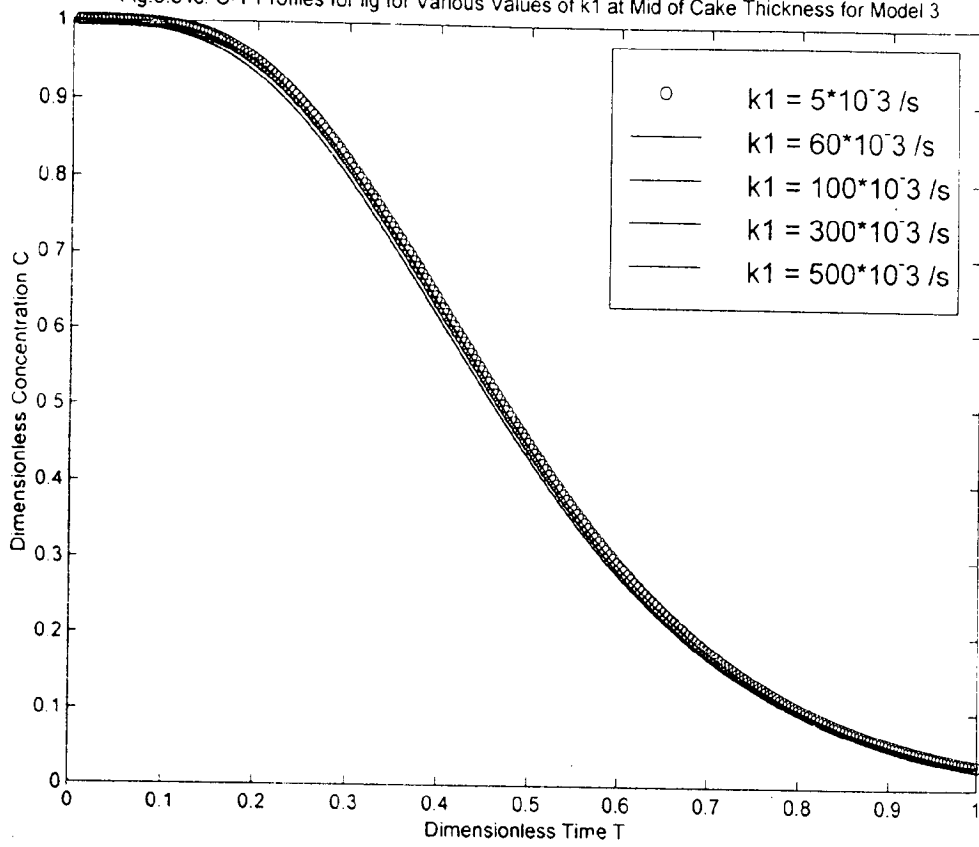
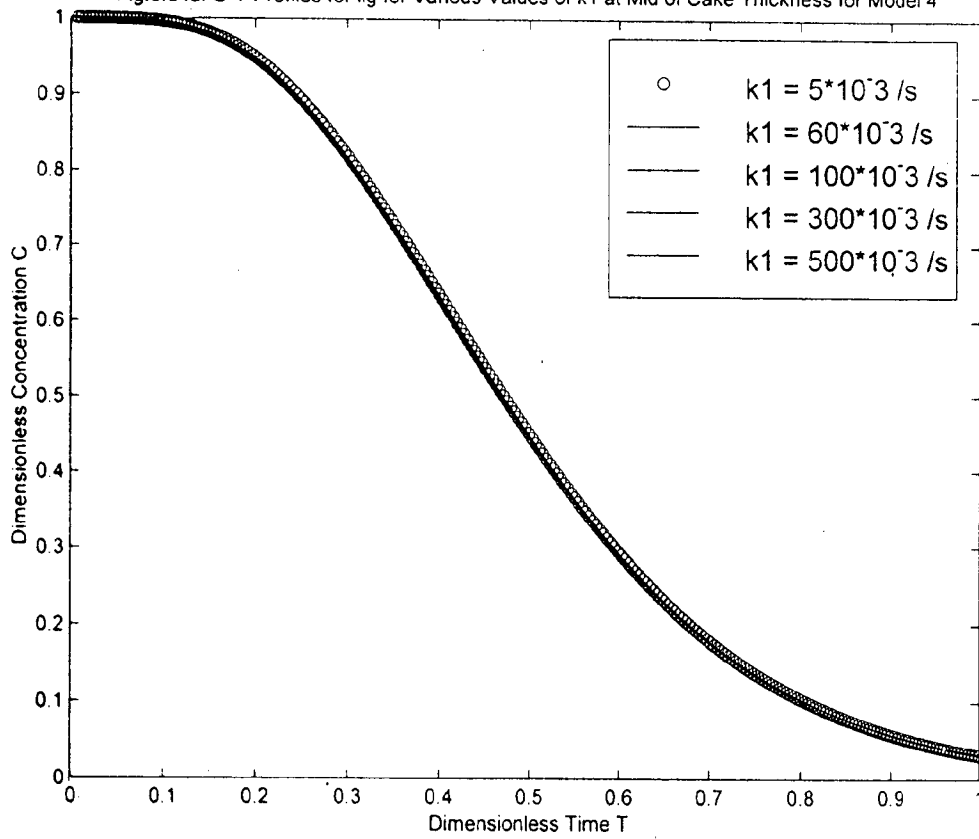


Fig.6.34d. C-T Profiles for lig for Various Values of k1 at Mid of Cake Thickness for Model 4



influence of this parameter. Grah [24] in fact considered the value of k_1 of the order of $7 \cdot 10^{-3}$ 1/s which lies within the ranges considered in this present investigation.

Figs. 6.34a-6.34d are drawn to show C-T profiles for lignin for five values of mass transfer coefficient k_1 varying from $5 \cdot 10^{-3}$ / s to $500 \cdot 10^{-3}$ / s for models 1-4 respectively. The behavior of the profiles is exactly the same as that of profiles for Sodium. Similar explanation can be given for the case of lignin also.

Figs. 6.35a-6.35d are drawn to show N-T profiles for Sodium for five values of mass transfer coefficient k_1 ranging between $5 \cdot 10^{-3}$ / s to $500 \cdot 10^{-3}$ / s for models 1-4 respectively. The profiles show increasing trend throughout for models 1 and 3 but first increasing and then decreasing for models 2 and 4. Adsorption is more for larger value of k_1 for all the four models.

Figs. 6.36a-6.36d are also drawn for lignin species. The behavior of the profiles is found almost increasing in all the cases.

6.1.30 Effect of mass transfer coefficient k_2 on C-T and N-T profiles for Sodium and lignin

Figs. 6.37a-6.37d are drawn to show C-T profiles for Sodium for five values of mass transfer coefficient k_2 varying from $0.0002 \cdot 10^{-3}$ / s to $2 \cdot 10^{-3}$ / s for models 1-4 respectively. The profiles show that there is no effect of varying value of k_2 on C-T profiles for Sodium for any of the model considered. This fact is also in agreement with those of Grah [24].

Similarly Figs. 6.38a-6.38d are drawn for lignin species. Like for Sodium there is no effect of varying value of k_2 on C-T profiles for lignin also for any of the model considered. The fact is still strengthened by the fact that the value of k_2 is of very low order for Na^+ and of much lower (of the order of 10^{-100}) for lignin.

Figs. 6.39a-6.39d are drawn to show N-T profiles for Sodium species. The profiles show increasing trend throughout the span for models 1 and 3 and increasing till midway and then decreasing for models 2 and 4. The most striking feature to be noticed is that lesser value of k_2

Fig.6.35a N-T Profiles for Na+ for Various Values of k1 at Mid Points of Cake Thickness for Model 1

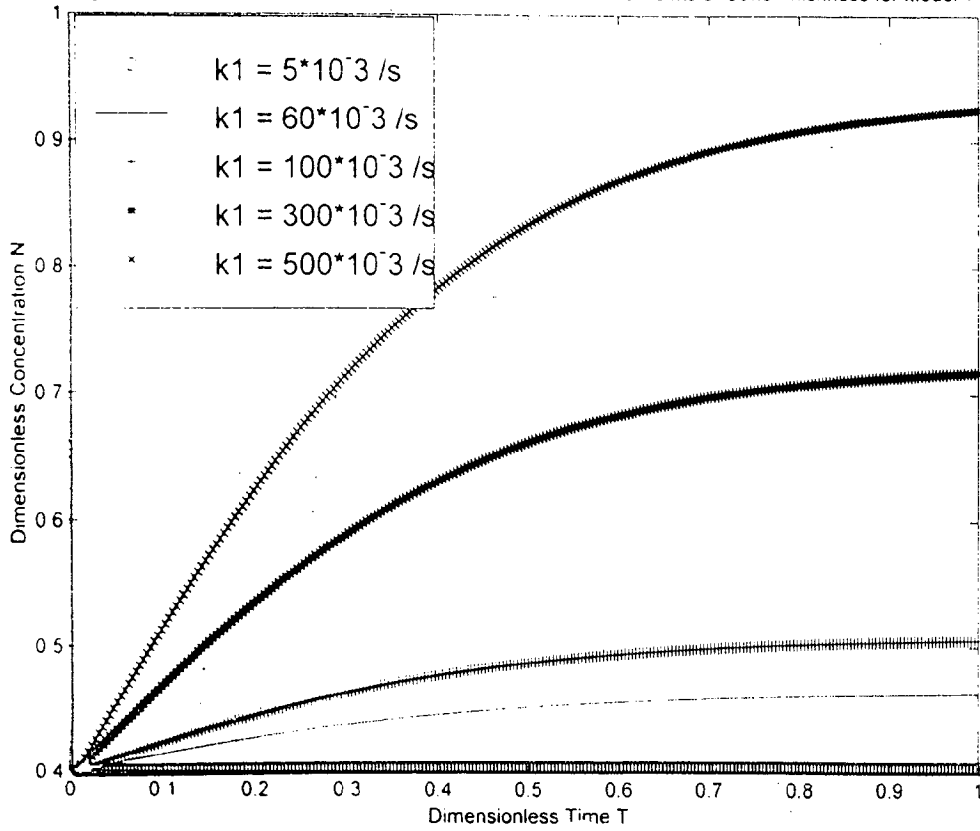


Fig.6.35b N-T Profiles for Na+ for Various Values of k1 at Mid of Cake Thickness for Model 2

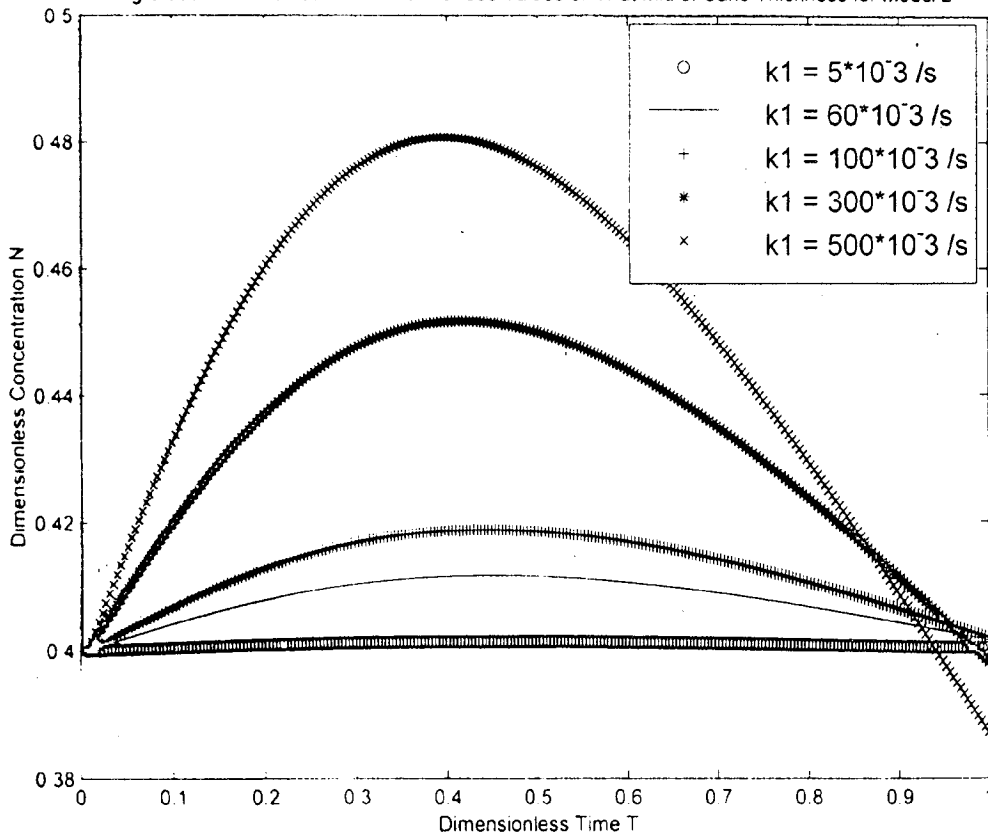


Fig.6.35c. N-T Profiles for Na+ for Various Values of k1 at Mid of Cake Thickness for Model 3

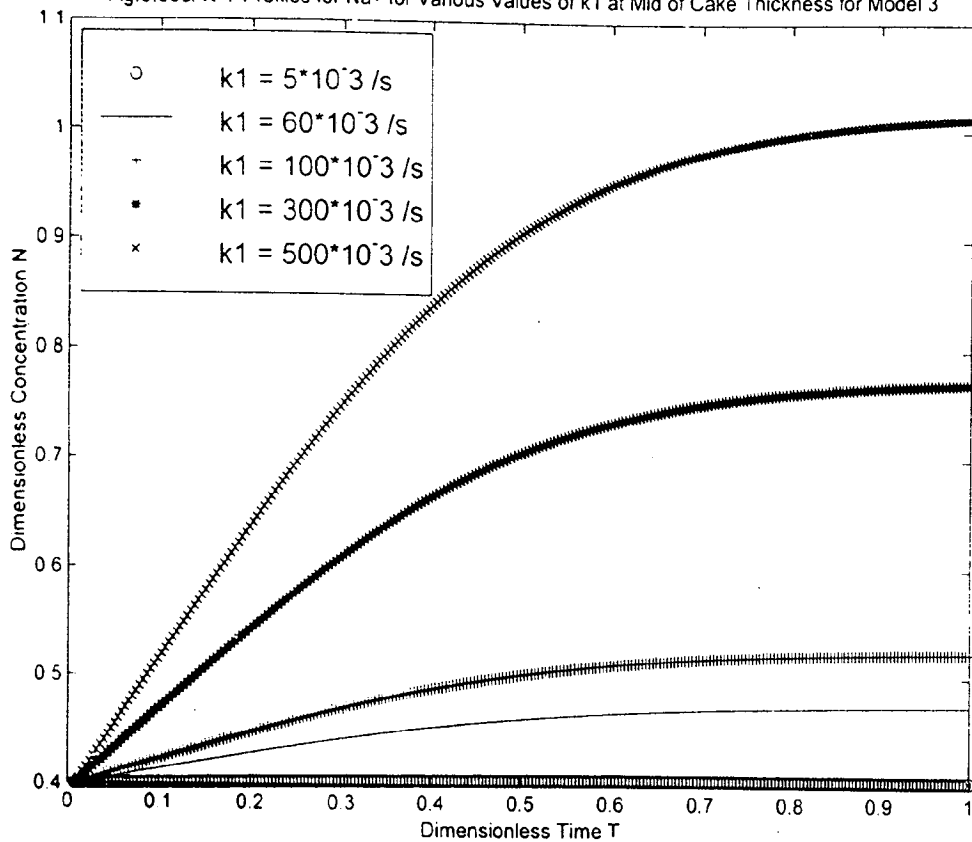


Fig.6.35d. N-T Profiles for Na+ for Various Values of k1 at Mid of Cake Thickness for Model 4

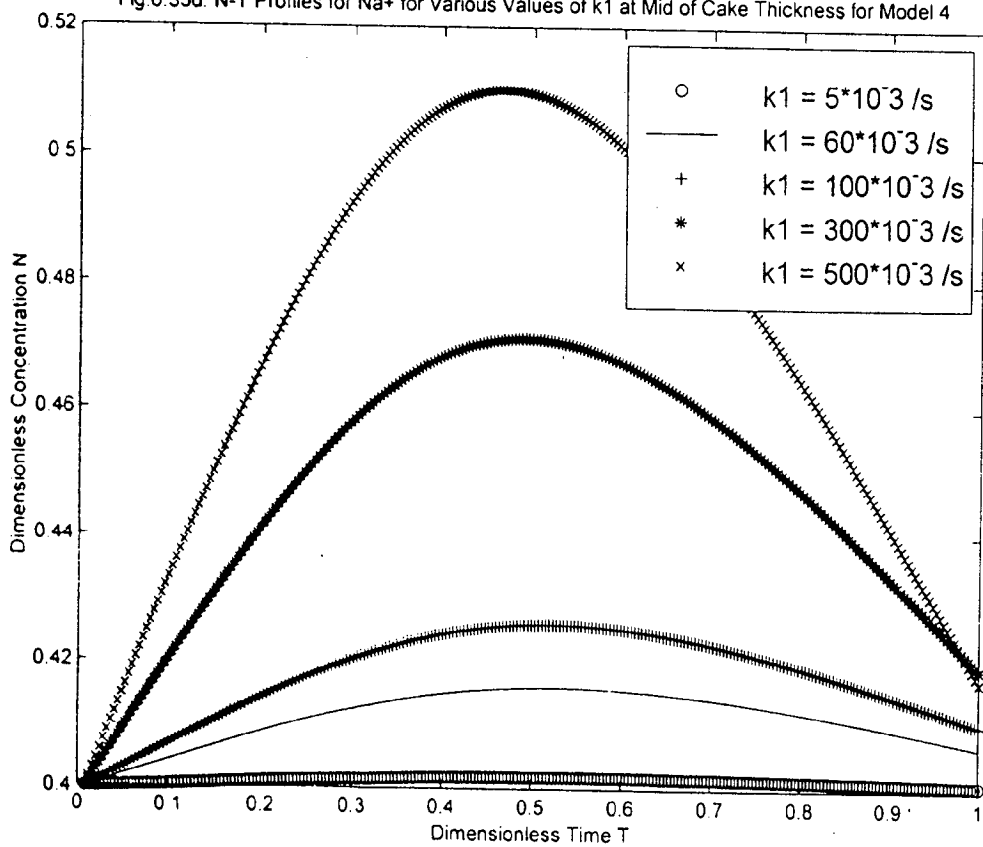


Fig.6.36a. N-T Profiles for lig for Values of k1 at Mid of Cake Thickness for Model 1

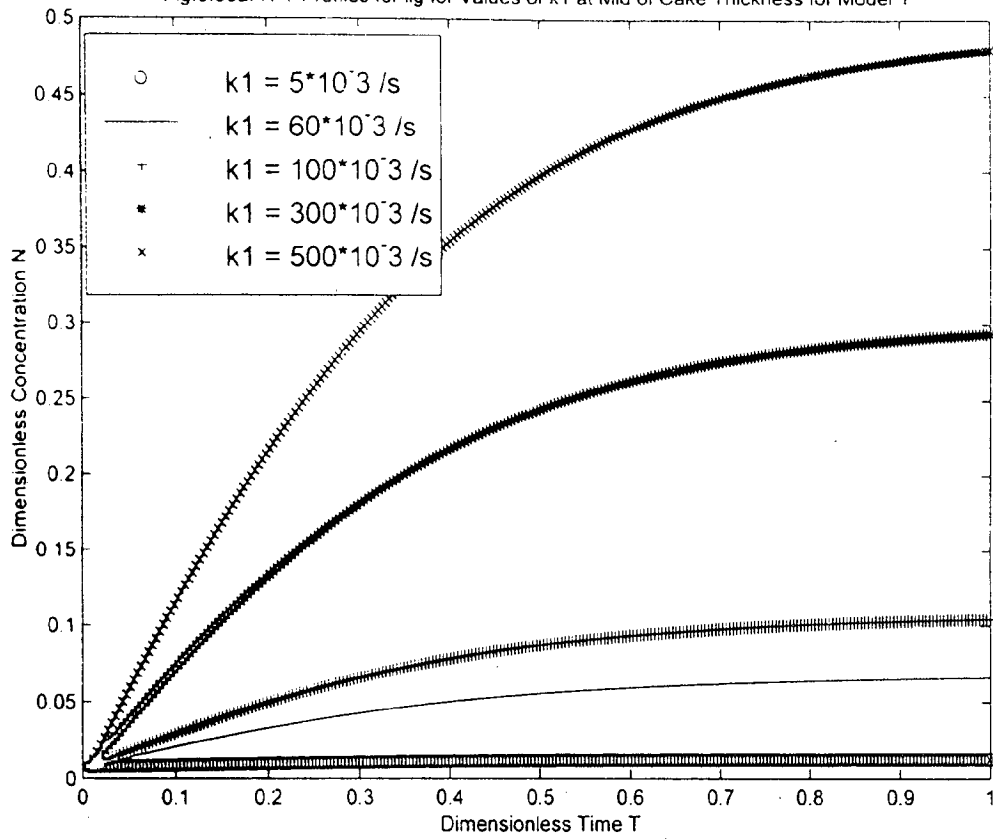


Fig.6.36b. N-T Profiles for lig for Values of k1 at Mid of Cake Thickness for Model 2

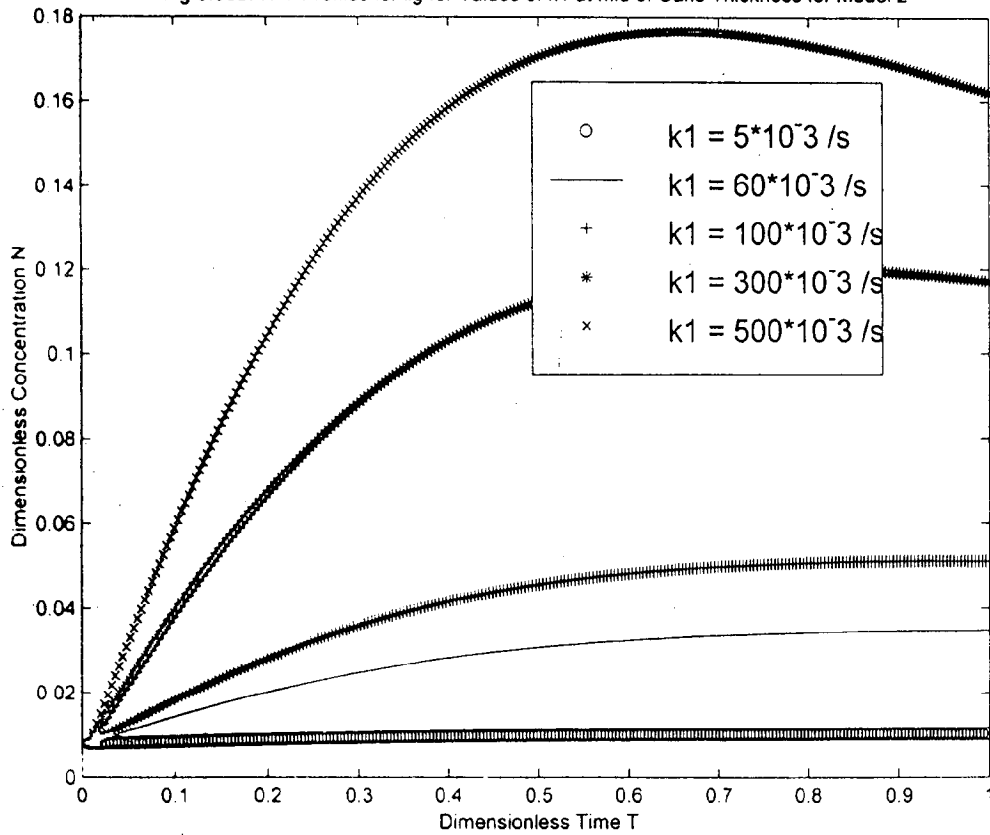


Fig.6.36c. N-T Profiles for lig for Values of k_1 at Mid of Cake Thickness for Model 3

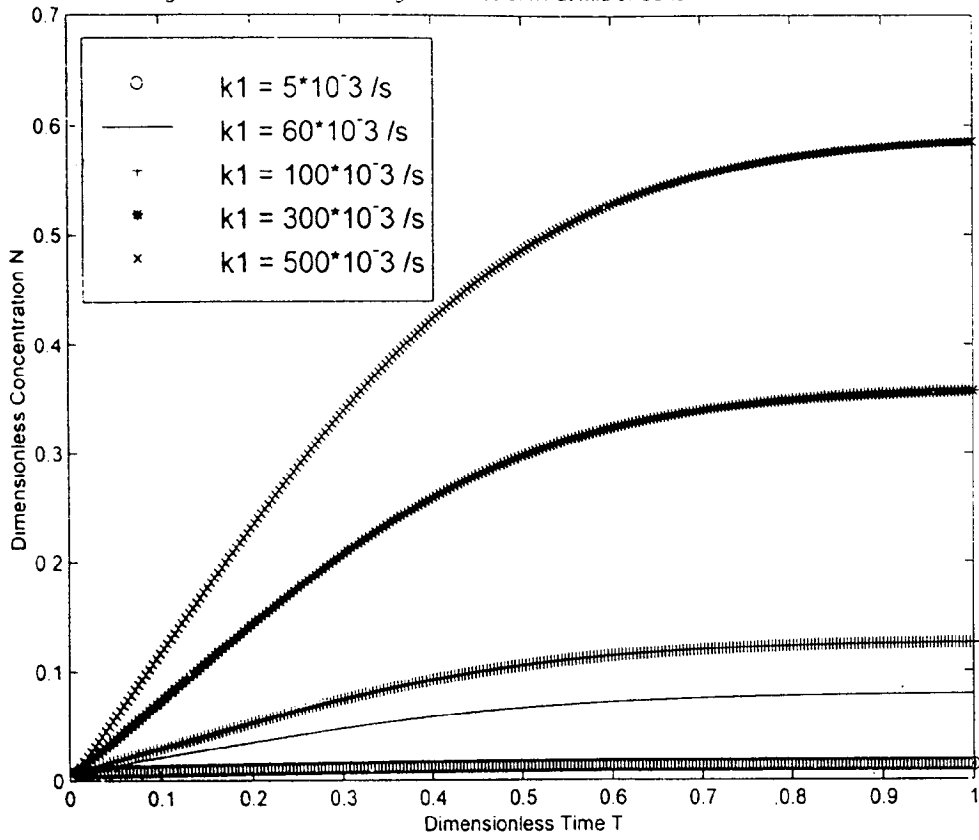


Fig.6.36d. N-T Profiles for lig for Values of k_1 at Mid of Cake Thickness for Model 4

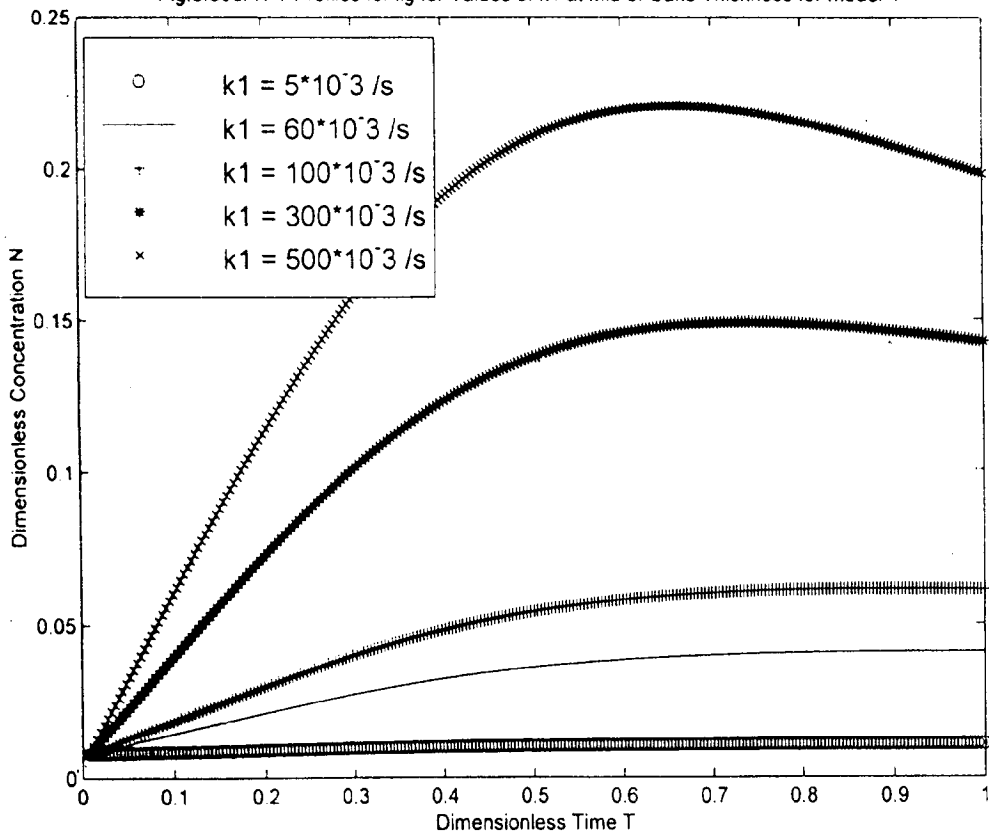


Fig.6.37a C-T Profiles for Na⁺ for Various Values of k₂ at Mid of Cake Thickness for Model 1

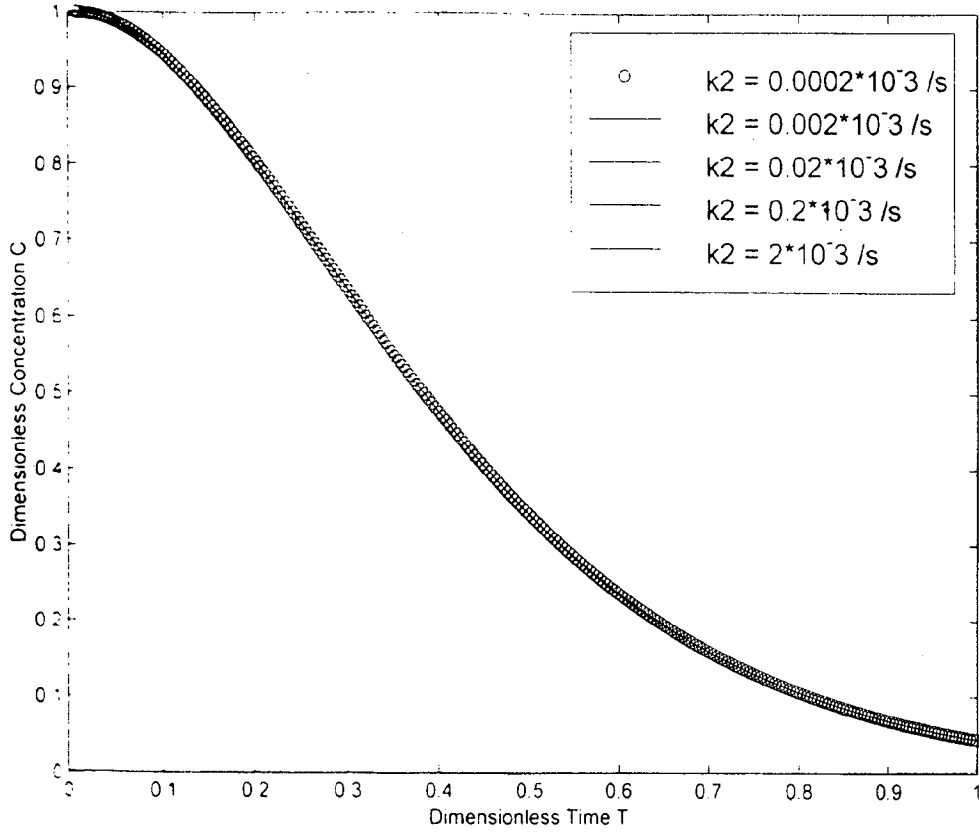


Fig.6.37b C-T Profiles for Na⁺ for Various Values of k₂ at Mid of Cake Thickness for Model 2

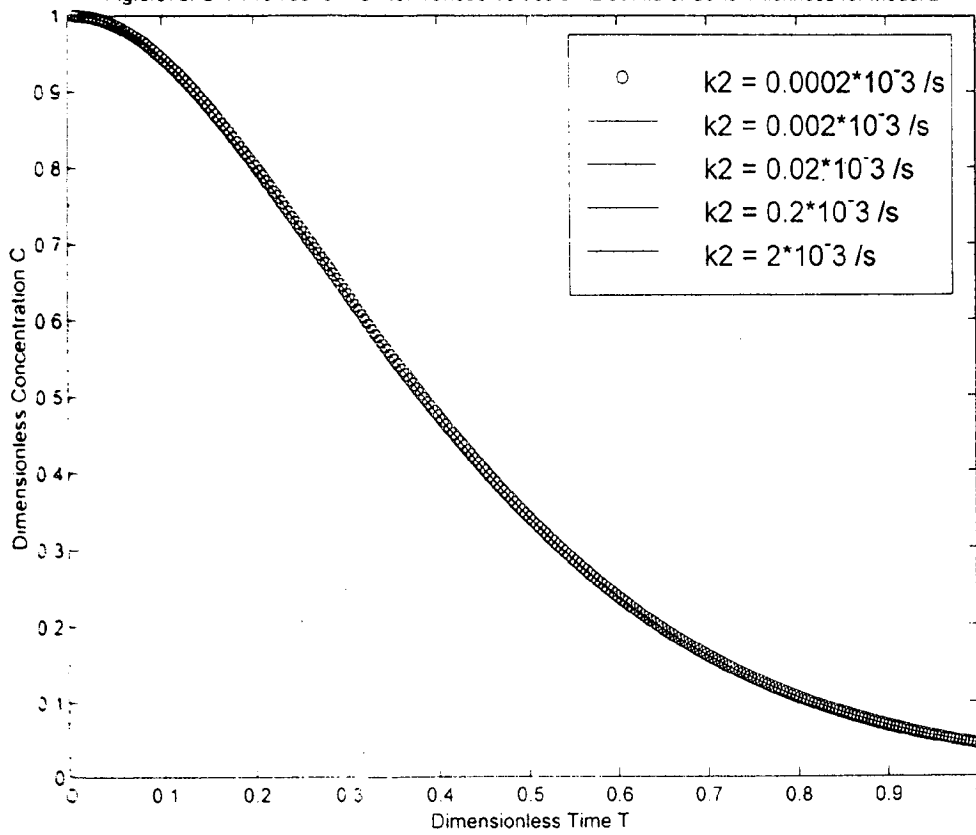


Fig.6.37c. C-T Profiles for Na+ for Various Values of k2 at Mid of Cake Thickness for Model 3

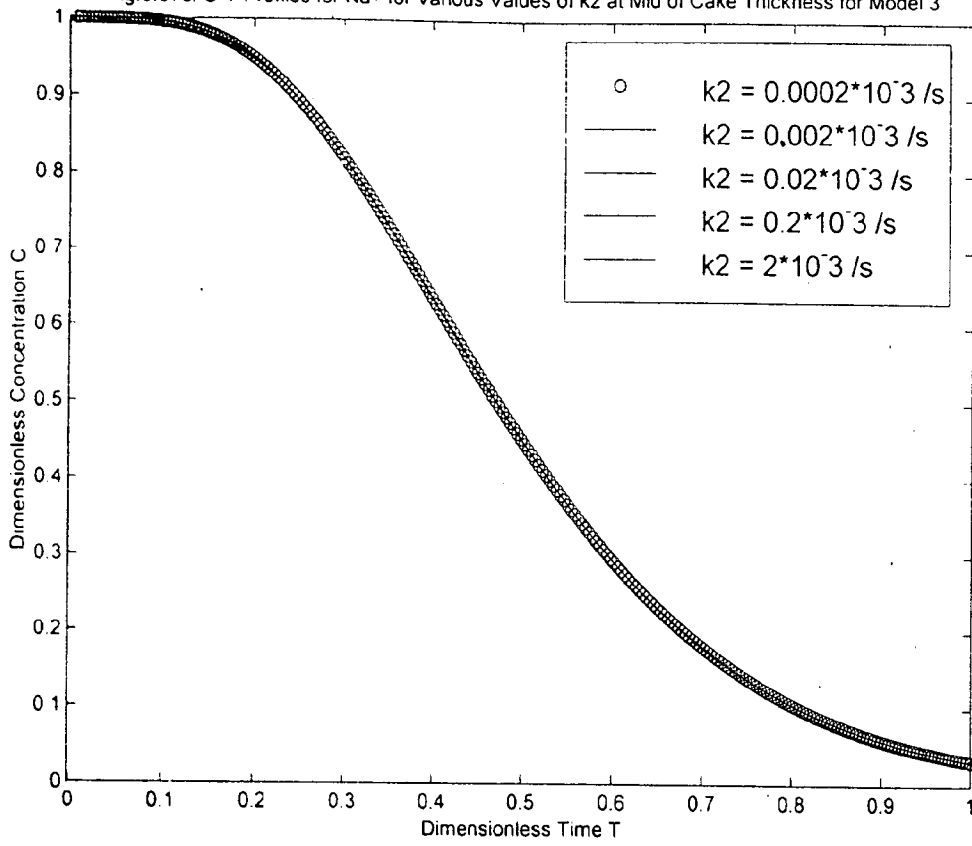


Fig.6.37d. C-T Profiles for Na+ for Various Values of k2 at Mid of Cake Thickness for Model 4

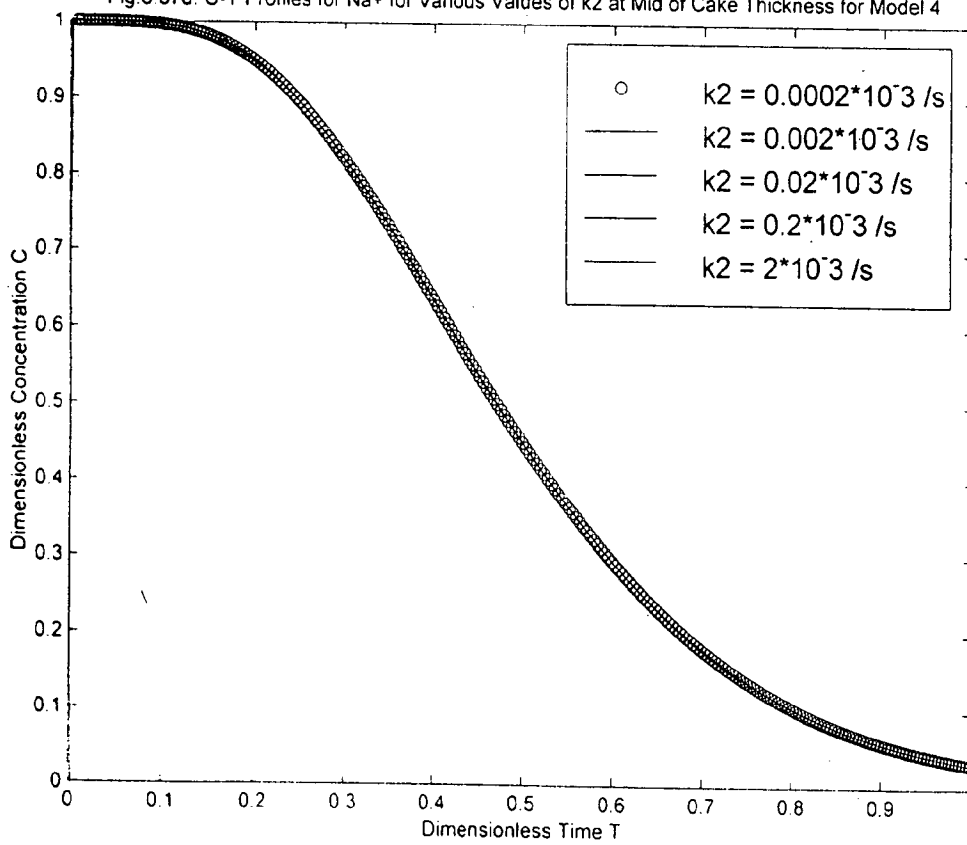


Fig.6.38a. C-T Profiles for lig for Various Values of k_2 at Mid of Cake Thickness for Model 1

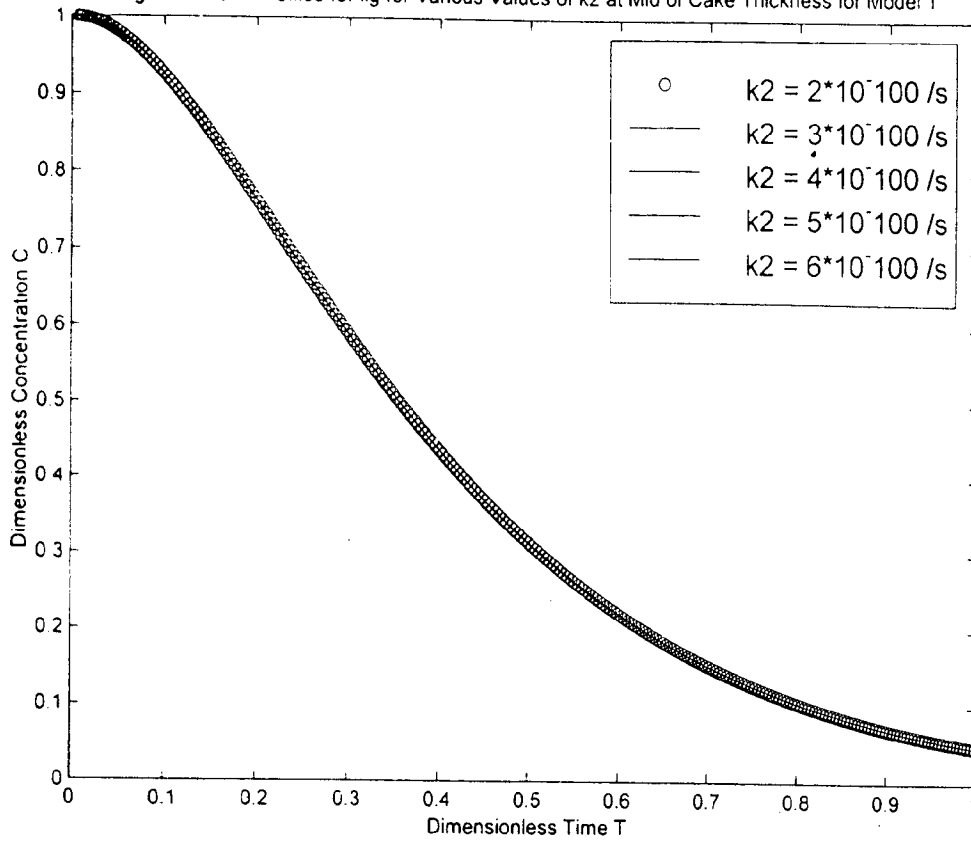


Fig.6.38b. C-T Profiles for lig for Various Values of k_2 at Mid of Cake Thickness for Model 2

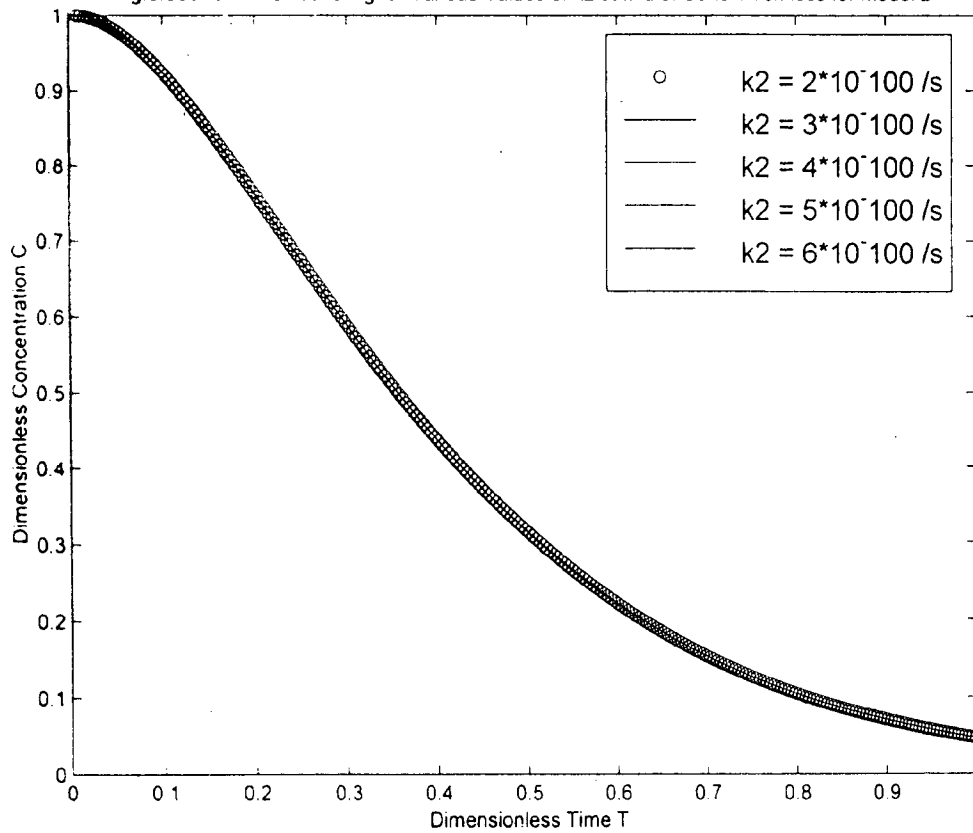


Fig.6 38c. C-T Profiles for lig for Various Values of k2 at Mid of Cake Thickness for Model 3

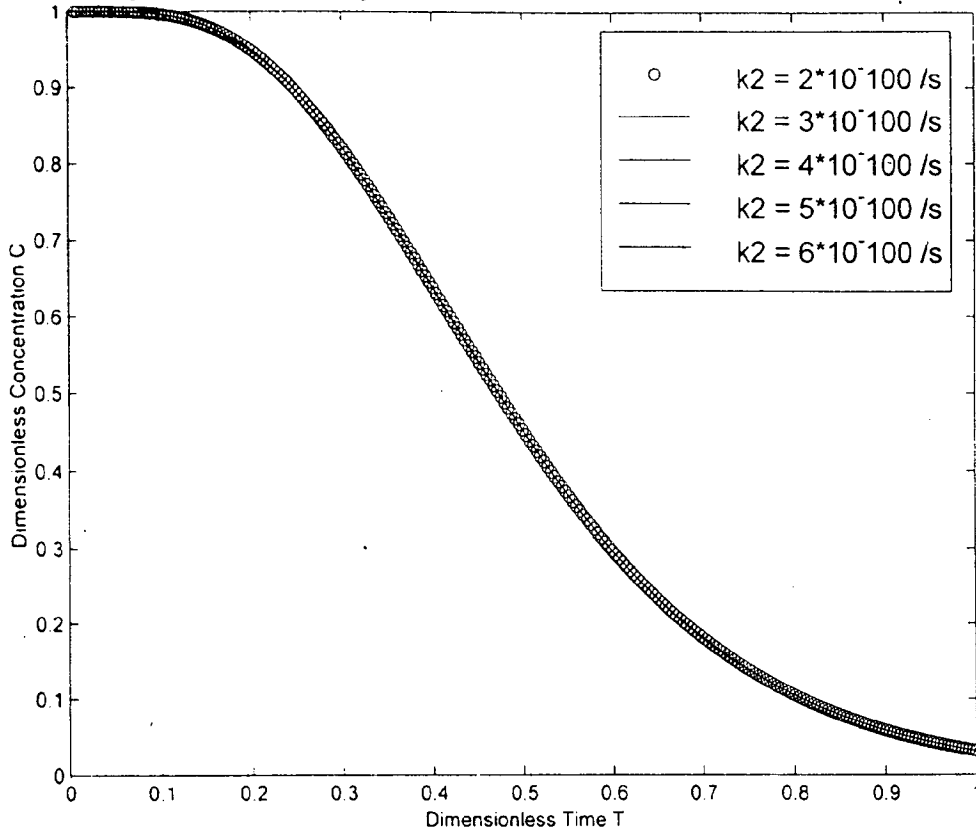


Fig.6 38d. C-T Profiles for lig for Various Values of k2 at Mid of Cake Thickness for Model 4

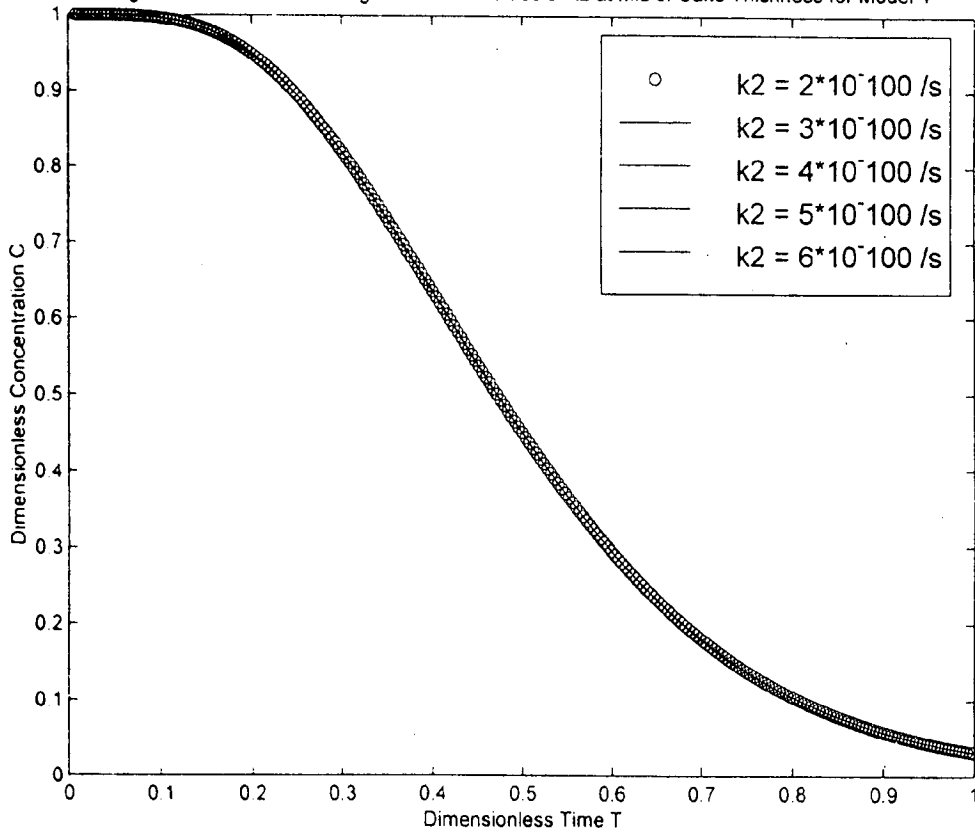


Fig.6.39a. N-T Profiles for Na+ for Various Values of k2 at Mid of Cake Thickness for Model 1

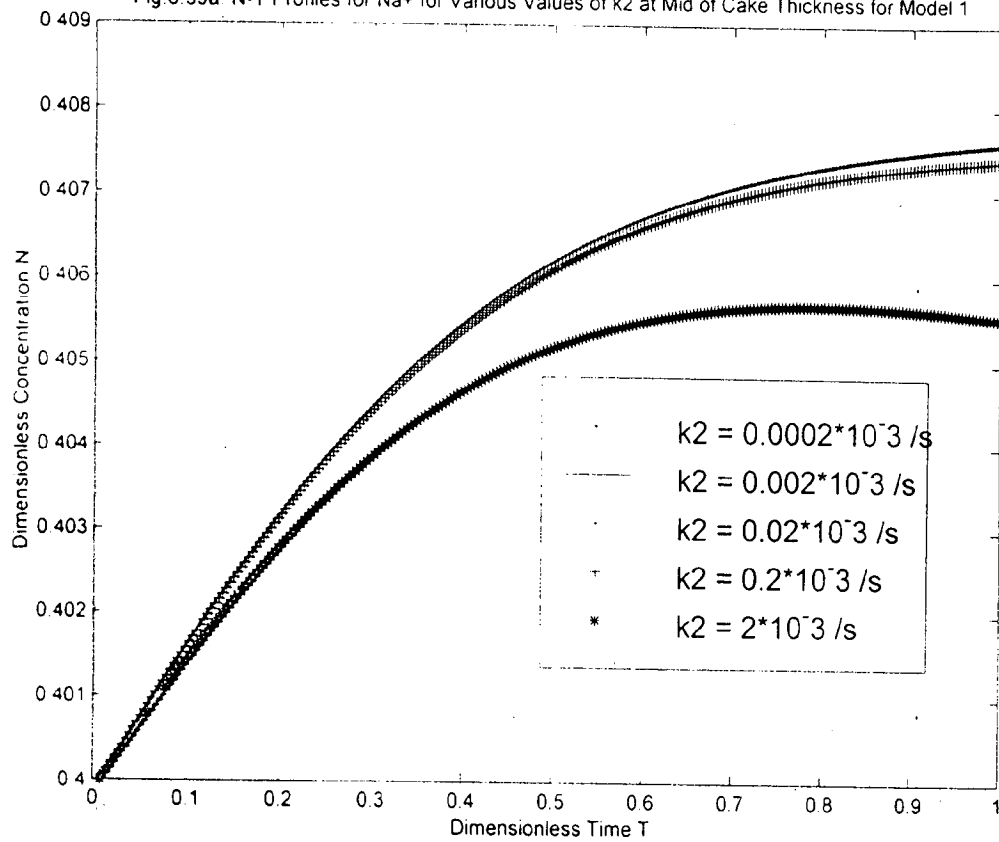


Fig.6.39b. N-T Profiles for Na+ for Various Values of k2 at Mid of Cake Thickness for Model 2

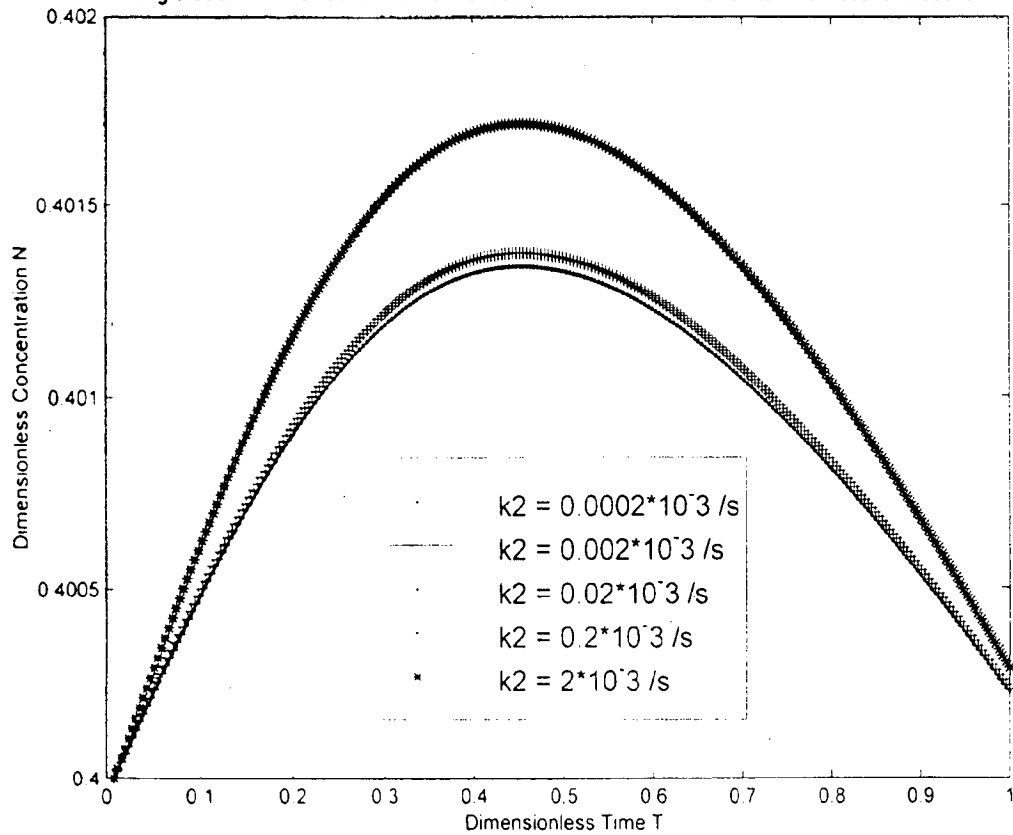


Fig.6.39c. N-T Profiles for Na⁺ for Various Values of k₂ at Mid of Cake Thickness for Model 3

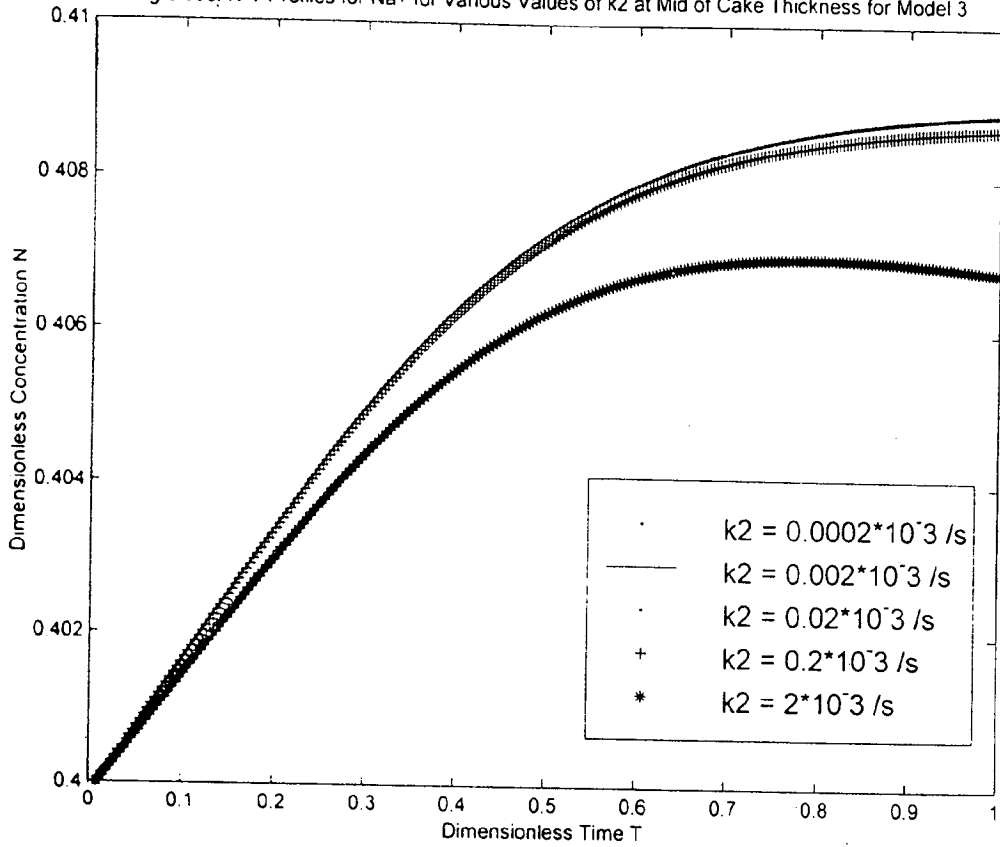
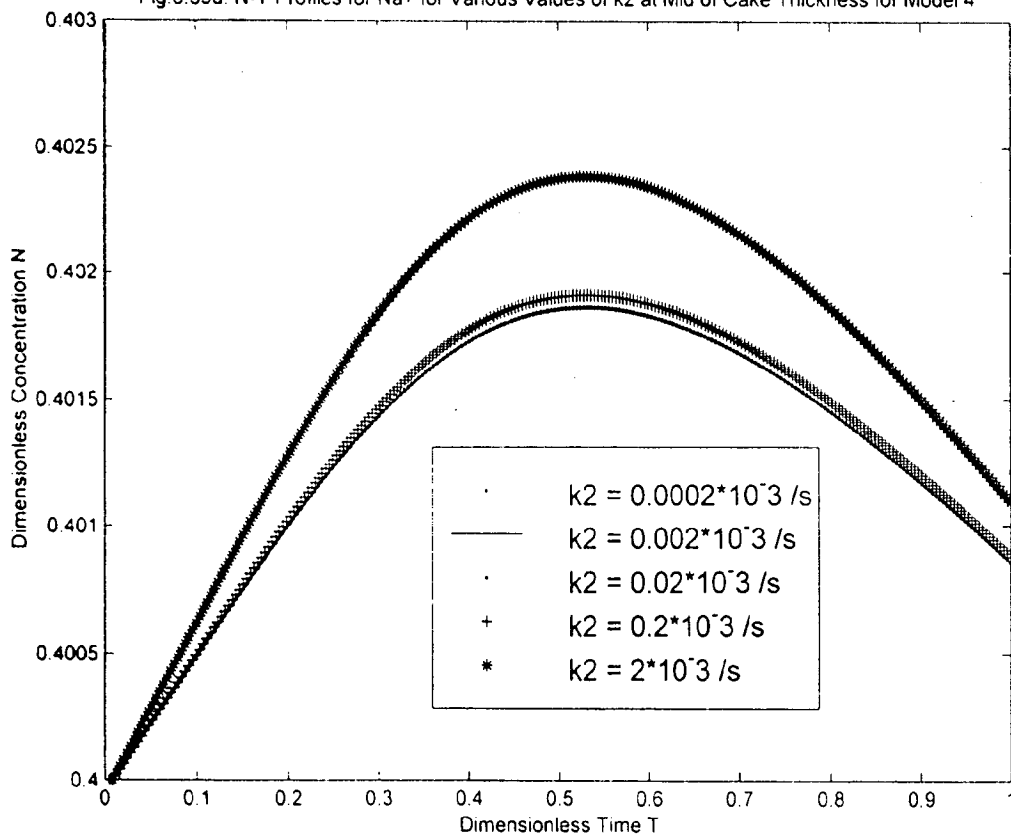
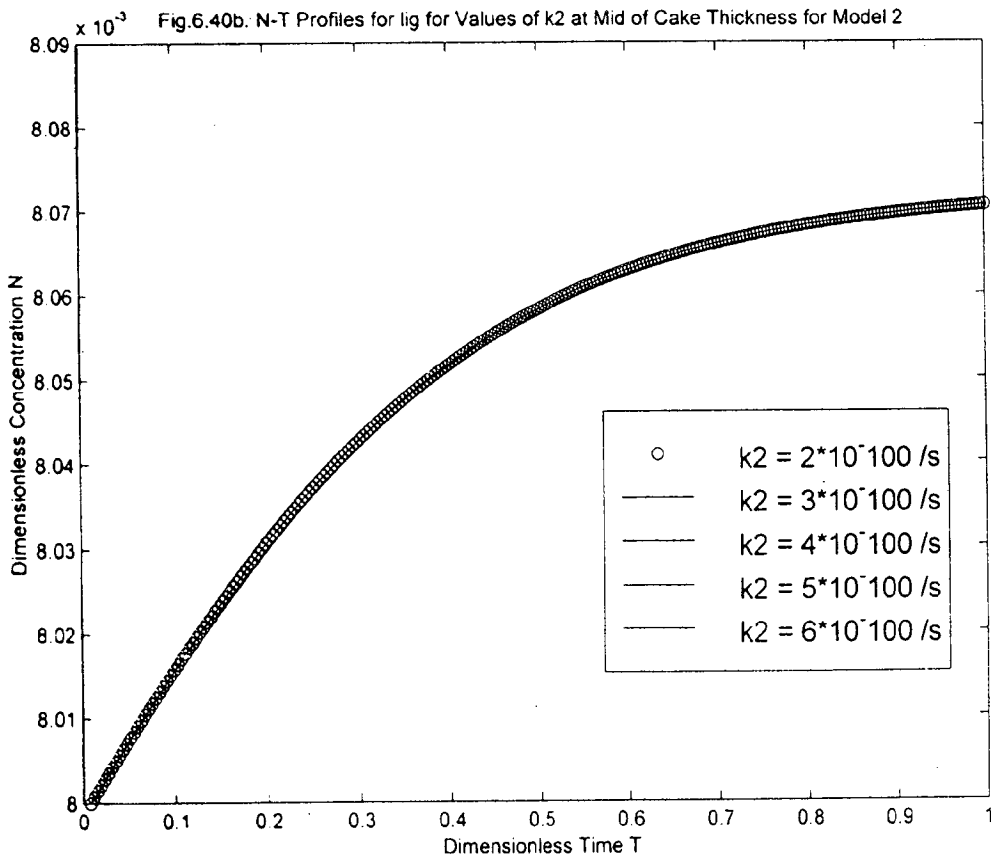
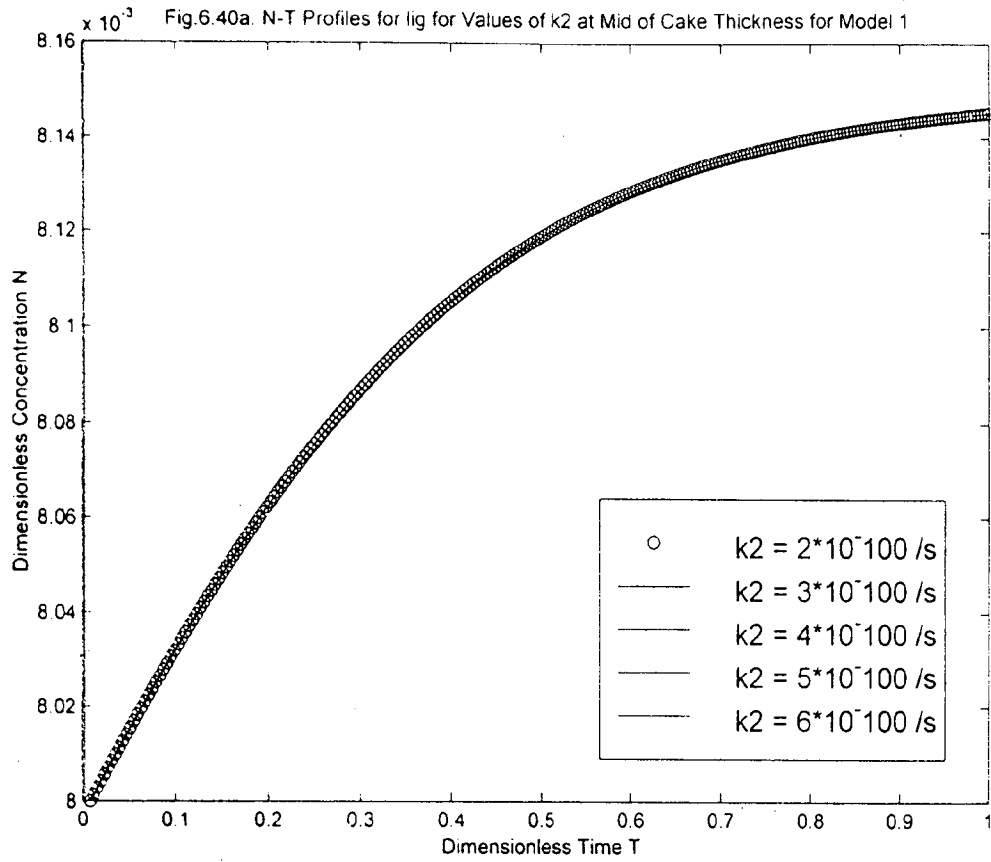
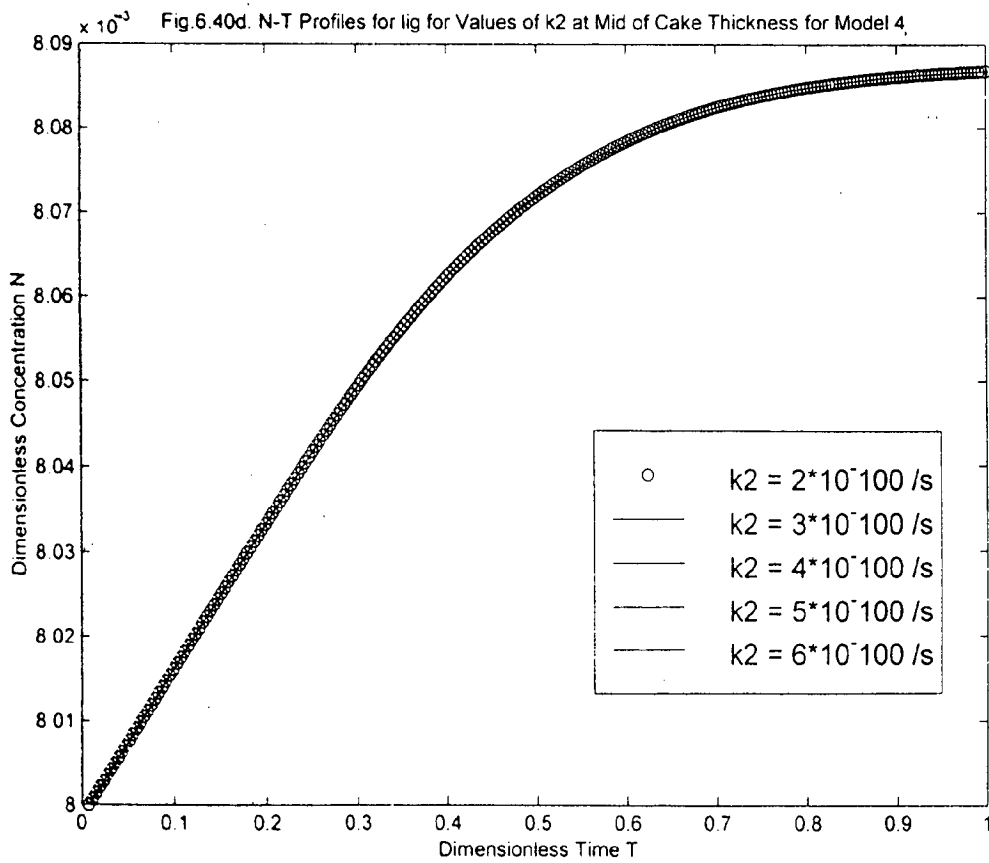
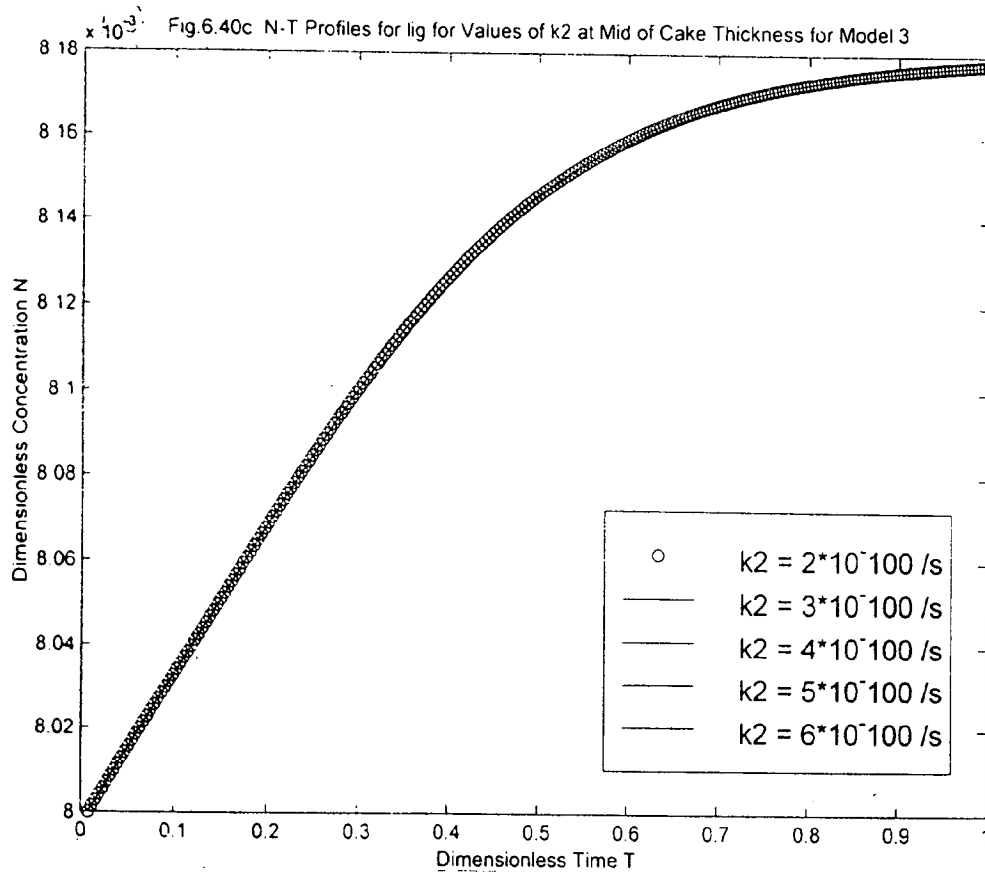


Fig.6.39d. N-T Profiles for Na⁺ for Various Values of k₂ at Mid of Cake Thickness for Model 4







show higher adsorption for models 1 and 3 while lesser value of k_2 show lesser adsorption for models 2 and 4.

Figs. 6.40a-6.40d are also drawn to show N-T profiles for lignin species. All the profiles coincide for varying values of k_2 . This may be due to the fact that the value of k_2 is of the order of 10^{-100} . Unlike N-T profiles for Sodium the profiles for lignin show the increasing trend for all the models.

6.1.31 Effect of C–T Profiles for Sodium as a function of Peclet number

Peclet number is a dimensionless parameter which takes care of various local velocities u , bed thickness L and longitudinal dispersion coefficient D_L . For a constant bed depth it can show the variational effect of both u and D_L . These are shown in Figs. 6.41a–6.41b for the models 1 and 2 respectively. Peclet number is varied from 20 to 110. This range is valid for pulp washing as suggested by various investigators including Grah [25]. The calculated values of Peclet number from Grah's data is shown in Table 5.8, Section 5.3.5 though some authors considered lower range of values in their depiction. For Peclet number below 20 (say 13 to 18) it is observed that there is erratic behavior of profiles. This is in conformity with the comments of Pourier et. al.[79]. It is surprising that in spite of so much observed findings Potucek [81] and some other investigators considered the value of Peclet number lower than 20. It is observed that Peclet number has significant influence on C–T profiles. Higher the Peclet number, better is the shape of the break through curves.

Streams of curves originates from $C = 1$, depends from each other ($Pe = 30$ to 110) and thus coincide at $T = 0.8$ and again diverge from each other in topsy-turvy manner. It means C–T profiles for $Pe = 30$ to 110 which were at the lower side of the curve, go upward This is true for Peclet number 20 also.

Fig.6.41a C-T Profiles for Na+ for Various Values of Pe at Bed Exit for Model 1

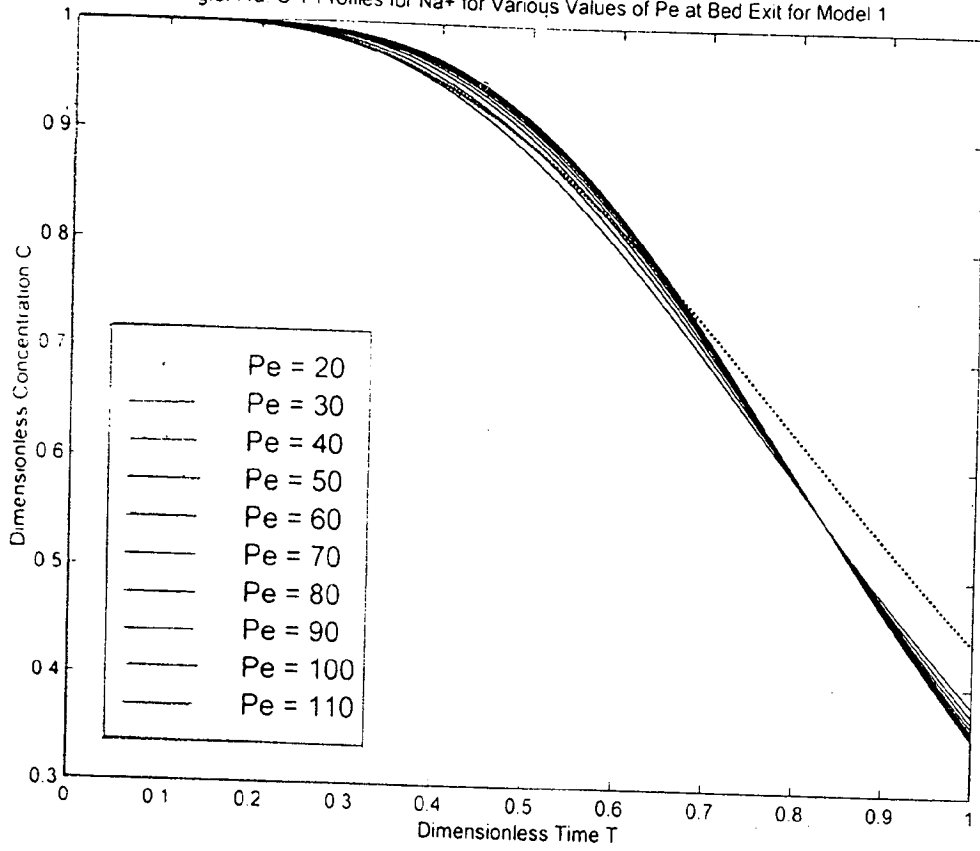
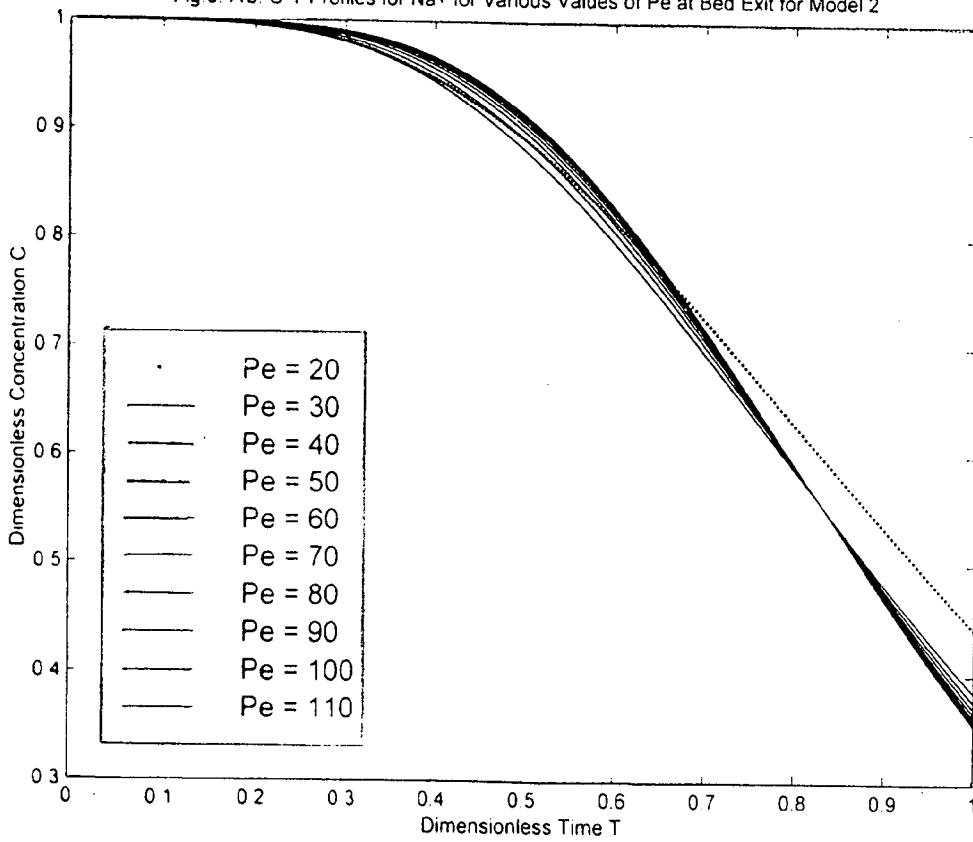


Fig 6.41b. C-T Profiles for Na+ for Various Values of Pe at Bed Exit for Model 2



6.1.32 Comparison of C–T profiles for the models 1-4 for Sodium for fixed value of Peclet number (Pe = 100)

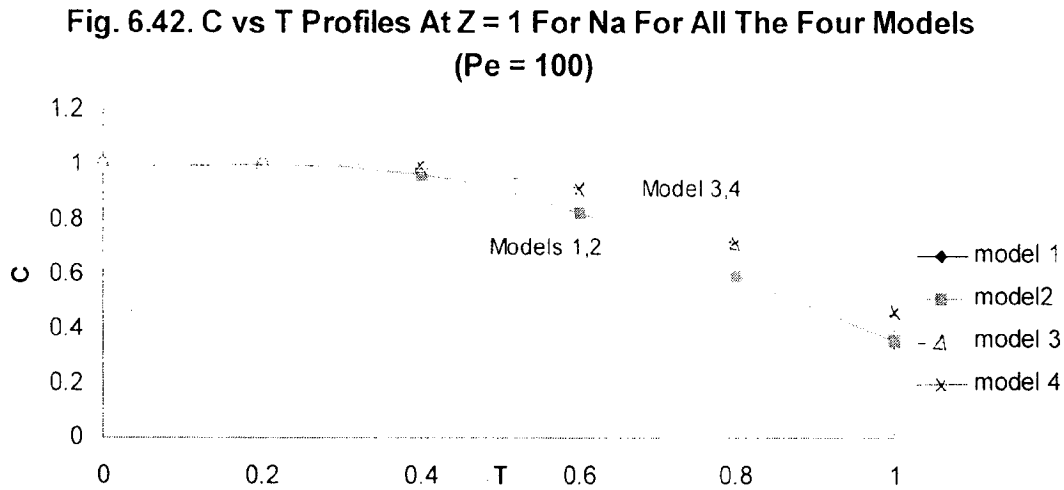


Fig. 6.42 shows the comparison among models 1-4 for C–T profiles for Sodium at constant Peclet number 100 at bed exit point. Similar trend can be found for lesser Peclet Number (Pe = 27) as shown in Fig. 6.10. It seems that Peclet number has no appreciable effect on concentration of solute in filtrate with time at bed exit conditions. Although models 3 and 4 do not have Peclet number directly in the mathematical formulation but have other parameters u and L which indirectly influence the trend.

6.1.33 Effect of C–T Profiles for lignin as a function of Peclet number

Fig. 6.43a – 6.43b show the C–T profiles for lignin at the various values of Peclet number at the bed exit. The nature of the curves and the profiles show the same behavior as the C–T profiles for Sodium. The figures can be explained in the same way as that for Sodium.

6.1.34 Comparison of C–T profiles for the models 1-4 for lignin for fixed value of Peclet number (Pe = 100)

Fig. 6.44 shows the comparison among models 1-4 for C–T profiles for lignin at constant Peclet number 100 at bed exit point. The profiles are similar to those for Peclet number 20 as shown in

Fig.6.43a. C-T Profiles for lig for Various Values of Pe at Bed Exit for Model 1

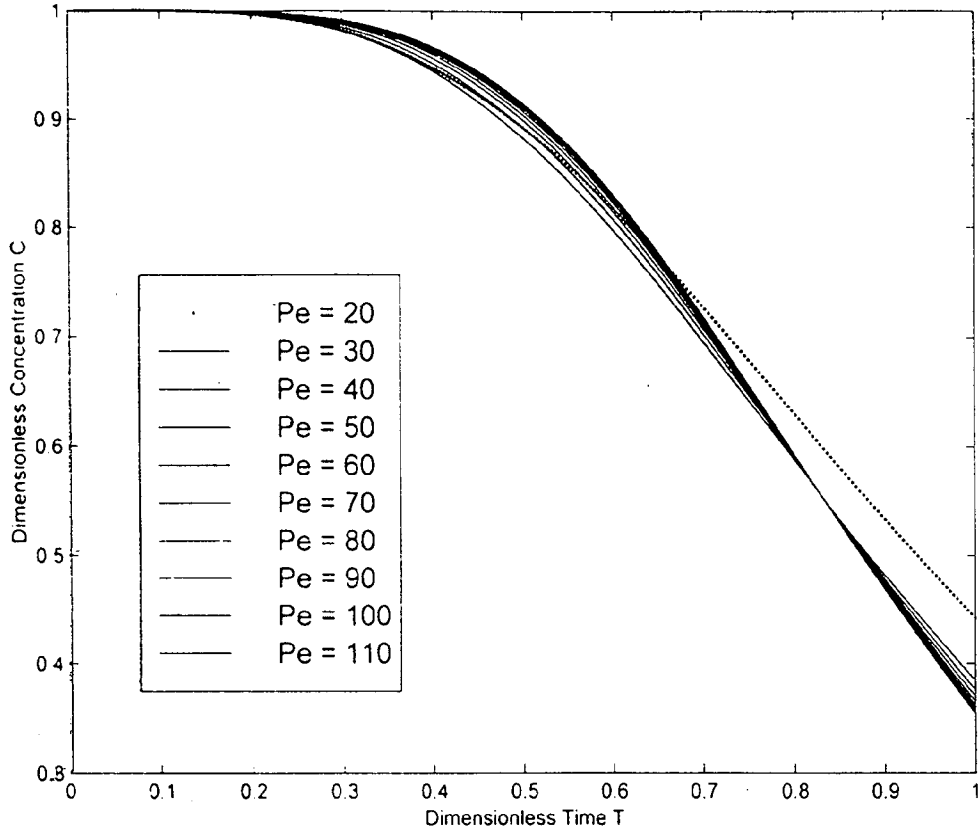


Fig.6.43b. C-T Profiles for lig for Various Values of Pe at Bed Exit for Model 2

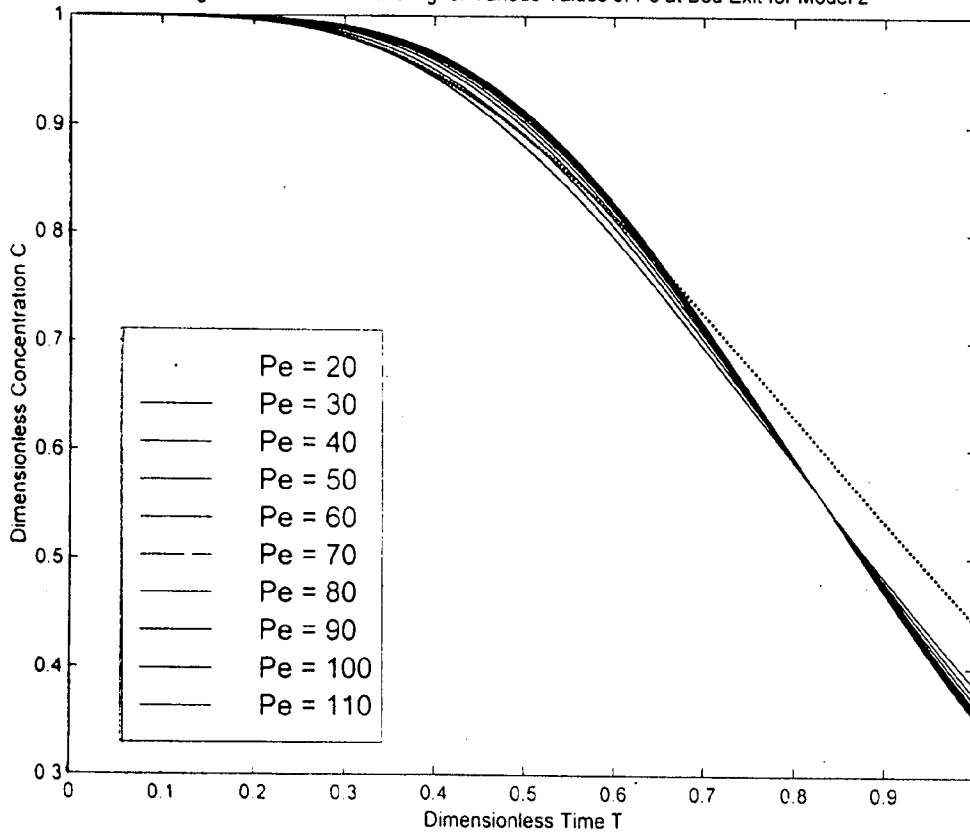


Fig 6.45a N-T Profiles for Na⁺ for Various Values of Pe at Bed Exit for Model 1

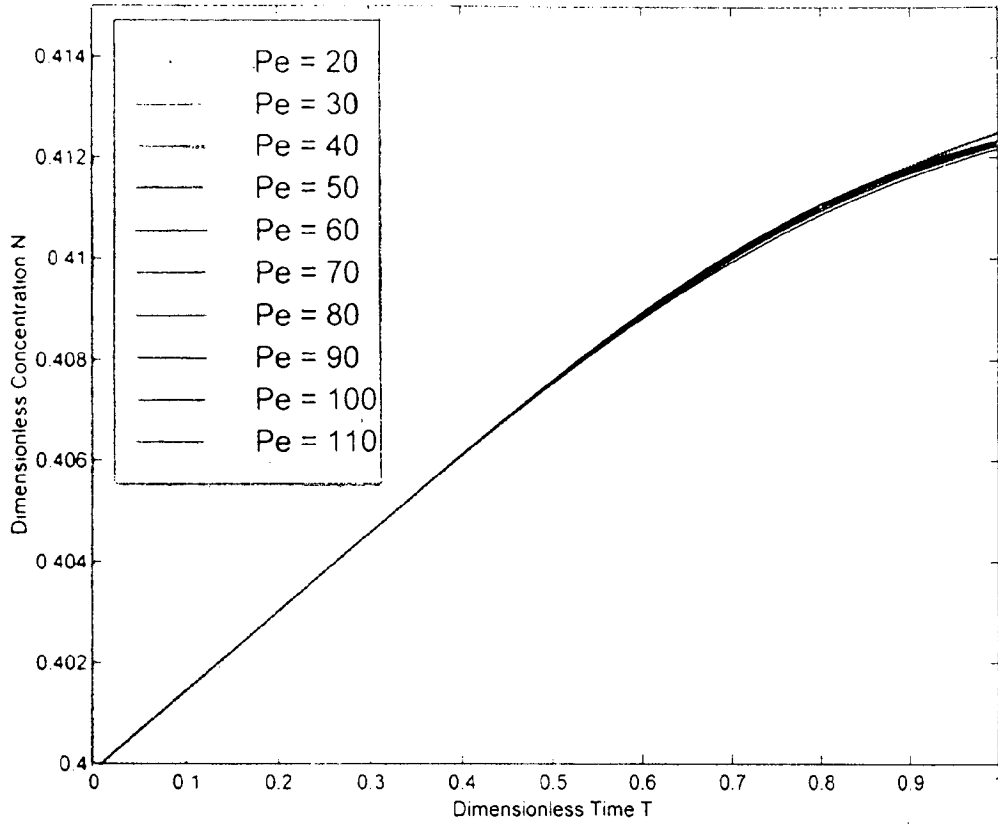


Fig.6.45b. N-T Profiles for Na⁺ for Various Values of Pe at Bed Exit for Model 2

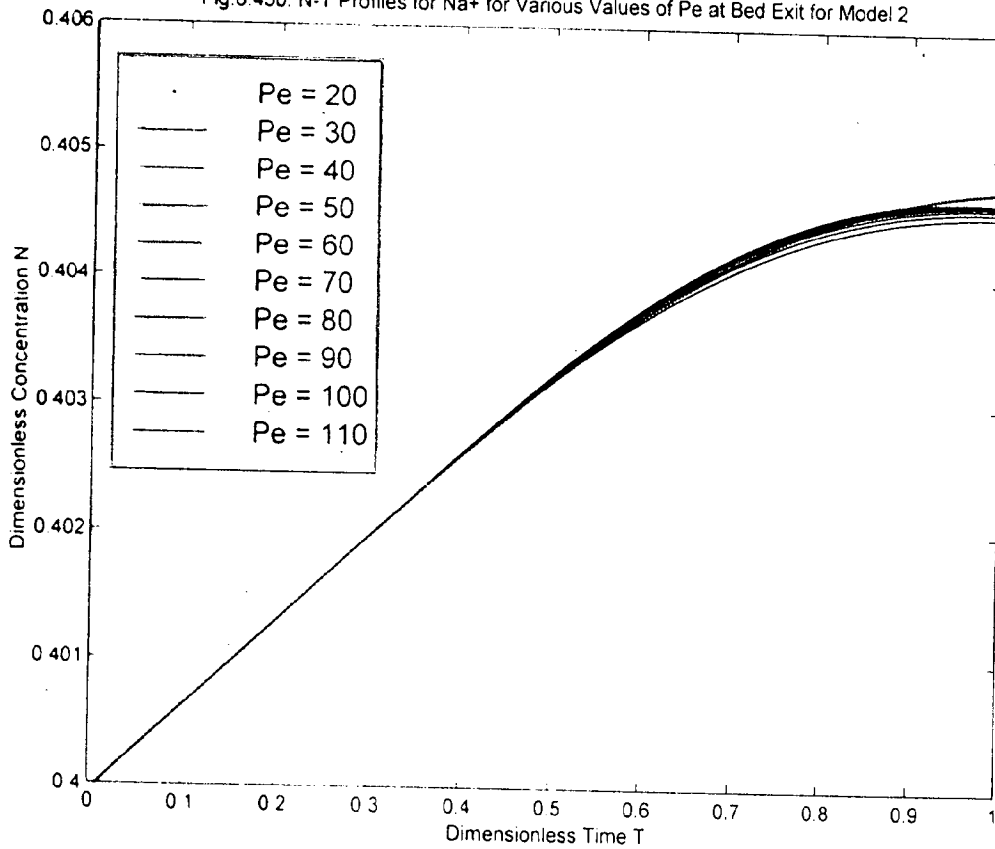
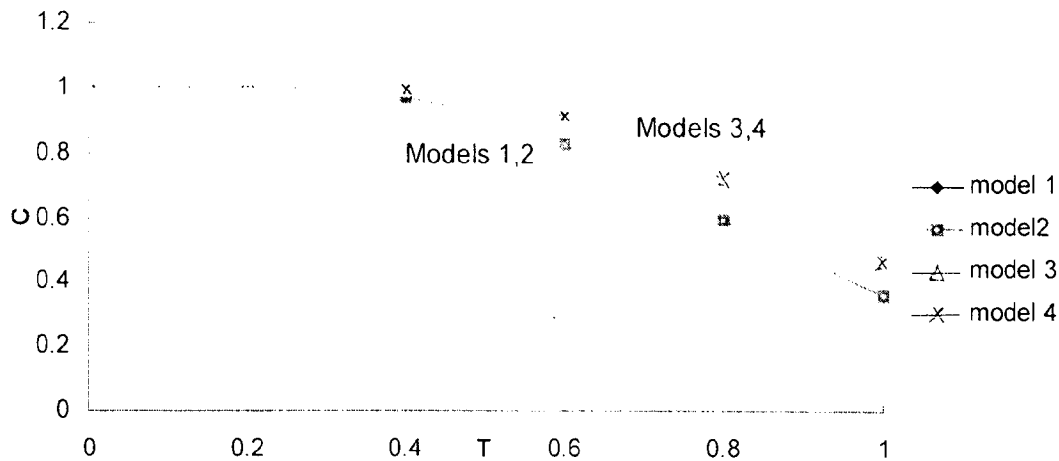


Fig. 6.12 except that the difference of concentration at $T = 1$ is slightly larger between models with and without dispersion in case of $Pe = 100$ than in the case of $Pe = 20$.

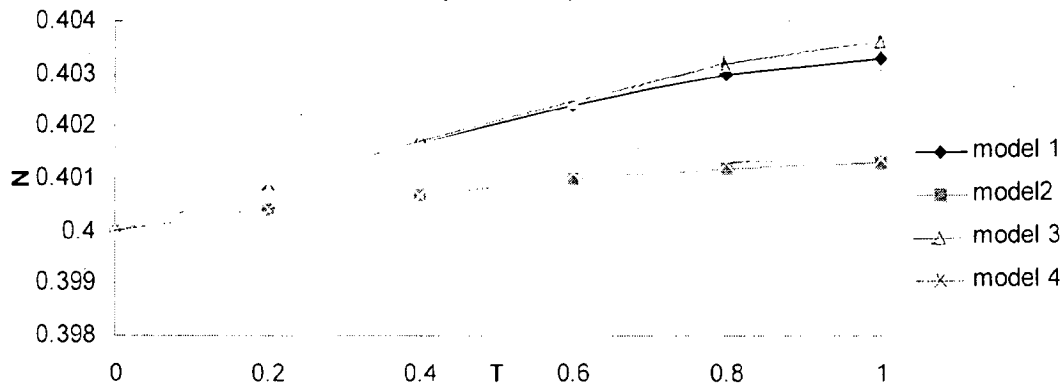
Fig. 6.44. C vs T Profiles At Z = 1 For lignin For All The Four Models (Pe = 100)



6.1.35 Effect of N–T Profiles for Sodium as a function of Peclet number

Figs. 6.45a–6.45b depict the N–T profiles for Na^+ for models 1 and 2 respectively. For all the Peclet numbers the profiles coincide with each other upto $T = 0.5$ to 0.6 and then diverge from each other beyond a certain value of T . The figures also display upside down trend similar to the case of C–T profiles.

Fig. 6.46. N vs T Profiles At Z = 1 For Na For All The Four Models (Pe = 100)



6.1.36 Comparison of N–T profiles for the models 1-4 for Sodium for Pe = 100

Fig. 6.46 shows the comparison among model 1-4 for N-T profiles for Sodium at constant Peclet number 100 at bed exit. The trend is the same as also clearly seen in Fig. 6.14 for lower Peclet number ($Pe = 27$).

6.1.37 Effect of N-T Profiles for lignin as a function of Peclet number at bed exit

Figs. 6.47a–6.47b are drawn to show the N-T profiles for lignin as a function of Peclet number at the bed exit for models 1 and 2 respectively. The profiles are almost identical as those for Sodium. The only difference between the Sodium and lignin species is the extent of linearity and curvilinearity at certain values of T upto certain point. The lignin curves become more elongated compared to those of Sodium though the values of N for lignin is much smaller than those of Sodium.

6.1.38 Comparison of N-T profiles for the models 1-4 for lignin for ($Pe = 100$)

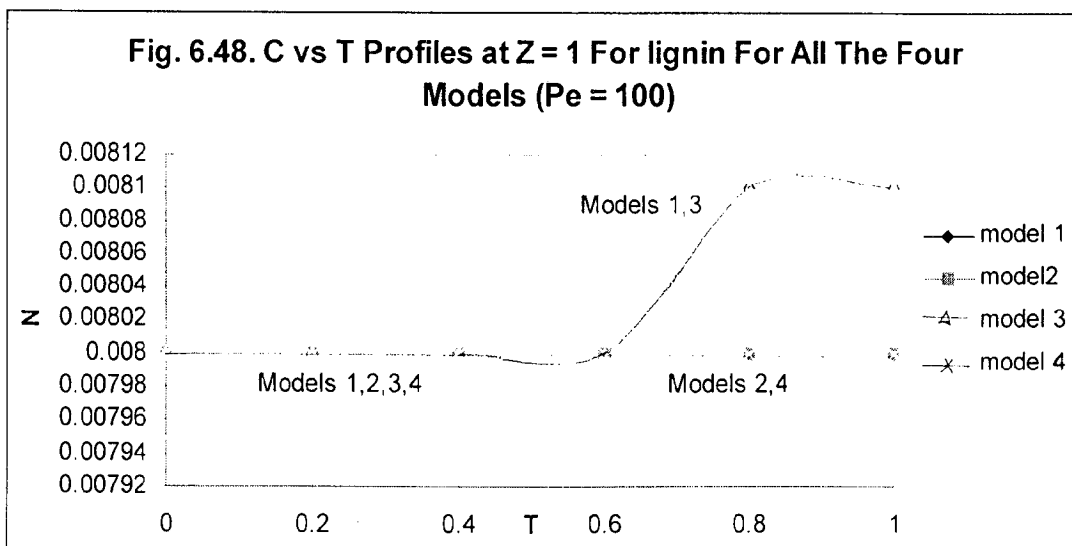
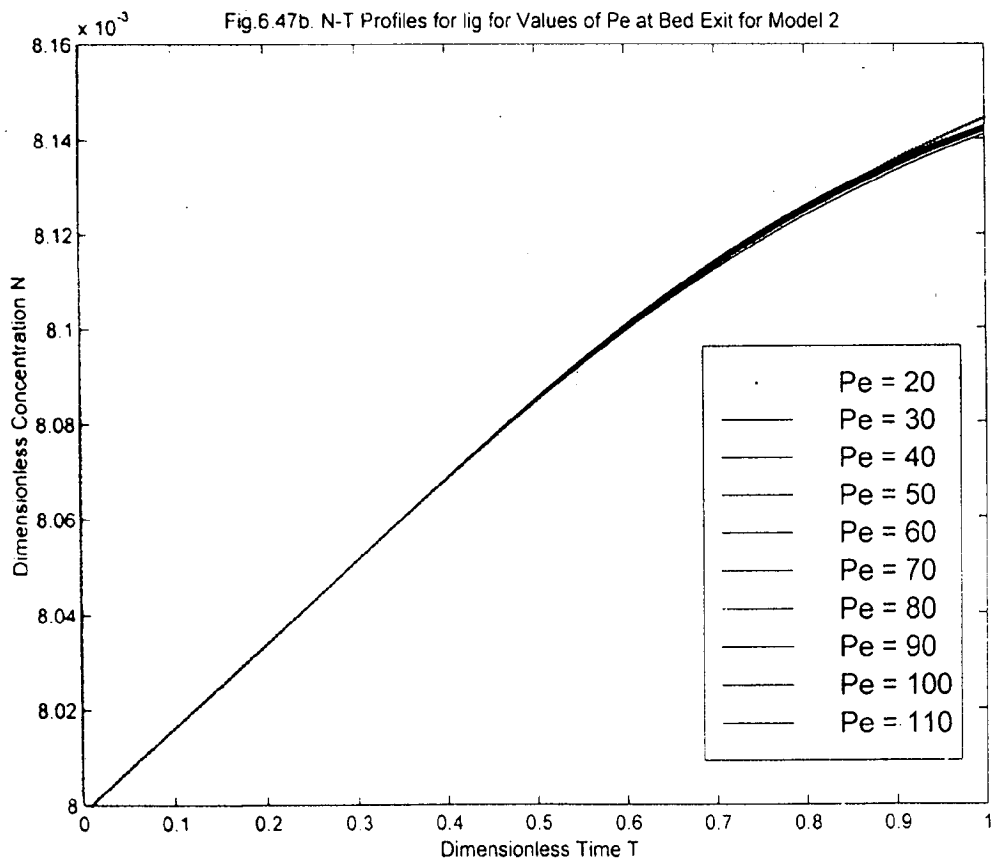
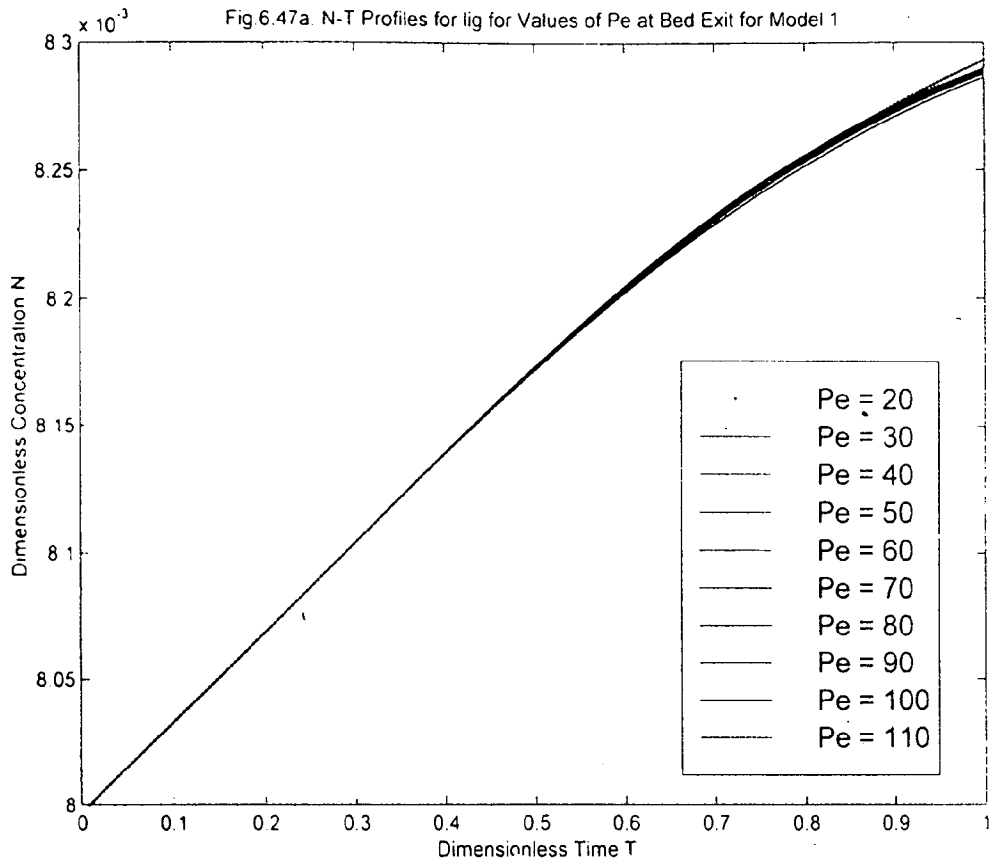


Fig. 6.48 shows the comparison among models 1-4 for N-T profiles for lignin at constant Peclet number 100 at bed exit. The trend is slightly different for lower Peclet number ($Pe = 20$) as already revealed. The models merge with each other displaying almost constancy of values of N till $T = 0.6$. Beyond this point though models 2 and 4 maintain the same trend, the models 1 and 3 rises sharply slightly above 0.6 and then becomes constant.



6.1.39 Effect of Peclet Number on C-T profile of Sodium for model 1 at bed exit

Fig. 6.49. comparison of numerical solutions of model 1 for two different Peclet numbers

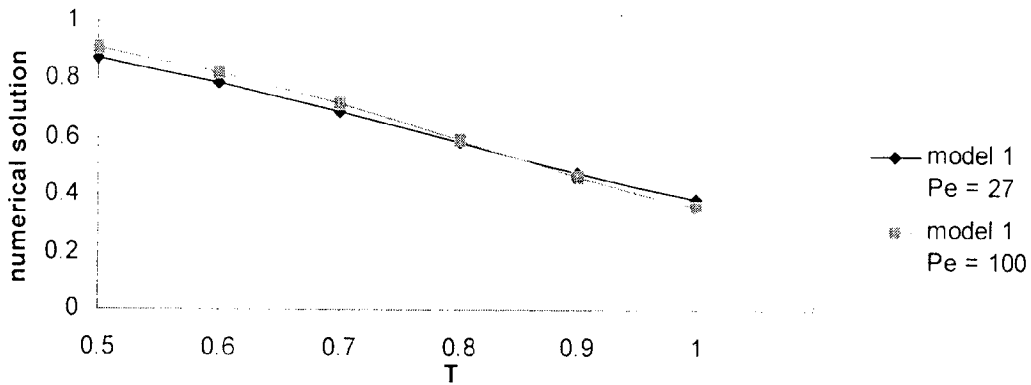
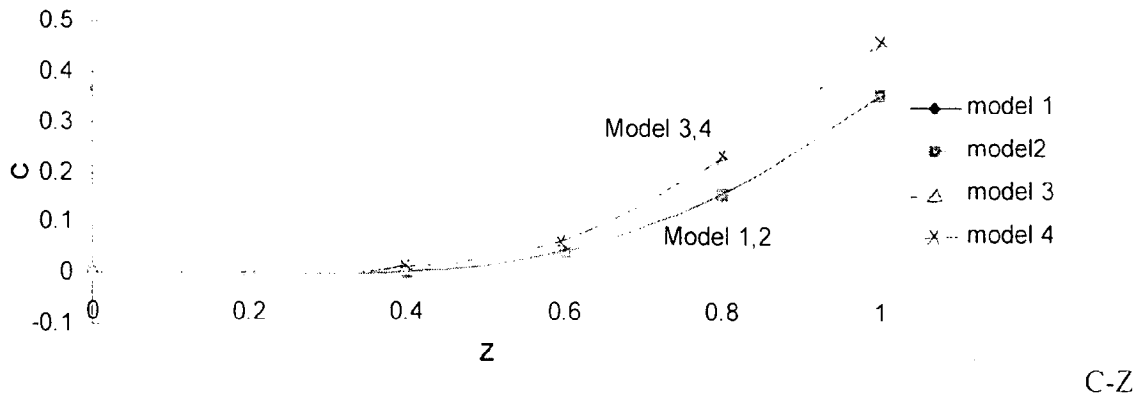


Fig. 6.49 is drawn to show the effect of Peclet number using model 1 (with dispersion) for C vs. T plot at bed exit. Peclet numbers used were 27 and 100. The profiles reveal that at lower value of T there is a slight difference of C value. The difference becomes narrower as one goes on increasing the value of T, then the graphs coincide at $T = 0.83$, then further diverge from each other in reverse manner. In the later case also the divergence is marginal.

6.1.40 Comparison of C-Z profiles for Sodium for all the four models at Pe = 100

Profiles have also been drawn for Sodium for all the four models at $T = 1$ for Peclet number $Pe = 100$ in Fig. 6.50. As shown the profiles for models 1 and 2 coincide and those for models 3 and 4 also coincide with each other separately. The same are drawn for $Pe = 27$ in Fig 6.2 where it is noticed that reverse trends are found above and below $Z = 0.7$. Obviously they merge each other at this value. The difference is however marginal. Only difference found in the former case is that there is no merge at an inflexion point.

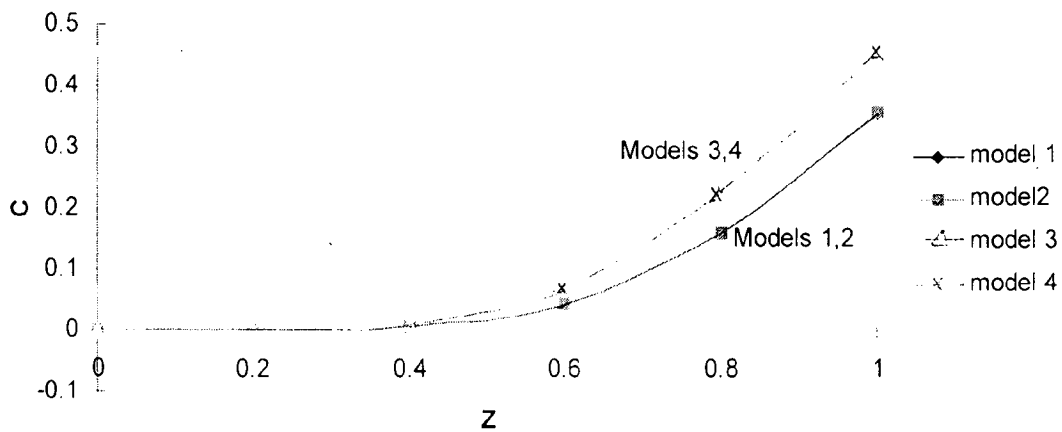
Fig. 6.50. C vs Z Profiles At T = 1 For Na For All The Four Models (Pe = 100)



6.1.41 Comparison of C-Z profiles for lignin for all the four models at Pe = 100

C-Z profiles have also been drawn for lignin in Fig. 6.51. Like Sodium the profiles for lignin display the same trend. For Pe = 20 shown in Fig 6.4 where it is observed that reverse trends are found above and below Z = 0.83, merge each other at this value, unlike for Pe = 100 the figures cross over each other. The difference is however marginal. Only difference found in the former case (Pe = 100) is that there is no merge at an inflexion point.

Fig. 6.51. C vs Z Profiles At T = 1 For lignin For All The Four Models (Pe = 100)



6.1.42 Comparison of N-Z profile for Sodium and lignin for all the four models at Pe = 100

N-Z profiles are shown for Sodium for all the four models in Fig. 6.52 at $Pe = 100$ and also at $T = 1$. The figures reveal that all the curves are distinctly different, having upward trends in almost linear manner. Similar trend is already found for lower Pe number ($Pe = 27$) shown in Fig 6.6. Adsorption is found higher at a lower Peclet number though the difference is marginal.

Fig. 6.52. N vs Z Profiles At T = 1 For Na For All The Four Models (Pe = 100)

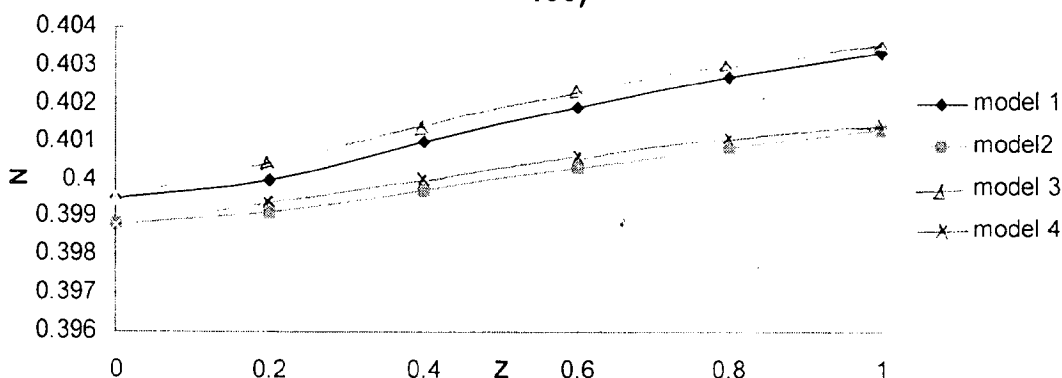
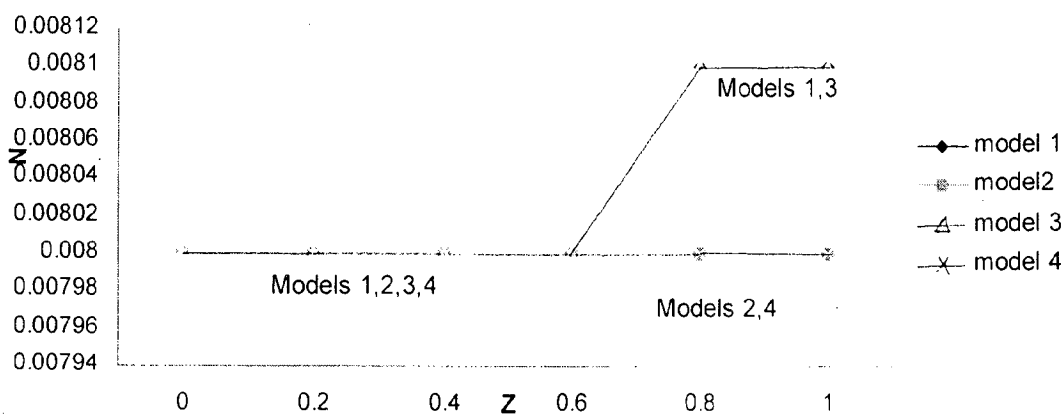


Fig. 6.53. N vs Z Profiles At T = 1 For lignin For All The Four Models (Pe = 100)



N-Z profiles are shown for lignin in Fig. 6.53. The figures reveal that all the curves coincide upto $Z = 0.6$ having linear trend parallel to Z axis. Afterward curves of models 2 and 4 maintain the same trend while those of models 1 and 3 show sharp increase till $Z = 0.8$ and then become

constant again till bed exit. Profiles for lower Pe number ($Pe = 20$) are shown earlier in Fig 6.8. The profiles for two different Peclet numbers have some different trends.

6.1.43 Effect of the nature of species on N–T profiles

The profiles have been drawn for both the species i.e. Na^+ and lignin in the Figs. 6.54a-6.54d regarding their characteristic features in respect to their desorption rates. Effect of both the species namely Na^+ and lignin on N–T profiles is shown at mid points of the cake thickness. It is interesting to note that for the N–T profiles for Na^+ there is a steep curve observed, strongly non linear in character. It is evident from the graphs that N increases rapidly, almost linearly, with smaller T, goes to a maximum at $T = 0.7$ approximately and then becomes almost constant at value $T = 0.8$ for models 1 and 3. For models 2 and 4 there is a rising trend upto midway and then drops afterwards. The same for lignin exhibits a linear trend with slightly increasing magnitude with time T at a much slower rate. This is attributed to the greater affinity of Na^+ ions compared to Lignin with the pulp fibers. This fact is verified from the experimental data of Trinh et al.[100].

The above fact is in close agreement with the findings of Grah [25] and Hartler & Rydin [33]. It is concluded that adsorption of lignin on the pulp is considerable lower than the adsorption of Na^+ and as a result Grah [25] has neglected adsorption of lignin on pulp fibers during his investigation.

6.1.44 Effect of t on c for Sodium for all the four models

A comparison has been made for Sodium for bed inlet and bed exit conditions by plotting absolute value of concentration c (kg / m^3) vs. time t (sec) in Figs. 6.55a-6.55d. As expected, the exit displays a breakthrough curve whereas the bed inlet represents an asymptotic curve where there is practically no displacement stage observed.

Figs. 6.55a1-6.55d1 are plotted for c as a function of time t at five equi-spaced bed depths. These curves also explain the absence of displacement stage in the upper layers (near bed inlet) whereas

Fig. 6.54a N-T Profiles for Na⁺ and lignin at Mid of Cake Thickness for Model 1

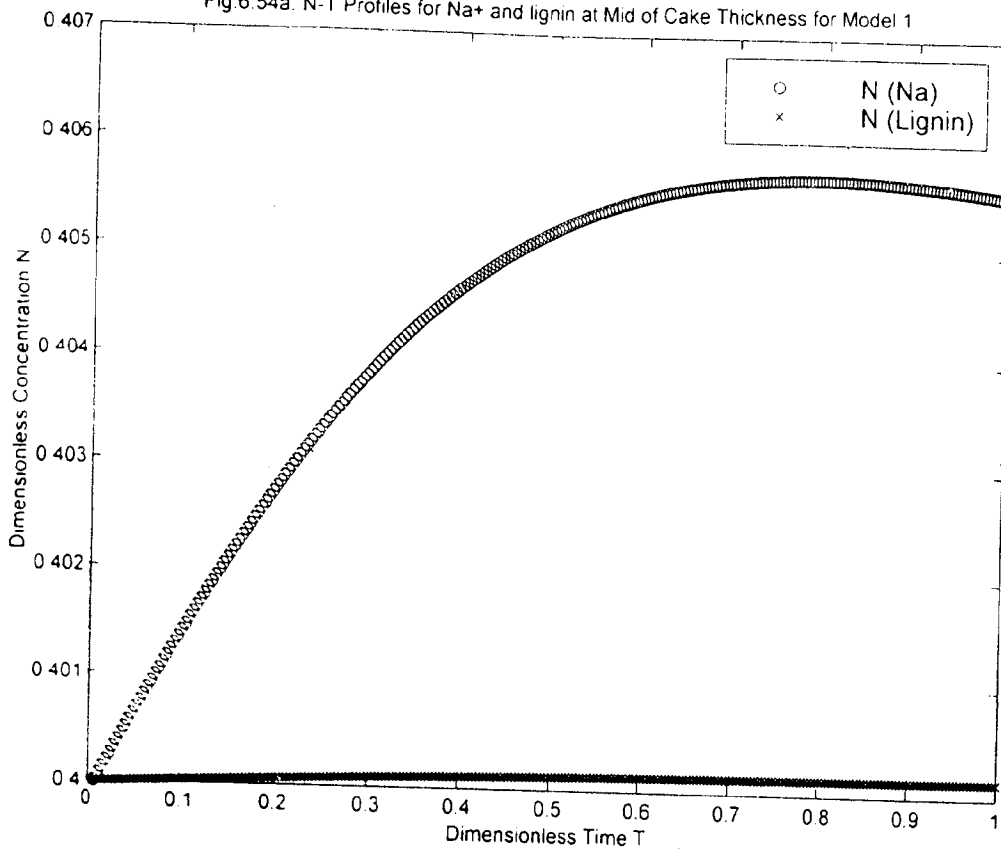


Fig. 6.54b N-T Profiles for Na⁺ and lignin at Mid of Cake Thickness for Model 2

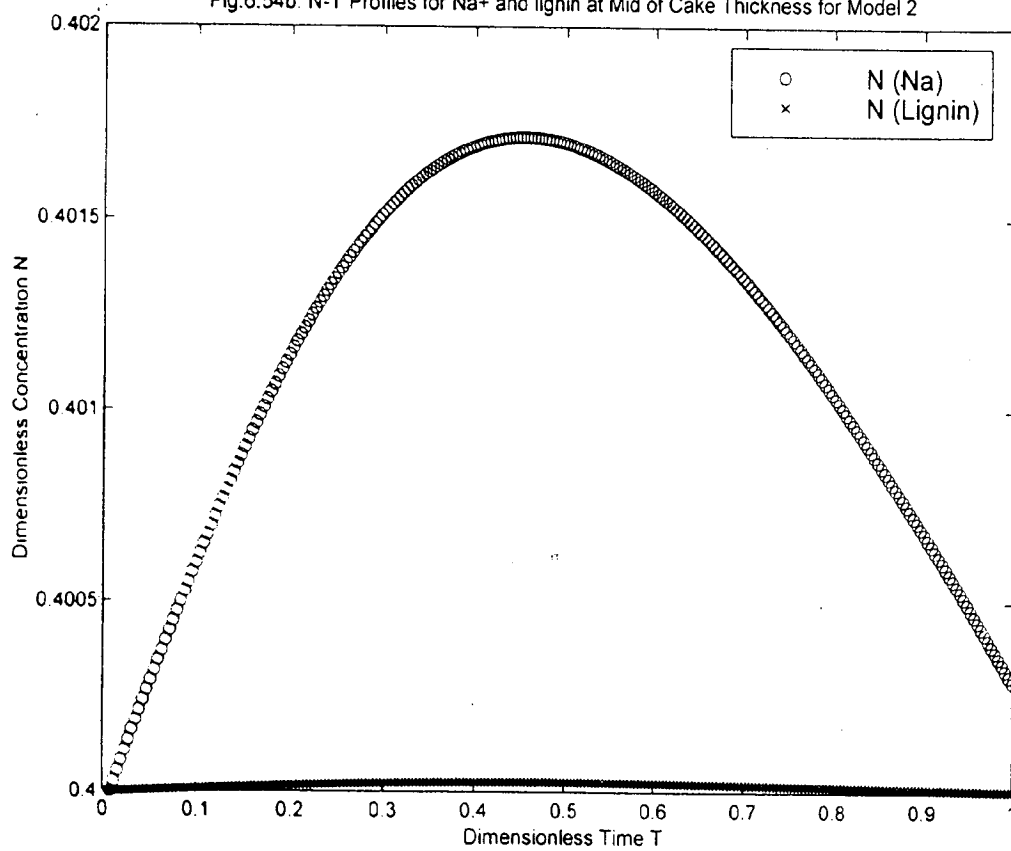


Fig. 6.54c. N-T Profiles for Na⁺ and lignin at Mid of Cake Thickness for Model 3

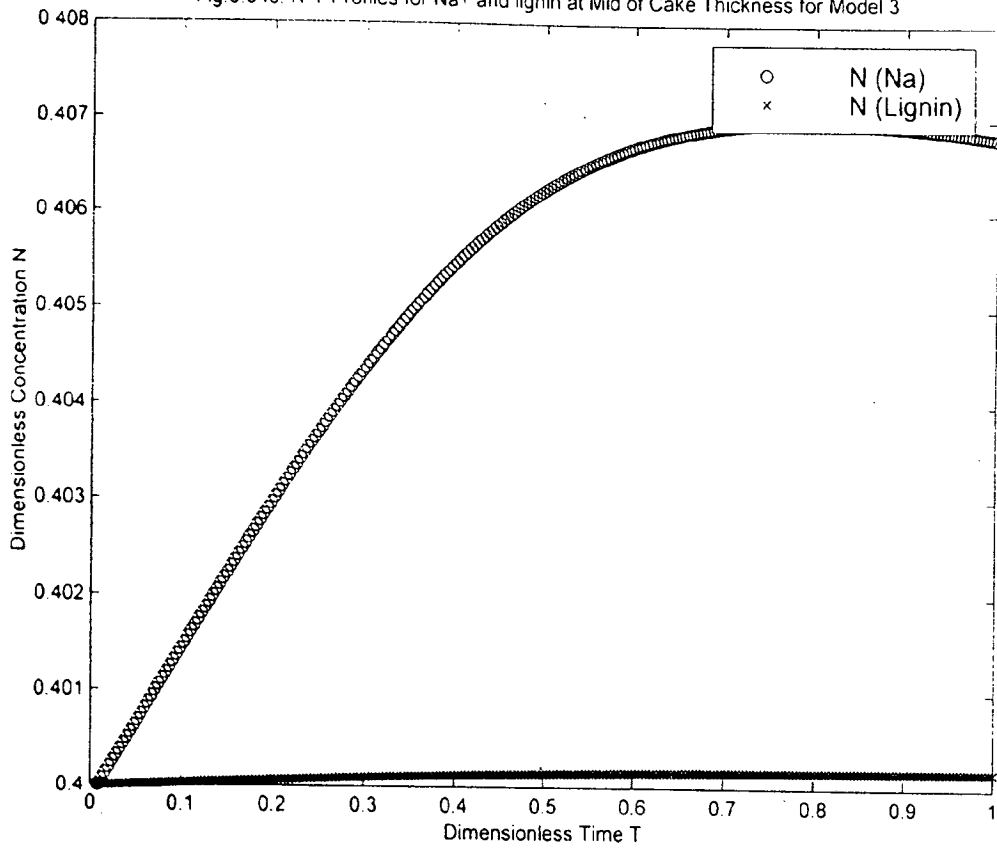


Fig. 6.54d. N-T Profiles for Na⁺ and lignin at Mid Points of Cake Thickness for Model 4

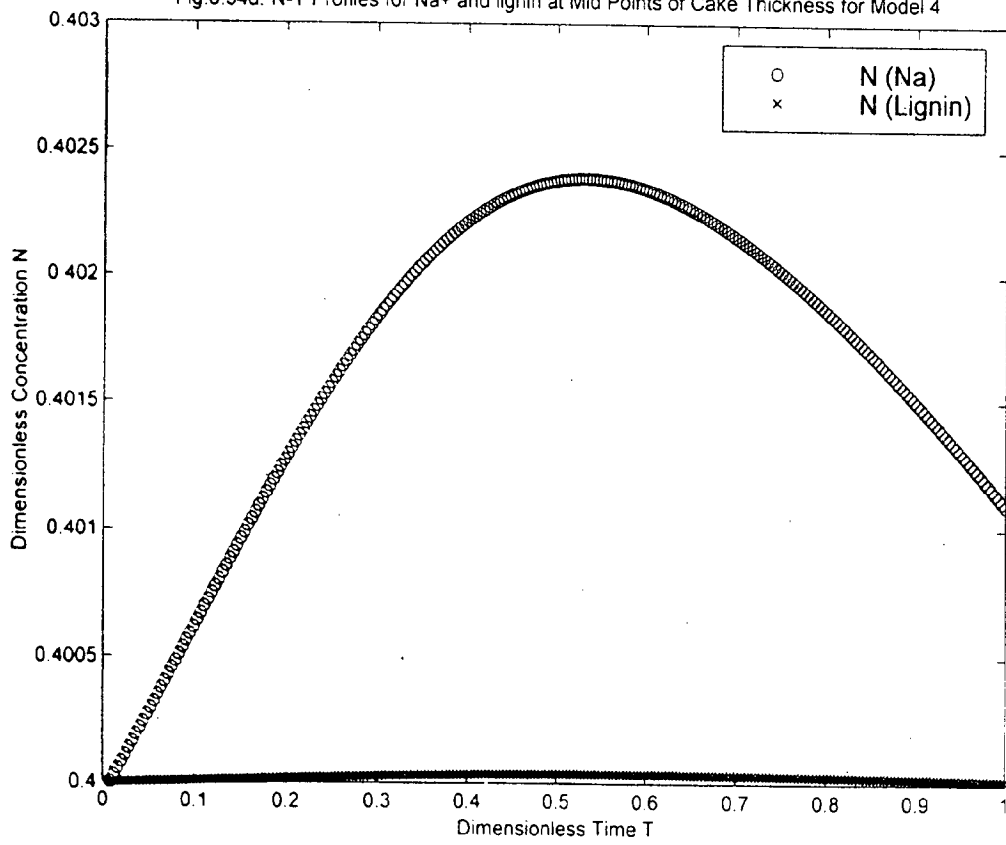


Fig.6.55a. c vs. t Profiles for Na⁺ at Bed Inlet and Bed Exit for Model # 1

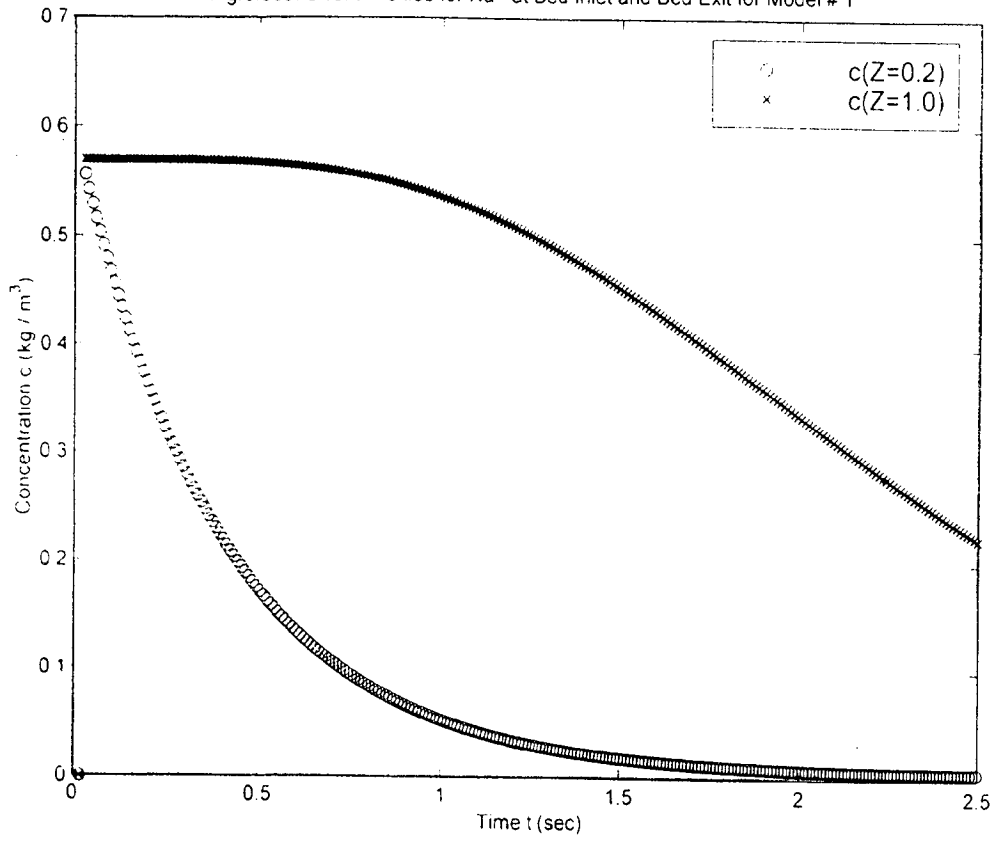


Fig.6.55b. c-t Profiles for Na⁺ at Bed Inlet and Bed Exit for Model 2

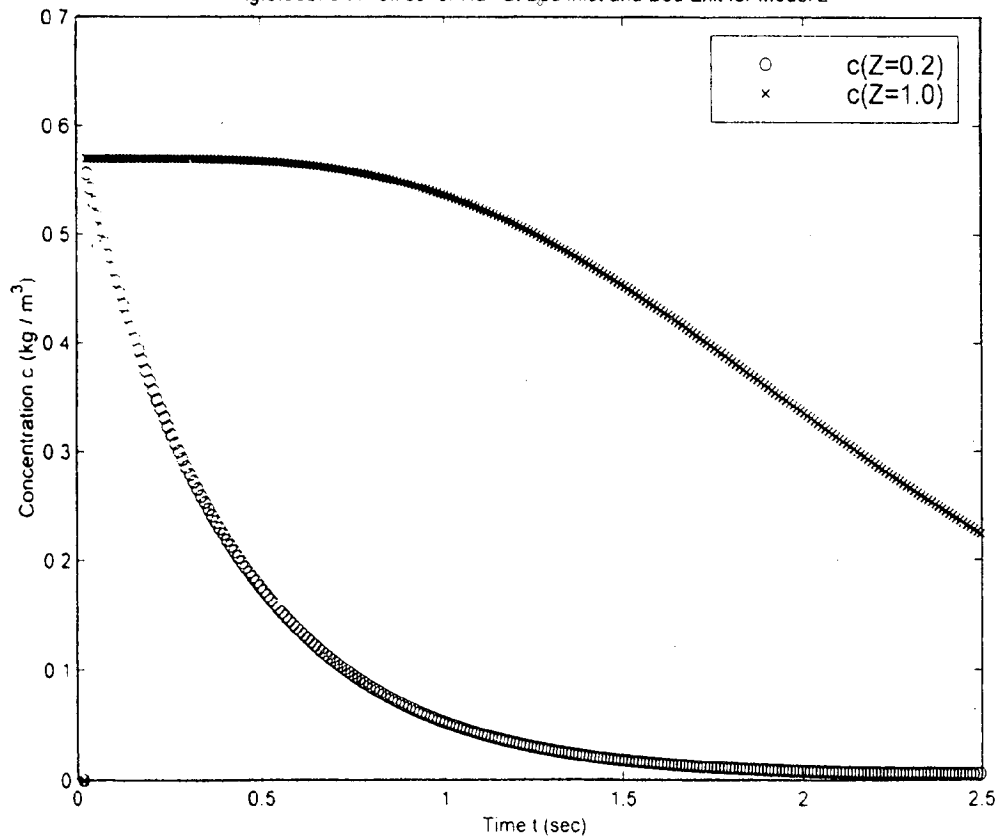


Fig 6.55c: c-t Profiles for Na⁺ at Bed Inlet and Bed Exit for Model 3

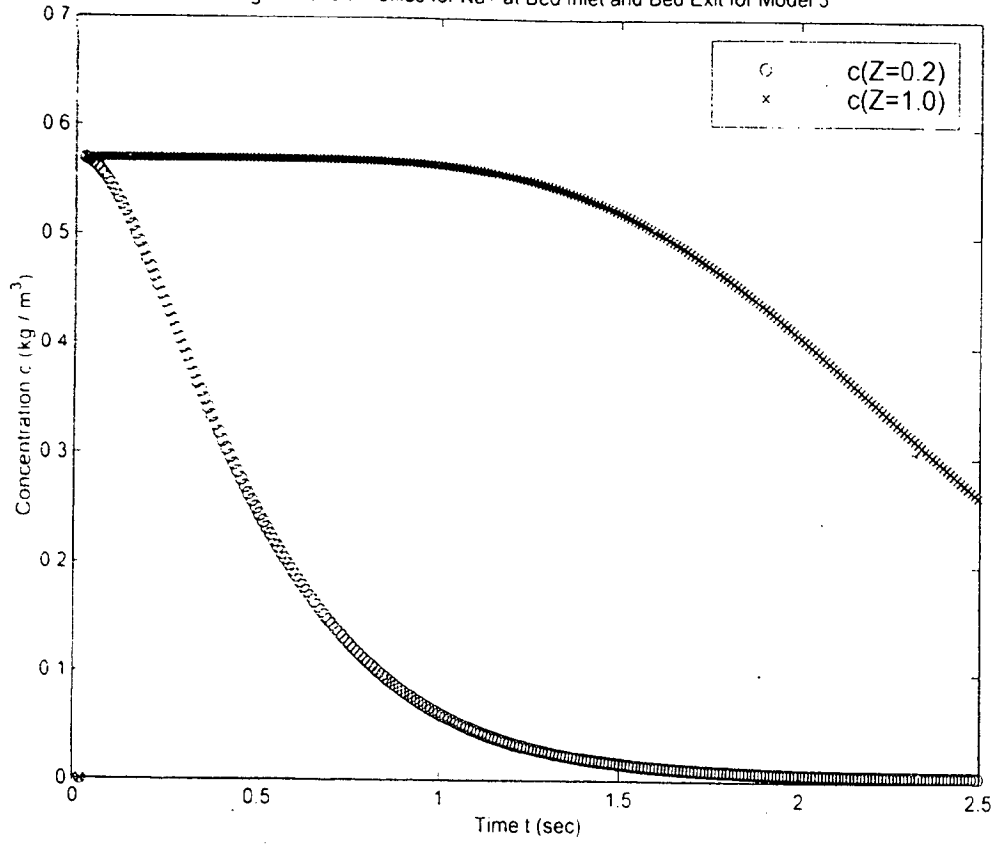


Fig.6.55d. c-t Profiles for Na⁺ at Bed Inlet and Bed Exit for Model 4

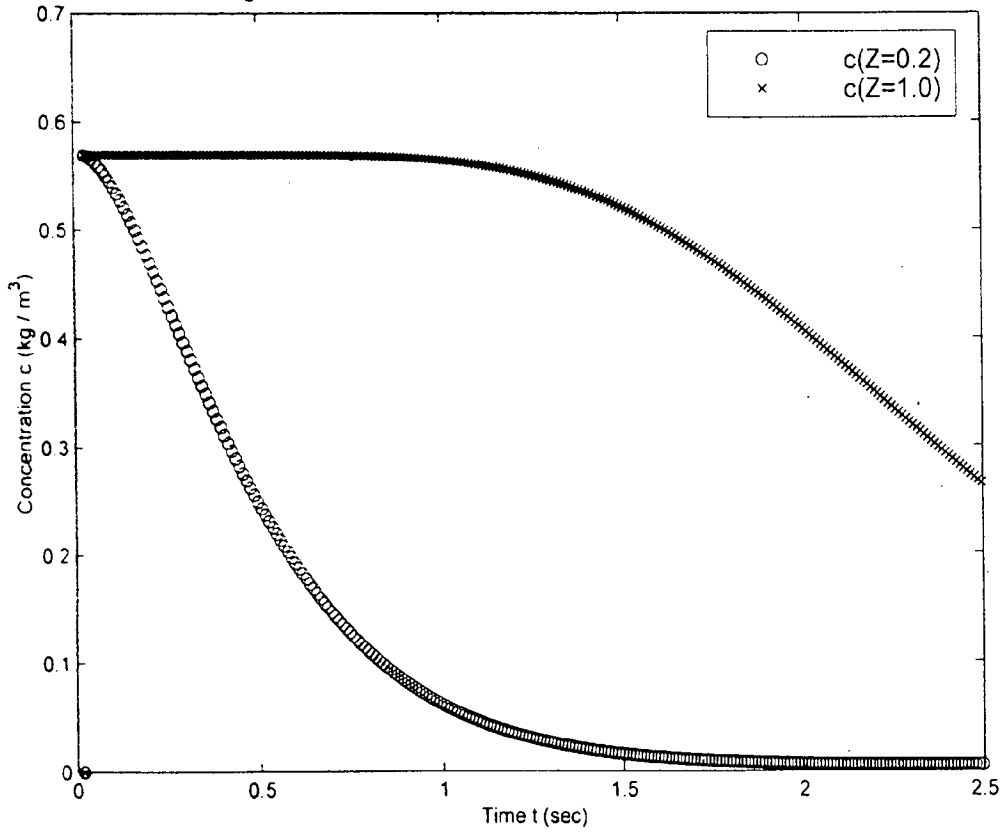


Fig 6 55a1 c vs t Profiles for Na+ at Various Bed Depths for Model # 1

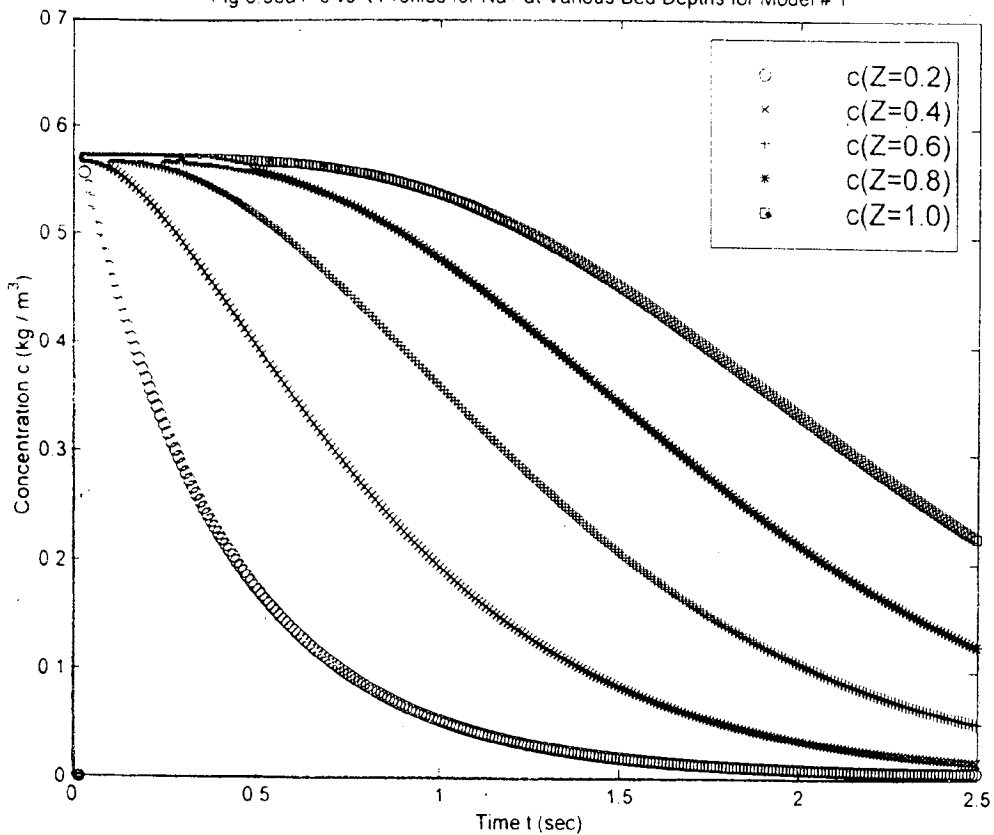


Fig 6 55b1 c-t Profiles for Na+ at Various Bed Depths for Model 2

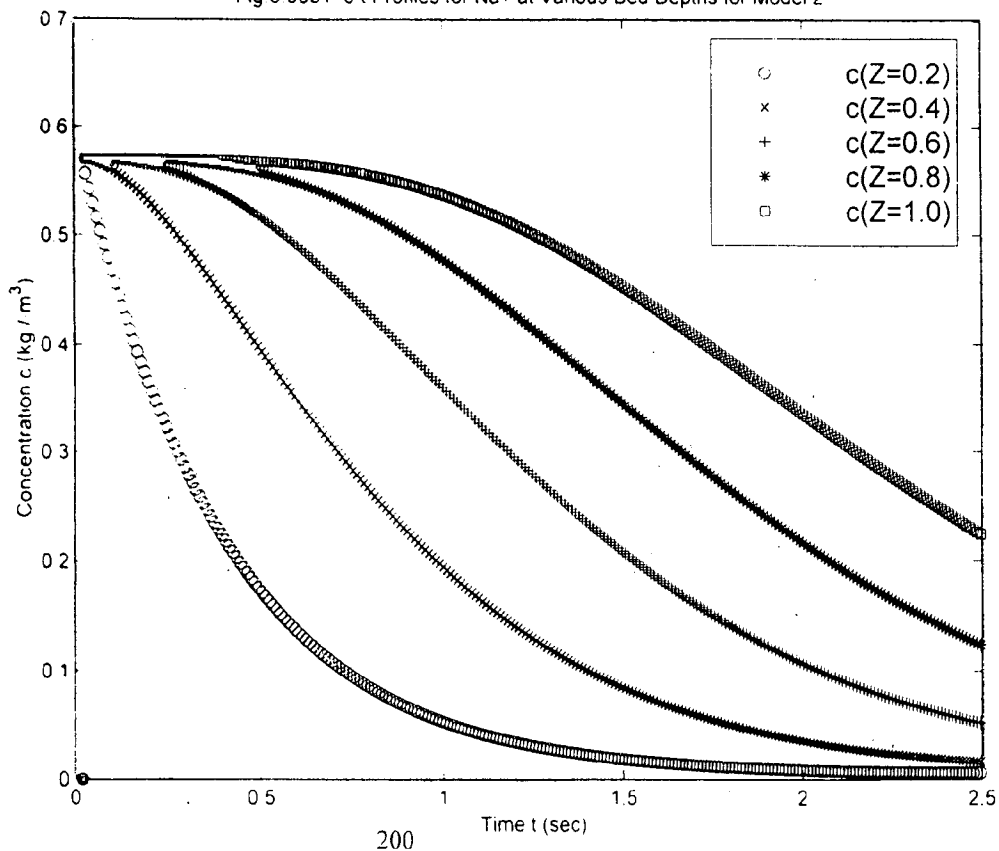


Fig.6.55c1 c-t Profiles for Na⁺ at Various Bed Depths for Model 3

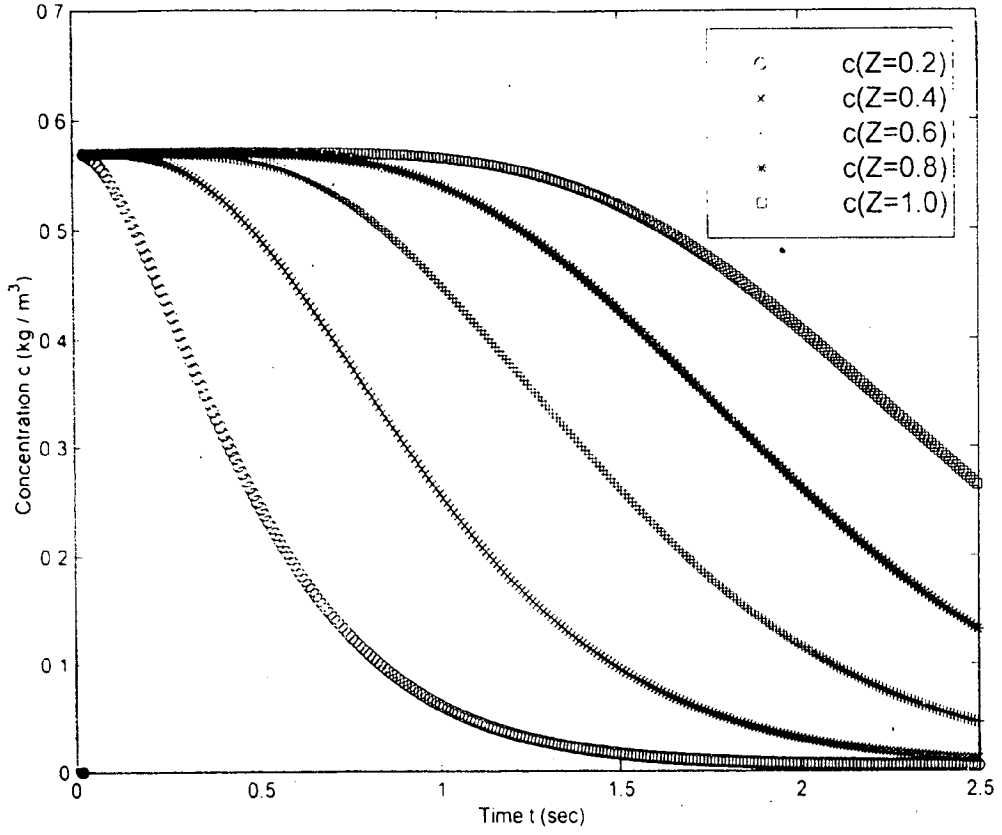
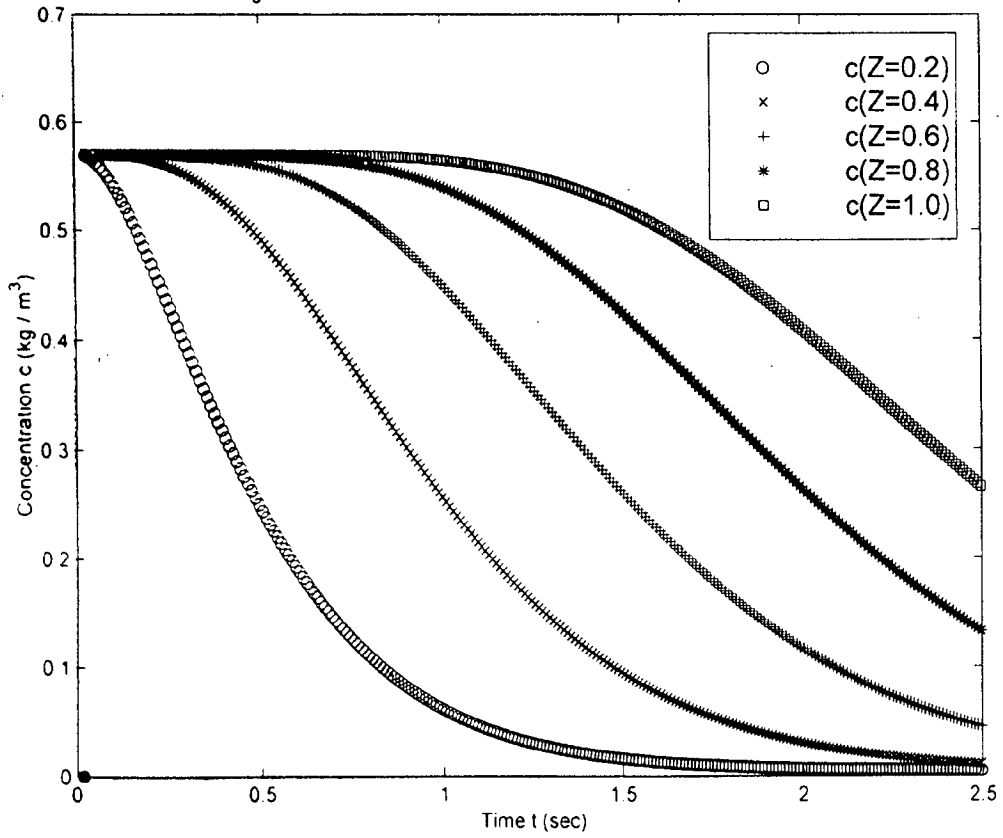


Fig.6.55d1 c-t Profiles for Na⁺ at Various Bed Depths for Model 4



appreciable magnitude of displacement stage can be found out in the lower-most layer (near bed exit). A sample set of values is given in Appendix-VI.

6.1.45 Effect of t on c for lignin for all the four models

A comparison has also been made for lignin for bed inlet and bed exit conditions by plotting absolute value of concentration c (kg / m^3) vs. time t (sec) graph in Figs. 6.56a-6.56d. Like Sodium the exit concentration of lignin also displays a breakthrough curve whereas the bed inlet represents an asymptotic curve where there is practically no displacement stage noticed.

Figs. 6.56a1-6.56d1 are plotted for c as a function of time t at five equi-spaced bed depths. The behavior is exactly the same as that of Sodium. These curves also explain the same behavior as displayed by Na^+ species.

6.1.46 Efficiency parameters

The data of concentration profile as a function of dimensionless time T is now required to be translated in terms of the parameters normally used by process engineers in pulp & paper industry. To achieve the above interrelation for the benefit of the practicing engineers and also to compare various washing systems one requires the variation of c as a function of t or its dimensionless form i.e. C as a function of T for all the proposed models.

The most important and widely used parameters in industry are: Wash liquor ratio (WR), and Washing efficiency (WE) or sometimes, wash yield (Y). These terms are exclusively detailed in Chapter 7.

To calculate efficiency one has to consider firstly the breakthrough curve of c as function of time t . A breakthrough curve is the response to a perfect step change in concentration. The slope of the breakthrough curve indicates that the flow through the pulp pad during displacement washing is non-ideal i.e. it is between the ideal limits of plug flow and perfectly mixed flow.

Fig 6.56a. c-t Profiles for lignin at Bed Inlet and Bed Exit for Model 1

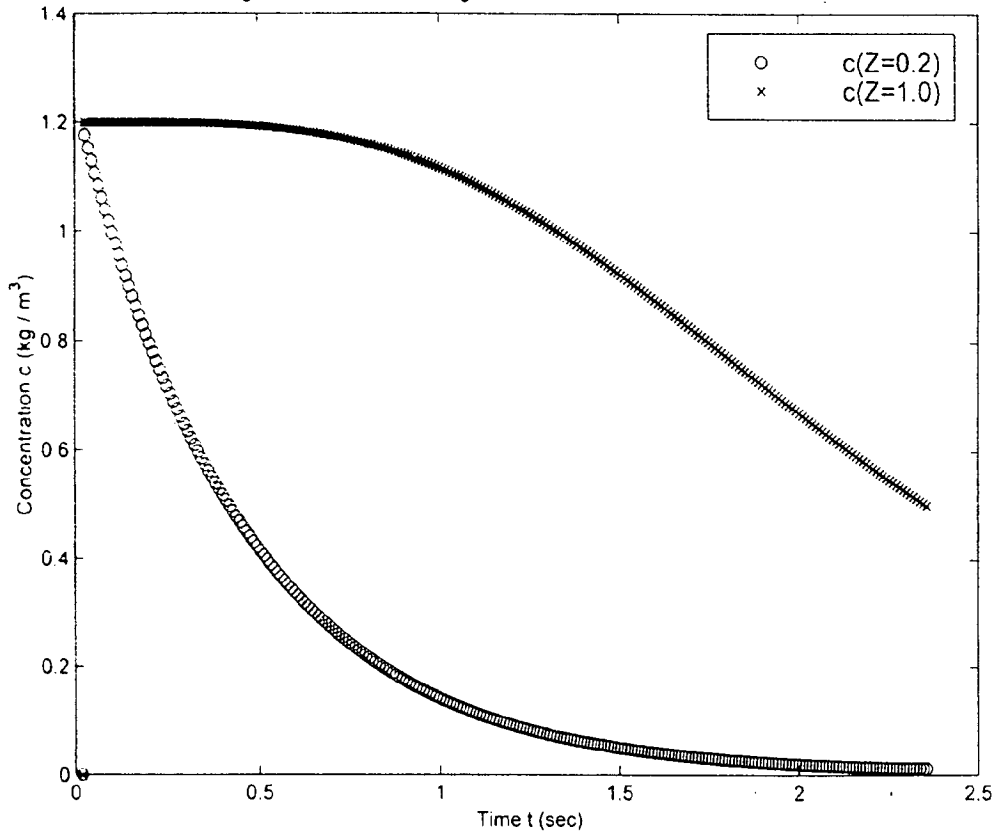


Fig 6.56b. c-t Profiles for lig at Bed Inlet and Bed Exit for Model 2

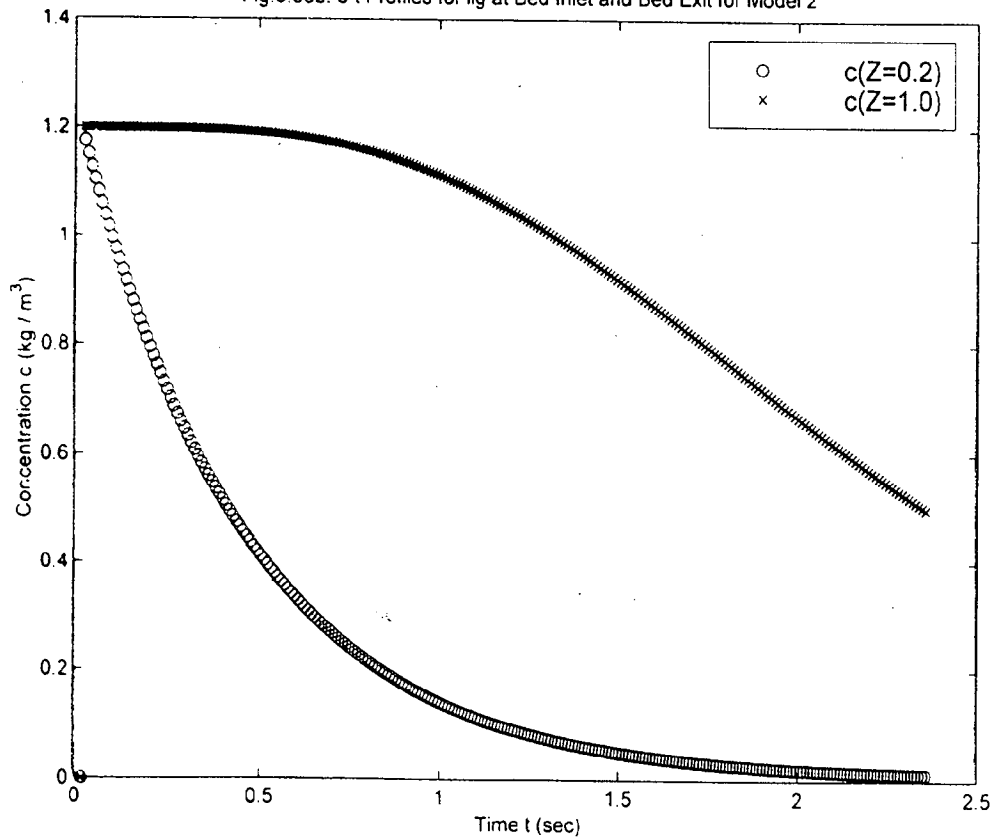


Fig 6.56c c-t Profiles for lig at Bed Inlet and Bed Exit for Model 3

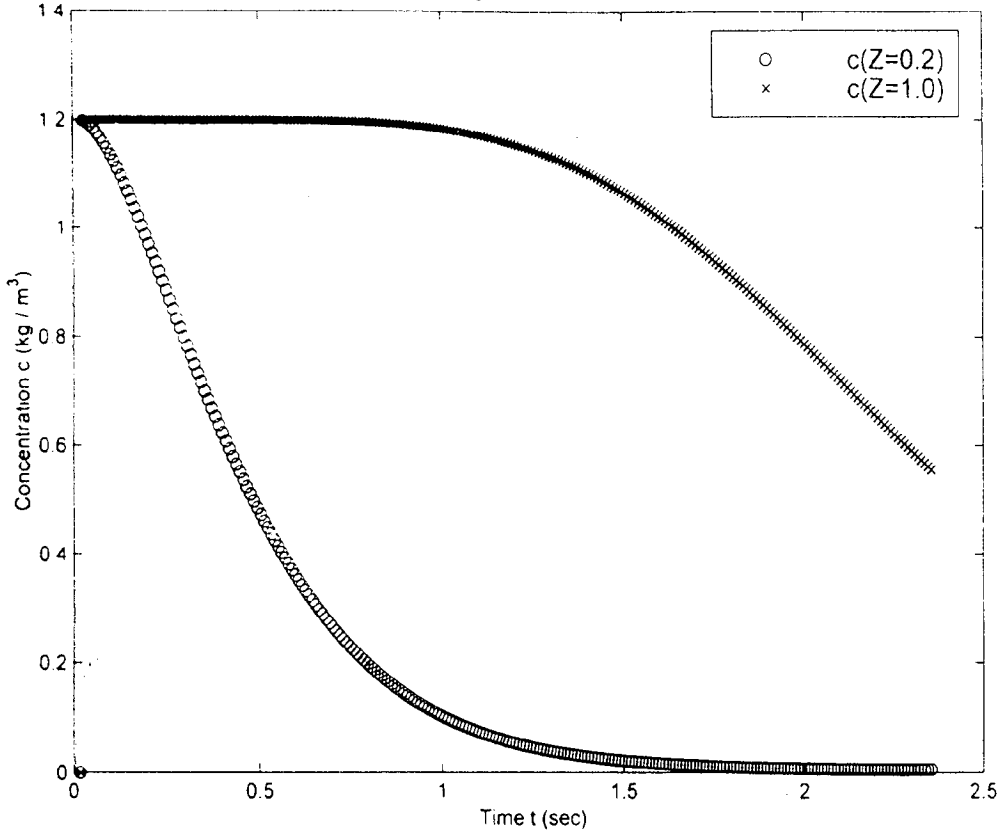


Fig 6.56d c-t Profiles for lig at Bed Inlet and Bed Exit for Model 4

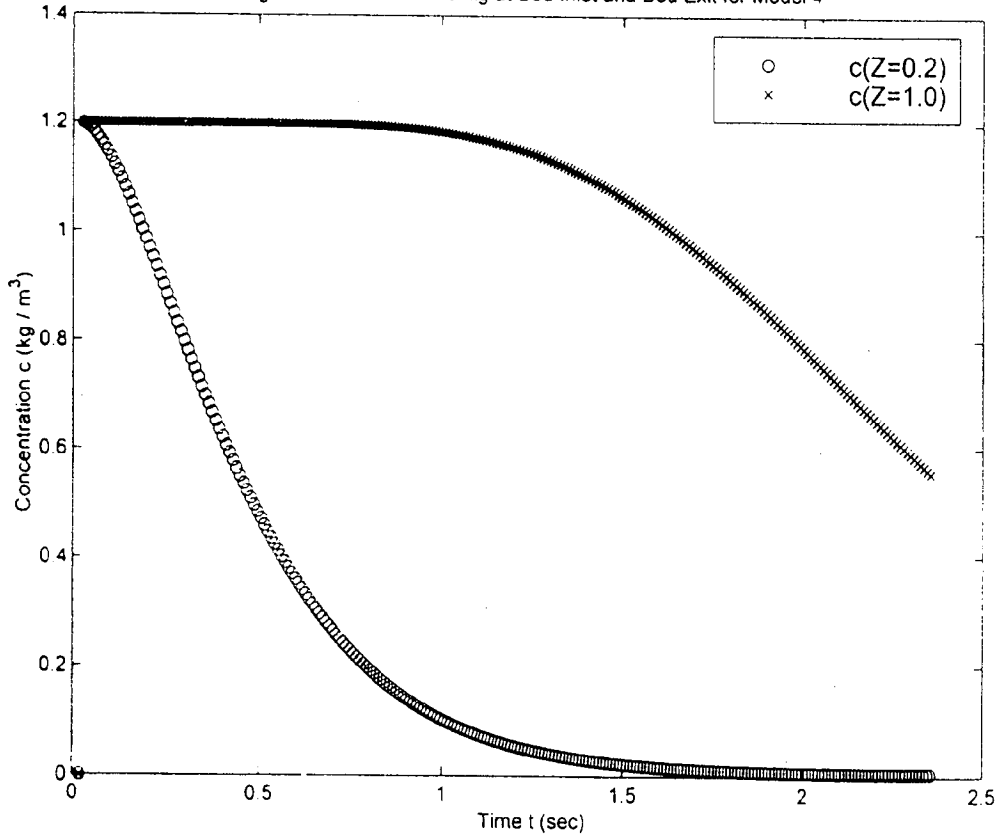


Fig. 6.56a1. c-t Profiles for lignin at Various Bed Depths for Model 1

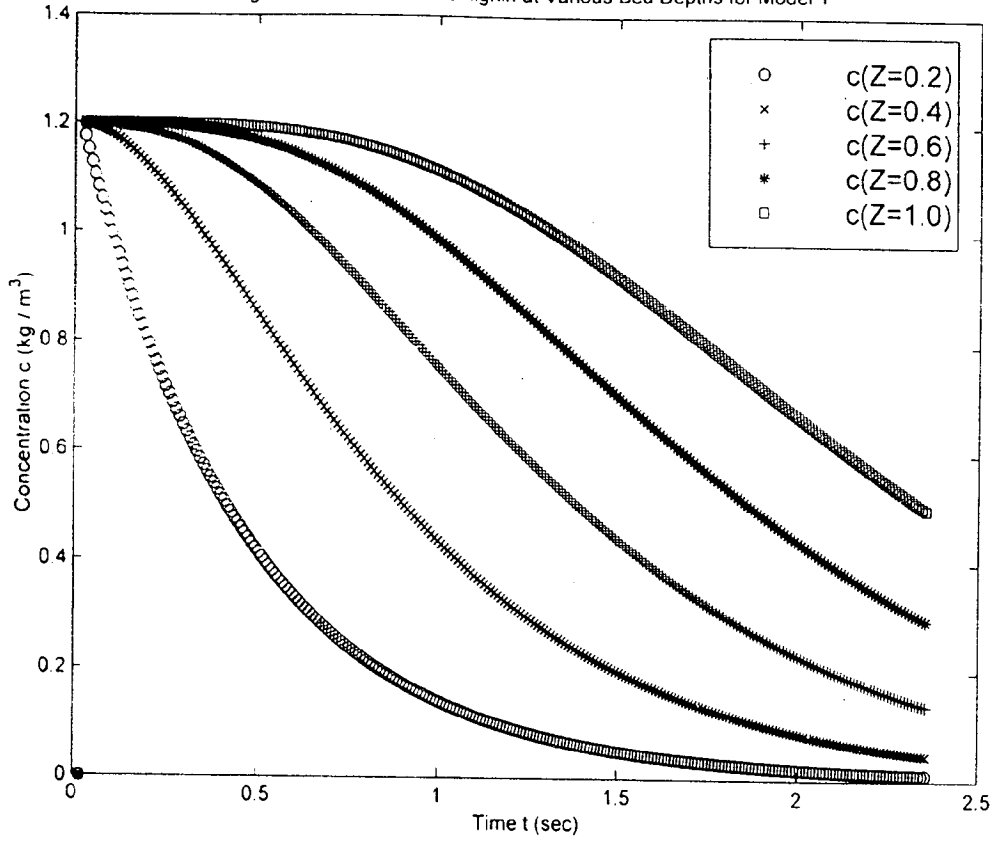


Fig. 6.56b1. c-t Profiles for lig at Various Bed Depths for Model 2

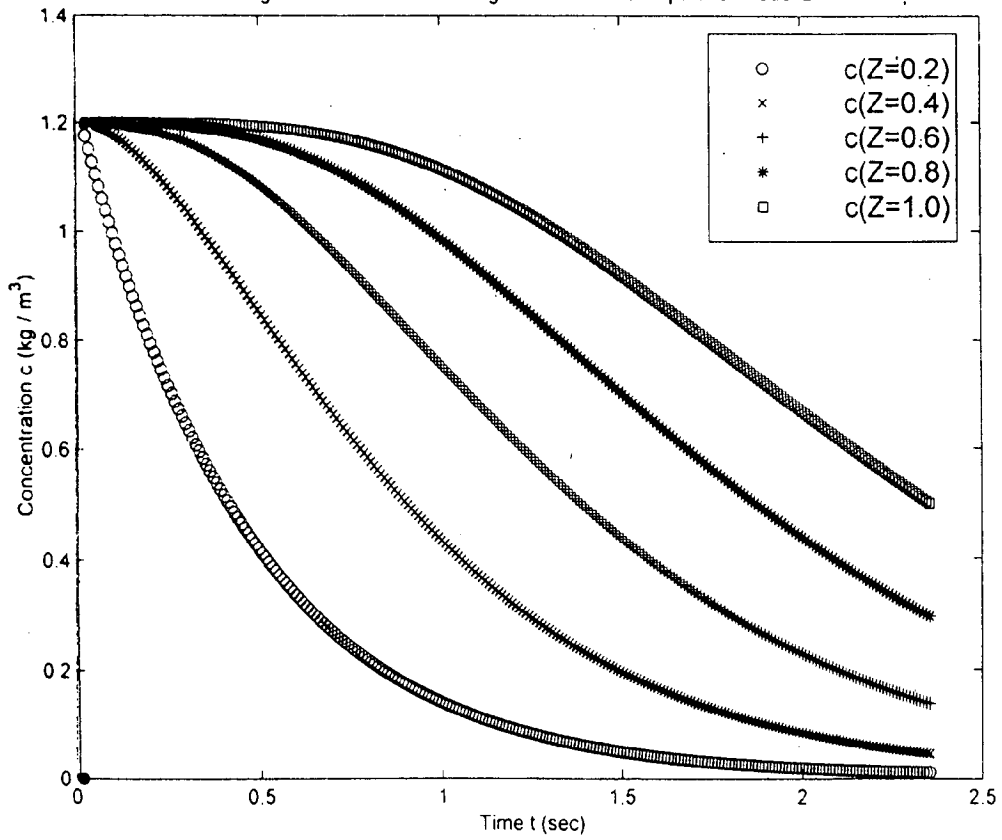


Fig 6.56c1. c-t Profiles for lig at Various Bed Depths for Model 3

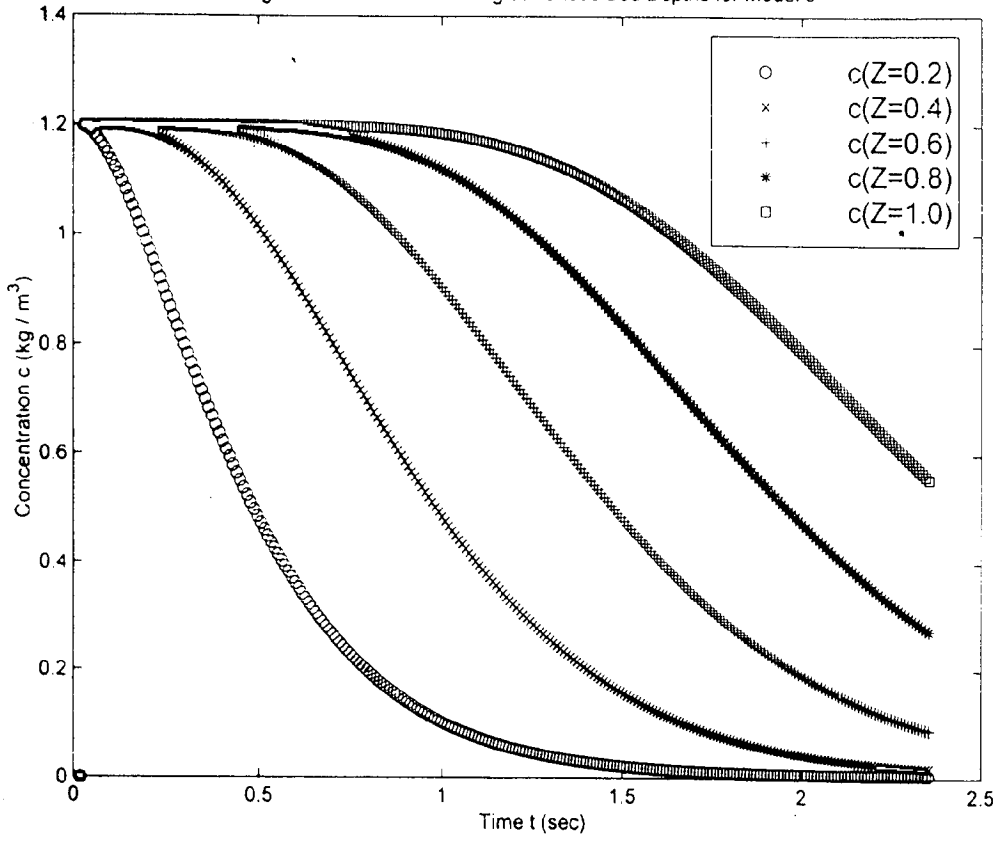
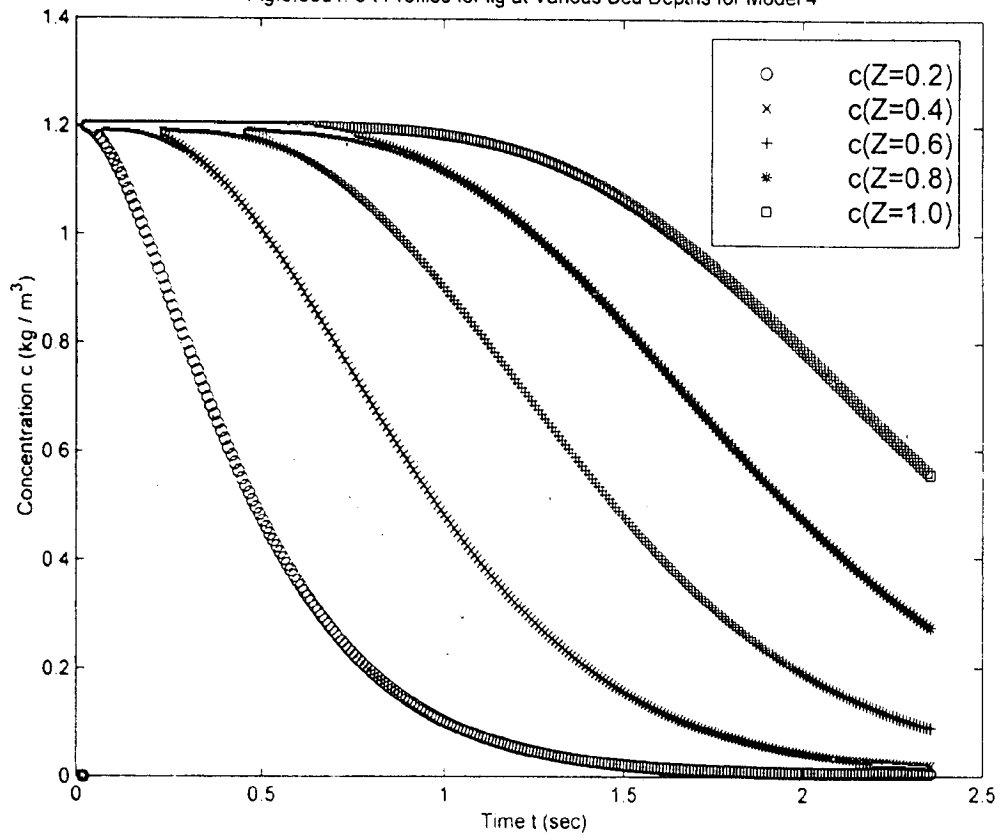


Fig 6.56d1. c-t Profiles for lig at Various Bed Depths for Model 4



This area must be divided by the area under the concentration- time profile for washing with infinite time. Mathematically, it can be represented as

$$\text{Washing efficiency (WE}_1\text{)} = \int_0^t c \, dt / \int_0^{\infty} c \, dt.$$

However, traditionally the expression for the breakthrough curve is subjected to normalization. After normalizing, the area under the curve needs to be evaluated. The estimation of efficiency thus followed. The normalized breakthrough curve area is directly proportional to the amount of solute removal.

The traditional displacement efficiency, WE is defined as the amount of solute washed out at some wash liquor ratio WR, divided by the total amount of solute removed during the washing period. This is also defined by Potucek [81] as displacement washing yield WY though the wash yield is defined by Crotofino et. al.[10], Smith and Duffy [91] ,Baldus and Warnqvist [4] in a different way. The displacement washing yield (WE₁, or the displacement washing efficiency evaluated at T = 1 or evaluated at WR = 1) is often used as a standard basis of comparison.

$$\text{WE}_1 = \text{WY}_{T=1} = \int_0^{T=1} C \, dT / \int_0^{T=\infty} C \, dT.$$

Analogously the washing yield (washing efficiency) in terms of wash ratio may be defined as WE₁

$$= \text{WE}_1 \text{ (at WR=1)} = \text{WY}_{\text{WR=1}} = \int_0^{\text{WR}=1} C \, d(\text{WR}) / \int_0^{\text{WR}=\infty} C \, d(\text{WR}),$$

where $C = (c - C_s) / (C_i - C_s)$ and $T = u t / L = U_{\text{superficial}} t / \varepsilon L$.

Though the above dimensionless concentration term in the ordinate has been used in the present investigation as well as by many other investigators including Grah [23] during model solution, Poirier et. al.[79]. Potucek [81] on the other hand have normalized the breakthrough ordinate in a different way. They divided each outlet concentration c (displaced liquor concentration) by the initial liquor concentration C_i (the plateau concentration) to get C, the ordinate. The breakthrough curve abscissa has been normalized by converting the t to the dimensionless time T in usual way. The abscissa however can also be normalized in terms of wash liquor ratio WR, which is defined

as the amount of wash water passed through the bed divided by the amount of liquor originally present in the bed following the suggested procedure given in Section 5.1.2.6 with only one set of experimental data. The value of WR hardly exceeds 2.5 in actual practice. It may be mentioned that in pulp and paper mill the range is between 0.8-1.5. Now, one can write

$$WE_1 = WY_{T=1} = \int_0^{T=1} (c / C_i) dT / \int_0^{T=1} (c / C_i) dT.$$

$$WE_1 = WY_{WR=1} = \int_0^{WR=1} (c / C_i) dWR / \int_0^{WR=1} (c / C_i) dWR.$$

The above expressions can be employed for two breakthrough curves, one for lignin and the other for Na⁺ species. Poirier et. al.[77,100]. have used the former expression for low initial liquor concentration and the later for high initial liquor concentration.

It must be noted that WY = DR if incoming pulp consistency and outgoing pulp consistency are the same. The denominator of the above equations should be equal to 1 for solutes which do not desorb from the fibers but are found only in the liquor permeating the pad. Since Sodium is known to desorb from the pulp fibers, the area under the sodium breakthrough curve is expected to be > 1, especially at low initial pad liquor concentrations where desorbed solute represents a significant proportion of the area under the breakthrough curve.

It is usual practice to translate the breakthrough curve in form of a polynomial approximation or a non-linear regression equation. As already indicated the area under the curve is proportional to the solid removal. Once C as a function of T is known, area under the curve can be found out for both Na⁺ and lignin or any other species. The values can be evaluated graphically / analytically / numerically / statistically. The normalized breakthrough curve area A_T, is expressed as under:

$$A_T = \int_0^T C dT.$$

In the present investigation numerical integration of the C-T profiles for all the models is performed using 1 / 3 Simpson's Rule for both the species i.e. Na⁺ and lignin at WR = 1. The dimensionless time T has been however limited to 1. The exponential tails were not fitted to the

breakthrough curves by extending T to 5 or higher values 10 as have been done by Trinh et. al.[100]. Nauman and Ruffham [c.f.100] recommended exponential type tails as diffusion ensures that the asymptotic form of the distribution will always be exponential. Truncating the breakthrough curve at T = 1 can yield only small percentage of errors in the estimation of total breakthrough curve area. As the integral $\int_0^1 (c / C_i) dT$ yields a value equal to 1 for the components which does not desorb from the fibers but are found only in the liquor permeating the bed. Since pulp fibers contain both Na⁺ and lignin, which are released in to the wash liquor, the total areas of the displacement washing breakthrough curves will exceed 1. Poirier et. al.[78] have shown that the error introduced is of the order of only 2% by truncating to T = 5.

Trinh et. al.[100] have further found the mean values of the integral, A_∞ for low initial liquor concentration (0.548 kg / m³ - 4 kg / m³ for Na⁺ and 1.455 kg / m³ - 8.1 kg / m³ for lignin) of the order of 1.167 for Na⁺ and 1.005 for lignin. Using these average values, the efficiency of washing WE_1 can be estimated approximately. The values are presented in Table 6.4. The two areas can be compared because they are based on normalized concentrations. Since Sodium and lignin are evenly dispersed throughout the fluid in the pulp bed, the removal of any part of this fluid would remove the same (normalized) amount of each solute. For comparison, the data presented by various investigators is given in Table (6.3) given in Appendix IV.

Table (6.4): Comparison of solute removal parameter (A_T) and washing efficiency (WE_1) from the present investigation.

| Models | A_T | A_T | $WE_1(Na^+)$ | $WE_1(lig.)$ | Comments |
|----------------------|--------------------|----------|--------------|--------------|--|
| | (Na ⁺) | (lignin) | % | % | |
| Modell, (Tab.3.1) | 0.8051 | 0.8122 | 68.99 | 81.82 | $A_T(L) > A_T(Na)$ $WE_1(L) > WE_1(Na)$ |

| | | | | | |
|-----------------------|--------|--------|-------|-------|--|
| Model2, (Tab.3.1) | 0.8054 | 0.8122 | 69.01 | 81.82 | $A_T(L) > A_T(Na)$ $WE_1(L) > WE_1(Na)$ |
| Model 3, (Tab.3.1) | 0.8741 | 0.8740 | 74.90 | 86.97 | $A_T(L) \cong A_T(Na)$ $WE_1(L) > WE_1(Na)$ |
| Model 4, (Tab.3.1) | 0.8744 | 0.8740 | 74.93 | 86.97 | $A_T(L) \cong A_T(Na)$ $WE_1(L) > WE_1(Na)$ |

Poirier et al. further reported that Sodium washing efficiency ranges from 66% (for very low concentration 5.48 kg / m³) to 80 % (for relatively high concentration 4.0 kg / m³) and lignin removal efficiency ranges from 77 % to 84 %. The later does not depend on liquor concentration.

From the table following noteworthy conclusions can be drawn.

- At the same time interval the A_T values of lignin are equal to or higher than those of Na^+ for the models 1 and 2 but it is reverse in case of models 3 and 4 (i.e. A_T value is higher for Na^+ than for lignin) though the differences are very marginal. Poirier however found the similar or slightly higher values in case of Na^+ . It is probable that Poirier et. al. did not consider the dispersion effect.
- For Na^+ the values of A_T are almost the same for models 1 and 2 and the same is true for models 3 and 4. WE_1 values also follow the same trend.
- For lignin, similar conclusions can be drawn i.e. models 1 and 2 give same order of magnitude and models 3 and 4 predict similar values.
- Models 1 and 2 predict lower values compared to models 3 and 4.
- The range of A_T values for Na^+ is between 0.80 and 0.874 and that for lignin is between 0.81 and 0.874. The values predicted by Poirier et. al. lie in the approximately same ranges 0.79-0.88 and 0.77-0.89 respectively. The mean values are 0.85 for Na^+ and 0.81 for lignin. Therefore there is an excellent agreement between this investigation and those from Poirier et. al. although the

parameters such as superficial velocity (1.8 mm / s), pad thickness (25 mm) and consistency (10 %) are different. Present investigation is based on Grah's data with pulp pad thickness (20mm), interstitial velocity (8 mm / s) and pulp consistency (9.16 %). The marginal difference is thus expected.

- The washing efficiency for lignin is found to be always higher (10-12 %) compared to those for Na^+ . Poirier also found the values either greater than or at least equal to those of Na^+ ranging from 0.0 to 17. The values of A_T and average WE_l are in excellent agreement with those of Trinh et. al.[100].

6.2 Conclusion

- The computed parameters in terms of C vs. T (dimensionless concentration in liquid phase vs. dimensionless pseudo time) and N vs. T (dimensionless concentration in solid phase vs. dimensionless pseudo time) from various models through MATLAB are now interpreted in terms of various characteristic graphs.

- It is evident that deeper bed gives the higher washing efficiency. The conclusion excellently agrees with the findings of Grah [24], Grah and Gren [27], Gren & Strom[28] and Trinh et. al.[100]. However, the influence of bed depth is found to be rather weak.

- This is also verified from the fact that the dimensionless concentration of lignin also increases as we move towards the bottom layer starting from the top layer where the dimensionless concentration of lignin is zero.

- Thereafter there is increasing trend of N with further increase of Z. It is an expected behavior as adsorbed N will be higher for higher concentration. This is verified by Trinh & Crotofino [98] in their experiment. The concentration C in fact, as earlier explained increases with bed depth.

- Lowering the bed depth (from top to bottom), the shape of the breakthrough curves C vs. T changes to a non-linear curve which is asymptotic in nature. These curves show insignificant

displacement wash whereas the diffusional and dispersion washing become predominant. This is in agreement with those of Grah [24], Poirier et. al.[78] Potucek [81] etc. This is attributed to the dispersion becoming more predominant after few layers from the top. The profiles of the curves surprisingly display the same characteristics as shown by Kukreja [40] and Kuo & Barrett [43] who used calcium carbonate cake containing ammonium chloride solute with water as washing medium.

- The N vs. T profiles dealing with pulp black liquor washing system, seem to have not been reported so far in any publications. This is opposite to those presented by Kukreja [40] and Kuo & Barrett [43] as the authors presented N (the concentration in stagnant liquor as a function of T instead of the concentration in solid phase vs. T as used in the present investigation. However they closely agree with recent investigations of Liao & Shiau [51], where they developed a similar axial dispersion model for the operation of a fixed bed adsorber with a linear adsorption isotherm using the experimental data for the removal of phenol from the solution of activated carbon and the Amberlite resin XAD-4. The model is further verified from the results of Lai & Tan [45] who have used a pore diffusion model assuming quartic profile and parabolic profile of exit concentration as a function of dimensionless time T. The nature of the curve is found tallying very well with the present investigations. The model is also verified with the recent results of Sridhar [92] who has developed a model based on the isothermal sorption of a single solute in dispersed plug flow through a packed column of mono-dispersed porous particle and applied one point Orthogonal Collocation method to solve the model. The results of the present model are also found in close agreement of the results of the Sridhar [92]. The observations are also similar to those for a linear isotherm as pointed out by Do & Rice [45]. Therefore the behavior displayed by the Na^+ during pulp washing in a paper mill in this present study must likely to occur. These findings claim a new dimension in the area of pulp and paper practices.

- There is no noticeable change of the $C - T$ profiles with ϵ ranging from 0.4 to 0.95. However there is small change observed if one attempts to use very low consistency pulp. This deviation can be ignored in engineering practice. This fact is in agreement with many earlier investigators [24,28]. This might be due to the fact that for medium to high porosity values the effect is shrouded by the concomitant effect of longitudinal dispersion coefficient, tortuosity and local flow velocity. The longer range considered in this present investigation is to cover not only the entire range of suspension habituated by the stock in paper making process in practice but also to cover the porosity value of the flowing zone (0.7 to 0.85), the same for stagnant zone (0.1 to 0.2) and total mean porosity.
- The rate of transfer is also very different for that of sodium because of mobility of lignin species is much smaller in magnitude than that of sodium species. Therefore it is expected that the performance of any given washing system with respect to lignin fragment removal must be quite different from its performance with respect to sodium removal. From the study of the various models for Na^+ one can find as under:
 - Boundary conditions do not influence the shape of the profiles and the value of the parameters.
 - Adsorption-desorption dynamics has little role to play.
 - The difference is mainly due to dispersion effects.
 - Model 1 and model 2 has no displacement part due to predominant effect of dispersion.
 - The difference of the value of C at a fixed T is not very significant
 - It is apparent therefore that dispersion has minor role compared to adsorption. It is also interesting to note that the porosity has no influence at a lower time values but deviates larger and larger for higher time values. For porosity values higher than 0.4, as earlier found, there is no difference noticed.

- For lignin it is clear from the graphs that neither dispersion nor adsorption influenced to a great extent. In fact some earlier investigators assumed that adsorption of lignin is negligible.
- The D_L is varied from 0.59×10^{-6} to 5.9×10^{-6} . Like u values, it displays same characteristics as those of Grah [24]. There is also an appearance of an inflexion point between $T = 0.3$ and $T = 0.4$. Thereafter the profile becomes reversed. This is in excellent agreement with those of Grah [24]. The deviation is quite significant from $T = 0.1$ to 0.2 and from 0.6 to 0.8 .
- The dispersion coefficient D_L increases when the rate of flow of liquor in bed is increased. This is in agreement with the other investigators such as Pellett [71]. This is corroborated with the fact that the mean value of porosity in the zone of flowing liquor is increasing too when the liquor flow rate increases. That means that a larger part of the bed volume is used for liquor in motion when the flow rate is increased. A breakthrough curve becomes less steep when the D_L value is increased as a consequence of elongated mixing zone in the bed.
- For Peclet number below 20 (say 13 to 18) there is erratic display of profiles. This is in confirmity with the comments of Pourier et. al.[79]. It is surprising that in spite of so much observed findings Potucek [81] and some other investigators considered the value of Peclet number lower than 20. It is observed that Peclet number has significant influence on $C - T$ profiles. Higher the Peclet number, better is the shape of the breakthrough curves.
- It is interesting to note that for the $N-T$ profiles for Na^+ there is a steep curve observed, strongly non linear in character. It is evident from the graphs that N increases rapidly, almost linearly, with smaller T , goes to a maximum at $T = 0.7$ approximately and then becomes almost constant at a value $T = 0.8$. However the same of lignin exhibits a linear trend with slightly increasing magnitude with time T at a much slower rate. This is attributed to the affinity of Na^+ ions compared to lignin with the pulp fibers. This fact is verified from the experimental data of Trinh et al.[100]. The above fact is also in close agreement with the findings of Grah[25] and

Hartler & Rydin [33]. It is concluded that adsorption of lignin on the pulp is considerable lower than the adsorption of Na^+ and as a result Grah [25] has neglected adsorption of lignin on pulp fibers during his investigation.

- At the same time interval the A_T values of lignin are equal to or higher than those of Na^+ for the models 1 and 2 but it is reverse in case of models 3 and 4 (i.e. for Na^+ it is higher than for lignin) though the differences are very marginal. Poirier however found the similar or slightly higher values in case of Na^+ . It is probable that Poirier et. al. did not consider the dispersion effects.
- For Na^+ the values of A_T are almost the same for models 1 and 2 and the same is true for models 3 and 4 which coincide each other. WE_1 values also follow the same trend.
- For Lignin, similar conclusions can be drawn i.e. models 1 and 2 give same order of magnitude and models 3 and 4 predict similar values.
- Models 1 and 2 predict lower values compared to models 3 and 4.
- The range of A_T values for Na^+ is between 0.80 and 0.874 and that for lignin is between 0.81 and 0.874. The values predicted by Poirier et. al. lie in the approximately same ranges 0.79 - 0.88 and 0.77 - 0.89 respectively. The mean values are 0.85 for Na^+ and 0.81 for lignin. Therefore there is an excellent agreement between this present investigation and those from Poirier et. al. although the parameters such as superficial velocity (1.8 mm / s), pad thickness (25 mm) and consistency (10 %) are different. Present investigation is based on Grah's data with pulp pad thickness (20mm), interstitial velocity (8 mm / s) and pulp consistency (9.16 %). The marginal difference is thus expected.
- The washing efficiency for lignin is found to be always higher (10-12 %) compared to those for Na^+ . Poirier also found the values either greater than or at least equal to those of Na^+ . The values of A_T and average WE_1 are in excellent agreement with those of Trinh et. al.[100].

CHAPTER-7

SIMULATION OF MODEL FOR EFFICIENCY FOR SINGLE AND MULTI-STAGE WASHER

7.0 Models to predict washing efficiency in mill equipment

Various types of mathematical models are available in the literature to assess the performance of a brown stock washer operations in a mill. These range from very simple to rather complex equations. Baldus and Warnqvist [4] and Pekkanen and Norden [70] have classified these models as zero parameter models, one-parameter models and detail (total) models. The later expressions are somewhat complex. Models used in research can be as complicated as desired, but models intended for use in engineering practice must not be more complicated than is absolutely necessary. This is a very severe restriction on modeling work for industrial practice. The above stipulations have been advocated by many practicing researchers including Norden [63]. Therefore the multi-parameter models, microscopic in nature, are not commonly practiced by the industry particularly the Indian pulp and paper industry. In this investigation therefore zero and one parameter models relating to some efficiency parameters for performance prediction of brown stock washer are discussed. Some interrelations between various efficiency parameters have been cited. Comparisons of various values of parameters are made to examine the magnitude of values obtained by macroscopic equations and also the model predicted data. The actual mill data measured by Perron and Lebeau [75], Turner et al.[104], Luthi [53], Han and Edwards [32] and others are compared with those from the displacement washing data of Grah [25], Trinh et. al.[100] and Potucek [81].

Before simulation work one has to define the most important washing performance indicators. These are wash liquor usage parameters, solute removal parameters and efficiency parameters. As there are numerous definitions with different nomenclatures used by different workers in this field, some of more relevant parameters need to be explained in brief as under.

There are three kinds of filter washer performance parameters belonging to zero or one - parameter models. The parameters are: wash liquor usage parameters such as dilution factor, wash liquor ratio, dilution ratio, effective wash liquor ratio, weight liquor ratio, filter entrainment etc.; Solute removal parameters such as wash yield, displacement ratio, thickening factor, solid reduction ratio etc. and Efficiency parameters such as % efficiency, Norden's efficiency factor, modified Norden efficiency factor, equivalent displacement ratio, overall efficiency, bed efficiency etc. The most important relevant macroscopic parameters required in this investigation and their inter-relationships are categorized and defined in Tables (7.1) to (7.5).

As already indicated zero parameter, includes displacement ratio, equivalent filtrate volume factor, filter entrainment and wash yield. One-parameter models have been derived to directly include the dependence of washing efficiency on amount of wash liquor. These models involve one empirical parameter that must be determined from mill data. These are efficiency factor, number of mixing cells, Peclet number [79] and reduced time.

The displacement ratio concept was introduced by Perkins et al.[74]. It is not a calculation method but a concept for evaluating the effectiveness of pulp washing. Baldus and Warnqvist [4] mentioned that the zero parameter model with the displacement ratio is one way of describing the overall effect of the displacement operation and has the advantage of allowing the quality of the wash liquor to change and still be valid under reasonable operating conditions. Edwards, Perron and Minton [15a] have reported that out of the dependent variables involved in washing, the displacement ratio (DR) is the best and most fundamental representation of the washing quality. Again this ratio appears when the basic equations describing washing are made dimensionless.

Brenner [6] accounts for the non-perfect displacement using axial dispersion coefficient and the Peclet number. Pellett [71] extended this work to include both the Peclet number and mass transfer from pockets of stagnant liquid trapped in the mat. Both of these models show that the

wash liquor ratio and displacement ratio are the proper descriptive variables. In addition, by looking at the dimensionless forms of these theoretical models the Peclet number appears in both cases.

A primary value of these models is in identifying the basic dimensionless variables. The number of variables is significantly reduced once they are combined in dimensionless form.

Armstrong [3] showed based on the work of Laxen [49] that calculation of the displacement ratio, DR is an easy way to compare the washing efficiency for the different black liquor components. The DR can also be related to filter entrainment or wash yield or equivalent filter volume factor. For constant pulp consistency in the displacement zone Baldus and Warnqvist [4] have shown DR and wash yield, Y are identical for x_s equal to zero.

Therefore, in this present study, the zero parameter model with the DR values and one-parameter models with Peclet number are attempted during simulation.

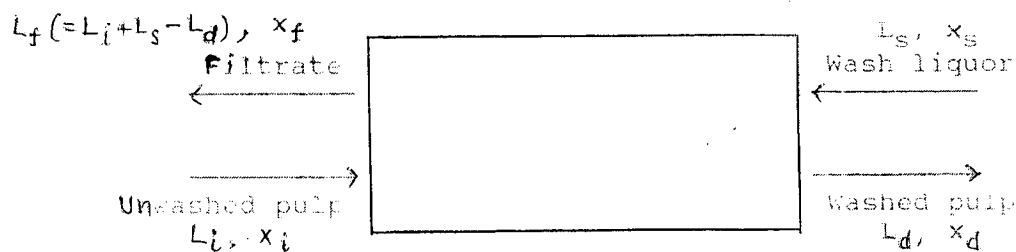


Figure 7.1 A single stage brownstock washer

To understand the basic definition of the terms some nomenclature is required for this purpose, various streams entering and leaving a brown stock washer are given in Fig. 7.1.

7.1 Steady state material balance around single stage brown stock washer

Overall Material Balance

$$L_i + L_s = L_d + L_f.$$

Material Balance for Solids

$$L_i x_i + L_s x_s = L_d x_d + L_f x_f.$$

An algorithm is developed to compute all values relating to performance prediction of BSW required for comparison. The following Tables are used for the development of the Algorithm and for subsequent simulation.

The computed data from the present models for displacement washing have been simulated, using the process and design values for BSW used in pulp and paper mill, given in various tables for calculation. These are described in subsequent paragraphs.

7.2 Selected Process and Design Parameters from the respective models

For the estimation of area of the washing zone of a filter, the time required for washing, the superficial or actual velocity through cake pores, and many more parameters required for simulation, one has to select the most accurate equations from fluid- mechanical theory. Some of them are reviewed in Chapter-5 explaining the merits and demerits. For this present investigation Table (7.1) is used for further calculation. A sample set of data based on BSW plant is also presented therein.

Table (7.1): Selected Process and Design Parameters from the respective models

Values from Perron and Lebeau: RPM = 1.5, $C_{yd} = 10\%$, $\rho = 1000 \text{ kg/m}^3$, $\rho_f = 1560 \text{ kg/m}^3$, $\Delta P = 2 \times 10^4 \text{ Pa}$, $\mu = 0.62 \times 10^{-3} \text{ kg/ms}$; $\theta = 2.14 \text{ rad}$, $R = 1.75 \text{ m}$.

| Variables | Equations | Approximate values |
|--|---------------------------------------|--------------------|
| C_{sl} , Concentration of pulp slurry, kg/m^3 | $C_{sl} = \rho C_{yi} / (1 - C_{yi})$ | 10.1 |

| | | |
|---|--|--|
| V_w , Volumetric flow rate. m^3/s | $V_w = [(100 - C_{yd}) / C_{yd} + DF] \text{ FPR} / \rho_w$ | 0.267 |
| L, Length of cake. m | $L = (1 / N) * \text{FPR} / (1 - \epsilon_t) \rho_f$ A | 0.028 |
| M, Mass of wet cake / mass of dry cake | $M = [\epsilon_t \rho + (1 - \epsilon_t) \rho_f] / [(1 - \epsilon_t) \rho_f]$ | 11.043 |
| m_p , Mass of particles deposited in filter per unit volume of filtrate, kg / m^3 | $m_p = C_{sl} \rho / [\rho - (m - 1) C_{sl}]$ | 11.241 |
| ϵ_t , Total porosity | $\epsilon_t = (1 - C_y) \rho_f / [\rho C_y + \rho_f(1 - C_y)]$ | 0.92 - 0.94 |
| f, Fraction of submergence | $(\theta / 2\pi) = (1 / \pi) \cos^{-1} [(R_0 + R - N_2) / R]$, where $\theta = 2 \cos^{-1} [(R_0 + R - N_2) / R]$ | 0.34 |
| K, Permeability constant Davis Eq. / Kozeny Equation, m^2 | $K = [K_1 S_0^2 (1 - \epsilon_t)^{3/2} \{1 + K_2 (1 - \epsilon_t)^3\}]^{-1}$. $K = \epsilon_t^3 / [k_1 S_0^2 (1 - \epsilon_t)^2]$. | $0.789 * 10^{-11}$. $1.7082 * 10^{-11}$ |
| α , Specific cake resistance, m/kg | $\alpha = k_1 (1 - \epsilon) (S_p / v_p)^2 / \epsilon^3 \rho_s$ $= k_1 (1 - \epsilon) (S_0)^2 / \epsilon^3 \rho_s = 1 / [K \rho_s (1 - \epsilon)]$ $= 2 A^2 g_c (-\Delta P) (1 - mw) / \rho C \mu w$ | $0.01354 * 10^{11}$ (Davis) $6.254 * 10^8$ (Kozeny) |
| s, compressibility coefficient | $(\text{Log } \alpha - \text{Log } \alpha_0) / \text{Log } (-\Delta P)$ | 0.78 |

| | | |
|--|--|---------------------|
| FPR, Fiber Production rate, kg/s Loading Factor, W, kg / m ² s | $FPR = (1 - \epsilon_t) N A L \rho_f = A [2 (-\Delta P)^{1-s} \rho C_{vi} f N / \mu \alpha_0 (1 - C_{vi})]^{0.5}$ $W = FPR/A$ | 2.9753 |
| A, Area of Filter | $A = FPR / (1 - \epsilon_t) * N * L * \rho_f$ | - |
| A, Area of Filter, m ² | $A = (V / t_c) [\mu \alpha_0 c t_c / 2 f (-\Delta P)^{1-s} g_c]^{0.5}$ | 44.56 |
| C _y , % Consistency, C _F , kg / m ³ | $C_y \% = C_F / (1000 + C_F)$ | - |
| u, liquor speed in cake pores (interstitial speed), m / s | $u = v_w / A_c \epsilon_t$ (t = total or mean value for displacable liquids, dm) $u = K (-\Delta P) / \mu \epsilon_t L$ | $8.01378 * 10^{-3}$ |
| T _w , Total time of washing, s | $T_w = V_w / u \epsilon_d N A$ | 5.543 |

7.3 Parameters required for evaluating washer performance

In addition to the fluid-mechanical parameters, some washing variables as mentioned in Section 7.0 are also required for simulation. The parameters important in this present work is depicted in the following Table (7.2).

Table (7.2): Various parameters used in the present work

| | | |
|---|--|--|
| Dilution Factor, DF | (Wash liquor entering - Liquor in washed pulp) / O.D. washed pulp | $DF = L_s - L_d$ $DF = 1 + (V_w \rho_s / P_f) - (100 / C_{yd})$ |
| Wash Liquor Ratio, WR | Wash liquor entering / Wash liquor leaving with washed pulp | $WR = L_s / L_d$ $WR = V_w \rho_s C_{yd} / \{P_f (100 - C_{yd})\}$ $WR = W_{tw} / W_o$ |
| Wash Yield, Y | Dissolved solids removed with the filtrate / Dissolved solids entering with unwashed pulp | $Y = L_f x_f / L_i x_i = (L_i + DF) x_f / L_i x_i$ |
| Wash Yield = Y* [Crotogino et. al.] = Theoretical Washing Efficiency[Lafreniere et. al.] | Assuming the solute is split in the same proportion as the liquor | For dilution- Extraction stage: $Y = \{(C_{yd} - C_{yi}) / C_{yd} (100 - C_{yi})\} \times 100$. |
| Displacement Ratio, DR | Actual reduction of dissolved solids / Maximum reduction of dissolved solids | $DR = (x_i - x_d) / (x_i - x_s) = \{(C_i / \rho_i) - (C_d / \rho_d)\} / \{(C_i / \rho_i) - (C_s / \rho_s)\}$ $DR = (C_i - C_d) / (C_i - C_s)$. |
| % Efficiency, WE | Percent of black liquor solids removed | $\% E = [1 - (C_d - C_s) (100 - C_{yd}) \rho_i / (C_i - C_s) (100 - C_{yi}) \rho_s] \times 100$. |

| | | |
|------------------------------------|--|--|
| Entrainment Ratio, FE | Weight of undisplaced vat liquor remaining in washed pulp per unit of dry fibers | $FE = L_d (1 - DR) m$ $FE = ((100 - C_{yd}) / C_{yd}) (1 - DR) m$ $m = [\epsilon_i \rho + (1 - \epsilon_i) \rho_f] / [(1 - \epsilon_i) \rho_f]$ = mass of wet cake / mass of dry cake |
| Equivalent displacement Ratio, EDR | Evaluated at standardized inlet consistency ($C_y = 1\%$) and discharged consistency ($C_{yd} = 12\%$) | $EDR = 1 - (1 - DR) (DCF)$ (ICF) $DCF = (1 / 7.33) L_d$ $ICF = 99 (L_i - DF) / [L_i (99 - DF) - L_d (99 - L_i) (1 - DR)]$ $L_i = (100 - C_{yi}) / C_{yi}$ For dilution / thickening washers $ICF = 99 / (99 + DF + L_d)$ |
| Overall System Efficiency, E | Consider all the washers in series | $E = [(1 - DR_1) (1 - DR_2) (1 - DR_3) \dots (1 - DR_n)]$ |

7.4 Interrelationship among different parameters

As already mentioned there are parameters diverse in nature and also used with diverse nomenclature by different investigators, these are required to express with common symbols in order to perform simulation. The parameters employed by the investigators and practicing engineers are also in many cases different. Therefore, the interrelations between different

parameters are required for performance assessment of BSW operation. These are shown below.

Table (7.3): Interrelations between different parameters

| | |
|-----------------------|--|
| DF and DR | $DF = \{(100 - C_{yd}) / C_{yd}\} (WR - 1).$ $WR=1, DF=0$ |
| DR and %WE | $\% E = \{1 - (1 - DR) (100 - C_{yd}) / (100 - C_{y1})\} \times 100$ |
| DR, Efficiency and WR | $DR = 1 - \exp(-Eff_1.WR).$ |
| R (% recovery) and WR | $\% R = WR \{(C - C_s) / (C_i - C_s)\} \times 100.$ |

7.5 Comparison of data among various investigators

For comparison of data one has to estimate various data i.e. the time required for washing T_w , V_w , WR, DF, WE, Y, Y^* and E limiting to brown stock washer only. The total time of washing T_w can be calculated as under:

$T_w = A * (\text{Time of one revolution}) * \text{Angle subtended for washing zone} / 360 / 2\pi R * \text{width of the drum}.$

Under normal operating conditions time of one revolution for BSW varies between 30-40 seconds. The angle for the washing zone is normally considered 60° .

To perform the above calculations an Algorithm is developed given in Appendix-V. The parameters are calculated based on their individual data obtained from pulp and paper mill. These data can be found elsewhere [75,32,53,54,104,40]. Using the Algorithm a C++ program is developed to generate data for simulation of BSW for a paper mill. The calculated value of efficiency indicators of a real washing system (rotary vacuum filter) is presented in the following Table.

Table (7.4): Calculated value of efficiency indicators of a real washing system

| Variables | Perron & Lebeau 1 | Han & Edwards 2 | Luthi 3 | Luthi 4 | Turner et al. I II 5 | | Kukreja (based on data of 1) | Perkins I II | |
|------------------|----------------------------|-----------------------|------------|------------|----------------------------|-------|------------------------------------|-----------------|------|
| | DF | 2.844 | 0.281 | 2.2 | 3.00 | 2.28 | 2.28 | 2.81 | 2.13 |
| WR | 1.51 | 1.058 | 1.42 | 1.448 | 1.32 | 1.29 | 1.50 | 1.29 | 1.30 |
| DR | 0.553 | 0.674 | 0.75 | 0.800 | 0.81 | 0.815 | 0.5988 | 0.75 | 0.75 |
| WE | 61.66 | 72.28 | 78.46 | 82.33 | 82.88 | 83.14 | 65.56 | 0.78 | 0.77 |
| Y | - | 0.978 | - | 0.998 | 0.998 | 0.99 | - | 0.99 | |
| Y* | 0.934 | 0.873 | - | 0.865 | 0.918 | 0.91 | - | 0.91 | |
| EDR | - | 0.653 | 0.758 | 0.810 | - | | - | - | |
| T _{w,s} | 5.794 | - | - | - | 5.18 | | - | - | |
| E | - | - | - | - | 96.44 | | - | 95.0 | |

7.6 Data obtained from Potucek models

It is imperative to compare the calculated data from mill conditions reported by various workers, those from Potucek [81] models and from the present investigation. For this comparison the models proposed by Potucek [81] are reproduced here. These models can be referred as one-parameter models. The data estimated from the models at low Peclet number are given below: The following Table shows the dependence of wash yield and bed efficiency predicted from Potucek' one parameter or two parameter models

Table (7.5): Dependence of wash yield and bed efficiency predicted from Potucek one parameter or two parameter models

X_0 is initial bed liquor concentration, kg of lignin / kg of oven dried pulp, E = Bed efficiency

| Equation | Pe | X_0 | $WY_{RW=1}$ | E |
|--|-----|-------|-------------|-----------|
| $WY_{RW=1} = 0.65 Pe^{0.016} X_0^{-0.15}$ $E = 0.95 Pe^{0.031} X_0^{-0.41}$ | 2 | 0.20 | 0.8367107 | 0.5325578 |
| Do | 20 | 0.20 | 0.8681111 | 0.4958687 |
| Do | 50 | 0.20 | 0.8809319 | 0.4819818 |
| Do | 100 | 0.20 | 0.8907562 | 0.4717356 |
| Do | 2 | 0.40 | 0.7540859 | 0.707602 |
| Do | 20 | 0.40 | 0.7823855 | 0.6588537 |
| Do | 50 | 0.40 | 0.7939403 | 0.6404023 |
| Do | 100 | 0.40 | 0.8027944 | 0.6267884 |
| $WY_{RW=1} = 0.65 X_0^{-0.18}$ $E = 0.94 X_0^{-0.46}$ | - | 0.20 | 0.8684162 | 1.9708522 |
| Do | - | 0.40 | 0.7665536 | 1.4327825 |

7.7 Data for multistage BSW

Laxen [49] has reported data of DR calculated on birch sulphate pulp washing. Four days mean values at two different mills for four stage drum filter on two different lines are shown in Table (7.6). Laxen [49] has indicated that the differences in DR values reveal that there are differences in washing efficiency between different black liquor components, between different stages and between differently equipped washing lines. These differences don't depend on liquor volumes alone; physico-chemical phenomena are also important. Similar data are also reported by Perkins et. al.[74] and Turner et al.[104] for two stage washer. The values are compared in Table (7.6) as under:

Table (7.6)

| Investigators | DR | F1 | F2 | F3 | F4 |
|---------------|----|--------|--------|------|------|
| Laxen | Na | 0.79 | 0.96 | 0.74 | 0.56 |
| Perkins | DS | 0.7525 | 0.7489 | - | - |
| Turner et al. | DS | 0.807 | 0.815 | - | - |

7.8 Simulation of BSW with the present investigation

The displacement washing data on C-T and c-t for both Na⁺ and lignin obtained from this present investigation are shown in Appendix-VI. The values of c, t and DR are obtained as follows: $c = C_s + C (C_i - C_s)$, kg / m³ and $t = T * L / u$, s.

$$DR = (C_i - c) / (C_i - C_s).$$

The results are shown in the following tables for three cases.

Case A: Efficiency Parameter for Sodium using Grah's data

$C_i = 0.57$ kg / m³; $C_s = 0.005$ kg / m³; C_{yd} = mean consistency = 106 kg / m³ \cong 9.617 %; Wash Ratio = 0.8; $C_{yi} = 1.5$ %; $Pe = 27$ at bed exit point ($Z = L$).

| Parameters | Model I | | Model II | | Model III | | Model IV | |
|------------|---------|-------|----------|-------|-----------|-------|----------|-------|
| | T = 0 | T = 1 | T = 0 | T = 1 | T = 0 | T = 1 | T = 0 | T = 1 |
| DR | 0 | 0.612 | 0 | 0.612 | 0 | 0.54 | 0 | 0.54 |
| WE | | 64.63 | | 64.60 | | 58.0 | | 58.0 |

Case B: Efficiency Parameter for Lignin using Grah's Data: $C_i = 1.20 \text{ kg / m}^3$; $C_s = 0.005 \text{ kg / m}^3$; $C_{yd} = \text{mean consistency} = 106 \text{ kg / m}^3 \cong 9.617 \%$; Wash Ratio = 0.8; $C_{y1} = 1.5 \%$ and $Pe = 20$ at the bed exit point ($Z = L$).

| Parameters | Model I | | Model II | | Model III | | Model IV | |
|------------|---------|-------|----------|-------|-----------|-------|----------|-------|
| | T = 0 | T = 1 | T = 0 | T = 1 | T = 0 | T = 1 | T = 0 | T = 1 |
| DR | 0 | 0.586 | 0 | 0.586 | 0 | 0.54 | 0 | 0.54 |
| WE | | 62.17 | | 62.17 | | 58.0 | | 58.0 |

Case C: At $Pe = 100$ for both Na^+ and lignin at the bed exit point ($Z = L$) for model I

| Parameters | Sodium | | Lignin | | Model III | | Model IV | |
|------------|--------|-------|--------|-------|-----------|-------|----------|-------|
| | T = 0 | T = 1 | T = 0 | T = 1 | T = 0 | T = 1 | T = 0 | T = 1 |
| DR | 0 | 0.644 | 0 | 0.644 | 0 | 0.54 | 0 | 0.54 |
| WE | | 67.50 | | 67.50 | | 58.0 | | 58.0 |

The value of t is approximately half of the total washing time required for a single stage BSW.

The predictions of DR and WE are made on this point.

From the inspection of all the data depicted above the following noteworthy conclusions can be made:

- The WE values proposed by Poirier et al. is different from those of wash yield proposed by Potucek. The Wash yield of Potucek gives higher value than the efficiency values of Poirier et. al., contrary to the data of other mill observers i.e. those of Grah and the present investigation.
- The Wash yield, WY is different from Y obtained by overall and component material balance. This is in conformity with Norden et. al. Similarly the values of Y and Y^* are not identical. Y yields always higher value than Y^* .
- The model predicted data can be used reliably for brown stock washer simulation.

- The simulated data on DR from displacement washing are in close agreement with mill data.
- The washing efficiency WE based on total solute removal in a brown stock washer closely tally with data calculated from the breakthrough curve obtained from the model. The difference arises due to different conditions employed by different investigators for brown stock washer. It however does not consider the removal efficiency of nature of solutes namely, Na⁺ and lignin species.
- The DR and WE values increases with time, valid for both Na⁺ and lignin. This is in excellent agreement with those of Grah.
- The DR and WE data for sodium are slightly higher than those for lignin for model 1 and model 2. However, for the case of model 3 and model 4 they yield identical values.
- Model 1 and model 2 give the same value whereas model 3 and model 4 yield identical value for both Na and lignin species. However model 1 and model 2 predict always higher value irrespective of the nature of species. Presence of dispersion- diffusion probably increases this value.

7.9 Conclusions

From the comprehensive study on the simulation of BSW from the data obtained from the model the following conclusions can be drawn:

- The simulated data on DR from displacement washing are in close agreement with mill data. The washing efficiency WE based on total solute removal in a brown stock washer also closely tally with data calculated from the breakthrough curve obtained from the models. The difference arises due to different conditions employed by different investigators for brown stock washer .It however does not consider the removal efficiency of nature of solutes namely, Na⁺ and lignin species.

- The DR and WE values increases with time, valid for both Na and Lignin. This is in excellent agreement with those of Grah. Therefore, the model predicted data can be used reliably for brown stock washer simulation.
- The DR and WE data for sodium are slightly higher than those for lignin for model 1 and model 2. However, for the case of model 3 and model 4 identical values of the above parameters are obtained.
- For Na^+ species the model 1 and the model 2 give the same order of value whereas model 3 and model 4 yield identical value. The above trend is also true for the other species namely lignin. However model 1 and model 2 predict always higher value irrespective of the nature of species. Presence of dispersion-diffusion probably increases this value.
- The WE values proposed by Poirier et al. is different from those of wash yield proposed by Potucek. The Wash yield of Potucek gives higher value than the efficiency values, contrary to the data of other mill observers, those of Grah and the present investigation.
- The Wash yield, WY is different from Y obtained by overall and component material balance. The values of Y and Y^* are not identical. Y yields always higher value than Y^* .

CHAPTER-8

CONCLUSION AND RECOMMENDATIONS

8.1 Main conclusions from the present study

Brown stock washing has manifold effects in the pulp and paper industry. On one hand it produces clean pulp for paper making and on the other hand it separates black liquor solids (Na^+ -salts and lignin based solutes) from the pulp. Various types of expressions are available in the literature to assess the performance of a brown stock washer. These expressions are somewhat complex. Therefore these are not commonly practiced by the industry particularly the Indian pulp and paper industry.

It is an established fact that a rotary vacuum filter (brown stock washer abbreviated as BSW) operation inducts various zones. These are: Cake formation zone, first dewatering zone, washing zone, second dewatering zone, blow and discharge zone, and the dead zones. The cake blow, discharge and dead zones have practically little contribution towards the brown stock washing operation while the models for cake forming zone is well known to the plant engineers. Therefore, there is only a need for investigating cake washing zone in order to find out the washing efficiency of a washer. In fact earlier investigators followed this practice. Hence in this present study emphasis is laid on investigating cake washing zone most explicitly.

In order to achieve the goal, available models are inspected in terms of their discrepancies. In this investigation mathematical models are derived firstly for displacement washing and then these are extended to washing zone of a practical rotary vacuum washer. A mathematical formulation has been made in the same manner as has been done by different investigators [6,88,71,23,24,42,33,57,75,105,63,4,10,64,15,82] for pulp washing system along with the effect of dispersion-diffusion as used by some workers [6,88,71,57,23,33]. Two different porosity values used by some researchers [23,24,75] for displaceable solutes and non-displaceable solutes and

adsorption-desorption isotherms have been considered. Majority of investigators have not taken into account the parameters related to diffusion, dispersion, adsorption, desorption, multiporosity values for inter particle and intra particle voids. It may be mentioned that some authors [81] neglected adsorption desorption isotherms. Many investigators [88,71,82,105] did not consider the difference of porosity values in different layers (stagnant and movable) during washing. While some other school of thoughts have neglected dispersion effects [14,48,42]. Even in adsorption-desorption isotherms investigators used different type of equations [Eqs.3.18,3.19,3.20]. The solution techniques are also remarkably different. No investigator has ever compared the results evolved out by assuming different adsorption isotherms that too for different boundary conditions.

The present investigation as indicated, limiting to the cake washing zone has been attempted to derive models from basic continuity equation of flow through porous media which incorporates all possible pertinent parameters (fluid dynamic and others) involved in the system. As the model is extremely complex, this is somewhat simplified to some extent, primarily for comparison purposes with few rival models. The later models have been solved for different adsorption isotherms along with varying initial and boundary conditions. This has led to formation of four different models with different adsorption-adsorption isotherms of finite and linear type only but with same initial and boundary conditions.

Finite difference method which appear to be simpler than many other numerical methods like Orthogonal Collocation, Galerkin finite element method etc. is used to solve these models, basically to examine the prediction capability compared to other more accurate numerical methods. The four different models are solved through MATLAB coupled with specially developed computer programs on C++ language. The validity of the models is checked with the simulated value given by Brenner using analytical methods and also with those from Grah who has used numerical technique –the orthogonal collocation.

The models are subjected with the data from Grah's experimental work on displacement washing. For some parameters most suitable equations for parameter estimation are used and in some cases models are specially developed.

Expressions are given for dimensionless concentration of solute in liquid phase C at any dimensionless pseudo time T , and dimensionless concentration of solute in solid phase, N as a function of T and also as a function of dimensionless distance (bed depth). The C - T profiles are in excellent agreement with those of Grah [24], Trinh et. al.[100] Sherman [88] as well as Brenner [6]. The C - T profile closely agrees also with Kuo and Barrett [43] and Kukreja [40]. However, there is no work available for pulp washing system with N - T profiles using solid phase though Kuo [42], Kuo and Barrette [43] and later Kukreja [40] have attempted to show the profile for stagnant liquor which will be obviously oppositely in trend as usual. The N - T profile for the present investigation has been in close agreement with many other investigators [17,45,51,92] working with adsorption in solid phase for allied type of systems. Therefore this investigation with N - T profile can claim for the first time a new dimension for solving adsorption related issues in pulp washing situation. As expected, the N - T profile in the present study gives an opposite trend with C - T profile of solute in liquor phase or solute in stagnant liquor phase as advocated by Kuo [42] and Kukreja [40]. The four different models are used to predict for two species, namely Na^+ and lignin to examine their washing behavior. Parameters like bed thickness, Peclet number, liquor velocity through cake pores, dispersion coefficient, porosity and mass transfer coefficients are varied in the C - T and N - T profiles of both Na^+ and lignin species to examine their influences.

From the displacement washing study for which our models are based the following important conclusions can be drawn.

Investigations of the simultaneous displacement washing of Na^+ and Lignin in sulphate pulp have shown great difference between the two substances in their behavior during washing.

At the same time interval the A_T values (proportional to solute removal) of lignin are equal to or higher than those of Na^+ for the models 1 and 2 but it is reverse in case models 3 and 4 (i.e. Na is higher than lignin) though the differences are very marginal. Poirier however found the similar or slightly higher values in case of Na^+ . It is probable that Poirier et. al. did not consider the dispersion effects.

For Na^+ the values of A_T are almost the same for model 1 and model 2 and the same is true for model 3 and model 4.

For lignin, similar conclusions can be drawn i.e. models 1 and model 2 give same order of magnitude and model 3 and model 4 predicts similar values.

Models 1 and 2 predict lower values compared to models 3 and 4.

The range of A_T values for Na^+ is between 0.80-0.874 and the same for lignin is between 0.81 – 0.874. The values predicted by Poirier et al. lie in the same range 0.79-0.88 and 0.77-0.89 respectively. The mean values are 0.85 for Na^+ and 0.81 for lignin. Therefore there is an excellent agreement between this investigation and those from Poirier et al. although the parameters such as superficial velocity (1.8mm/s), pad height (25mm), consistency (10%) are different. Present investigation is based on Grah's data with pulp pad thickness (20mm), interstitial velocity (8mm/s) and pulp consistency (9.16%). The marginal difference is thus expected.

The following striking features are noticed:

- The total amount of substance in different zones changes during simulation.
- Increased flow velocity results in a higher washing yield in spite of the simultaneous decrease in the degree of dispersion.
- Increase in the bed depth causes increase in washing efficiency but the effect is small.
- The mathematical model is found to be well suited for the analysis of results from the washing experiments due to Gren and Grah [27] and Trinh et al.[100].

The parametric values are valid for conditions existing in the pulp industry for wide range of conditions.

The model predicted data based on displacement washing is required to be applied for a real problem with an example of brown stock washer for a paper mill for the benefit of the industry. For this purpose the data are suitably modified using the procedure of Grah and other workers in this field. It may be mentioned that there is a number of empirical approaches available along with many macroscopic design equations. An investigation has therefore been called for design aspects of rotary vacuum filter used for washing of brown stock in a paper industry. This in turn demanded adjustment of parameters for displacement washing suitable for brown stock washing. The results are reported however for a single washer in terms of certain well known performance parameters.

The model predicted data using displacement washing process are compared with those of Perron and Lebeau [75] , Turner et al.[104] , Han and Edwards [32], Perkins et. al.[74] and also with Potucek [81]. The approach for evaluating the performance has been multi-directional. Detailed literature survey indicated that there was non-homogeneity of definitions and imperfections in defining the widely accepted parameters used in practice. In this investigation therefore, an attempt has also been made to define possible applicable performance evaluation parameters used by various investigators and to compare each other.

Majority of parameters are found to be a function of two variables only namely, concentration of dissolved solids and amount of liquor present in different streams.

The most important parameters are the displacement ratio and the efficiency of washing expressed in terms of the solute concentration in the inlet liquor, discharged as well as the extracted liquor. The interrelations between the different parameters are also reported. This is an important area as these can help the designers and the practicing engineers to predict, to compare, to optimize and to design the washing systems and equipments for mill practice. Expressions for, displacement ratio,

% efficiency, adsorption in terms of Na^+ loss and lignin have been reported. This will be further helpful to find out the efficiency of brown stock washers in paper mill.

Results from some models [75,32,53,54,104] are found closer to the earlier predicted equations, largely employed for process and design of industrial set up. The results from few rival models predicted by Potucek [81] are also compared.

All the above experimental and theoretical findings suggest that the present model agrees quite well with the experimental data and takes care of many of the important aspects of diffusion, dispersion, adsorption-desorption and different porosity values in the system.

The presents computer simulation can be employed to find optimum operating conditions for practical washers, however, it is limited to only washing zone of BSW and also for a single stage equipment.

The present mathematical model is suitable for the simulation of displacement washing in other existing equipment and in equipment under design.

- This present analysis can also be extended for the simulation of the washing operation on a multistage rotary washing filter for pulp mill.

8.2 Recommendations based on present study

Based on the entire investigation the following recommendations can be made for future work in this area:

- Weighted residual methods like Galerkin finite element and Orthogonal Collocation can be attempted to examine the computer time needed to solve the problem and also with better accuracy.
- The method of moments and the detailed equation of Laan (c.f.118) can be used to determine the value of Pe number.

- The model can also be applied for many other species present in brown stock of pulp like BOD₅ or BOD₇ (due to dissolved carbohydrates with a low D.P., and Uronic acids etc.)
- Non-linear adsorption isotherm like Langmuir or Goggenheim can be used in the models.
- Detailed study on the influence of mass transfer coefficient, k_1 and k_2 is required as the value in this present investigation has been taken from Grah. Experimental determination is thus necessary.
- The reverse trend of N-T profile of this present investigation and reported by other investigators [17,45,51,92] with C-T profile for stagnant liquor of Kuo [42], Kuo and Barrette [43] and Kukreja [40] must carefully examined . An inter-relation of these aspects has to be established.
- Nonlinear multi-variate statistical analysis of the effects of the operating variables can be attempted to examine the effect of temperature, thickness and consistency of mat (at inlet and discharge conditions), and superficial velocity of liquor/ wash water on washing efficiency.

Elaborate experiments should be conducted in an industrial BSW with various kinds of pulp obtained from hardwood, bamboo, and non-woods like bagasse, and straw which are main raw material for pulp and paper industry. It may be mentioned that this present work is based on softwood (Pine) sulphate pulp. Unfortunately no data is available on the above raw materials. The parameters might be significantly changed.

Experiments can be conducted on the pulp obtained from different pulping methods like CMP, CTMP, NSSC etc.

NOMENCLATURE

| | |
|------------|---|
| A. | : Surface area of drum, m^2 |
| Ac | : Area of cross section of washing zone, m^2 |
| ABC/(1+BC) | : Langmuir adsorption isotherm |
| B | : Constant for a given flow condition, geometry, fluid and pressure drop |
| c | : Concentration of the solute in the liquor, kg/m^3 |
| C_s | : Solute concentration in stagnant zone, kg/m^3 |
| C_s^* | : Solute concentration in stagnant zone at equilibrium, kg/m^3 |
| C_b | : Concentration of solute in blow liquor, kg/m^3 |
| C_d | : Concentration of solute in the discharged pulp, kg/m^3 |
| C_e | : Exit concentration of solute leaving the bed, kg/m^3 |
| C_f | : Concentration of solute in the filtrate, kg/m^3 |
| C_i | : Concentration of solute inside the vat, kg/m^3 |
| C_m | : Mean concentration of the filtrate collected through the washing zone, kg/m^3 |
| C_s | : Concentration of solute in the wash liquor, kg/m^3 |
| C_{sl} | : Concentration of the pulp slurry, kg/m^3 |
| C_F | : Fibre consistency, kg/m^3 |
| C_{Fm} | : Mean fibre consistency, kg/m^3 |
| C_o | : Fiber concentration in bed, kg/m^3 |
| C_y | : Pulp consistency, kg of fibers/kg of liquor |
| C_{yb} | : Blow consistency of pulp, kg of fibers/kg of liquor |
| C_{yd} | : Discharged consistency of pulp, kg of fibers/kg of liquor |
| C_{yi} | : Inlet vat consistency of pulp, kg of fibers/kg liquor |
| C_{yo} | : Fiber consistency in bed, %. |
| C_{yst} | : Standard consistency typically 10% or 12%. |
| D_L | : Longitudinal dispersion coefficient, m^2/s |
| D_v | : Molecular diffusion coefficient, m^2/s |
| erf | : Error function |
| g | : Gravitational acceleration, m/s^2 |
| I_0 | : Zero order Bessel function with imaginary argument |
| k, k', k'' | : Mass transfer coefficients, dimensionless |

| | |
|-----------------|---|
| k_1, k_2, k^* | : Mass transfer coefficients, l/s |
| K | : Permeability constant of cake, m^2 |
| K_e | : Relative permeability of cake |
| L | : Cake thickness, m |
| l | : Arbitrary cake thickness, m |
| l_d | : Length of dewatering zone, m |
| l_w | : Length of washing zone, m |
| L_b | : Amount of liquor in the pulp coming from blow tank, kg of liquor/kg of pulp |
| L_c | : Amount of liquor in the pulp leaving for bleaching section, kg of liquor/kg of pulp |
| L_d | : Amount of liquor in discharged pulp, kg of liquor/kg of pulp |
| L_e | : Liquor speed inside the vat, m^3/s |
| L_f | : Amount of filtrate, kg of liquor/kg of pulp |
| L_i | : Amount of liquor inside the vat, kg of liquor/kg of pulp |
| L_p | : Amount of liquor in the pulp coming from previous stage, kg of liquor/kg of pulp |
| L_r | : Amount of liquor recycled to previous washer, kg of liquor/kg of pulp |
| L_s | : Amount of wash water, kg of water/kg of pulp |
| L_{st} | : Amount of liquor in the pulp at standard consistency, kg of liquor/kg of pulp |
| m | : Mass of wet cake / mass of dry cake, kg/kg |
| m_p | : Mass of particles deposited in filter per unit volume of filtrate, kg/m^3 |
| N | : Speed of the drum, rpm/60, l/s |
| N_2 | : Level of slurry in the drum, m |
| N_i | : Concentration of solute in the fibers, kg/m^3 |
| n | : Concentration of solute on the fibres, kg/m^3 |
| P | : Width of the drum, m |
| Pe | : Peclet number, dimensionless |
| P_a | : Atmospheric pressure, Pascal |
| P_h | : Hydrostatic pressure, Pascal |
| P_v | : Vacuum, Pascal |

| | |
|--------------|--|
| ΔP | : Pressure drop, Pascal |
| ΔP_c | : Pressure drop across the cake, Pascal |
| ΔP_f | : Pressure due to friction, Pascal |
| ΔP_i | : Inlet pressure, Pascal |
| ΔP_k | : Kinetic pressure, Pascal |
| ΔP_m | : Pressure due to medium, Pascal |
| ΔP_t | : Total pressure, Pascal |
| ΔP_v | : Pressure due to vacuum, Pascal |
| q | : Local shower flow (zero for drying zone), m/s |
| r | : Radial distance from the centerline of the capillary, m |
| R | : Radius of the drum, m |
| R_o | : Perpendicular distance between axis of rotation and surface of slurry, m |
| R' | : Arbitrary distance between axis of rotation and surface of slurry, m |
| R_o'' | : Vertical distance between drum and vat, m |
| s | : Constant for a particular cake |
| S_o | : Specific surface of fibres, m^2/m^3 |
| S_e | : Effective saturation, % |
| S_r | : Residual saturation, % |
| S_s | : Real saturation, % |
| t | : Time, s |
| t_d | : Time of drying zone, s |
| t_w | : Time of washing zone, s |
| t | : Time to deposit a cake layer with a resistance equal to that of the filter cloth, s |
| T | : Time, dimensionless |
| u | : Liquor speed in cake pores, m/s |
| V | : Filtrate volume, m^3 |
| V' | : Filtrate collected during deposition of a pulp mat with a resistance equal to filter cloth, m^3 |
| V_c | : Volume of filtrate collected during deposition of a cake of resistance equivalent to the cloth per m^2 , m^3/m^2 |
| V_d | : Filtrate flow rate through cake drying zone, m^3/s |

| | |
|------------|---|
| V_f | : Filtrate flow rate through cake formation zone, m ³ /s |
| V_w | : Filtrate flow rate through cake washing zone, m ³ /s |
| V_t | : Total filtrate flow rate, m ³ /s |
| WW | : Amount of wash water added, liters per hour |
| x | : Dummy variable of integration |
| x_b | : Dissolved solids in pulp coming from blow tank, % |
| x_c | : Dissolved solids in pulp going for bleaching section, % |
| x_d | : Dissolved solids in discharged pulp, % |
| x_f | : Dissolved solids in the filtrate, % |
| x_i | : Dissolved solids inside the vat, % |
| x_p | : Dissolved solids in pulp coming from previous stage, % |
| x_s | : Dissolved solids in the washed pulp, % |
| X_i | : Mass of fibres / liquor in the vat, $C_{yi} / (1-C_{yi})$, kg/kg |
| y | : Constant depending on particle size |
| z | : Variable cake thickness, m |
| Δz | : Small increment in cake thickness, m |

Greek Symbols

| | |
|-------------------|---|
| α | : Specific resistance, kg/m |
| α_o | : Constant for a particular cake |
| β | : Variable angle in the cake formation zone, Radian |
| β_n | : Roots of transcendental equation |
| γ, γ' | : Constants |
| ϵ_d | : Interfiber porosity of cake, dimensionless |
| ϵ_s | : Intrafiber porosity of cake, dimensionless |
| ϵ_t | : Total porosity of cake, dimensionless |
| ϵ_{dm} | : Mean interfiber porosity of cake, dimensionless |
| ϵ_{tm} | : Mean total porosity of cake, dimensionless |
| η | : Viscosity of the liquor, kg/ms |
| θ | : Angle of submergence, Radian |
| ρ | : Density of water, kg/m ³ |

| | |
|---------------------|---|
| ρ_f | : Density of fibres, kg/m^3 |
| ρ_{sus} | : Density of suspension, kg/m^3 |
| ρ_d | : Density of liquor in washed pulp, kg/m^3 |
| ρ_i | : Density of liquor inside the vat, kg/m^3 |
| ρ_o | : Density of liquor in the bed, kg/m^3 |
| ρ_s | : Density of wash water, kg/m^3 |
| σ | : Surface tension of the liquor, kg/m^3 |
| ϕ | : Angle subtended by point area with horizontal, Radian |
| ϕ_1 | : Angle subtended by point area with horizontal when the drum enters the slurry, Radian |
| ϕ_2 | : Angle subtended by point area with horizontal when the drum leaves the slurry, Radian |
| ψ | : Fractional submergence of drum, dimensionless |
| ξ | : Dimensionless distance, dimensionless |
| τ | : Dimensionless time, dimensionless |

REFERENCES

1. Al Jabari M., Van Heiningen A.R.P. and Van De Ven T.G.M., *Modelling the flow and the deposition of fillers in packed beds of pulp fibers*. J. of Pulp and Paper Science, 20(9), pp.J249-J253, (1994).
2. Aris R. and Amundson N. R., *Some remarks on longitudinal mixing or diffusion in fixed beds*. AIChE J., 3(2), pp.280-282, (1957).
3. Armstrong B., *Analysis of a pulp washing system*, The Paper Industry, 38(Jan.), pp.854, (1957); Southern Pulp Paper, 20(2), pp.56-62, (1957).
4. Baldus R.F., Warnqvist B. and Edwards L.L., *Washing models for use in pulp mill, Material balance calculations*, Pulp and Paper Canada, 78(6), pp. TR56- TR63, (1977).
5. Bastian W.C. and Lapidus L., *Longitudinal diffusion in ion exchange and chromatographic columns, Finite column*, J. of Physical Chemistry, 60, pp.816-817, (1956).
6. Brenner H., *The diffusion model of longitudinal mixing in beds of finite length, Numerical values*, Chemical Engineering Science, 17, pp.229- 243, (1962).
7. Brinkley S.R. (Jr), *Tables of the temperature distributing functions for heat exchange between fluid and porous solid*, US Deptt. of Interior, Bureau of Mines, Pittsburgh, Pennsylvania, (1951).
8. Carman P.C., *Fundamental principles of industrial filtration*, Trans. Institute of Chemical Engineers (London), 16, pp.168, (1938).
9. Cheng Z., Leminen J., Ala-Kaila K. And Paulapuro H., *The basic drainage properties of Chinese wheat straw pulp*, Tappi Proceedings, Pulping Conference, pp.735-744, (1994).
10. Crotagino R.H., Poirier N.A. and Trinh D.T., *The principles of pulp washing*, Tappi J., 70(6), pp.95-103, (1987).
11. Cullinan H. T., *The efficiency of pulp washing with regard to lignin removal*, Appita, 44(2), pp.91-94, (1991).
12. Cullinan (Jr.) H. I., *A unified treatment of brown stock washing on rotary filters*, Tappi J., 69(8), pp.90-94, (1986).
13. Davis C.N., Proc. Institute of Mechanical Engineers (London), 1B,185, (1952).
14. Edeskuty F.J. and Amundson N .R., *Mathematics of adsorption, Part-4 : Effect of intraparticle diffusion in agitated static systems*, J. of Physical Chemistry, 56, pp.148-152, (1952).
15. Edwards L. and Rydin S., *Washing of pulps, Part-5: A dispersion model for washing of pulp in mill continuous diffusers*. Svensk Papperstidning, 79(11), pp.354-358, (1976).

- 5a. Edward L., Peyron M. and Minton M., *Models for cross-flow pulp washing calculations*, Pulp and Paper Canada, 87(1), pp.T17-T21, (1986).
6. Emersleben O., *Physikal. Z.*, Vol.26, pp.601, (1925).
7. Farooq S. and Ruthven D.M., *Dynamics of kinetically controlled binary adsorption in a fixed bed*, AIChE J., 37(2), pp.299-301, (1991).
8. Fenghua Shen , Teruo Takahashi and Takashe Korenaga, *a numerical solution for the dispersion in laminar flow through a circular tube*, The Canadian Journal of Chemical Engineering, 68(4), pp191-196, (1990).
9. Fitch B. and Pitkin W.H., *Analysis of brown stock washing systems*, Tappi J., 47(10), pp.170A-81A, (1964).
10. Foscolo P.U., Gibilaro L.G. and Waldram S.P., *Chem. Eng. Sci.*, 39(12), pp.1667, (1983).
11. Goldstein S., *On the mathematics of exchange processes in fixed columns, Part-1: Mathematical solutions and asymptotic expansions*, Proc. of Royal Society of London, A 219, pp.151-171, (1953).
12. Grah L.E., *Washing of cellulose fibres, analysis of displacement washing operation*, Ph.D. Thesis, Chalmers University of Technology, Goteborg, Sweden, (1974).
13. Grah L.E., *Displacement washing of packed beds of cellulose fibres, Part-1: Mathematical model*, Svensk Papperstidning, 78(12), pp.446- 450, (1975).
14. Grah L.E., *Displacement washing of packed beds of cellulose fibres, Part-2: Analysis of laboratory experiments*, Svensk Papperstidning, 79(3), pp.84-89, (1976).
15. Grah L.E., *Displacement washing of packed beds of cellulose fibres, Part-3 : A comparison of the washing behaviour of sodium and lignin*, Svensk Papperstidning, 79(4), pp.123-128, (1976).
16. Gren U., *Compressibility and permeability of packed beds of cellulose fibres, Part-2 : The influence of permeation temperature and electrolytes*, Svensk Papperstidning, 76(6), pp.213-218, (1973).
17. Gren U. and Grah L.E., *Washing of cellulose fibre beds*, Svensk Papperstidning, 76(16), pp.597-601, (1973).
18. Gren U .B .and Strom K.H. U ., *Displacement washing of packed beds of cellulose fibres*, Pulp and Paper Canada, 86(9), pp.T261-264, (1985).
19. Gullichsen J., *Experience accumulated from tests with a pilot diffuser*, Pulp and Paper Canada, 74(8), pp.80-85, (1973).
- 19a. Gullichsen J. and Ostman H., *Sorption and diffusion phenomena in pulp washing*, TAPPI, 59(6), pp. 140-143, (1976).

30. Hakamaki R. and Kovasin K., *The effect of some parameters on brown stock washing: A study made with a pulp tester*, Pulp and Paper Canada, 86(9), pp.45-52, (1985).
31. Han C.D., *Washing theory of the porous structure of aggregated materials*, Chemical Engineering Science, 22, pp.837-846, (1967).
32. Han Y. and Edwards L., *Optimization of filter washer operation and control*, Tappi J., 71(6), pp.101-104, (1988).
33. Hartler N. and Rydin S., *Washing of pulps, Part-1: Equilibrium studies*, Svensk Papperstidning, 78(10), pp.367-372, (1975).
34. Ingmanson W.L., Andrews B.D. and Johnson R.C., *Internal pressure distributions in compressible mats under fluid stress*, Tappi J., 42(10), pp.840-849, (1959).
35. Jahnke E. and Emde F., *Tables of Functions*, Dover, (1945).
36. Josephson W., Cullinan H.T. and Krishnagopalan G.A., *The environmental impact of acidic shower water usage on the final stage of a brown stock washing system*, Appita, 49(1), pp.43-49, (1996).
37. Josephson W.E., Krishnagopalan G.A. and Cullinan H. T., *Multi component control of brown stock washing*, Tappi J., 76(9), pp.197-204, (1993).
38. Kasten P.R., Lapidus L. and Amundson N.R., *Mathematics of adsorption in beds, Part-5: Effect of intraparticle diffusion in flow systems in fixed beds*, J. of Physical Chemistry, 56, pp.683-688, (1952).
39. Kerekes R. J. and Schell C.J., *J. Pulp Paper Sci*, 18(1), pp.J32, (1992).
40. Kukreja V.K., *Modelling of washing of brown stock on rotary vacuum washer*, Ph.D. Thesis, University of Roorkee, Roorkee, India, (1996).
41. Kukreja V.K., Ray A.K., Singh V.P. and Rao N.J., *some rotary vacuum washer performance parameters and their correlations*, TAPPI Proceedings, Pulping Conference, pp.837-847, (1996).
42. Kuo M.T., *Filter cake washing performance*, AIChE J., 6(4), pp.566- 568, (1960).
43. Kuo M.T. and Barrett E.C., *Continuous filter cake washing performance*, AIChE J., 16(4), pp.633-638, (1970).
44. Kyan C.P., Wasan D.T. and Kintner R.C., *Ind. Eng. Chem. Fundam.*, 9(4), pp.596,(1970).
45. Lai Ching-Chih and Tan Chung-Sung, *Approximate models for nonlinear adsorption in a packed-bed adsorber*. AIChE J., 37(3), pp.461-465, (1991).

46. Lafreniere S., Dessureault S. and Barbe M.C., *Recycled pulp washing, Part-I: Comparison of washing equipment and subsystems*, Pulp and Paper Canada, 96(2), pp. T55-62, (1995).
47. Lapidus L. and Amundson N .R., *The rate determining steps in radial adsorption analysis*, J. of Physical Chemistry, 56, pp.373-383, (1952).
48. Lapidus L. and Amundson N.R., *Mathematics of adsorption in beds, Part-VI: The effect of longitudinal diffusion in ion exchange and chromatographic columns*, J. of Physical Chemistry, 56, pp.984-988, (1952).
49. Laxen T., *Dynamic and physical- chemical aspects of sulphate pulp washing*, Pulp and Paper Canada, 87(4), pp.T148-152, (1986).
50. Lee P.F., *Optimizing the displacement washing of pads of wood pulp fibres* , Tappi J., 62(9), pp.75-78, (1979).
51. Liao Hsin-Tzu and Shiau Ching-Yeh, *analytical solution to an axial dispersion model for the fixed-bed adsorber*, AIChE J., 46(6), pp.1168-1176, (2000).
52. Lindsay J.D., *Relative flow porosity in fibrous media: Measurements and analysis, including dispersion effects*, Tappi J., 77(6), pp.225-239, (1994).
53. Luthi O., *Equivalent displacement ratio -Evaluating washer efficiency by comparison*, Tappi J., 66(4), pp.82-84, (1983).
54. Luthi O., *Different approaches to modelling displacement ratio*, Pulp and Paper Canada, 86(7), pp. T201-205, (1985).
55. McCubbin N. and Folke J., *Significance of AOX vs unchlorinated organics*, Pulp and Paper Canada, 96(2), pp. T63-68, (1995).
56. Neretnieks I., *Analysis of some washing experiments of cooked chips*, Svensk Papperstidning, 75(20), pp.819-825, (1972).
57. Neretnieks I., *A mathematical model for continuous counter current adsorption*, Svensk Papperstidning, 77(11), pp.407-411, (1974).
58. Neretnieks I., *Note on some washing results with a Kamyr Hi-Heat washer*, Svensk Papperstidning, 77(13), pp.486-490, (1974).
59. Neretnieks I., *Adsorption in finite bath and counter current flow with systems having a nonlinear isotherm*, Chemical Engineering Science, 31, pp.107-114, (1976).
60. Neretnieks I., *Adsorption in finite bath and counter current flow with systems having a concentration dependent coefficient of diffusion*, Chemical Engineering Science, 31, pp.465-471, (1976).

61. Nierman H.H., *Optimizing the wash water rate of counter current washing systems*, Tappi J., 69(3), pp.122-124, (1986).
62. Nierman H.H., *More on data adjustment for counter current washer efficiency calculations*, Tappi J., 69(8), pp.85-89, (1986).
63. Norden H.V., Pohjola V.J. and Seppanen R., *Statistical analysis of pulp washing on an industrial rotary drum*, 74(10), pp.83-91, (1973).
64. Norden H. V. and Tiainen P., *The use of matrices in pulp washing calculations*, Proc. of the Symposium on Recovery of Pulping Chemicals, Ekono, Helsinki, pp.47-63, (1968).
65. Norden H. V. and Viljakainen E., *The calculation of pulp washing processes influenced by adsorption*, Svensk Papperstidning, 83(2), pp.50-56, (1980).
66. Norden H. V. and Viljakainen E., *Calculation of pulp washing by the Z method*, Paperi ja Puu, 65(4), pp.281-285, (1983).
67. Norden H.V., Viljakainen E. and Nousiainen H., *Calculation of the efficiency of multizone pulp washers using a mass transfer model and the superposition principle*, Pulp and Paper Canada, 83(6), pp. TR21- 26, (1982).
68. Oxby P.W., Sandry T.D. and Kirkcaldy D.M., *A method for quantifying pulp washer performance that does not use flow rate measurements*, Tappi J., 69(8), pp.118-119, (1986).
69. Peck R.E. and Chand J., *Filtration rates in rotary leaf vacuum filters*, Trans. Indian Institute of Chemical Engineers, XIV, pp.48-50,(1961-62).
70. Pekkanen M. and Norden H.V., *Review of pulp washing models*, Paperi ja Puu, 67(11), pp.689-696, (1985).
71. Pellett G .L., *Longitudinal dispersion, intra particle diffusion and liquid-phase mass transfer during flow through multiparticle systems*, Tappi J., 49(2), pp.75-82, (1966).
72. Pelton R., *A review of brown stock defoamer fundamentals*, Pulp and Paper Canada, 90(2), pp.T61-68, (1989).
73. Penttila M., Laxen T. and Virkola N.E., *Laboratory simulation of kraft pulp washing*, Pulp and Paper Canada, 87(1), pp.T31-37, (1986).
74. Perkins J.K., Welsh H.S. and Mappus J.H., *Brown stock washing efficiency: Displacement ratio method of determination*, Tappi J .,37(3), pp.83-89, (1954).
75. Perron M. and Lebeau B., *A mathematical model of pulp washing on rotary drums*, Pulp and Paper Canada, 78(3), pp. TR1-5, (1977).
76. Phillips J.R. and Nelson J ., *Diffusion washing system performance*, Pulp and Paper Canada, 78(6), pp. T123-127 , (1977).

77. Poirier N.A., Crotogino R.H., Trinh D.T. and Douglas W.J.M., *displacement washing of wood pulp - An experimental study at low initial liquor concentration*, Pulp Washing Symposium, Helsinki, pp.1-19, May18-21, (1987) .
78. Poirier N.A., Crotogino R.H. and Douglas W.J.M., *Displacement washing of wood pulp – A model with source term for low initial liquor concentration*, Pulp Washing Symposium, Helsinki, pp.35-48, May18-21, (1987).
79. Poirier N.A., Crotogino R.H. and Douglas W.J.M., *Displacement washing of wood pulp – A one parameter model for high initial liquor concentration*, Pulp Washing Symposium, Helsinki, pp.49-72, May18-21, (1987).
80. Potucek Frantisek and Milichovsky Miloslav, *Efficiency of pulp washing with regards to energy consumption*, INPAP-94, pp.38-48, Lodz, 18-19.10.1994 r.
81. Potucek Frantisek, *Washing of pulp fibre bed*, Collect. Czeck. Chem. Commun., 62, pp.626-644, (1997).
82. Rasmuson A. and Neretnieks I., *Exact solution of a model for diffusion in particles and longitudinal dispersion in packed beds*, AIChE J., 26(4), pp.686-690, (1980).
83. Ray A.K. and Singh V.P., *On the mathematical modelling of multistage rotary drum brown stock washing system for paper industry*, Proc. of first annual conference of Indian Society of Industrial and Applied Mathematics, University of Roorkee, Roorkee, India, pp.281-286, (1992).
84. Rosen A., *Adsorption of sodium ions on krait pulp fibers during washing*, Tappi J., 58(9), pp.156-161, (1975).
85. Ruth B.F. and Kempe L.L., *An extension of the testing methods and equations of batch filtration practice to the field of continuous filtration*, Trans. AIChE J., 33, pp.34-83, (1937).
86. Sampson W.W. and Kropholler H.W., *Batch-drainage curves for pulp characterization; Part 2: Modeling*, Tappi J., 79(1), pp.151-160, (1996).
87. Service G.G. and Seymour G.W., *Black liquor losses*, Tappi J., 64(7), pp.90-92, (1981).
88. Sherman W.R., *The movement of a soluble material during the washing of a bed of packed solids*, AIChE J., 10(6), pp.855-860, (1964).
89. Sherratt M.J., *The pore structure of fiber mats*, M.Sc. Thesis, Dept. of Paper Science, UMIST, Manchester, U.K., (1992).
90. Smith A.J., Gustafson R.R. and McKean W.T., *Enhanced lignin removal in brown stock washing*, Tappi J., 76(6), pp.81-86, (1993).
91. Smith R.J. and Duffy G.G., *Pulp washing by dilution thickening without remixing*, Appita, 44(4), pp.265-269, (1991).

92. Sridhar P., *Implementation of the one point Orthogonal Collocation method to an affinity packed bed model*, Indian Chemical Engr., 41(1), pp.T36-T42, (1999).
93. Stromberg C.B., *Washing for low bleach chemical consumption*, Tappi J., 74(10), pp.113-122, (1991).
94. Stromberg C.B., *Washing of dissolved organic solids from pulp*, Paper Asia, October, pp.32-39, (1994).
95. Sun L.M. and Levan M.D., *Numerical solution of diffusion equations by the finite difference method: efficiency improvement by iso-volumetric spatial discretization*, Chemical Engineering Science, 50(1), pp.163-166, (1995).
96. Szukiewicz M.K., *New approximate model for diffusion and reaction in a porous catalyst*, AIChE J., 46(3), pp.661-665, (2000).
97. Tiller F.M. and Cooper H.R., *The role of porosity in filtration: IV. Constant Pressure Filtration*, AIChE J., 6(4), pp.595-601, (1960).
98. Trinh D.T. and Crotagino R.H., *Sodium equilibrium in kraft pulp washing*, J. of Pulp and Paper Science, 13(3), pp.J93-J98, (1987).
99. Trinh D.T. and Crotagino R.H., *The rate of solute removal from kraft pulp fibres during washing*, J. of Pulp and Paper Science, 13(4), pp.J126-J132, (1987).
100. Trinh D.T., Poirier N.A., Crotagino R.H. and Douglas W.1.M., *Displacement washing of wood pulps -An experimental study*, J. of Pulp and Paper Science, 15(1), pp.J28-J35, (1989).
101. Tomiak A., *Theoretical recoveries in filter cake reslurrying and washing*, AIChE 1.,19(1), pp.76-84, (1973).
102. Tomiak A., *Counter current pulp washing, recovery calculations*, Pulp and Paper Canada, 75(9), pp.T331-336, (1974).
103. Tomiak A., *Solve COMPLEX WASHING PROBLEMS*, Chemical Engineering, October 8, pp.109-113, (1979).
104. Turner P.A., Roche A.A., McDonald J.D. and Van Heiningen A.R.P., *Dynamic behaviour of a brown stock washing system*, Pulp and Paper Canada, 94(9), pp.T263-268, (1993).
105. Viljakainen E., *Mass transfer models and multizone washing efficiency calculations*, Pulp & Paper Canada, 86(10), pp.T301-305, (1985).
106. Walker D., *Structural mechanisms of sheet formation in papermaking systems*, Ph.D.Thesis, Dept. of Paper Science, UMIST, Manchester, U.K., (1989).
107. Wong B.M. and Reeve D. W., *Diffision in fibre beds*, J. of Pulp and Paper Science, 16(2), pp.172-176, (1990).

108. Westerterp K., Dil'man V.V. and Kronberg A.E., *Wave model for longitudinal dispersion: development of the model*, AIChE J., 41(9), pp.2013-2028, (1995).
109. Xie Lai Su, *Washing characteristics of different pulps and productivity of drum washer*, Pulp washing Symposium, Helsinki, pp.73, May18-21, (1987)
110. Xuan N.N., Venkatesh V., Gratzl J.S. and McKean W.T., *The washing of soda-oxygen pulps, sorption phenomena of cations*, Tappi J., 61(8), pp.53-56, (1978).

BOOKS

111. Badger W.L. and Banchero J. T., *Introduction to Chemical engineering*, McGraw-Hill Book Company, Inc., (1955).
112. Balagurusamy E., *Numerical Methods*, Tata McGraw-Hill Publishing Company Limited, New Delhi, (1999).
113. Brown G.G., *Unit Operations*, John Wiley and Sons, (1950).
114. Coulson J.M., Richardson J.F., Backhurst J.R. et.al., *Chemical Engineering Vol. 2 – Particle Technology and Separation Processes*, 4th edn., Pergamon Press, Oxford, 1991.
115. Gerald Curtis F. and Wheatley Patrick O., *Applied Numerical Analysis (Fifth Edition)*, Addison-Wesley Publishing Company, (1998).
116. Higgins H. and de Young J., *Visco-elasticity and Consolidation of the Fiber Network During Free Water Drainage; in consolidation of the paper web*, F. Bolam, Ed., vol. (I), Tech. Sect. BPMBA, London, pp.242-268, (1966).
117. Jain M.K., Iyengar S.R.K. and Jain R.K., *Numerical Methods for Scientific and Engineering Computation (Second Edition)*, Wiley Eastern Limited, New Delhi, (1987).
118. Levenspiel O., *Chemical Reaction Engineering*, Wiley Eastern Private Limited, New Delhi, (1974).
119. McCabe W.L. and Smith J. C., *Unit Operations of Chemical Engineering*, McGraw-Hill Book Company, Second Edition, (1967).
120. Orr C., *Filtration: Principles and Practices*, Part-1, Marcel Dekker Inc., (1977).
121. Peters M.S. and Timmerhaus K.D., *Plant Design and Economics for Chemical Engineers*, McGraw-Hill Kogakusha lid., (1980).
122. Sastry S.S., *Introductory Methods of Numerical Analysis*, 3rd Ed., Prentice Hall of India Limited, New Delhi, (2000).
123. Scheidegger A.E., *The Physics of Flow Through Porous Media*, 3rd edn., University of Toronto, ON, 1974.

124. Smith G.D., *Numerical Solution of Partial Differential Equations*, Oxford University Press, London, (1965).

125. Smook G.A., *Handbook for Pulp and Paper Technologists*, Joint Textbook Committee of the Paper Industry, (1989).

APPENDIX-I

BASE DATA FOR THE PRESENT WORK FOR CHAPTER-5

Table (5.2): Summary of displacement washing studies on fibrous beds

| Author(s) | Pad Thickness (mm) | Pad Consistency (%) | Temperature (°C) | Superficial Liquor Vel(mm/s) | Fiber Type | Liquor to be Displaced |
|---------------------|--------------------|---------------------|------------------|------------------------------|------------------------------------|--|
| Sherman [88] | 30.5-53.9 | - | - | 0.2-10 | V&D fibres | Diacetyl solution |
| Pellet [71] | 30.5-82.9 | - | - | 2-20 | All-skin viscose yarn | Three coloured solution |
| Gren and Grahs [27] | 40-90 | 6-11 | - | 0.1-0.5 | PSP(30-60% yield) Kappa No. 16-81 | Various electrolyte solution |
| Grahs [25] | 100-170 | 6-10 | 21 | 0.1-1.1 | PSP,Ka No.49.7 | Spent sulphite liquor,0.2-0.3 kg Na/m ³ |
| Grahs[25] | 100 | 8-10 | 50 | 0.07 | PSP, Kappa No. 30 | Spent sulphite liquor,0.57-0.655 kg Na/l,1.2-1.42 |

| | | | | | | kg lignin/l |
|-------------------------------|-------|----------|-------|------------|--|--|
| Lee [50] | 25.4 | 3.5-17.3 | 20-55 | 0.072-0.75 | HW & SW kraft pulp | Kraft black liquor, 15.6% solids, 4% Na |
| Gren and Strom [28] | 20-80 | 5-21 | 20 | 0.04-0.4 | SW Sulphate Pulp, kappa No.31-34 | Spent sulphite liquor |
| Hakamaki & Kovasin [30] | - | 1-12 | 30-90 | 2-12 | Pine kraft pulp ,Kappa No.27-32 | Kraft black liquor |
| Trinh et al.[100] | 25-85 | 2.9-17.4 | 30-60 | 0.028-0.9 | Kraft black spruce, Kappa No. 27 | Kraft black liquor, 8-13 g Na/l, 22-33 g lignin/l |
| Xuan et. al. [110] | - | - | - | - | Kappa No.35-41 | 250-452ppm |
| Hartler et. al. [33] | - | 10% | - | - | Kappa No.19-55 | 0-400ppm |
| Smith et. al. [90] | - | - | 20-90 | - | Kappa No.30-48 | - |

Note: VD = Viscose and Decron, PSP = pine sulphate pulp.

Table (5.3): Compressibility parameters of different pulp samples at temperature of 60°C
 (due to Cheng, Leminen, Kaila and Paulapuro)

| Pulp | Spec.Vol m ³ / kg | Specific Surface, m ² / m ³ | N | M, kg/m ³ /Pa ^N | SR No. | Kapp a No. | Drain. Rα, m / kg | Drain. Vel., mm / s |
|------------------------|---------------------------------|---|-------|--|-----------|------------------|-------------------------|---------------------------|
| Larch | 0.00220 | 581,000 | 0.349 | 5.35 | 13.1 | 41.0 | 6.7x10 ⁹ | 5.2 |
| Southern Pine | 0.00236 | 426,000 | 0.361 | 4.84 | 12.9 | 28.8 | 4.8x10 ⁹ | 7.4 |
| Wheat Straw | 0.00244 | 1,809,00 0 | 0.346 | 5.50 | 35.1 | 14.9 | 79.3x10 ⁹ | 1.1 |
| Wheat Straw (Bl) | 0.00223 | 1,377,00 0 | 0.369 | 4.95 | 36.5 | 2.8 | 56.4x10 ⁹ | 1.6 |
| WS, R>200 | 0.00272 | 671,000 | 0.375 | 3.967 | - | - | 17.0x10 ⁹ | 2.1 |
| WS, R>100 | 0.00292 | 503,000 | 0.394 | 3.287 | - | - | 10.3x10 ⁹ | 3.3 |

Table (5.5a): Constants for Langmuir adsorption isotherm for Na⁺

| A, kg / t of pulp | B, m ³ / kg | Raw Material | Kappa Number | Investigators |
|-------------------|------------------------|--------------|--------------|-------------------------|
| 2.9 | 23 | Pine Kraft | - | Hartler & Rydin [33] |
| 3.1 | 42 | Birch Kraft | - | Do |
| 4.04 | 16.8 | | | Gullichsen [29a] |
| 2.9 | 47 | Birch | 18 | Grah [24] |
| 2.2 | 56 | Birch | 20 | Do |
| 2.7 | 55 | Do | 26 | Do |

Table (5.5b): Constants for Langmuir adsorption isotherm For Na⁺

| A, m ³ liquor/kg Na | B, m ³ liquor/kg Na | Raw Material | Kappa Number | Investigators |
|-----------------------------------|-----------------------------------|-----------------------|--------------|---------------|
| 0.01324 | 6.586 | Pine Sulphate Pulp | 22.4 | Grah[24] |
| 0.01401 | 5.232 | Do | 43.4 | Do |
| 0.01263 | 3.955 | Do | 49.7 | Do |
| 0.01195 | 2.708 | Do | 72.6 | Do |

Table (5.5c): Constants for Langmuir adsorption isotherm for Na⁺

| A, mg/g | B, 1/mg | Raw Material | Kappa Number | Investigators |
|---------|---------|------------------------------|--------------|------------------------|
| 3.1 | 0.069 | Pine craft pulp | 28 | Hartler and Rydin [33] |
| 2.7 | 0.016 | Do | 30 | Do |
| 1.8 | 0.013 | Do | 38 | Do |
| 2.3 | 0.009 | Do | 40 | Do |
| 4.6 | 0.007 | Do | 48 | Do |
| 2.9 | 0.047 | Birch Kraft Pulp | 18 | Do |
| 2.2 | 0.056 | Do | 20 | Do |
| 2.7 | 0.055 | Do | 26 | Do |
| 4.4 | 0.011 | Do | 36 | Do |
| 0 | 0 | Bisulphite pulp of spruce | 27 | Do |
| 0 | 0 | Do | 33 | Do |
| 0 | 0 | Do | 40 | Do |
| 2.1 | 0.001 | Do | 55 | Do |

Table (5.5d): Constants for Langmuir adsorption isotherm for lignin

| A, mg/g | B, 1/mg | Raw Material | Kappa Number | Investigators |
|---------|---------|------------------------------|--------------|---------------------------|
| 0 | 0 | Pine kraft pulp | 28 | Hartler and Rydin [33] |
| 25 | 0.001 | Do | 30 | Do |
| 1 | 0.002 | Do | 38 | Do |
| 1 | 0.001 | Do | 40 | Do |
| 1 | 0.131 | Do | 48 | Do |
| 6 | 0.0010 | Birch Kraft Pulp | 18 | Do |
| 4 | 0.0003 | Do | 20 | Do |
| 7 | 0.0032 | Do | 26 | Do |
| 9 | 0.0017 | Do | 36 | Do |
| 0 | 0 | Bisulphite pulp of spruce | 27 | Do |
| 0 | 0 | Do | 33 | Do |
| 0 | 0 | Do | 40 | Do |
| 0 | 0 | Do | 55 | Do |

APPENDIX-II

BASE DATA FOR CHAPTER-5

Table (5.4): Calculated porosity values obtained from different model equations

Fixed values: Consistency = 10 %; WRR = 1.7; $\rho_s = 1550-1560 \text{ kg / m}^3$; $\rho = 100 \text{ kg / m}^3$

| Models | ϵ_t (total) | ϵ_d (displaceable) | ϵ_s (stagnant) | ϵ_{eff} (effective) | ϵ_{ret} (relative) |
|---------------|--------------------------------|---------------------------------------|-----------------------------------|--|--|
| Grah | 0.924 (Eq.5.30) | 0.806 | 0.118 | - | - |
| Lindsay | 0.935 | - | - | 0.738 | 0.796 |
| Kyan | 0.928 | - | - | 0.536 | 0.578 |

Table (5.6): Calculated values of Permeability constant K, m² from different models

Fixed values: $K_1 = 3.5$, $K_2 = 57$, $k_1 = 5.55$, $\epsilon_1 = 0.928$.

| Pulp | Sp. Sur. Area S_o (m ² /m ³) | Kozeny Equation K (m ²) | Davis Equation K (m ²) | Perron & Lebeau K (m ²) | Ref. |
|--------------------------|---|---|--|--|---------------------|
| - | 1.56×10^6 | 1.141×10^{-11} | 0.5950×10^{-11} | 0.69×10^{-11} | Perron & Leb.[75] |
| - | 1.388×10^6 | 1.440×10^{-11} | 0.752×10^{-11} | - | Lindsay [52] |
| Southern Pine | 0.426×10^6 | 15.306×10^{-11} | 7.979×10^{-11} | - | Cheng Z., et.al.[9] |
| Wheat Straw (R > 100) | 0.503×10^6 | 10.979×10^{-11} | 5.723×10^{-11} | - | Do |
| Larch | 0.581×10^6 | 8.229×10^{-11} | 4.290×10^{-11} | - | Do |
| Wheat Straw (R > 200) | 0.671×10^6 | 6.170×10^{-11} | 3.216×10^{-11} | - | Do |
| Wheat Straw Bleached | 1.377×10^6 | 1.465×10^{-11} | 0.764×10^{-11} | - | Do |
| Wheat Straw | 1.809×10^6 | 0.849×10^{-11} | 0.443×10^{-11} | - | Do |
| Wood, Ka No21.5 | 0.243×10^6 | 47.041×10^{-11} | 24.523×10^{-11} | - | Potucek [81] |
| Wood, Ka No.17.6 | 0.333×10^6 | 25.05×10^{-11} | 13.059×10^{-11} | - | Do |

Table (5.7a): Calculated data of amount adsorbed of Na⁺ and soda loss using non-linear Langmuir adsorption isotherm as a function of Kappa number based on Grah [24] data

Raw material: Pine sulphate pulp; Temperature = 21°C, C_i (kg / m³)

| Kappa No. | Amount of Na ⁺ sorbed, kg / t | | Soda loss (as Na ₂ SO ₄), kg / t | |
|-----------|--|-------|---|-------|
| | C _i ,0.57 | 0.655 | C _i ,0.57 | 0.655 |
| 22.4 | 1.587 | 1.632 | 4.905 | 5.043 |
| 43.4 | 2.005 | 2.073 | 6.196 | 6.405 |
| 49.7 | 2.212 | 2.304 | 6.836 | 7.119 |
| 72.6 | 2.677 | 2.822 | 8.275 | 8.719 |

Table (5.7b): Data on Na⁺ adsorbed and soda loss as a function of initial sodium concentration at a fixed Kappa Number of 49.7, based on Grah [24] data

Raw material: Pine sulphate pulp; Temperature = 21°C.

| C _i , kg / m ³ | Na ⁺ , kg / t | Soda loss as Na ₂ SO ₄ , kg / t |
|--------------------------------------|--------------------------|---|
| 0.225 | 1.504 | 4.646 |
| 0.263 | 1.628 | 5.031 |
| 0.264 | 1.631 | 5.040 |
| 0.278 | 1.672 | 5.168 |
| 0.290 | 1.706 | 5.271 |
| 0.315 | 1.771 | 5.474 |
| 0.319 | 1.781 | 5.505 |
| 0.365 | 1.886 | 5.829 |

Table (5.7c): Calculated data of amount adsorbed of Na⁺, soda loss and lignin using Non-linear Langmuir adsorption isotherm as a function of kappa number based on Hartler & Rydin [33] data

Raw material: Pine kraft pulp; Temperature = 170°C, C_i (kg / m³)

| Kappa No. | Amount of Na ⁺ sorbed, kg / t | | Soda loss (as Na ₂ SO ₄), kg / t | | Amount of Lignin, kg / t | |
|-----------|---|-------|--|--------|-----------------------------|--------|
| | C _{i,0.57} | 0.655 | C _{i,0.57} | 0.655 | C _{i,1.2} | 1.42 |
| | 28 | 3.023 | 3.032 | 9.341 | 9.372 | 0.000 |
| 30 | 2.433 | 2.465 | 7.519 | 7.616 | 13.636 | 14.669 |
| 38 | 1.586 | 1.611 | 4.901 | 4.977 | 0.706 | 0.740 |
| 40 | 1.925 | 1.966 | 5.948 | 6.076 | 0.545 | 0.587 |
| 48 | 3.678 | 3.776 | 11.366 | 11.669 | 0.994 | 0.995 |

Table (5.7d): Calculated data of amount adsorbed of Na, soda loss and lignin using Non-linear Langmuir adsorption isotherm as a function of kappa number based on Hartler & Rydin [33] data

Raw material: Birch kraft pulp; Temperature = 170°C, C_i (kg / m³)

| Kappa No. | Amount of Na ⁺ sorbed, kg / t | | Soda loss (as Na ₂ SO ₄), kg / t | | Amount of Lignin, kg / t | |
|-----------|---|-------|--|--------|-----------------------------|-------|
| | C _{i,0.57} | 0.655 | C _{i,0.57} | 0.655 | C _{i,1.2} | 1.42 |
| | 18 | 2.796 | 2.809 | 8.639 | 8.679 | 5.538 |
| 20 | 2.133 | 2.142 | 6.591 | 6.618 | 3.130 | 3.240 |
| 26 | 2.617 | 2.627 | 8.085 | 8.118 | 6.822 | 6.849 |
| 36 | 3.795 | 3.864 | 11.726 | 11.939 | 8.579 | 8.642 |

Table (5.7e): Calculated data of amount adsorbed of Na, soda loss and lignin using Non-linear Langmuir adsorption isotherm as a function of kappa number based on Hartler & Rydin [33] data

Raw material: Bisulphite pulp of Spruce; Temperature = 170°C, C_i (kg / m³)

| Kappa No. | Amount of Na ⁺ sorbed, kg / t | | Soda loss (as Na ₂ SO ₄), kg / t | | Amount of Lignin, kg / t | |
|-----------|---|-------|--|-------|-----------------------------|-------|
| | $C_i, 0.57$ | 0.655 | $C_i, 0.57$ | 0.655 | $C_i, 1.2$ | 1.42 |
| | 27 | 0.000 | 0.000 | 0.000 | 0.000 | 0.000 |
| 33 | 0.000 | 0.000 | 0.000 | 0.000 | 0.000 | 0.000 |
| 40 | 0.000 | 0.000 | 0.000 | 0.000 | 0.000 | 0.000 |
| 55 | 0.762 | 0.831 | 2.356 | 2.568 | 0.000 | 0.000 |

APPENDIX-III

ALGORITHM FOR CALCULATING APPROXIMATE PECLET NUMBER

- Obtain c vs t data.
- Find out the mean time $t_i = \int_0^\infty t C dt / \int_0^\infty C dt$.
- For discrete values time values $t_i \cong \sum t_i C_i \Delta t_i / \sum C_i \Delta t_i$.
- Find the spread of the distribution, measured by the variance representing the spread of the distribution $\sigma^2 = \int_0^\infty (t - t_i)^2 C dt / \int_0^\infty C dt = \int_0^\infty t^2 C dt / \int_0^\infty C dt - t_i^2$.
- Convert step- 4 to discrete form, $\sigma^2 \cong \sum t_i^2 C_i \Delta t_i / \sum C_i \Delta t_i - t_i^2$.
- Fit the dispersion model for small extent of dispersion, ($D_L / u L$ is small)

$$\sigma_\theta^2 = \sigma^2 / t_i^2 = 2 (D_L / u L) \text{ or } \sigma^2 = 2 (D_L L / u^3).$$

- Fit the dispersion model for large extent of dispersion,

For Closed vessel:

$$\sigma_\theta^2 = \sigma^2 / t_i^2 = 2 (D_L / u L) - 2 (D_L / u L)^2 (1 - e^{-uL/D_L}) = 2 / Pe - (2 / Pe^2)[1 - \exp(-Pe)]$$

$$\sigma^2 = 2 (D_L L / u^3)$$

For Open vessel:

$$\sigma_\theta^2 = \sigma^2 / t_i^2 = 2 (D_L / u L) + 8 (D_L / u L).$$

- Estimate the value of Peclet Number, Pe.
- Estimate D_L .

Though the above algorithm is valid, the terms of the calculation is slightly changed as follows for the packed bed washing.

If τ is the time from the moment of introduction of solute(tracer/ indicator) and c is the concentration of the same at outlet, then for $\Delta\tau = \text{constant}$ one can approximately write for average time spent by solutes

$$\tau_{av} = \int_0^\infty \tau c d / \int_0^\infty c dt.$$

$$\int_0^{\infty} c \, dt \cong \Delta\tau \sum_{i=1}^n (c_i + c_{i-1}) / 2 = \Delta\tau / 2 (\sum_{i=1}^n c_i + \sum_{i=1}^n c_{i-1})$$

$$\int_0^{\infty} \tau c \, dt \cong 0.5 \Delta\tau \sum_{i=1}^n \tau_i c_i + \sum_{i=1}^n \tau_{i-1} c_{i-1}$$

The variance can be calculated as

$$\sigma^2 = \int_0^{\infty} \tau^2 c \, dt / \int_0^{\infty} c \, dt.$$

$$\text{Now, } \sigma^2 = \int_0^{\infty} \tau^2 c \, dt \cong \Delta\tau \sum_{i=1}^n (\tau_i^2 c_i + \tau_{i-1}^2 c_{i-1}) / 2 \cong 0.5 \Delta\tau \sum_{i=1}^n (\tau_i^2 c_i) + \sum_{i=1}^n (\tau_{i-1}^2 c_{i-1}).$$

$$\sigma_{\theta}^2 = \sigma^2 / \tau_{av}^2 = 2 (D_L / u L) - 2 (D_L / u L)^2 (1 - e^{-uL/D_L}) = 2 / Pe - (2 / Pe^2) [1 - \exp(-Pe)] = 2 / Pe^2 [Pe - 1 + e^{-Pe}].$$

Now solve the above equation by the method of consecutive approximation for the exact value of Peclet number and then the coefficient of longitudinal mixing, $D_L = u L / Pe$.

APPENDIX-IV

BASE DATA FOR COMPARISON BETWEEN DISPLACEMENT WASHING
AND BROWN STOCK WASHING IN ROTARY VACUUM FILTER OF A
MILL

Table (6.1): Conditions of experiment and the data reported by Grah [25] for Kappa
Number = 49.7

| N0. | L (m) | C_{Fm} (kg /m ³) | V. 10 ⁶ (m ³ /s) | D_L 10 ⁷ m ² /s | $K_{i,10}$ ⁵ (1/s) | ϵ_{dm} | ϵ_{Tm} | $u \cdot 10^4$ (m/s) | C_i (kg/m ³) | C_s (kg/m ³) | k_2 (1/s) |
|-----------------|-------|-----------------------------------|---|---|-------------------------------------|-----------------|-----------------|-------------------------|-------------------------------|-------------------------------|----------------|
| 1. | 0.166 | 63.8 | 1.65 | 0.9 | 3 | 0.845 | 0.957 | 2.05 | 0.264 | 0.043 | 0.01 |
| 2. | 0.166 | 63.8 | 3.23 | 3.2 | 5 | 0.885 | 0.957 | 3.84 | 0.315 | 0.043 | 0.01 |
| 3. | 0.124 | 85.5 | 1.63 | 1.5 | 2 | 0.765 | 0.942 | 2.24 | 0.290 | 0.043 | 0.01 |
| 4. | 0.124 | 85.5 | 3.63 | 3.5 | 7 | 0.81 | 0.942 | 4.72 | 0.319 | 0.043 | 0.01 |
| 5. | 0.124 | 85.5 | 7.90 | 7.7 | 5 | 0.81 | 0.942 | 10.27 | 0.278 | 0.043 | 0.01 |
| 6. | 0.103 | 100.9 | 1.86 | 2.8 | 3 | 0.725 | 0.931 | 2.68 | 0.263 | 0.034 | 0.01 |
| 7. | 0.104 | 106.9 | 4.73 | 4.0 | 0.4 | 0.77 | 0.927 | 6.47 | 0.365 | 0.042 | 0.01 |
| 8. | 0.102 | 104.4 | 8.73 | 5.1 | 4 | 0.82 | 0.929 | 11.23 | 0.225 | 0.043 | 0.01 |
| Na ⁺ | 0.105 | 106.4 | 5.64 | 10.8 | 70 | 0.81 | 0.928 | 7.33 | 0.570 | 0.005 | 0.002 |
| lig. | 0.105 | 106.4 | 5.64 | 14.8 | 1.5 | 0.76 | 0.928 | 7.81 | 1.200 | 0.005 | 0.0 |
| Na ⁺ | 0.104 | 84.0 | 5.22 | 12.2 | 15 | 0.84 | 0.943 | 6.54 | 0.655 | 0.006 | 0.002 |
| lig. | 0.104 | 84.0 | 5.22 | 12.8 | 1.0 | 0.76 | 0.943 | 7.23 | 1.420 | 0.005 | 0.0 |

Table (6.3): Hydrodynamic data for simulation of filter washer for Na⁺

| Parameter | Grah [25] | Perron & Lebeau [75] | Han [31] | Turner[104] (Washer 1) | Turner[104] (Washer 2) |
|---------------------------------------|------------------------|----------------------|----------|------------------------|------------------------|
| L (m) | 0.02 | 0.029567 | 0.0346 | 0.0250 | 0.0282 |
| A _c (m ²) | 6.1 | 43 | 37.3 | – | – |
| C _{Fm} (kg/m ³) | 106.4 | – | – | – | – |
| D _L (m ² /s) | 5.9 × 10 ⁻⁶ | – | – | – | – |
| ε _{dm} (DL) | 0.88 | – | – | – | – |
| ε _t (DL) | 0.928 | 0.94 | 0.93 | – | – |
| ε _{dm} / ε _t (DL) | – | 0.5 | – | – | – |
| C _i (kg/m ³) | 0.570 | 11.05 | 38 | 52.9 (kg/t) | 18.9 (kg/t) |
| C _s (kg/m ³) | 0.005 | 0.00 | 15 | 18.30 (kg/t) | 5.90 (kg/t) |
| C _o (kg/m ³) | – | – | 36.91 | – | – |
| C _d (kg/m ³) | – | – | 22.5 | 25.0 (kg/t) | 8.30 (kg/t) |
| C _{yi} (%) | – | – | 2.58 | 1.140 | 1.120 |
| C _{yo} (%) | – | – | 17.2 | – | – |
| C _{yd} (%) | – | – | 17.2 | 12.3 | 11.32 |
| K ₁ (1/s) | 70 × 10 ⁻⁴ | – | – | – | – |
| K ₂ (1/s) | 20 × 10 ⁻⁴ | – | – | – | – |
| ρ (kg/m ³) | – | 1000.0 | 1000.0 | – | – |
| ρ _i (kg/m ³) | – | – | 1008.9 | – | – |
| ρ _o (kg/m ³) | – | – | 992.12 | – | – |
| ρ _s (kg/m ³) | – | – | 997.67 | – | – |
| ΔP (Pascal) | – | 20000 | 43989 | – | – |

APPENDIX- V

ALGORITHM FOR CALCULATION OF RELEVANT WASHING PERFORMANCE PARAMETERS IN BROWN STOCK WASHING OPERATION

- Calculate from the pressure-volume of filtrate data, the resistances due to cake α , filter medium resistance R_m and compressibility coefficient s
- Estimate Permeability constant K , porosity ϵ , specific cake resistance α , C_F , cake thickness L , c_{sl} , m_p , fraction submergence f and other design parameters
- Estimate fiber production rate FPR
- Estimate area requirement A
- Estimate loading factor W
- Estimate Volume of filtrate V
- Compute superficial velocity, and interstitial velocity through the mat of fibers
- Compute time of washing T_w and volumetric flow rate of washing
- Estimate wash ratio WR , DF , DR and Wash yield Y^*
- Perform mass balance for single and multi-stage washers
- Find the exit concentration of filtrate during washing and the value of Y and WE
- Estimate order of Peclet number (Pe) or Bodenstein number (Bo)
- Estimate the Wash yield proposed by Potucek and the bed efficiency E
- Compare the results of WF , WR , WE , Y , Y^* and E obtained from the experimental displacement washing of Grah, Poirier et al. and Potucek and rotary vacuum brown stock washers data reported by various investigators (Perron & Lebeau, Han & Edwards, Luthi and Turner et al.)
- Compare the above results with those from present investigation

APPENDIX-VI

A SET OF DATA OBTAINED FROM MODEL SOLUTION

Table (8.1): Values of C at bed exit for various values of T for Na⁺ from all the four models for Peclet number 27

| T | C (Model 1) | C (Model 2) | C (Model 3) | C (Model 4) |
|-----|-------------|-------------|-------------|-------------|
| 0.0 | 1 | 1 | 1 | 1 |
| 0.1 | 0.9996 | 0.9997 | 0.9999 | 0.9999 |
| 0.2 | 0.9953 | 0.9954 | 0.9997 | 0.9998 |
| 0.3 | 0.9778 | 0.9780 | 0.9982 | 0.9984 |
| 0.4 | 0.9387 | 0.9389 | 0.9900 | 0.9903 |
| 0.5 | 0.8748 | 0.8751 | 0.9647 | 0.9650 |
| 0.6 | 0.7895 | 0.7898 | 0.9114 | 0.9118 |
| 0.7 | 0.6900 | 0.6904 | 0.8259 | 0.8263 |
| 0.8 | 0.5850 | 0.5854 | 0.7136 | 0.7140 |
| 0.9 | 0.4822 | 0.3878 | 0.5868 | 0.5873 |
| 1.0 | 0.3874 | 0.0198 | 0.4599 | 0.4603 |

Table (8.2): Values of C at bed exit for various values of T for lignin from all the four models for Peclet number 20

| T | C (Model 1) | C (Model 2) | C (Model 3) | C (Model 4) |
|-----|-------------|-------------|-------------|-------------|
| 0.0 | 1 | 1 | 1 | 1 |
| 0.1 | 0.9997 | 0.9997 | 1.0000 | 1.0000 |
| 0.2 | 0.9953 | 0.9953 | 0.9999 | 0.9999 |
| 0.3 | 0.9778 | 0.9778 | 0.9985 | 0.9985 |
| 0.4 | 0.9394 | 0.9394 | 0.9905 | 0.9905 |
| 0.5 | 0.8781 | 0.8781 | 0.9653 | 0.9653 |
| 0.6 | 0.7971 | 0.7971 | 0.9120 | 0.9120 |
| 0.7 | 0.7031 | 0.7031 | 0.8265 | 0.8265 |
| 0.8 | 0.6037 | 0.6037 | 0.7142 | 0.7142 |
| 0.9 | 0.5134 | 0.5134 | 0.5874 | 0.5874 |
| 1.0 | 0.4144 | 0.4144 | 0.4604 | 0.4604 |

Table (8.3): Values of c at bed exit for various values of t for Na⁺ from all the four models for Peclet number 27

| t | c (Model 1) | c (Model 2) | c (Model 3) | c (Model 4) |
|--------|-------------|-------------|-------------|-------------|
| 0.0198 | 0.5700 | 0.5700 | 0.5700 | 0.5700 |
| 0.2675 | 0.5698 | 0.5699 | 0.5699 | 0.5700 |
| 0.5152 | 0.5674 | 0.5698 | 0.5698 | 0.5699 |
| 0.7629 | 0.5576 | 0.5690 | 0.5690 | 0.5681 |
| 1.0106 | 0.5355 | 0.5644 | 0.5644 | 0.5645 |
| 1.2583 | 0.4994 | 0.5501 | 0.5501 | 0.5502 |
| 1.5060 | 0.4512 | 0.5199 | 0.5199 | 0.5201 |
| 1.7537 | 0.3951 | 0.4716 | 0.4716 | 0.4719 |
| 2.0014 | 0.3357 | 0.4082 | 0.4082 | 0.4084 |
| 2.2491 | 0.2777 | 0.3366 | 0.3366 | 0.3368 |
| 2.4967 | 0.2241 | 0.2648 | 0.2648 | 0.2651 |

Table (8.4): Values of c at bed exit for various values of t for lignin from all the four models for Peclet number 20

| t | c (Model 1) | c (Model 2) | c (Model 3) | c (Model 4) |
|--------|-------------|-------------|-------------|-------------|
| 0.0187 | 1.2000 | 1.2000 | 1.2000 | 1.2000 |
| 0.2523 | 1.1997 | 1.1997 | 1.2000 | 1.2000 |
| 0.4859 | 1.1944 | 1.1944 | 1.1999 | 1.1999 |
| 0.7195 | 1.1734 | 1.1734 | 1.1983 | 1.1983 |
| 0.9532 | 1.1276 | 1.1276 | 1.1886 | 1.1887 |
| 1.1868 | 1.0543 | 1.0543 | 1.1585 | 1.1585 |
| 1.4204 | 0.9575 | 0.9575 | 1.0949 | 1.0949 |
| 1.6540 | 0.8452 | 0.8452 | 0.9927 | 0.9927 |
| 1.8876 | 0.7264 | 0.7264 | 0.8585 | 0.8585 |
| 2.1213 | 0.6094 | 0.6094 | 0.7070 | 0.7070 |
| 2.3549 | 0.5002 | 0.5002 | 0.5551 | 0.5551 |